UNIVERSITY OF MANITOBA

"IN-SITU CHARACTERIZATION OF MATERIAL PROPERTIES FOR THE DESIGN AND EVALUATION OF FLEXIBLE PAVEMENTS"

A Thesis
Presented to the Faculty of Graduate Studies
in Partial Fulfilment of the Requirements for
The Degree of **Doctor of Philosophy**
in
the Department of Civil and Geological Engineering

by

Gani Venkataraman GANAPATHY

VOLUME 1 - Text, Figures and Tables

February, 1994

IN-SITU CHARACTERIZATION OF MATERIAL PROPERTIES FOR THE THE DESIGN AND EVALUATION OF FLEXIBLE PAVEMENTS

BY

GANI VENKATARAMAN GANAPATHY

A Thesis submitted to the Faculty of Graduate Studies of the University of Manitoba in partial fulfillment of the requirements for the degree of

DOCTOR OF PHILOSOPHY

CHAPTER FIVE

ANALYSIS OF DEFLECTION DATA

5.1 GENERAL

An important task in this study was the analysis of deflection data collected with the FWD. In Chapter 3 an overview of different models for analyzing elastic layered systems was given. It was also mentioned that many computer algorithms are available at present. One deficiency with all the available computer algorithms is that they cannot consider anisotropy of the materials. Many theses have been written with some algorithm which would meet the quest of that particular researcher but would not be generalised or versatile enough to meet other requirements. Therefore, it was suggested that a general-purpose finite-element method (FEM) is best suited for the analysis of pavement systems. Two finite-element programs available with the University of Manitoba mainframe computer were not suited for this study, since they would have required extensive modifications and rewriting source codes to consider non- homogeneous, nonlinear or anisotropic behaviour. For this study the finite-element method chosen was the ANSYS system developed by Swanson Analysis System Inc (SASI) of Philadelphia in the USA. ANSYS is a commercial general-purpose finite-element program which can be used for a variety of problems in applied mechanics including the layered elastic models for pavements. One can use it for modelling the simple homogeneous, isotropic elastic solid or add in any other features such as non-homogeneity, anisotropy, non-linearity, plasticity and yield criteria and even temperature-dependent material properties. Even though ANSYS is a commercial program, and hence its source code is not available to its users, it provides enough flexibility that user-defined parameters can be input into the system. There are other similar commercially available finite-element programs. However, ANSYS was chosen for this study because it was readily available within the University with the Department of Mechanical Engineering.

5.2 FEATURES OF ANSYS FINITE-ELEMENT PROGRAM

5.2.1 General

ANSYS is a self-contained, general-purpose finite-element method having many capabilities. Fig. 5.1[1], which is reproduced from the ANSYS user manual, shows some of these capabilities. Most of these capabilities are in modules which are invoked with simple commands. Like many other good finite-element methods, ANSYS has, in general, three stages as shown in Fig. 5.2:

1. Pre-processing;
2. Analysis;
3. Post processing.

A fourth stage which was used in this study is the **OPTIMIZATION** module. Fig. 5.2 shows the tasks or activities that are undertaken in each of the three main sub-processes. The optimization module preserves the parameters which are specified as fixed by the user and varies the rest to arrive at the solution, within the constraints prescribed. The basic principles of optimization as used by ANSYS are discussed in a little more detail later in this chapter.

Fig. 5.3 shows a generalized flow chart giving the processes under the ANSYS program. Obviously, for layered elastic analysis of pavement structures only certain paths on

---

1 All figures and Tables are included in the Appendices at the end of the chapter.

this figure will be relevant or of interest. Two such subsystems of analysis procedures which could be of interest are shown in Fig. 5.4 and Fig. 5.5. The subsystem used in this study is the one shown in Fig. 5.4 with the addition of the optimization module. Fig. 5.5 shows the data flow in the solution of a simple linear or non-linear dynamic analysis.

5.2.2 Basic Theoretical Concepts in Ansys

As discussed in Chapter 3, the finite-element method is essentially an approximation of the original real problem. The structure is divided into a number of elements which are interconnected at a finite number of points. If the force-displacement relationships for each of the elements can be formulated then the force-displacement relations for the entire structure can be assembled in the form of matrices of the type shown in Eqn. (10) in Chapter 2. This matrix relates the stress and strain at any point in the structure using the material properties. These material properties are given by the modulus of elasticity and the Poisson's ratio. As has been discussed in great detail in Chapter 2 there will be two material constants (E and μ) for an isotropic solid and five for cross-anisotropic solids (E_x, E_y, μ_{vv}, μ_{vh}, and G_{xy}). Having defined the element geometry and the material properties the next step is to define the boundary conditions and the applied loads and displacement conditions.

In matrix formulation the basic equation relating force and displacement for the static

$$[K]\{u\} = \{F_{app}\} + \{F_{th}\} + \{F_{pr}\} + \{F_{ma}\} - \{F_{el}\} \qquad (109)$$

analysis in ANSYS is:

where,

[K]	=	sum of element stiffness matrices (total stiffness matrix)
$\{F_{app}\}$	=	applied load force vector (concentrated point loads)
$\{F_{th}\}$	=	applied element thermal vector
$\{F_{pr}\}$	=	applied element pressure vector (uniformly distributed loads)
$\{F_{ma}\}$	=	applied element body force vector
$\{F_{el}\}$	=	applied element elastic load vector (secondary forces due to non-linearity) and
$\{u\}$	=	displacement vector

In this study, thermal properties, body forces and non-linearities were not considered though ANSYS is capable of handling these cases. Also, the applied load is considered to be uniformly distributed. Therefore, the terms $\{F_{app}\}$, $\{F_{th}\}$, $\{F_{ma}\}$, and $\{F_{el}\}$ will vanish. Thus Eqn. (109) will reduce to:

$$[K]\{u\} = \{F_{pr}\} \qquad (109\ a)$$

finite-element program usually starts with the formulation of the matrices for all the elements. Then using matrix algebra the matrices are manipulated so that as many matrix elements as possible can be reduced to zero. This helps reduce the computation time. This process is shown in Fig. 5.4 as "wavefront solution" and "triangularized stiffness matrix". Equations of the type of Eqn. (109a) give rise to a set of simultaneous equations, as many as there are elements. When these equations are solved for the known boundary and loading conditions in such a way that at all nodes the equilibrium and compatibility conditions are satisfied, a solution for the problem at hand has been found. By substituting the solutions in the individual element matrices, displacements, stresses and strains at every point in the structure can be obtained (shown as "back substitution" in Fig. 5.4).

5.2.3 Element Library

It was mentioned earlier that the finite-element model is an approximation to the real structure. The approximation is achieved by breaking down the structure into an assemblage of smaller elements connected at a number of nodal points. Therefore, in order that the behaviour of the assemblage would truly approximate that of the real structure, it is important that the individual elements are properly characterized. The formulation of the stiffness matrix will depend upon the type of element. For instance, a two dimensional plate cannot be truly represented by elements carrying axial loads only; nor will a prismatic flexural element be appropriate to represent a pin jointed truss. Thus all finite-element programs carry an element library. The element library contains different types of structural elements and information about how to define their geometry, their stiffness material properties and the degrees of freedom. Such information is the shape function, stiffness matrices, degrees of freedom, stress or strain parameters etc. in source code. This information is not transparent to the user, but the program accesses that information once a certain element type is specified. Fig. 5.6 shows a partial list of the library of elements carried by ANSYS. It is not necessary that a structure should contain only one type of element. It can be an assemblage of many different types of elements. The only caution is that they are all properly defined.

In the ANSYS program different types of elements are called by a nomenclature STIF<u>n</u> where n represents the library identification number. For example, referring to Fig. 5.6, STIF1 represents a spar element in a plane. The deformed geometry of such an element is completely defined by the two component displacements U_x and U_y in the Cartesian coordinate system. U_x and U_y are the two degrees of freedom (DOF) for such an element. Fig. 5.6-B explains the characteristics of the different STIF elements and what features of such elements can be handled by ANSYS at the present stage of development. Fig. 5.6-A shows some elements (STIF 45, STIF 64 and STIF 46) which can be used if one has to model the pavement as a three-dimensional solid.

5.2.4 Representation of Pavement Structure

Pavement structure is generally represented as a semi-infinite elastic continuum, layered or homogeneous. In most cases the problem can be analyzed as a plane strain problem. However, the loading on a pavement is over a finite area given by the tire foot-print. Thus, while the geometry of the pavement is a two-dimensional plane, the loading would strictly make it a three-dimensional solid. However, wheel loads are generally assumed to be circular having an axis of symmetry in the vertical direction. Thus the pavement structure can be represented by an axi-symmetrical solid, which is a plane strain problem.

The most appropriate element in the ANSYS element library to represent such a structure would be STIF42 (see Fig. 5.6a). This is a two dimensional, isoparametric elastic solid having two degrees of freedom U_x and U_y (planar structure). Fig. 5.6 shows the features that can be possibly handled by ANSYS using these elements. For instance plasticity can be handled. Thus if the complete stress-strain curve for the component materials can be defined (see Fig. 5.7 for examples) then the deformation of such elements can be computed. For pavement materials, particularly the unbound materials, one can prescribe a yield criterion and ensure that excessive deformations do not occur. Theories of elasticity generally assume small displacements so that the principle of superposition can be valid in many analyses. However, in pavement materials one might be occasionally interested in analyzing the structure under large deformations. With STIF42, ANSYS can handle such an analysis. Some earth materials are stress- stiffening.

According to Fig. 5.6 STIF42 will permit incorporation of such material properties. Therefore, in this study the pavement structure was represented as made up of STIF42 elements and an axi-symmetrical formulation was used. Because of the importance of STIF42 to this thesis, and in the opinion of the author to the analysis of pavements by ANSYS, the complete theoretical development of STIF42 as described in ANSYS "Theoretical Manual" is included as an appendix to this chapter (Appendix 5-I).

5.2.5 Optimization Module

Optimization as employed by ANSYS is a programmed mathematical technique which integrates the analysis procedures into an iterative search procedure to find the minimum value for a specified parameter subject to certain user-defined constraints. For example, if one were to use ANSYS to design a beam for minimum weight, subject to certain boundary and loading conditions, and subject to certain limiting stresses and physical dimensions, ANSYS would go through the analysis part first and determine the stresses in terms of the physical geometry of the beam. In the second part it would start an iteration process by which the dimensions would be chosen within the constraining conditions of size and stress until finally a least weight design would be obtained.

In the above example, the objective is the least weight design. For a simple beam, the weight can be explicitly written in terms of its physical dimensions and mass density. Such a function forms the **OBJECTIVE FUNCTION.** Similarly, the stresses can be computed in terms of the physical dimensions. The restrictions one places on these stresses and the physical dimensions are called the **CONSTRAINT EQUATIONS**. For the beam example both the objective function and the constraint equations can be explicitly written as functions of the physical dimensions of the beam. The physical dimensions form the **DESIGN VARIABLES**. The determinant to change and try different combinations of dimensions within the specified limits is the state of stress at various points in the beam. The stresses are called the **STATE VARIABLES.**

This example illustrates that in running an optimization module one should define four essential components:

1. The **OBJECTIVE FUNCTION**.
2. The **CONSTRAINTS** within which the system should seek an optimal solution.
3. The **DESIGN VARIABLE** which is the independent variable which should be modified in each iteration cycle, and
4. The **STATE VARIABLE** which is the outcome of the analysis in each iterative cycle.

In the example of the beam, all of these can be explicitly written in terms of the design variables. Thus, the optimization will converge to a unique value. However, in many problems for which one would seek a finite-element approximation, explicit relationships do not exist. In such a case the optimal solution will lie within a space bounded by the surfaces of the objective function plane, and the surfaces bounded by the design variables and state variables. By repeated optimization one can then arrive at a point in the surface where the gradient of the objective function is **minimum**. The concept of optimization as applied in ANSYS is illustrated in Fig. 5.8.

In the above discussion, it has been tacitly accepted that one is always seeking the **minimum** value for the objective function. The ANSYS optimization module will always seek the minimum value. Therefore, when using this module, one should write the objective function in such a way that the minimum solution is the appropriate one for the problem at hand.

5.3 MODEL GEOMETRY FOR THE PAVEMENTS ANALYZED

Fig. 5.9 shows the photograph of the finite-element mesh generated for the pavements in this study. Fig. 5.10 shows a hard copy printout of the mesh. All mesh elements were specified as rectangular. The mesh is finer near the load and becomes coarser as one gets farther and farther away from the load both vertically and horizontally. Because of the large amount of data to be analyzed, a generic type of mesh generation code was written to build the finite-element model.

5.3.1 Horizontal Direction

In heavy pavement structures, such as airfield pavements, the deflection bowls are usually large. Therefore, the vertical boundary of the model should be sufficiently far away from the load point so that the model can predict the real load distributing capacity of heavy pavements. This was also confirmed when some of the 1985 data was analyzed using the ISSEM-4 program. Also from these initial results it was decided to have the vertical boundary at twice the distance of the last sensor from the load point. At this boundary, only vertical movements are possible, but no horizontal movements. Twenty five node points were specified within this distance. Four of these nodes were under the loading plate, the next seventeen between the outside edge of the plate and the last sensor and the rest between the last sensor and the outer boundary as determined above (see Fig. 5.10).

5.3.2 Vertical Direction

In the vertical direction the number of elements and the node points depended on the structure. Generally the asphalt layer had an element height approximately equal to 40 or 50 mm. This was done to reflect general construction practice in the past where the lift thickness of the asphalt surface layer would be between 40 and 50 mm. Similarly, for the granular material the specifications, generally, called for compacted thicknesses of 150 to 200 mm. Therefore the mesh generation called for an element height in this range. The subgrade was always divided into 1.0 m thick layers and there were always fifteen layers in the subgrade. This amounts to assuming the thickness of the "semi-infinite" layer to be 15 m.

5.3.3 Boundary Conditions

Along the axis of symmetry and the vertical outer edge only vertical movements are possible. At the bottom of the fifteenth layer in the subgrade a rigid bottom was assumed. Thus there would be no movements at all at this boundary. The top horizontal boundary is a free surface. The choice of thickness of the semi-infinite layer was made after some trial runs with the model trying to reproduce results published by Gerrard (1968) and Bhattacharya (1968). Fig. 5.11 shows the results of these trial computations.

5.3.4 Loads

The final step in building the finite-element model is to specify the loads. Only vertical surface loads applied over a circular area centred on the axis of symmetry were considered. The load was specified as a uniformly distributed pressure equal to the applied FWD load. It was assumed that no shear forces exist between the loading plate and the surface of the continuum.

5.4 USER-DEFINED PARAMETRIC CODING FOR PROBLEM DEFINITION IN ANSYS

The main ANSYS program has three functions, to:

1. Create the model geometry as directed by the user or automatically under the limits specified by the user;
2. Run the analysis. This includes the formulation of matrices, triangularization of the matrices and solving the matrix equations;
3. To do specific post-analysis manipulation. This includes collecting the results, such as stress, strain, and deformations, at any user specified points and displaying them as graphs, charts, tables etc.

All these functions are contained in individual modules held in the ANSYS program library. The input directing the program to perform its functions must be created by the user by issuing the individual commands, if the user is solving the problem interactively, or through a set of macros if the program is run under a batch mode. Appendix 5-II shows the coding used in running ANSYS. Fig. 5.12 is a flow chart which shows how the different modules are invoked in sequence, to execute ANSYS for this thesis. It is not the intention here to discuss individual ANSYS commands, but merely to demonstrate how the different modules are built up and joined into a macro so that these can be submitted as batch files to a computer for processing, as shown in Appendix 5-II. The ANSYS program was run on a VAX-4.0 mini computer housed in the Department of Mechanical Engineering of the University of Manitoba.

5.5 LAYERED PAVEMENT SYSTEMS AT THE DIFFERENT SITES

The example shown in Appendix 5-II is for a specific site and shows the coding for a three-layered pavement (AC, Base and Subgrade) with four loading conditions. However, this is not the general case with all the sites presented in this thesis. Table 5.1 shows the layers at the different sites and the layered approximations used. In general, the pavement was represented as it was built (see also Table 4.2 to 4.6 in Chapter 4). Since airfield pavements are usually built up as the need arises this resulted in systems with up to six layers. In the literature, one often finds statements that there is no special advantage in idealizing the pavement as more than a three- or four-layer system. While this is true for homogeneous pavements, it becomes necessary to have the capability of analyzing a truly "n-layer" system such as the pavements analyzed in this thesis. Often the layers were so contrasting in their material properties that it would not have been possible to find a reasonable equivalent layer thickness by any of the methods described in Chapter 2.

Table 5.1 Layered System Approximation at Different Sites

Site	Date Built	Date Tested	Age Yrs.	Analysis System	Subgrade (USC)
BRANDON	1983	1985	2	3L 4P	CL-ML
THUNDER BAY	1984	1985	1	4L 4P	SP-SM-ML
ST. ANDREWS	1968	1988	20	3L 3P	CH
REGINA	1979	1988	9	5L 3P	CH
SASKATOON	1976	1988	12	6L 3P	CL-CH

Note: For the analysis system 3L 4P means a three-layer system with 4 loading cases was analysed.

It should be mentioned here that the use of a general-purpose finite-element program, such as ANSYS, proved to be advantageous in the analysis of composite pavements. For example, when it was attempted to analyze composite pavements, in which a rigid layer was overlain by a more flexible layer, using the ISSEM-4 program the program would often fail because of the proximity of a "rigid bottom" to the surface. In a general-purpose finite-element program this does not appear to be a problem. In fact the program helped to visualize the effectiveness of a rigid layer at different levels in the pavement structure in distributing the load. This will be discussed in the next chapter where results of stress analysis are presented. It is submitted that this might prove to be a useful tool in overlay designs.

5.6 METHODOLOGY OF ANALYSIS

In the previous sections the reasons for the choice and use of the ANSYS finite-element program for the analysis of pavements by the layered elastic theory were given. In this section the nature of the solutions to the problems and the criteria which were used to choose one or other of the solutions are discussed. In Chapter 6 the actual results are presented and discussed.

5.6.1 Solutions to the Layered Elastic Problem

In Chapter 2 it was mentioned that the layered elastic system has no unique solution. This is because the problem is basically indeterminate. The more the number of layers, the more indeterminate is the problem and hence the less unique are any solutions. Many combinations of the layer moduli can be found to yield the same deflection basin. It is then a matter of judging which combination of individual layer moduli is the most plausible. Therefore the experience of the engineer analyzing the problem becomes very important. It also becomes very important that the behaviour of the materials is well understood. However, when one is dealing with materials such as asphaltic concrete or earth materials, this becomes a very difficult, if not altogether impossible, task. Added to that, the solution appears to depend on the criterion used to judge the goodness of fit between observed and theoretical deflection basins. Similar observations were made independently by Sivaneswaran et al. (1991).

As far as the author is aware of, most of the back-calculation procedures aim at matching the maximum deflection (at the centre of applied load) as the criterion for selecting the layer moduli. Some other methods (e.g. ISSEM-4, SENOL) aim at matching deflections at discrete points (usually the sensor points, because these are the only points of certainty) as a criterion for a good fit. However, it is submitted that the volume of the deflection basin would form a better criterion to calculate the layer moduli.

The concept that the shape of the deflection basin is a unique characteristic of the pavement is not an entirely new concept. Vaswani's and Majidzadeh's concept of rigidity factor (Vaswani, 1971; Majidzadeh, 1982), already established this fact. Hoffman and Thompson (1982) also presented some evidence to this effect. However, a back-calculation method using this concept has not been presented so far. The method presented herein is not the ultimate development either. There are still significant improvements to be made. Intuitively, the deflection basin is the response of the pavement to an applied load at a given time with a certain combination of material properties.

In fact, it is the work done by the energy absorbed by the pavement from the total energy delivered to the pavement by the falling weight (in case of FWD) or the periodic load generated by other loading devices (e.g. the Dynaflect) that defines the deflection bowl. This capacity to absorb energy is a function of the material properties, most notably the dynamic moduli and the damping characteristics of the pavement materials. If resilient modulus, as is generally understood by pavement engineers, can be accepted as a surrogate to this dynamic modulus then the volume of the deflection basin can be used to calculate the resilient moduli. Normally, plane strain conditions or axi-symmetry is assumed. Therefore deflections are measured only along one line tacitly assuming that the deflections along any other line radiating from the load point would be identical[2]. As an initial attempt to use the concept the following

---

2 This was why it was felt it was unfortunate (see p. 171) that in the 1985 test series even though deflections were measured at five different points on a circle around a given station they were not measured radially. Such a measurement would have permitted the calculation of the actual deflection basin.

procedure was used.

It was assumed that the model was either isotropic and homogeneous or was cross-anisotropic and homogeneous. It will be emphasized that non-homogeneity can be very easily handled by the model presented here and by the ANSYS program. However, this will be left to future evaluation and research. In this thesis, it was attempted to simply determine a criterion that would lead to better results when back-calculating FWD data. Using the seed values, ANSYS would calculate the deflections at the sensor points. Then the optimization module would be called and ANSYS would be directed to optimize the modulus values by the following three criteria:

1. "AREA" of the deflection basin;
2. The maximum defection at the centre of the load; and
3. The Root Mean Square (RMS) value of the deflections at the seven sensor locations.

1. "AREA" of the Deflection Basin

The area of the deflection bowl was calculated by the trapezoidal rule using the deflection ordinates at the sensor locations. Thus the area became:

$$A = 1/2 \times (U_i - U_{i-1}) \times (d_i - d_{i-1})$$

where, the U_i's and the d_i's are the deflections and the distance from the centre of the load respectively of the i^{th} sensor. The program would calculate the square of the difference in the areas from the measured deflections and the calculated deflections after each valid iteration (feasible solutions) in the optimization loop. It was necessary to calculate the square of the differences in the area so that the objective function was a positive quantity and hence a

minimum value could be found. It might be recalled from the earlier section that ANSYS always ***minimizes*** the objective function.

2. Maximum Deflection

For this criterion the square of the difference between the calculated and measured deflection under the load is the objective function. Again, the square of the difference was used so that the objective function was a positive quantity and ANSYS could seek a **minimum** value to find an optimal solution.

3. Root Mean Square (RMS) Value of Deflections

The RMS value is the sum of the squares of the differences between the observed and calculated deflections at the seven sensor locations. Once again the squared value was needed to have the objective function positive. This is similar to the SENOL or ISSEM-4 programs where the deflection bowls are required to match at discreet points in addition to the point under the load. RMS values were used in an optimization technique suggested by Sivaneswaran et al. (1991).

It should be recognized that both the "AREA" method and the RMS method use the entire deflection bowl in an attempt to find an optimal solution. Therefore, based on the discussions in the previous sections, these are inherently better criteria than the one where just the maximum deflections are matched. The "AREA" method would be even better if a curve fitting program (such as the one used by ISSEM-4) were used prior to invoking ANSYS. ISSEM-4 attempts to fit a curve through the measured points by a smoothing function that considers the ordinates at every 30 mm. Thus a tight fitting smooth curve for the deflection bowl can be obtained. In future developments of the concepts developed in this thesis this should be explored.

ANSYS continued the optimization loops until one of the following criteria was met:

1. The solution had converged and therefore an optimal solution has been reached;
2. ANSYS had run through the specified number of loops requested by the user regardless of whether an optimal solution had been found or not;
3. The default limit for the number of loops had been reached regardless whether an optimal solution had been reached. This number is 50 for the system at the University of Manitoba. In such a case, the user has the option to choose the best (N + 2) solutions out of the 50 and re-start the optimization subroutine, where N is the number of design variables in the problem. This would lead to another set of 50 solutions, excluding the sets already rejected, or to convergence. Of course, one has to weigh the trade-off between computer time and the gain made by finding a near-true optimal solution;
4. The objective function showed constant oscillation so that an optimal solution was not feasible.

An example of the output from ANSYS optimization loop is shown on the next page.

In the solutions presented in this thesis, the number of loops varied mostly between 16 and 28 while there was a significant amount of calculations that used up the 50 loop limit. Only in a very few cases a second 50-loop routine was attempted. It will be shown later that the modulus per se, is not a high-sensitivity quantity in pavement analysis so that one should not over-emphasize the need to find a very precise value for this quantity.

EXAMPLE OF PARTIAL ANSYS OUTPUT AFTER OPTIMIZATION LOOPS

	SET 36 (FEASIBLE)	SET 37 (FEASIBLE)	SET 38 (FEASIBLE)	SET 39 (FEASIBLE)	SET 40 (FEASIBLE)
EY1	7016.38	7099.18	7200.43	6645.22	6826.22
EY2	7094.20	7110.79	3665.41	7050.52	5562.68
EY3	1913.19	1887.74	1895.35	1883.06	2782.10
EY4	489.723	490.117	298.822	303.295	305.838
EY5	130.682	130.800	130.744	130.755	130.726
EY6	157.137	160.355	173.771	177.744	179.913
R4	1.58309	1.53184	1.79652	2.52130	2.41822
R5	2.33054	2.28442	2.30967	2.29973	0.782592
NUV1	0.154949	0.229203	0.153660	0.153974	0.154030
NUV4	0.291917	0.398634	0.398963	0.399104	0.398965
NUV5	0.438754	0.438854	0.323614	0.332384	0.440269
NUH4	0.291917	0.398634	0.398963	0.399104	0.398965
NUH5	0.438754	0.438854	0.323614	0.332384	0.440269
TENS	0.000000E+00	0.000000E+00	0.000000E+00	0.000000E+00	0.000000E+00
AREA	798.746	15164.4	4693.31	155.658	170.406

	SET 41 (FEASIBLE)	SET 42 (FEASIBLE)	SET 43 (FEASIBLE)	SET 44 (FEASIBLE)	SET 45 (FEASIBLE)
EY1	7994.98	7753.67	9396.54	4009.51	4052.99
EY2	5200.12	6995.80	7019.66	6998.18	7088.75
EY3	1415.93	1562.95	2708.07	2097.00	2068.05
EY4	295.237	489.723	492.112	489.729	491.696
EY5	130.813	130.820	130.767	130.765	130.728
EY6	171.103	158.353	152.359	150.227	147.883
R4	1.84572	2.54200	1.27023	1.00411	1.06219
R5	2.32206	0.851659	0.740417	0.783059	0.831846
NUV1	0.154239	0.171258	0.171635	0.162808	0.154586
NUV4	0.290501	0.399059	0.399025	0.280758	0.398900
NUV5	0.440430	0.326193	0.438304	0.329002	0.438381
NUH4	0.290501	0.399059	0.399025	0.280758	0.398900
NUH5	0.440430	0.326193	0.438304	0.329002	0.438381
TENS	0.000000E+00	0.000000E+00	0.000000E+00	0.000000E+00	0.000000E+00
AREA	12011.6	1746.88	988.646	217.066	2947.75

	SET 46 (FEASIBLE)	SET 47 (FEASIBLE)	SET 48 (FEASIBLE)	SET 49 (FEASIBLE)	SET 50 (FEASIBLE)
EY1	6990.47	6961.79	7040.82	6430.69	7439.71
EY2	7064.67	7054.21	7115.86	6792.16	6784.13
EY3	2602.88	2685.87	2259.12	2661.75	2611.05
EY4	491.739	489.287	488.910	493.849	492.198
EY5	130.782	130.660	130.768	243.415	243.267
EY6	152.607	153.749	151.055	138.367	136.018
R4	1.14850	1.15728	1.12166	1.42584	1.13267
R5	0.748720	0.742756	0.745587	0.746974	0.740578
NUV1	0.164895	0.164243	0.163184	0.177806	0.158352
NUV4	0.282499	0.286426	0.399134	0.387222	0.383929
NUV5	0.330806	0.439943	0.329284	0.314995	0.431424
NUH4	0.282499	0.286426	0.399134	0.387222	0.383929
NUH5	0.330806	0.439943	0.329284	0.314995	0.431424

5.6.2 Model Definition

In Chapter 3, the requirements for a finite-element model to represent pavement structures were given. Two models were analyzed in the current work:

1. A homogeneous, elastic, isotropic model. In this model all layers were assumed to be isotropic;
2. A homogeneous, elastic, cross-anisotropic model. In this model all layers except bound layers (asphaltic concrete, Portland cement concrete and stabilized layers such as the econocrete layer in Brandon) were assumed to be cross-anisotropic.

While all stations at all the test sites were analyzed by the cross-anisotropic model, only five stations from each site were analyzed by the isotropic model for comparing with the cross-anisotropic solutions.

5.6.2.1 <u>Layer Definitions</u>

Table 5.1. in Section 5.5 lists the layered systems that were analyzed for the pavements at the different test sites. As shown in Table 5.1. the maximum number of layers used in this thesis is six. The program has no constraint regarding the number of layers. However, increase in the number of layers, particularly in the subgrade materials or at greater depths offers no special advantage. On the other hand, if starkly contrasting materials are present within 15 m of the surface they should be preferably treated as different layers. The layers were subdivided to roughly correspond to construction practice (compaction-lift thickness, different type of fill materials, etc.). This will be also useful if stress-dependency is to be included.

5.7 INPUT FOR OPTIMIZATION LOOPS

One of the distinctive features of the analyses presented in this thesis is the optimization procedure. This is not to be confused with the iteration procedures available in many algorithms, including ANSYS. It will be recalled that the optimization routine tries to find the minimum value for the objective function within the constraints specified by the user. Thus one can restrict the program not to seek solutions for material properties which are not generally found at a site or in a region or which do not correspond to the construction history of a project. The latter will be of interest if one is investigating a failure or problem areas, or evaluating a pavement for structural input into a pavement management system. In this investigation some of the material properties were available from original construction records kept by Transport Canada. Combining these with the general ranges found in the literature, particularly in the study by Emery (1983) for Ontario Ministry of Transportation, the following limits on the material properties were set for the optimization routine:

Limits on Moduli Values

Asphaltic Concrete:	1,000 - 10,000 MPa
Granular Base:	200 - 600 MPa
Granular Subbase:	120 - 250 MPa
Silty Sand to Sandy Silt (ML, SP, SM):	80 - 200 MPa
Silty Clay to Clayey Silt (CL) :	50 - 150 MPa
Plastic Clays (CH) (Stiff to firm):	80 - 200 MPa

Plastic Clays (CH) (Soft):	35 -120 MPa
Portland Cement Concrete:	25,000 - 50,000 MPa
Econocrete:	10,000 - 20,000 MPa

Limits on Poisson's Ratios

Asphaltic Concrete:	0.20 - 0.30
Portland Cement Concrete:	0.15 - 0.25
Granular materials:	0.30 - 0.40
Fine-grained sub-grade materials:	0.35 - 0.48

It should be noted that in many finite-element programs, including ANSYS, the Poisson's ratio cannot be 0.5. Saturated clays, which are virtually incompressible, and hence have a Poisson's ratio of nearly 0.5, can be modelled in ANSYS by a fluid element called STIF79 or STIF80. However, in this analysis it was decided to retain the STIF42 element throughout the analysis and not to let the Poisson's ratio approach the value of 0.50.

Anisotropy ratios in unbound layers were assumed to vary between 0.5 and 5.0. Bound layers were assumed to be isotropic regardless of whether one used the isotropic or the cross-anisotropic model. Anisotropic ratio is defined as E_h/E_v.

The design variables for the optimization routine were the different layer moduli. The state variables were the pavement response which were the surface deflections, stresses, strains, and deformations at different points within the pavement structure.

Another feature in the optimization routine was to restrict the tension in the unbound layer to zero. This was to ensure that during the analysis the unbound materials do not develop tension. The number of optimization loops were between 16 and 50. The program was asked to sort the solutions in an ascending order i.e. from minimum to maximum value of the objective function. From this sorted set, the top five solutions were picked as giving the most probable range of layer moduli for that station. The corresponding deflections and the stress distributions for these five solutions were also printed out. These calculations are repeated for all the three chosen criteria, namely:

1) "AREA" of Deflections Basin;
2) Maximum Deflection;
3) RMS value of Deflections.

The analyses and the results are presented and discussed in Chapter 6.

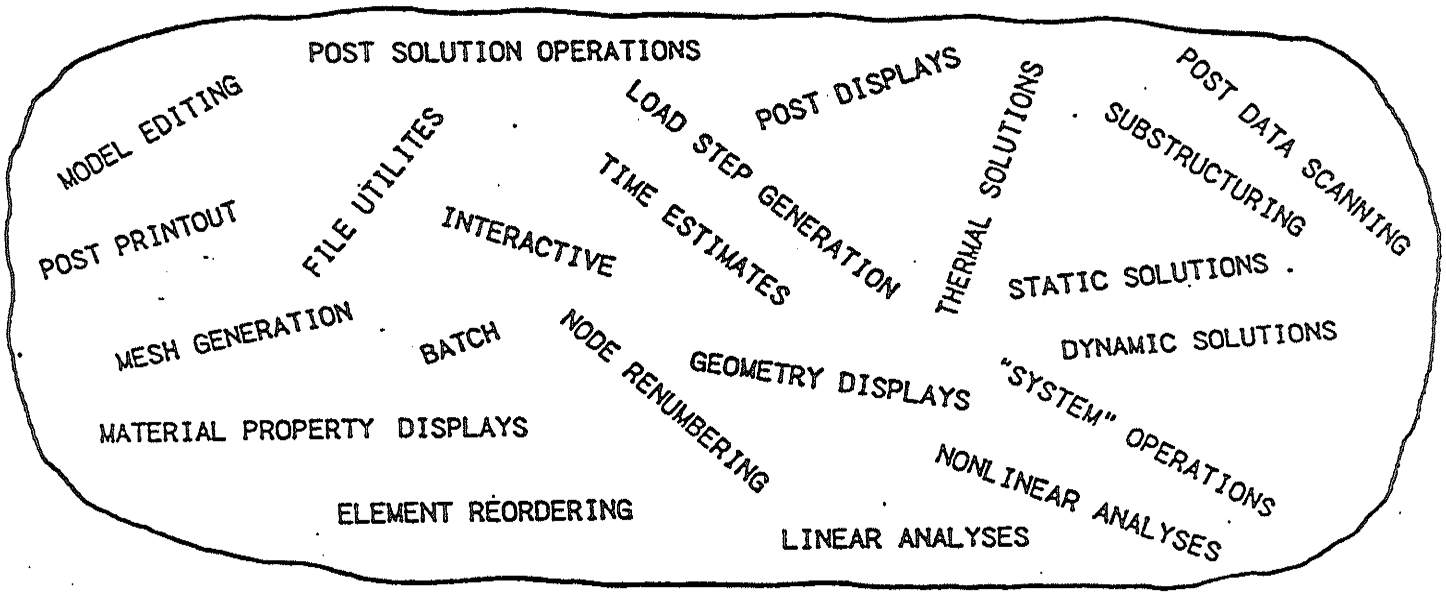

FIG. 5.1. OVERALL ANSYS PROGRAM AND SOME OF ITS CAPABILITIES

(FROM ANSYS 4.4.A. THEORETICAL MANUAL)

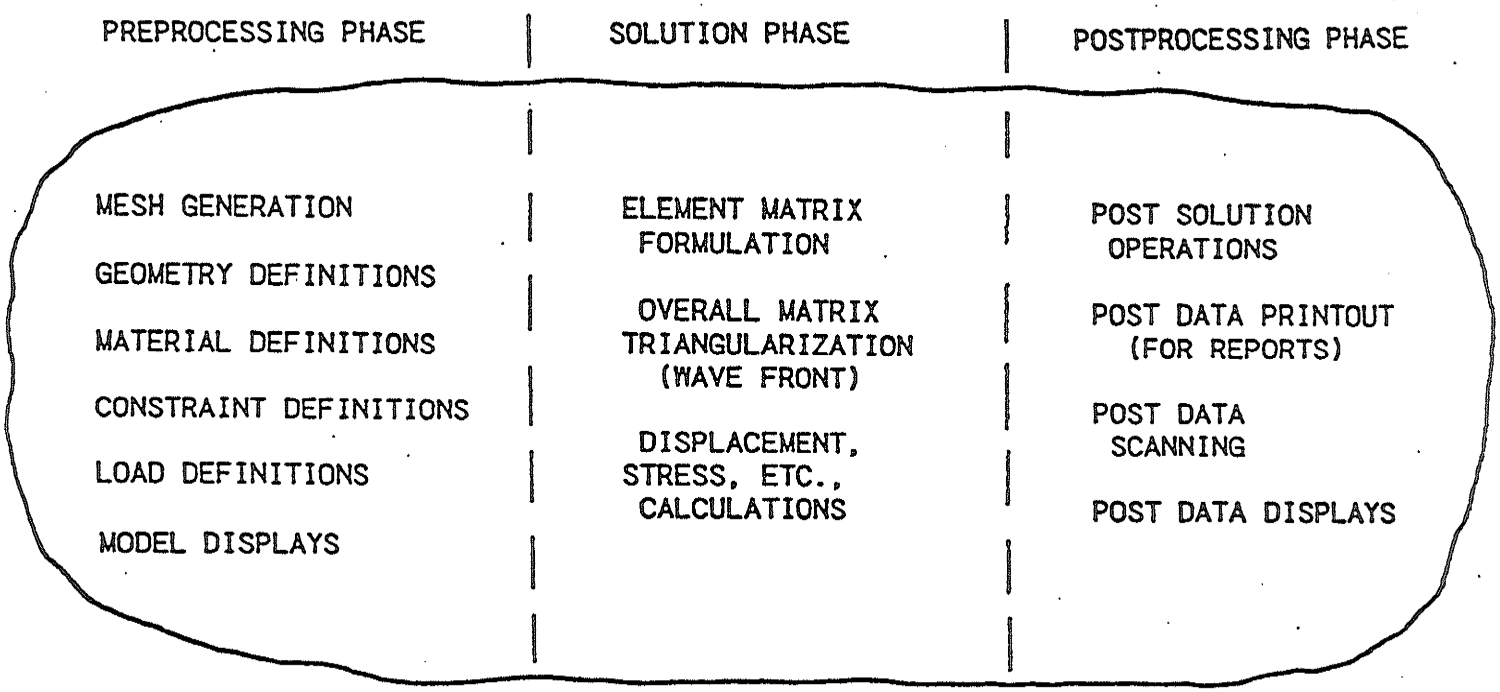

FIG. 5.2. MAJOR TASKS IN EACH OF THE SUBPROCESSES IN ANSYS

(FROM ANSYS 4.4.A. THEORETICAL MANUAL)

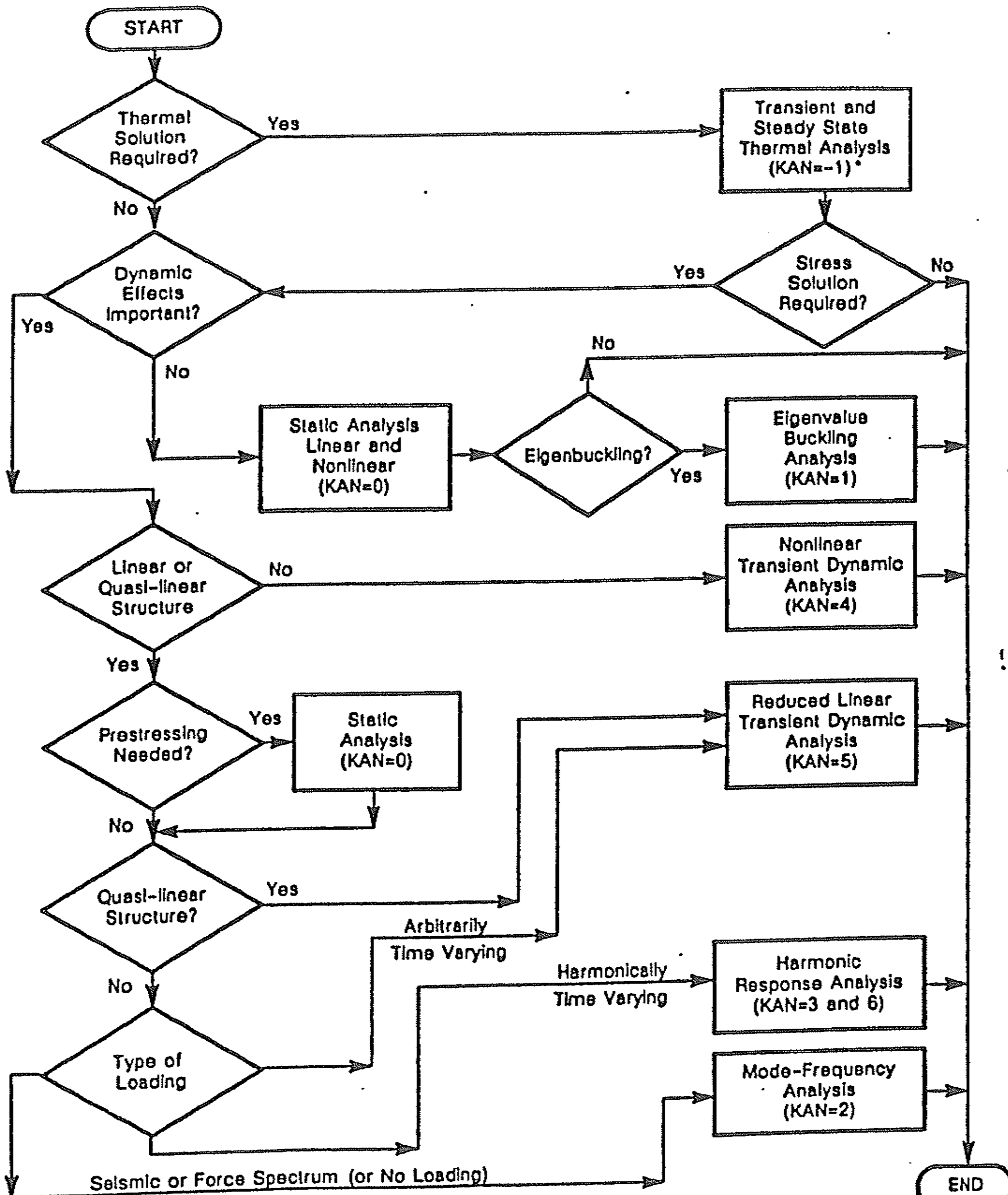

* KAN is the key input on the KAN command to select the analysis type
** Quasi-Linear – the structure is linear except for gaps

FIG. 5.3. FLOW CHART SHOWING GENARALISED PROCEDURES IN ANSYS (FROM ANSYS 4.4.A. THEORETICAL MANUAL)

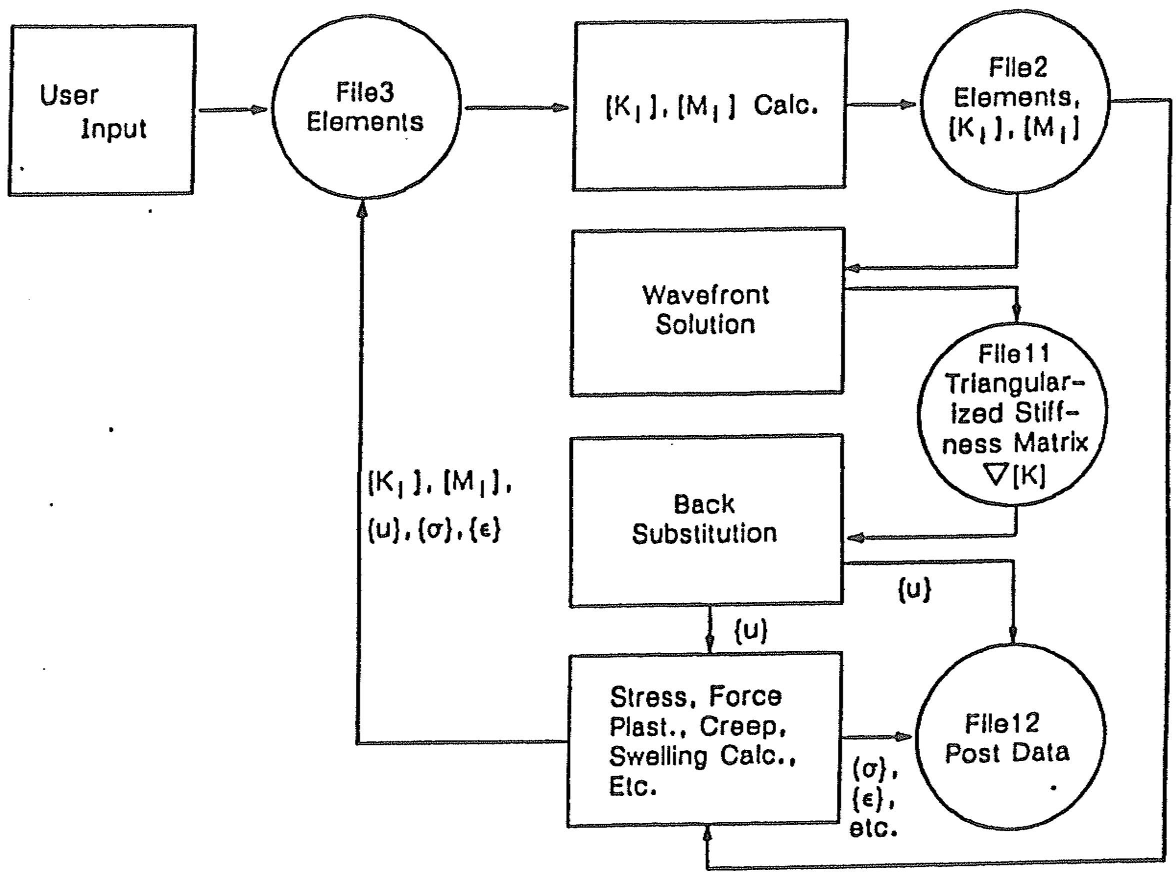

FIG. 5.4. FLOW CHART OF GENERALISED STATIC ANALYSIS IN ANSYS (FROM ANSYS 4.4.A. THEORETICAL MANUAL)

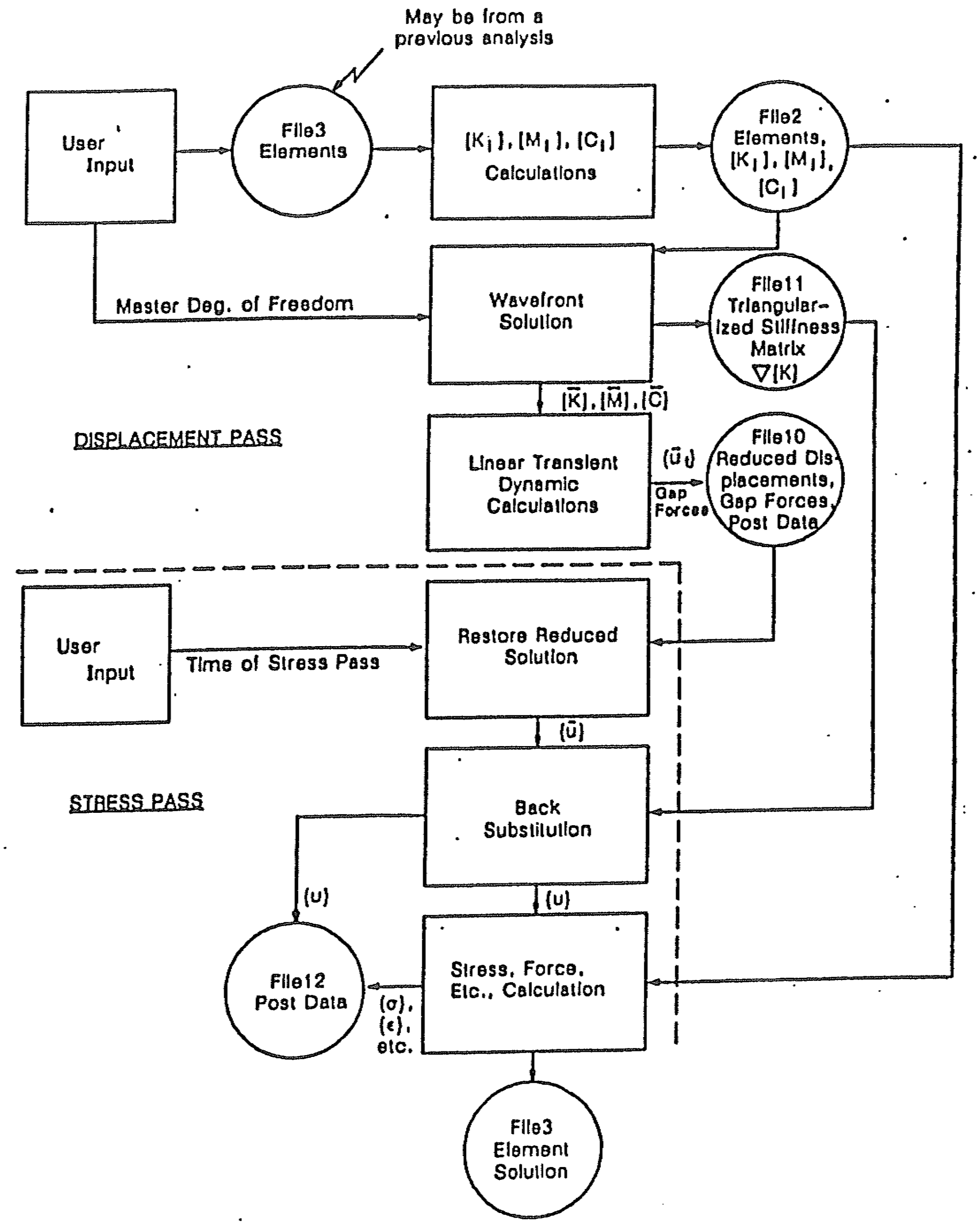

FIG. 5.5. FLOW CHART OF GENERALISED LINEAR TRANSIENT DYNAMIC ANALYSIS IN ANSYS (FROM ANSYS 4.4.A. THEORETICAL MANUAL)

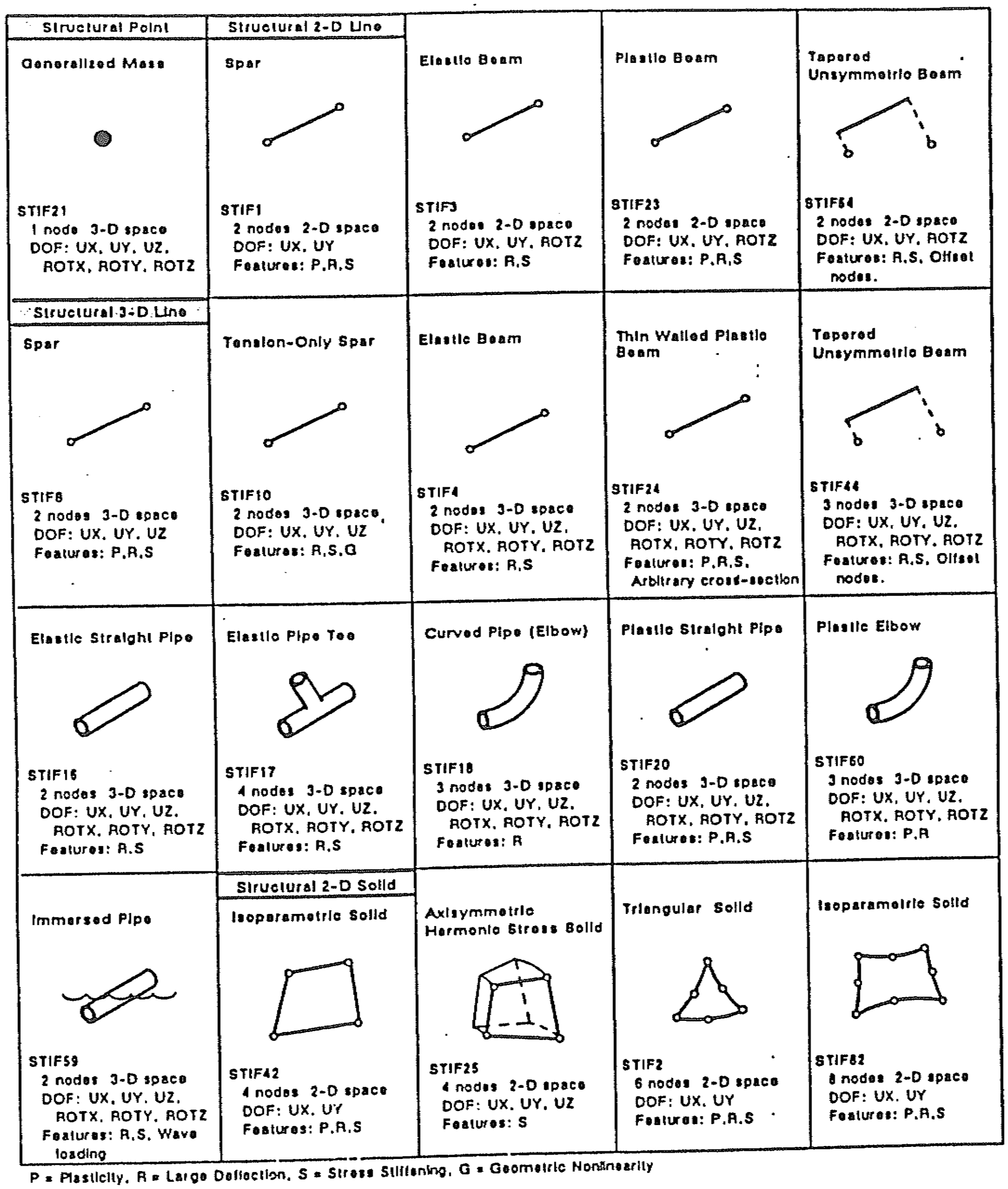

FIG. 5.6. PARTIAL LIST OF ELEMENT LIBRARY IN ANSYS

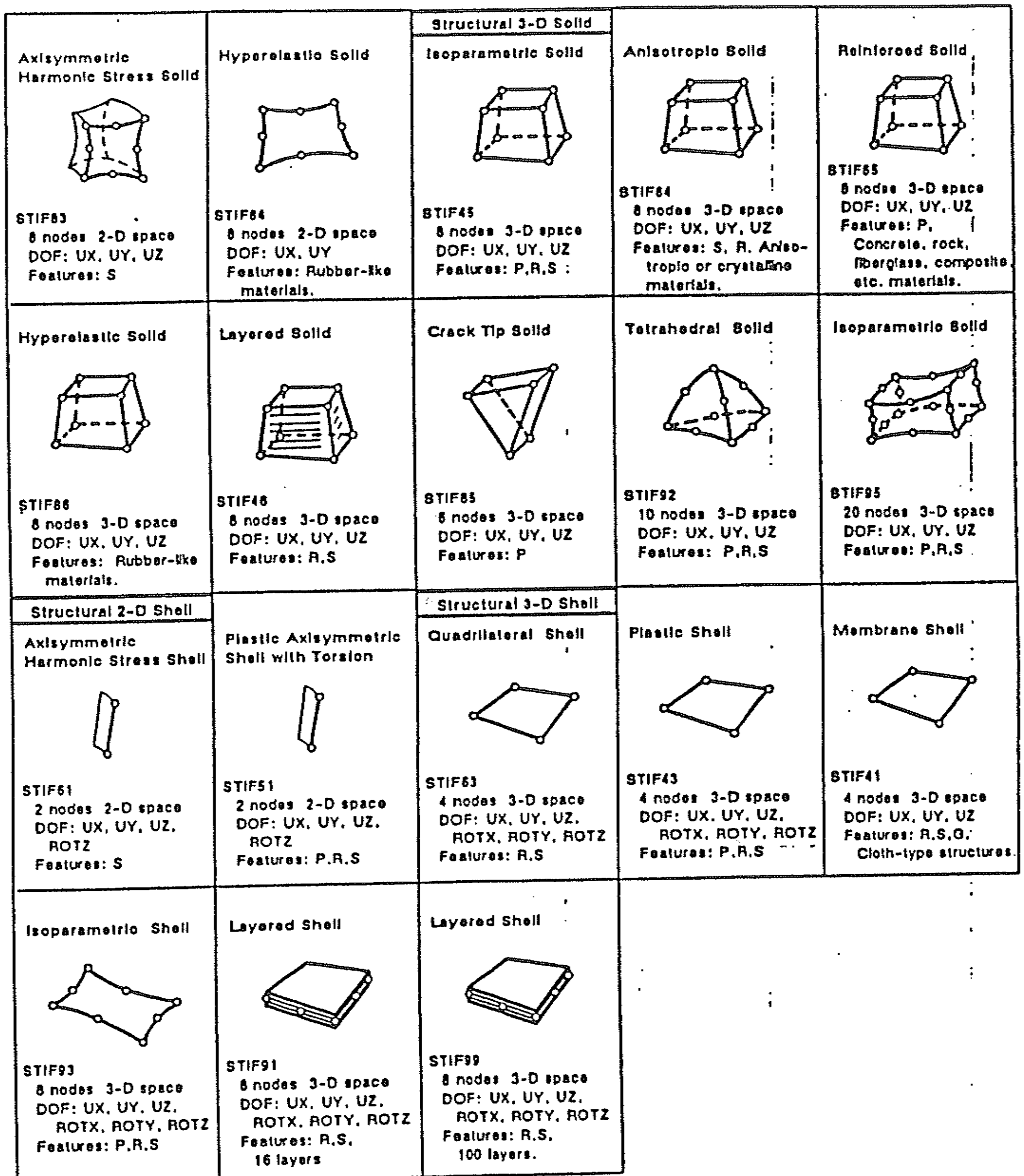

P = Plasticity, R = Large Deflection, S = Stress Stiffening, G = Geometric Nonlinearity

FIG. 5.6.A. PARTIAL LIST OF SOLID (3-D) ELEMENTS IN ANSYS LIBRARY

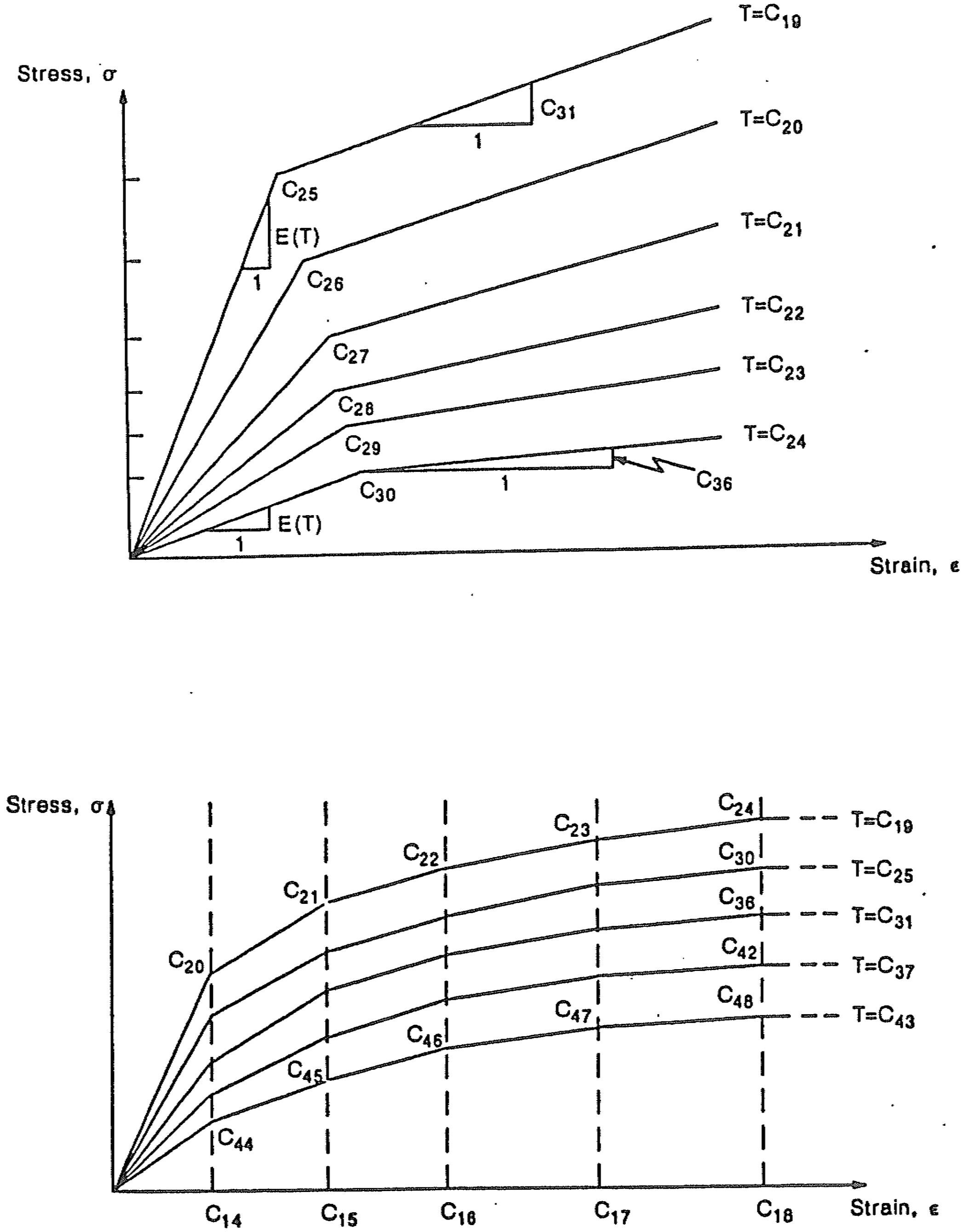

FIG. 5.7. DIFFERENT TYPES OF PLASTICITY HANDLED BY ANSYS

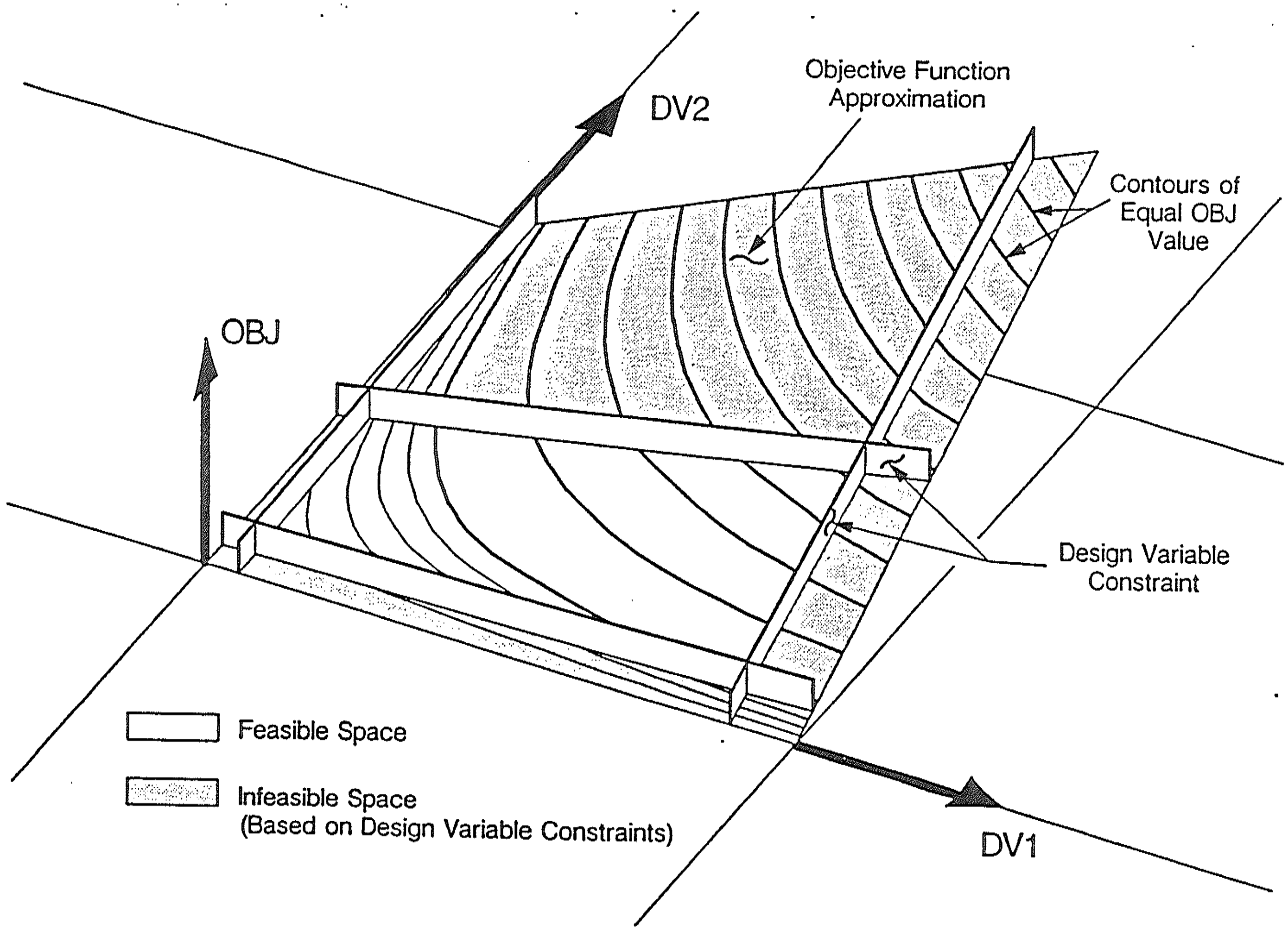

FIG. 5.8. CONCEPT OF OPTIMIZATION IN ANSYS

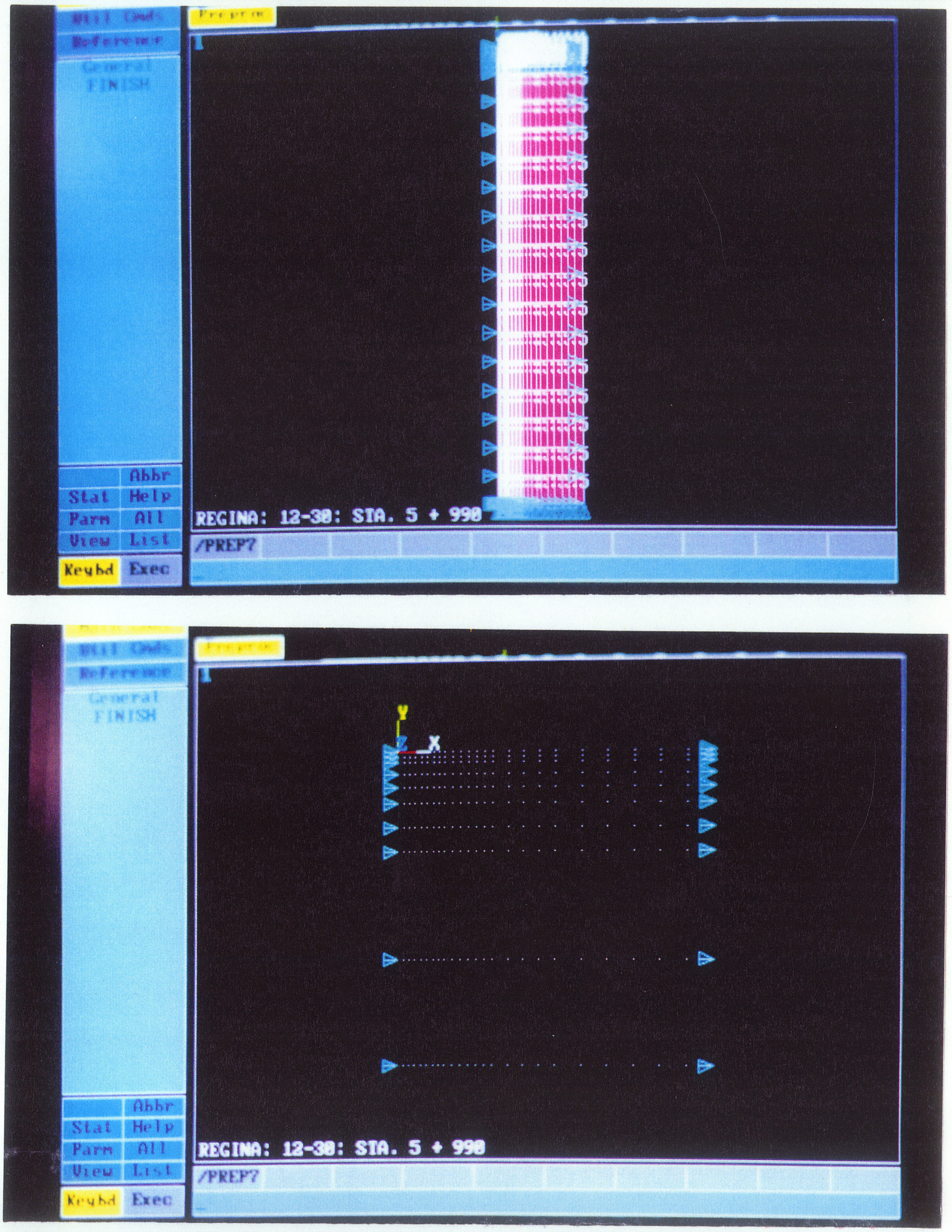

FIG. 5.9-A: PHOTOGRAPH OF MODEL GENERATED BY ANSYS

TOP: GENERAL VIEW OF THE MODEL IN FULL

BOTTOM: GENERATION OF NODES, BOUNDARY AND LOADING CONDITIONS

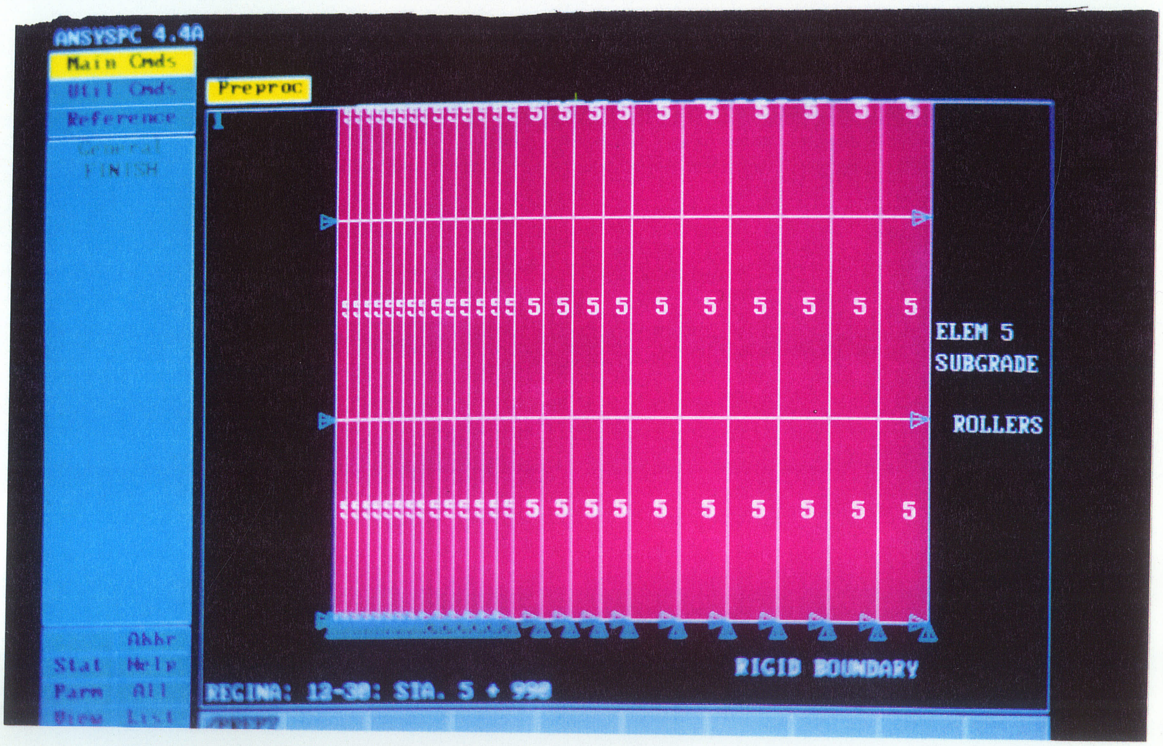

FIG. 5.9-B: ENLARGED VIEW OF MODEL GENERATED BY ANSYS

TOP: TOP PART OF THE MODEL

BOTTOM: BOTTOM PART OF THE MODEL

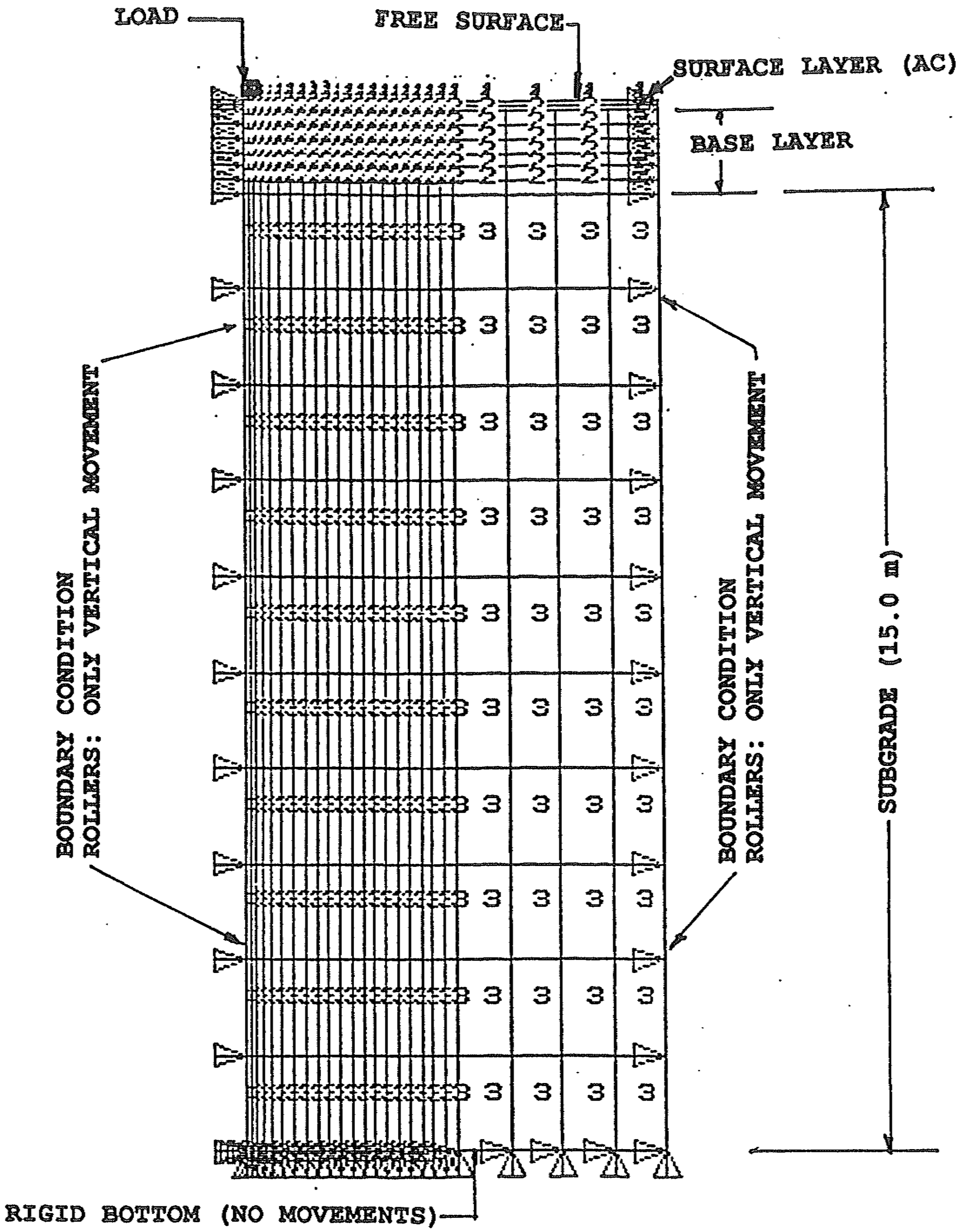

FIG. 5-10. EXAMPLE OF THE FINITE ELEMENT MESH GENERATED BY ANSYS

COMPARISON OF ANSYS SOLUTIONS WITH GERRARD

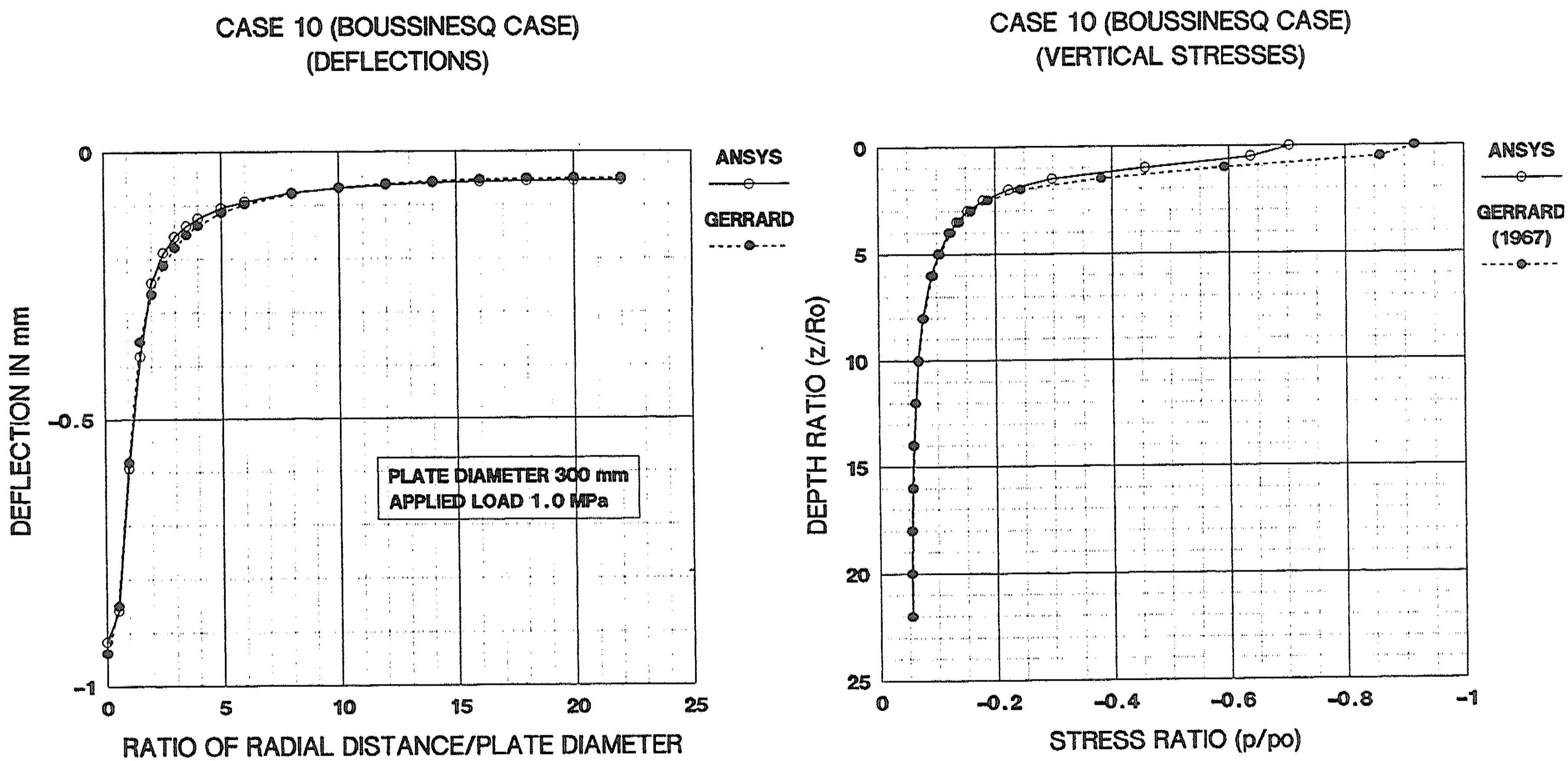

FIG. 5.11.A: VERIFICATION OF ANSYS MODEL

COMPARISON OF ANSYS SOLUTIONS WITH GERRARD

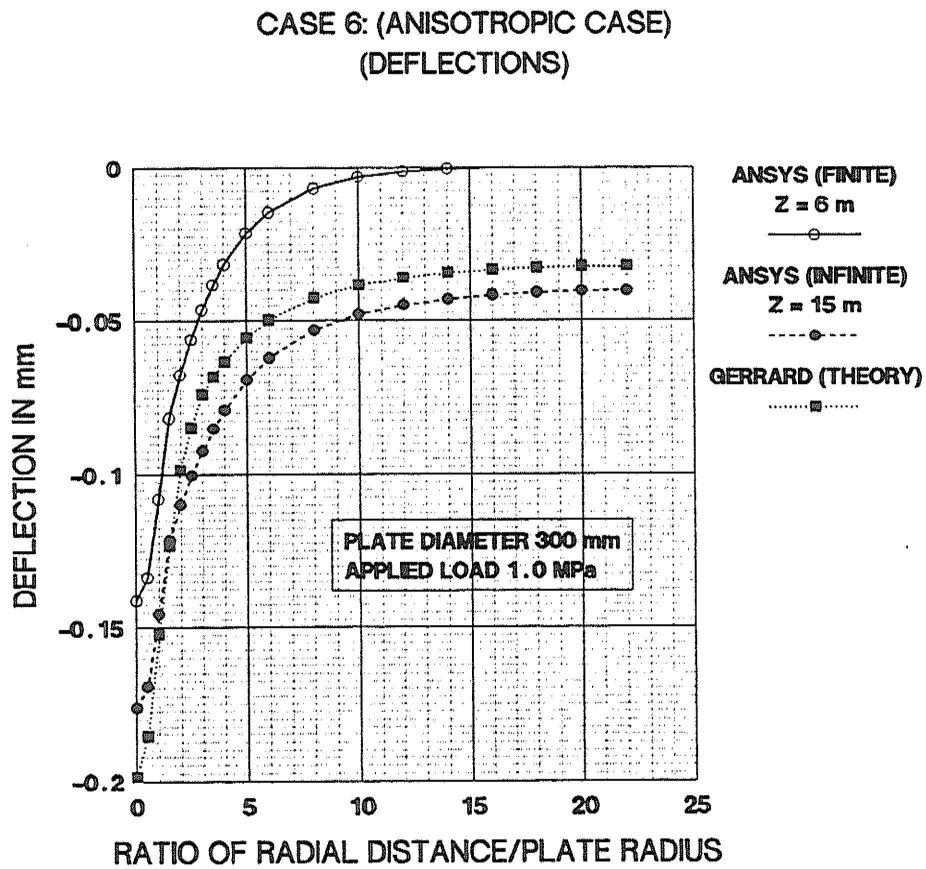

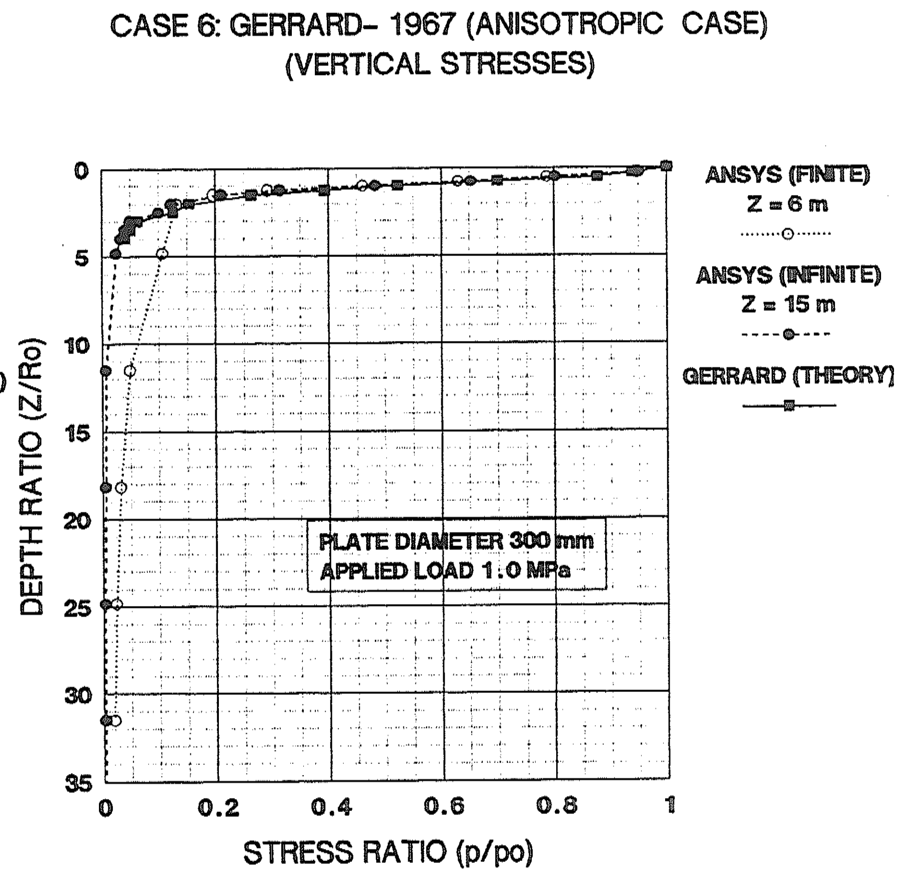

FIG. 5.11.B: VERIFICATION OF ANSYS MODEL

COMPARISON OF ANSYS SOLUTIONS WITH

BHATTACHARYA (1969) AND POULOS & DAVIS (1974)

BOUSSINESQ (POINT LOAD)
(DEFLECTIONS)

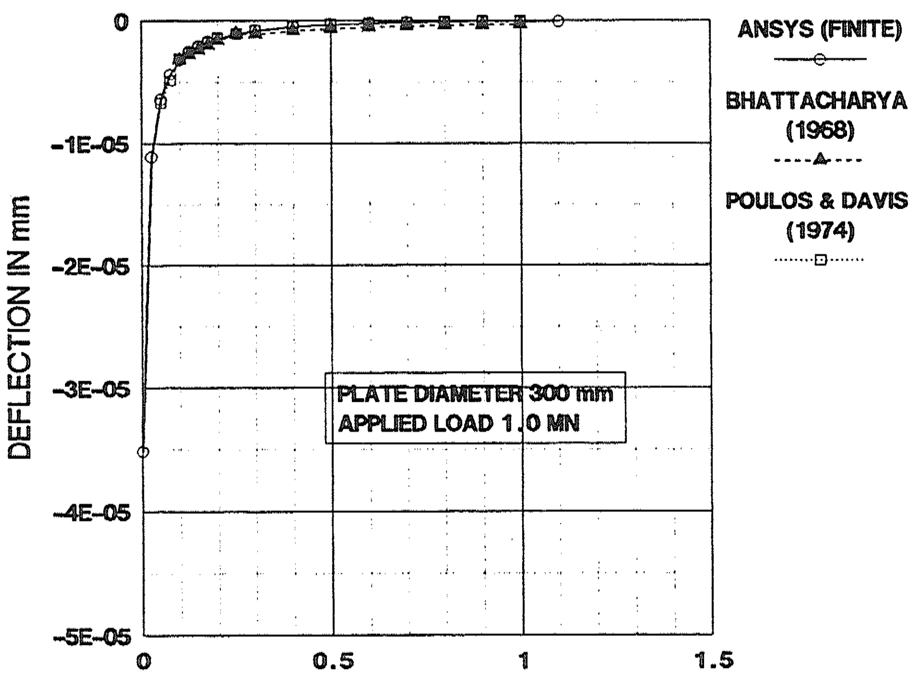

BOUSSINESQ (POINT LOAD)
(VERTICAL STRESSES)

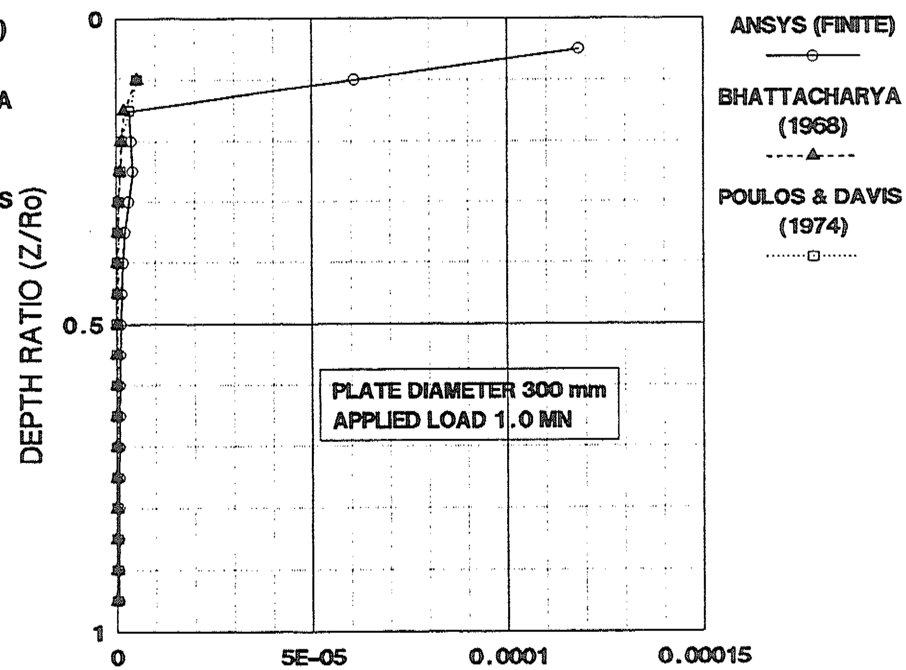

FIG. 5.11.C: VERIFICATION OF ANSYS MODEL

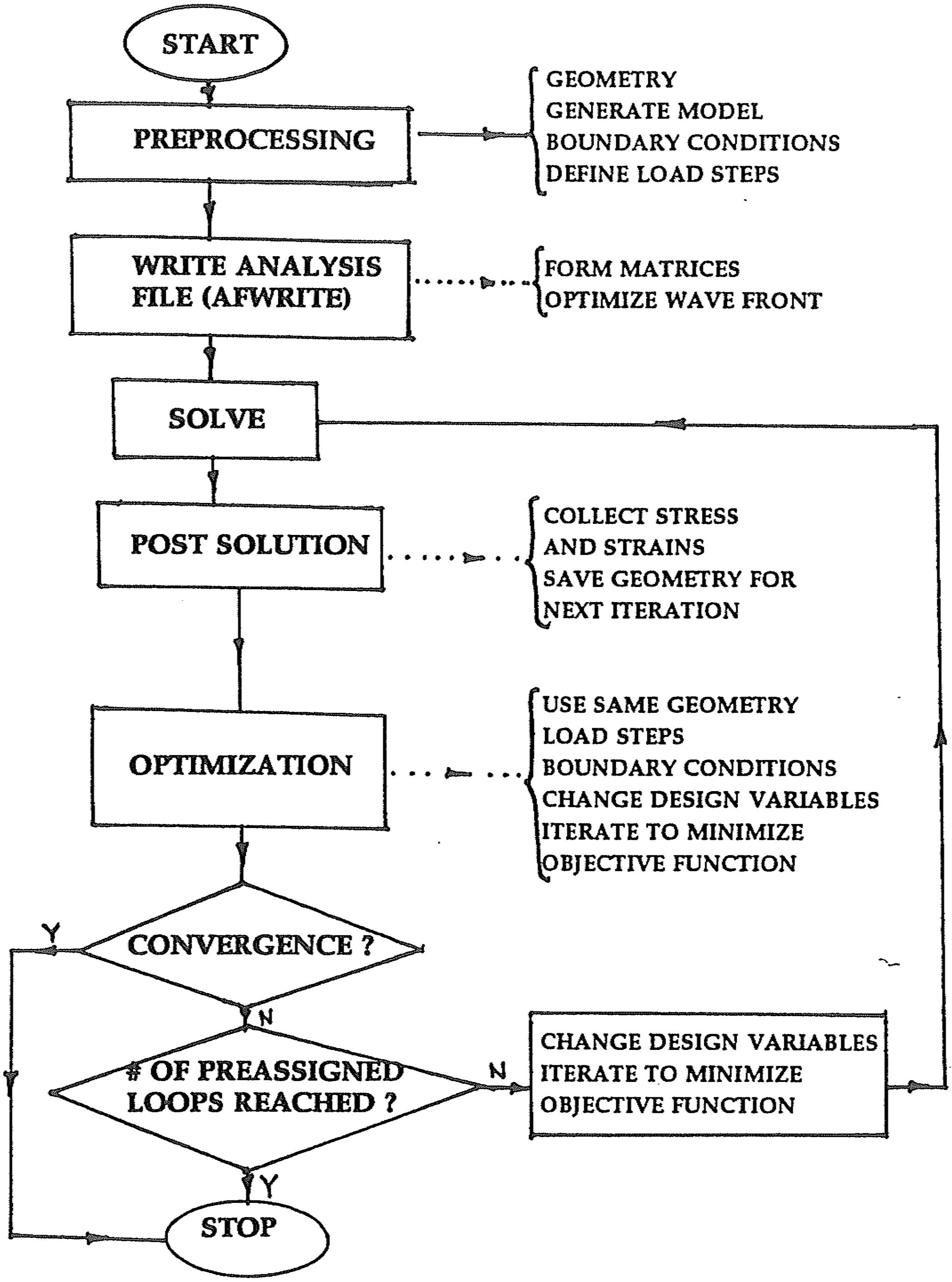

FIG. 5.12: FLOW CHART SHOWING THE STEPS IN PROCESSING BY ANSYS.

CHAPTER SIX

RESULTS AND DISCUSSIONS

6.1 GENERAL

In the previous two chapters the main work undertaken in this investigation was described. Chapter 4 described the field tests and presented the results obtained from this phase. Chapter 5 presented the analysis procedures used to back-calculate the FWD data from the five airport sites. It was mentioned that the analysis was carried out with a general purpose finite element program, ANSYS, available at the University of Manitoba. One of the distinctive features of the analysis was the use of an optimization routine available within the ANSYS program. The features of ANSYS and the optimization program were described. Some examples of input to and output from the ANSYS analysis were presented.

This Chapter presents the selected results of all the analyses for each site and discusses them. Conclusions are drawn from these results. These conclusions are again summarized and presented in a comprehensive form in Chapter 7 together with directions for future research. The volume of data collected from the five airports was quite large. Table 6.1[1] gives the stations tested, types of analyses done and the format of results presented. The results for all the individual stations for different loads at the different sites would form too bulky a volume to be included under one chapter. Therefore, they are bound as Volume 2 of this thesis. In this chapter only some examples and summary sheets are included and will be referenced. For the

---

1 Except for Table 6.3 all results in the form of Tables, charts and graphs are included in the different Appendices to the chapter. A list of Appendices, figures and tables will be found at the end of the chapter.

reader who would like to peruse the detailed results or the mass of raw data these are available in separate volumes.

6.2 GENERAL SCHEME FOR THE PRESENTATION OF ANALYSES AND RESULTS

As shown in Table 6.1 a cross-anisotropic analysis was run on all stations at all sites. The number of optimization loops were between 16 and 50. The program was asked to sort the solutions in an ascending order i.e. from minimum to maximum value of the objective function. From this sorted set, the top five solutions were picked as giving the most probable range of layer moduli for that station. The corresponding deflections and the stress distributions for these five solutions were also printed out. These calculations are repeated for all the three chosen criteria, namely:

1) "AREA" of Deflections Basin;
2) Maximum Deflection;
3) RMS value of Deflections.

Appendix VI-1 shows examples of such results for one arbitrarily selected station each site. Volume 2 of this thesis contains all the results for all the stations at all the sites for all the loading conditions for both isotropic and cross-anisotropic models. From these tables the average moduli are extracted and summarised in another table such as shown in Appendix VI-3. For cross-anisotropic model, in addition to the values of the layer moduli, the anisotropic ratios were also computed and are also presented in the tables in Appendix VI-3. The results are also presented graphically. The following results are shown graphically:

1. Deflection basins by the three criteria for all the stations and for all the load steps.

These are shown both for cross-anisotropic and isotropic models. (Appendix VI-2);

2. Modulus profile (bar charts) for each layer along the runways for both isotropic and cross-anisotropic models and for all load conditions. (Appendix VI-4);

3. For the anisotropic models, the anisotropy ratios in the unbound layers. (Appendix VI-4);

4. Stress distribution under the load at each station and for all loading conditions. Again both isotropic and cross-anisotropic models are presented. (Appendix VI-5).

Finally, the theoretical results are compared with the moduli measured in field with the pressuremeter (for unbound material) or the ones computed from laboratory tests on asphalt cements and using Van der Poel's nomographs. In the following sections, these results are discussed and some conclusions are drawn.

6.3 DISCUSSIONS

6.3.1 Deflection Basins

From the deflection basins presented in Appendix VI-2, one can see that all three criteria predict the deflection basin reasonably well considering the fact that the differences pertain to one tenth to one hundredth of a micron (10^{-3} metre). However, the "Area"-of-the-basin criterion provides the best match between the observed and calculated deflections followed by the RMS value and then the maximum deflection criterion. It is conceded that this is a subjective evaluation of the deflection results. One can numerically evaluate the match and provide an objective legitimacy to the above conclusion. **However, it is submitted that in a great majority of cases, the visual judgement is so convincing that it can be accepted that the "area" criterion provides the best match.** Often, the six curves (five top solutions from the optimization routine, and the actual measured values are indistinguishable from one another even on an enlarged scale. In the previous chapter a theoretical basis for this method of matching calculated and observed deflection basins was advanced. That hypothesis, based on the energy absorbed by the pavement, is strengthened by the fact that the RMS value provides the next-best match. In general, the more points in the deflection basin one tries to match the better will be the fit. While this is done in some programs such as SENOL and ISSEM-4, they do not have an optimization run and hence cannot limit the moduli values to within a plausible range. Such a feasible range can be arrived at by independent measurement of the moduli, from the experience of the engineer or from records of previous performance and evaluation of a pavement in a specific region. One improvement to the method used in this thesis would be to precede the ANSYS analysis with a curve fitting program such as the one used by ISSEM-4. Then the deflection bowl can be defined in tightly specified intervals and hence will more closely represent the energy absorbed. Another improvement would be to measure the deflection basin in different radial directions and use a three-dimensional solid model to calculate the **volume of the basin** instead of the area of the basin. Of course, if axi-symmetry is accepted, then theoretically the area method and the volume method are equivalent.

While in a great majority of cases the match between the observed and calculated deflection basins is satisfactory, particularly with the "Area" method, there are some cases where the theoretical predictions were significantly different from the observed deflections. Fig. 6.1[2] shows an example of such deviation. In almost all of these cases the load was

---

2 All figures and Tables are included as Appendices to each chapter.

dropped in the proximity of a crack as illustrated in Figs. 6.2 and 6.3. As far as the author is aware of, no results have been presented in the literature (to early 1993) indicating the relationship between the distance to the crack and the deviation from elastic layered theory. However, it does not need much convincing to accept that if a significant crack exists within the reach of the deflection basin, then the assumptions of the elastic layered theory are seriously violated. The load transfer across the crack at the surface layer is destroyed or diminished depending on the nature of the crack. Thus the surface layer merely acts as an extension to the loading plate and the underlying base layer is loaded with the full stress on the surface. Since the base material is much weaker than the surface layer there will be significantly higher deflections than if there were no cracks. Obviously the nearer the load is to the crack the more will be the divergence between observed and calculated basins. It is also interesting to note that the major divergence between observed and computed deflections occur only at the nearer sensors and not as much at the farther sensors. Because the effect of load redistribution, the stresses will be maximum near the cracked surface and insignificant or absent in the deeper layers. Hence, one should expect to observe the divergence only at the nearer sensors and much less so at the farther sensors. This is indeed the case in all the cases observed.

Unfortunately, during the test series, both in 1985 and in 1988, detailed notes on the pavement condition, distance of the load from the crack, the nature and width of the crack etc. were not kept except in a cursory way, and a few photographs taken, as shown in Figs. 6.2 and 6.3. Thus an analysis of these sections are not possible now. It is suggested that many of the discrepancies reported in the literature could be due to similar oversight. It is also, therefore, suggested that when testing a pavement with FWD such observation should be included in the input and analysis program should be able to handle such cases. It should be mentioned here that the ANSYS program has what is known as a "gap" element. Incorporation of such elements in the model would permit one to analyze precisely such problems as mentioned above. The gap elements permits the user to assign varying degrees of load transfer across the gap so that one could be able to accommodate cracks of different widths. Incorporation of cracks in the analysis of layered elastic computations may be a worthwhile future research program (e.g. Jung and Stolle, 1992).

6.3.2 Profile of Moduli

Appendix 6-III presents the mean moduli for the top five optimization solutions extracted from Appendix 6-I. These tables also give the average values of the anisotropic ratios for the unbound layers for the cross-anisotropic solutions. These results are represented graphically in the form of bar charts in Appendix 6-IV.

Studying these tables and charts one finds that:

1. At each site, the range of moduli is wide but reasonable. The range could be due to variation in materials, and/or construction. They could be also due to differences in usage. Airport runways, generally, receive selective usage because of the prevailing wind conditions. Thus there are more landings, take-offs and taxiing in some parts than the rest.
2. Some stations show extremely high moduli (between 8,000 MPa and 10,000 MPa) close to the upper limit given to ANSYS. It is submitted that these are not the real values. These sections have likely failed. The pavement is hard and brittle, and acts more like an extension of the loading plate than a continuous layer. ANSYS, in

attempting to match the deflection basin, artificially assigns a high value to one or more layers. Therefore these high values are suspect. This is a drawback with any of the back-calculation methods. With ANSYS this can be avoided by restricting the limiting values within a much narrower range.

3. At Regina, Saskatoon and Thunder Bay the pavement sections were composite. The pavements have been upgraded at various times since late 1940's or early 1950's. Thus one finds stiff or rigid layers followed by unbound layers placed on top of old pavements with stiff of rigid bound layers. However, the modulus calculations show that the older stiff bound layer at depth do not have the same stiffness or rigidity as the newer layers near the surface. It is suggested that the stiffness of a layer depends not only on the material but also on its position in the pavement structure. This was pointed out by Ahlvin in 1974. The author is not aware of previous back-calculations of deflection tests which analyzed this problem. It also suggested that this aspect should be more thoroughly investigated using deflection data on composite pavements. Such analysis will have implications for rehabilitation strategies for older pavements.

4. As a corollary, the unbound material between two layers of bound materials (the so-called "sandwich" construction) shows higher modulus or stiffness because of its confinement (compare Vaswani's result in Fig. 2.34 and the discussions under Section 2.2.2.1 in Chapter 2).

5. The anisotropic ratio of unbound materials varied from less than 1.0 to 3. There are odd stations which showed anisotropic ratios as high as 5. There are no published results of anisotropic ratios in granular base layers in pavements. However, Ingold's

work (Ingold 1979, 1980) with compacted backfills behind retaining walls suggests that this (1.0-3.0) is a plausible range. Lo et al. (1977), Yuen (1976), Graham and Houlsby (1983) and Graham et al. (1989), presented data which would support this range of anisotropic ratio for the soils that formed the subgrade at the five test sites. It is, therefore, submitted that the model presented herein predicted the anisotropic properties of the materials reasonably well.

6.3.3 Stress Distribution

The stresses at the centroid of all the vertical elements under the centreline of the load were calculated for all cases. The results are shown in Appendix 6-I (Tables) and in Appendix 6-II (charts). The stresses are presented as a normalized relationship between stress ratios (p/p_o) and depth ratio (z/r_o), where p is the calculated stress, p_o is the contact pressure at the surface, z is the depth and r_o is the radius of the loaded area. The ratio (p/p_o) is defined as the stress ratio and z/r_o as the depth ratio. Many inferences can be made from these diagrams.

The shape of the curves shows that the model predicts the stress distribution correctly, at least qualitatively. If one accepts that the influence of load can be neglected at depths where p/p_o reaches a value of 0.01, then for the pavements tested in this series, load influence will be felt for depth ratios between 6 and 20. Thus for the pavements tested, the load influence will extend between 3 m and 5 m for the 450 mm plate and between 1 m and 3 m for the 300 mm plate. Since airfield pavements are usually thick, extending to one metre or more, the influence of the light FWD loads with smaller plates might not extend deep enough into the pavement structure.

A more important and perhaps a more surprising result is that the stress distribution diagrams for all the five top optimization solutions from isotropic and anisotropic models practically overlap each other or lie in a very narrow band. In the final analysis, since the performance of the pavements depends on the stresses and strains in the pavement materials one should ask the question:

> "In the light of the results presented herein, is the importance given to the determination of the layer moduli with the high degree of precision in the analysis of pavement by back-calculation of deflection data warranted ?"

Based on the results presented here, the author would like to submit that the current fixation with trying to compute moduli with great accuracy is not warranted. In the same light it appears to be academic and irrelevant whether the layers possess some degree of anisotropy or not. In all cases the stresses in the pavement do not appear to vary significantly. Given this assumption, one can as well use a simple layer elastic model, wherein the layers are elastic, and isotropic. Non-homogeneity, stress dependency and non-linearity were not investigated in this thesis and hence the author cannot comment on these. Perhaps the data should be re-analyzed incorporating these features to see whether any significant effects are shown.

In this thesis, the stress distribution has not been quantitatively verified. Therefore, one does not know from this work whether the predicted stresses are the ones in the pavement layers. This can be verified only with controlled tests with instrumented pavements. Only then the question of required accuracy in back-calculation procedures to determine the moduli can be categorically answered one way or the other. Since the completion of the major part of the analysis for this thesis, the author had the opportunity to verify the model presented, herein, with two instrumented pavements in Thompson, Manitoba, Canada. The results confirm the validity of the ANSYS model. Therefore it is suggested that, in addition to the research efforts to better understand the material properties, there is an urgent need to test instrumented pavements so that a realistic layered elastic model for pavement can be presented with all the relevant factors properly included.

6.3.4 Correlation of In-situ Material Properties with Computed Properties

This investigation started with an objective of correlating back-calculated moduli to in-situ moduli measured by other independent means. The independent means for unbound material was to use the PENCEL pressuremeter. For bound materials (particularly asphaltic concrete), the Van der Poel-McLeod nomographic approach was used. In order to use the method, asphalt viscosities from recovered cores were determined and the Shell bituminous chart constructed for each station. From this, the bitumen stiffness and finally the mix stiffness were determined. These tests were described in Chapter 4 and the results were presented there. In this chapter those results are compared with ANSYS computed layer moduli.

6.3.4.1 Correlations for Bound Materials (Asphaltic Concrete)

Fig. 6.4 shows the linear regression of computed and "measured" asphaltic concrete moduli for the isotropic model while Fig. 6.5 shows the same results for the cross-anisotropic moduli. Before discussing the results, two points need to be clarified. First the "measured" moduli in Fig. 6.4 are actually the moduli obtained using McLeod's nomographs from measured bitumen viscosities. The moduli were not measured directly. Secondly it should be remembered that for both isotropic and cross-anisotropic models, the bound layers were always considered isotropic. Therefore, the comparisons are made here only to establish which model is likely to give a better correlation with the nomographic moduli. Table 6.2

shows the regression equations and the coefficient of correlation between the moduli at the different sites.

The results show at best some ambiguous trends and at worst no good correlations. Looking at Fig. 6.4, there appears to be two groups of trends. The first one concerns the pavements in Brandon, Regina and Thunder Bay. The second comprises St. Andrews, Saskatoon and the combined data from all the sites. The first group exhibits a positive relationship i.e. there is a positive slope for the regression line. They also show coefficients of correlation which, though not very high, are still fair. The intercept in these graphs have no real meaning. The slope of these lines vary between 0.2 and 0.3 indicating that the ratio of "measured" moduli to the computed moduli lies between 3 and 5. The nomographic moduli are based on dynamic tests done in the Shell Laboratories in Amsterdam in early 70's. Therefore, these modulus values represent the *dynamic response* of the pavement. On the other hand the back-calculation results are based on *static analysis.* The frequency, loading time, or the dynamic character of the loading by FWD is not considered in the model or the computations. Therefore, the "resilient modulus" is really a *static modulus*. Thus the slope of the line or the ratio of the two moduli can be looked upon as the dynamic effect of the loading. The ratio of dynamic to static moduli is generally reported in the literature, to be in this range.

Therefore, it is submitted that for the elastic layer analysis of pavements, the moduli of bound layers can be taken to be 0.2 to 0.3 times the modulus that would be computed by using McLeod's nomograph and from bitumen viscosities determined in the laboratory.

However, Figs. 6.4 and 6.5 present another problem. In Fig. 6.4 St. Andrews shows a negative trend while Saskatoon shows no trend at all. In Fig. 6.5 the trends shown in

Fig. 6.4 are reversed. Brandon, Regina and Thunder Bay show negative relationships with a correlation coefficient practically equal to zero while the other two show a positive relationship with low R^2 values. In both cases when one combines all data there is no relationship between the two modulus values. These observations lead to the following conclusions:

1. The data cannot be combined. There are individual site characteristics that should be accounted for in trying to arrive at a correlation between "measured" and computed values of asphalt moduli.
2. The individual site characteristics are the age of the pavement, the fatigue consumed at the date of testing, and the initial mix properties.
3. The crack density on the surface has an influence on the modulus values and should be somehow considered in the analysis.

Table 6.3 on the following page summarises these factors for the individual sites. As one can see from Table 6.3 the pavements which showed better correlations in Fig. 6.4 are the younger pavements while the ones which did not are the older pavements. It is suggested that the older pavements have fatigued, do not show resilience and elasticity, and the surfaces behave more like brittle and rigid materials; they are heavily cracked so that the application of layered elastic theory is questionable (cf. for example Jung and Stolle, 1992). Because of the brittleness and rigidity of the surface they are better modelled as a cross-anisotropic system rather than an isotropic model.

TABLE 6.3 Individual Site Characteristics That Influence Resilient Moduli

Site	Date Built[1]	Date Tested	Age Years	Crack Rating[2]
BRANDON	1983	1985	2	2/1, 2/1
REGINA	1979	1988	9	3/2, 3/2
ST. ANDREWS	1968	1988	20	4/3, 4/3
SASKATOON	1974	1988	14	4/2, 4/2
THUNDER BAY	1984	1985	1	2/1, 2/1

Note: 1. Date built is the date of last major rehabilitation

2. Crack Density is the condition rating taken from Transport Canada's annual pavement rating, for the year of testing. Rating gives Extent/Severity

It is, therefore, suggested that a back-calculation model should be able to consider the age and condition of the pavement in its algorithm. This would mean that one should be able to quantify these factors so that they can be incorporated in the model. This thesis does not offer any suggestion how this should be done. But it appears that this could form the basis of further research.

6.3.4.2 Unbound Materials

The moduli of the unbound materials were measured with the PENCEL pressuremeter. With unbound materials one should differentiate between the granular materials (base and subbase) and the native subgrade materials. The granular materials are processed materials, processed to conform to rigid specifications. In the region where the test pavements are situated, except Thunder Bay, the material is basically crushed limestone. In Thunder Bay the rock is generally igneous and hence could be granitic.

The subgrade materials, on the other hand, are natural materials. As shown in Table 4.1 (Chapter 4) these varied widely. The results of the gradation analyses on the unbound materials were presented in Chapter 4 (Figs. 4.18 to 4.22 and Tables 4.2 to 4.6).

A. Granular Materials

Appendix 6-VI contains the summary of results showing the correlation between the measured and computed values of the different layer moduli. Figs. 6.6 and 6.7 show these results in graphic form. Fig. 6.6 show the results from all the sites pooled together for both isotropic and for cross-anisotropic models. Fig. 6.7 shows the results for the individual sites. It is felt that the type of presentation made in Fig.6.7 will distort the true picture because the test points are all clustered in a narrow range. This should be expected because in any one project, the material will have properties within a narrow range subject only to minor variations during construction. However, when pooled together they would present a wider range and would permit a more meaningful interpretation. Therefore, the following comments will be based on the composite data, Fig. 6.6 only. Considering that the granular base is a processed material conforming to rigid specifications this is be permissible.

Examining Fig. 6.6 one sees immediately, that there is significant scatter of data about the suggested regression lines. The correlation factor (R^2) is not high. However, the R^2 value for the isotropic model is still acceptable permitting the conclusion that there exists a correlation between the pressuremeter moduli and the computed moduli.

The above observation leads the author to suggest that:

1. Despite the fact that the calculation shows that the anisotropy ratio for the granular base ranged between 1 and 3 an anisotropic model for the layered elastic system is not warranted.
2. One frequent criticism that the pressuremeter measures the horizontal modulus while the isotropic model for pavements uses the vertical modulus appears to be answered. Regardless of what the pressuremeter measures, the cyclic modulus appears to correlate well with the vertical modulus computed by the isotropic model.
3. Since the results and discussions presented in the previous section show that a simple isotropic model is just as good as any other model, the pressuremeter modulus can be used for the design and evaluation of pavements using the layered elastic model.

Having suggested these inferences from the results presented, it still behooves the author to explain the large unexplained variations. Therefore, the following explanations are offered.

In unbound materials a simple linear regression between two sets of modulus values is generally inadequate because, the mechanical properties of such materials depend upon many factors. Some more significant of these factors are:

1. Gradation;
2. Percent passing the 75 micron sieve;
3. Percent crushed faces;
4. Water content; and
5. Sum of the principal stresses.

Therefore, the regression analysis should be done as a multivariate analysis rather than a simple linear regression as done here. This thesis does not present such a correlation - this is left for future analysis. The data from the tests presented here should be re-analyzed or additional controlled tests might be done to establish the significance of these factors.

Another factor which could have distorted the results is the uncertainty that the pressuremeter was always in a single type of material. Though cores were taken and depth of construction carefully measured before inserting the pressuremeter, many factors such as the age of the pavements, possible intermingling of layers, migration of fines over the years and simply not having adequate depth to install the pressuremeter are beyond the control of the testing personnel. Thus it is not unlikely that the pressuremeter was standing in two layers or was measuring a composite modulus of two starkly contrasting layers, such as a crushed gravel base and a pit-run granular subbase. However, in the analysis these were assumed to be neatly separated layers. Thus some variations would be always present. However, it is hoped that such unavoidable errors contribute only to a small part of the variations.

The physical meaning of the parameters of the regression equations is not quite clear. The intercept of the equation corresponds to zero measured modulus, i.e. zero pressuremeter modulus. This would intuitively indicate that this should be related to the P_0 value in the pressuremeter test. Since P_0 in base and subbase layers is induced mainly by placing methods, it is suggested that these are the lateral residual stresses in the base layer. The slope of the line is simply the ratio E_y/E_r where, E_y is the vertical modulus computed from the model and E_r is the horizontal modulus measured. Thus this ratio will be the inverse of the anisotropic ratio as defined in Chapter 5. The regression equation shows that this ratio is 2.21, which is close to the average ratio of anisotropy computed by the model. It will be noticed that the author has refrained from calling this the ratio of dynamic to static modulus, unlike in the case of bound materials. This is because both the computations and the pressuremeter tests deal with the static case and therefore it might not be appropriate to call this the ratio of dynamic to static moduli.

B. Subgrade Materials

The evaluation of the results for the subgrade materials followed the same pattern as for the granular base or for the surface layer. Regression analyses of data were attempted both on the basis of individual sites as well as for pooled data from all sites. The analyses were carried out for both isotropic and cross-anisotropic models. The results are shown in Figs. 6.7 and 6.8.

It is clear from Fig. 6.7 that when data is analyzed for individual sites no correlation can be found. While the charts show some regression lines their R^2 value is too low to suggest any real correlation. That is not to say that there is no correlation, but only suggests that the range of points for any one site is too narrow. Looking at Fig. 6.7 one can fit many other lines in all possible directions to obtain better R^2 values than given on that figure. Since one is considering a relatively short total distance of not more than 2 km at any one site, the subgrade is bound to be relatively uniform and the points will tend to cluster around, in a narrow range. Furthermore, having only five or six points for regression may not provide meaningful results.

For these reasons Fig. 6.8 was prepared where all the data from all the sites were pooled. Now more acceptable trends are indicated both for the isotropic and for the cross-anisotropic models. The isotropic model shows, once again much better correlations than the cross-anisotropic. The R^2 value of 0.53 for the isotropic case is, though not very high, satisfactory when one considers that many other factors should enter the equation. As in the case of granular base materials, other factors such as gradation, percent finer than 75 micron size, the uniformity coefficient, in-situ moisture content and density, and the stress ratio might have to be considered. Therefore, a multivariate analysis rather than a single-variable analysis is indicated. This thesis does not present such an analysis. This will be left to future research.

It is even more difficult to attach any physical meaning to the regression parameters in this case than in the case of granular base. The slope, which should be still defined as the anisotropic ratio, does not correspond to the anisotropic ratios reported in the literature for these subgrades.

6.4 PRACTICAL APPLICATIONS

One of the objectives of this thesis was to suggest a finite element model of the layered elastic system which could be used in a typical design office to evaluate and design a pavement. The previous three chapters explained the philosophy and underlying concepts of the ANSYS model for this purpose. This chapter presented the results demonstrating the validity of the proposed model. The author considers himself extremely fortunate that just when the major part of the analyses was completed, Transport Canada had a requirement to rehabilitate certain airfield pavements giving him the opportunity to demonstrate the practical application of the results derived from this thesis.

What was more fortunate, was the fact that two of these pavements were instrumented to measure actual stresses in the various layers. These instrumented pavements provided the opportunity to compare the measured and predicted stresses in the various layers. The pavements were:

1. Runway 18-36 in Flin Flon, Manitoba; This was an interesting example because

steeply dipping bedrock was at a shallow depths. The pavement could be modelled with stepped bedrock profile and successfully analyzed. Fig. 6.9 shows the correlation between measured and computed deflection basins.

2. Taxi A in Thompson, Manitoba where a stone column test section was installed in an attempt to stiffen a very weak subgrade; ANSYS could model this very heterogeneous pavement and demonstrated that the stone columns were actually acting as discreet elements and were punching into the soft subgrade (Fig. 6.10).

3. Runway 05-23 in Thompson, Manitoba where a composite econocrete-asphalt pavement test section was built to avoid excessive deformations; Design of the econocrete-asphaltic concrete pavement was done using the optimization technique suggested in this thesis.

   The Taxiway and the runway in Thompson were instrumented with stress cells in the different layers; The correlations between measured and computed deflections as well as stresses are shown in Fig. 6.11 through and 6.14.

4. Runway 13-31 in Winnipeg International Airport in Manitoba where the runway showed premature rutting just two years after a major rehabilitation; ANSYS model showed that the stresses in the subgrade are much higher than permissible. The model was also used to design possible rehabilitation options (Fig. 6.15).

It is intended to discuss these in any greater detail in this thesis. These evaluations and designs have been reported to Transport Canada in various internal reports between 1990 and 1993.

6.5 SUMMARY

This chapter has presented the analysis of data presented in Chapter 4 (Field Testing) and in Chapter 5 (Analysis of Deflection Data). The appendices to this Chapter contain typical results from each site. The complete data is presented in a second volume of this thesis.

The results show that the "area" of the basin criterion for back-calculating the deflection data gives by far the best match between the observed and computed deflection basins. They also show that the FWD tests should identify the pavement condition, proximity of the test points to cracks etc., because these have been shown to influence the shape of the basin. The simple layered theory cannot handle such situations. It is therefore suggested that the current models should be expanded or enhanced to consider such cases.

The analysis in this thesis made use of an optimization technique in the ANSYS finite-element program. The average of the modulus values from the top five solutions from the optimization routine was taken to represent the most probable value of the layer moduli. Yet the moduli varied over a range. Even though there was quite a variation in the moduli, the stress distribution in the pavement was not materially affected. In most cases the stresses fell within a very narrow band. Since ultimately the stresses and strains are of prime importance for pavement performance, the analysis raises the question as to how much effort one should spend in determining the modulus values very accurately.

Moduli of the different layers in the pavement were also determined independently and compared to the computed values. The correlations were done by means of simple regression as a first step. This established that the measured and computed moduli have a fair correlation, with R^2 values generally in the range of 0.55 to 0.6. While this range for R^2 is not high, other factors which should enter into the equation were discussed. Thus multivariate analysis was suggested. Moduli of unbound layers can be correlated to the unload-reload moduli determined by the PENCEL pressuremeter.

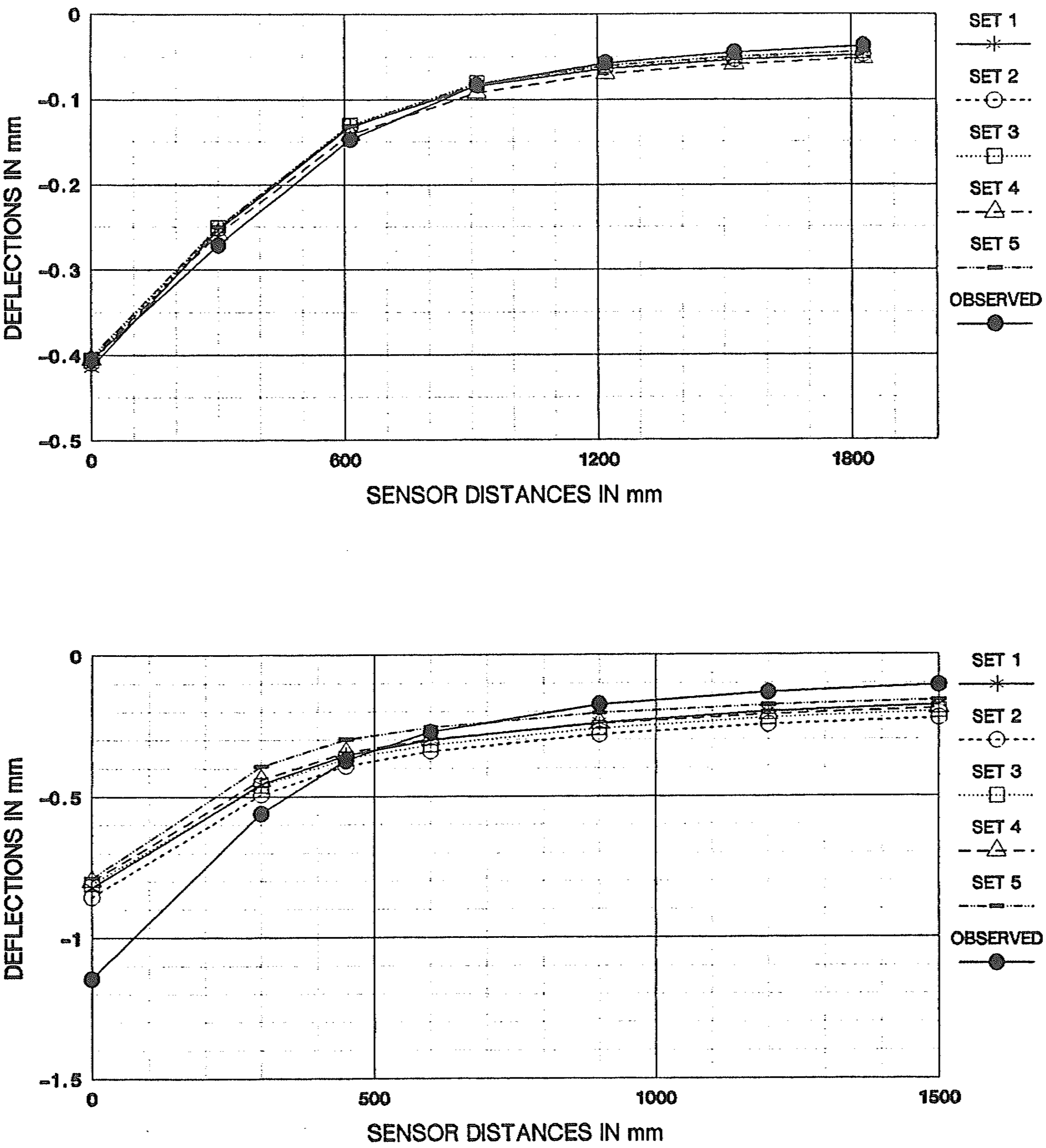

FIG. 6.1: EXAMPLE OF GOOD AND BAD MATCH BETWEEN COMPUTED AND OBSERVED DEFLECTION BASINS

FIG. 6.2. LOAD APPLICATION AT OR NEAR CRACKS COULD BE THE CAUSE OF POOR MATCH SHOWN ON FIG. 6.1(b)

(TOP: ST. ANDREWS: BOTTOM: SASKATOON)

FIG. 6.3. LOAD APPLICATION AT OR NEAR CRACKS COULD BE THE CAUSE OF POOR MATCH SHOWN ON FIG. 6.1(b) (SASKATOON)

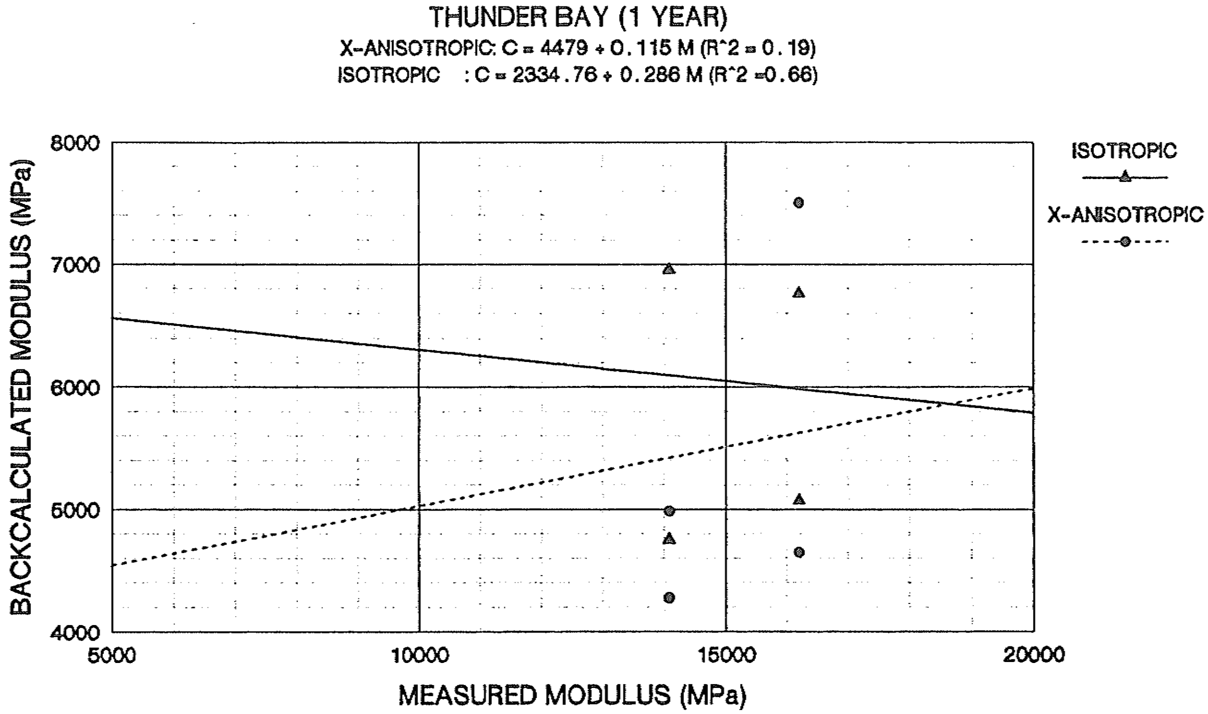

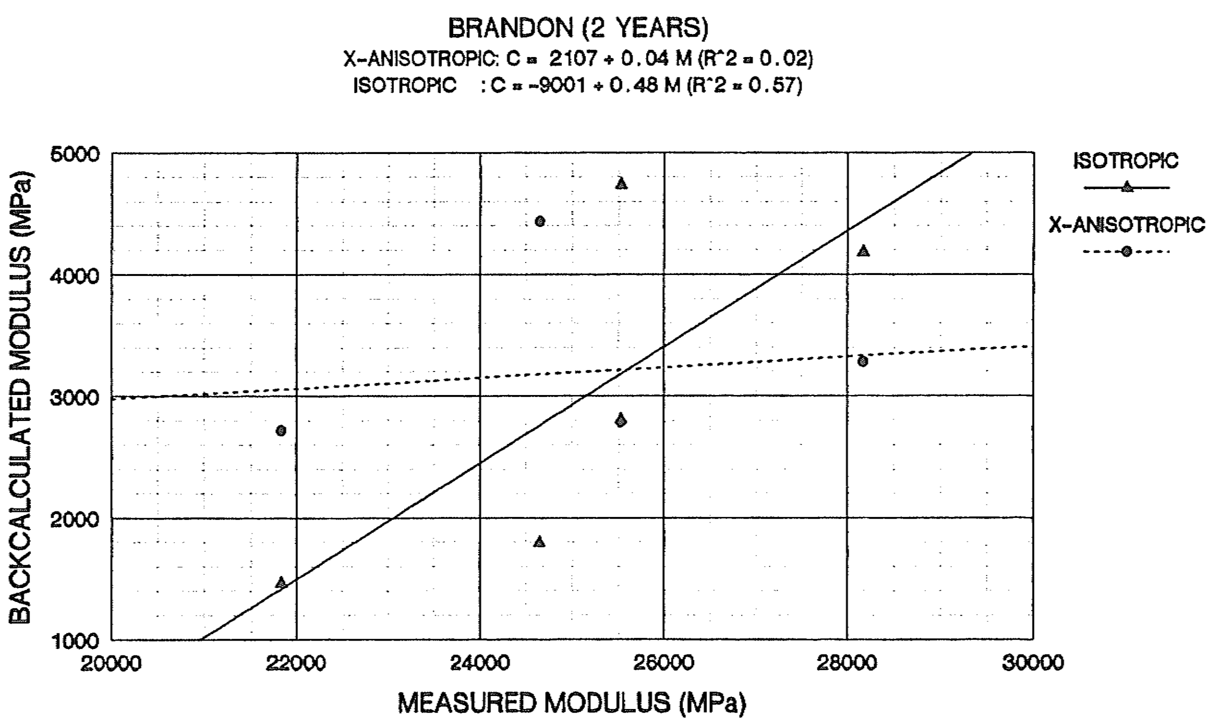

FIG. 6.4.A. CORRELATION BETWEEN MEASURED AND COMPUTED ASPHALTIC CONCRETE MODULI (THUNDER BAY AND BRANDON)

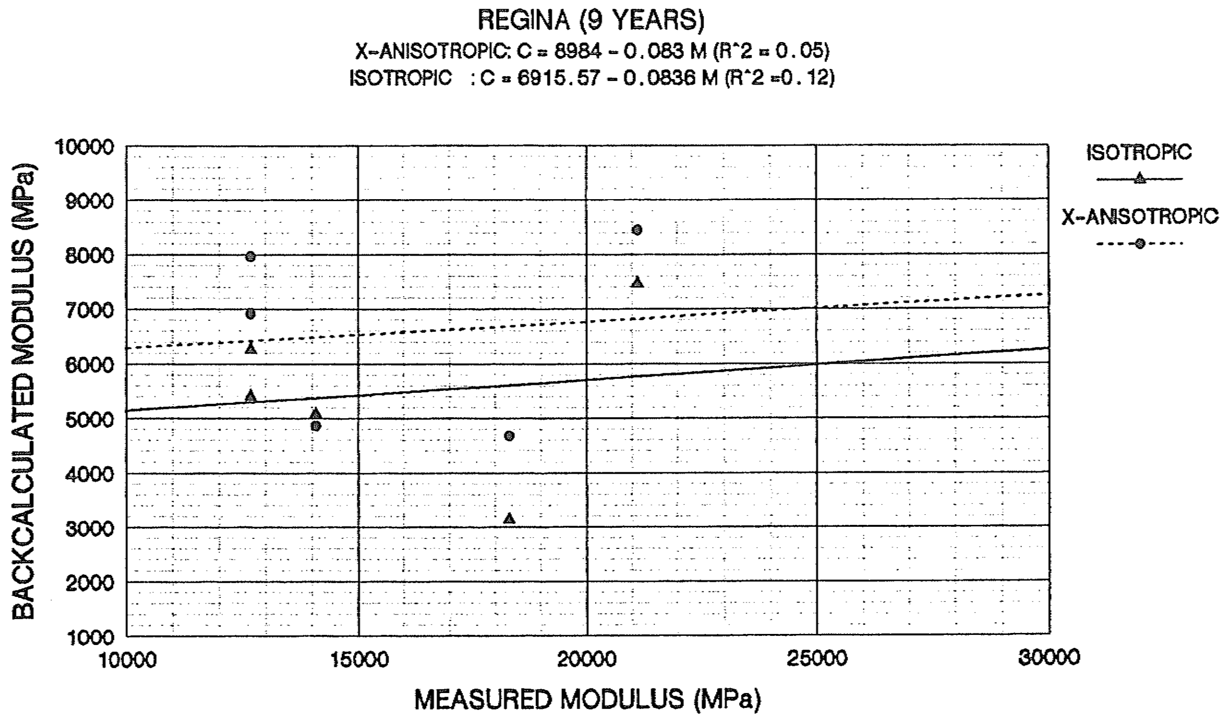

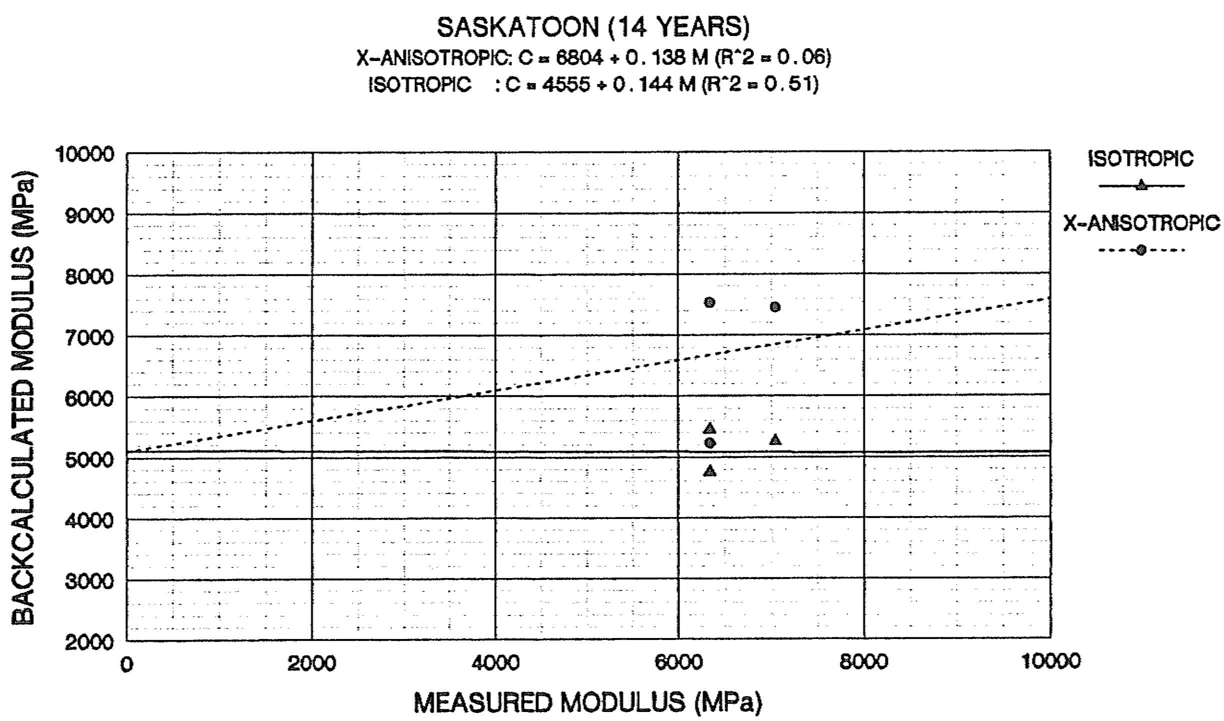

FIG. 6.4.B. CORRELATION BETWEEN MEASURED AND COMPUTED ASPHALTIC CONCRETE MODULI (REGINA AND SASKATOON)

ST. ANDREWS (20 YEARS)
X-ANISOTROPIC: C = 2519.73 - 0.482 M (R^2 =0)
ISOTROPIC : C = 4708.01 - 0.014 M (R^2 =0.45)

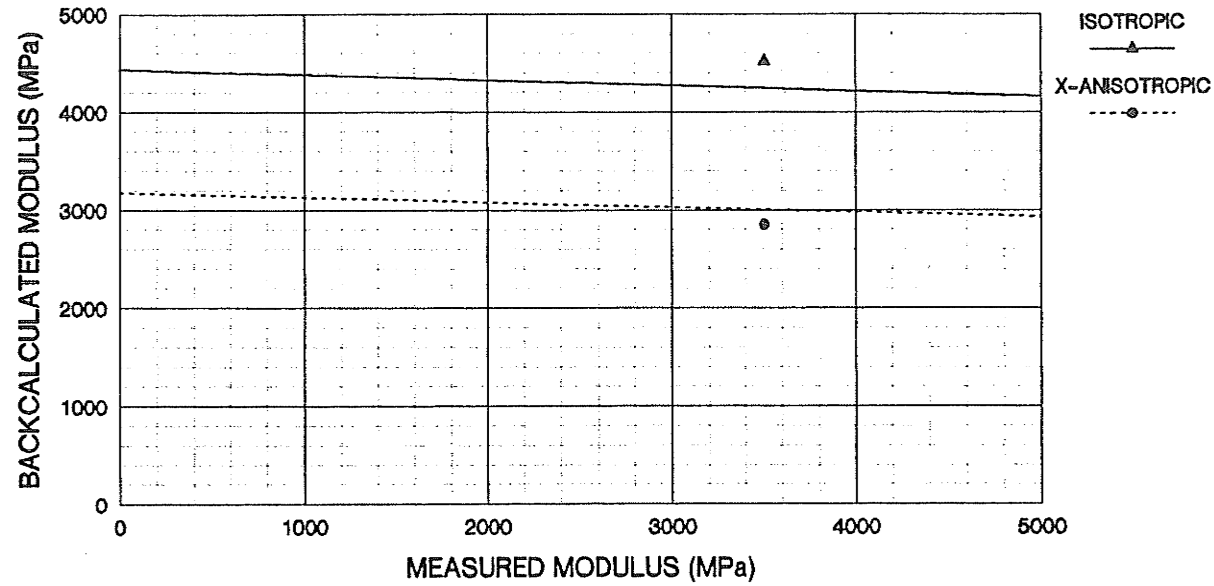

ALL DATA
X-ISOTROPIC: 5667 - 0.061 M (R^2 = 0.07)
ISOTROPIC : 6706 - 0.097 M (R^2 = 0.09)

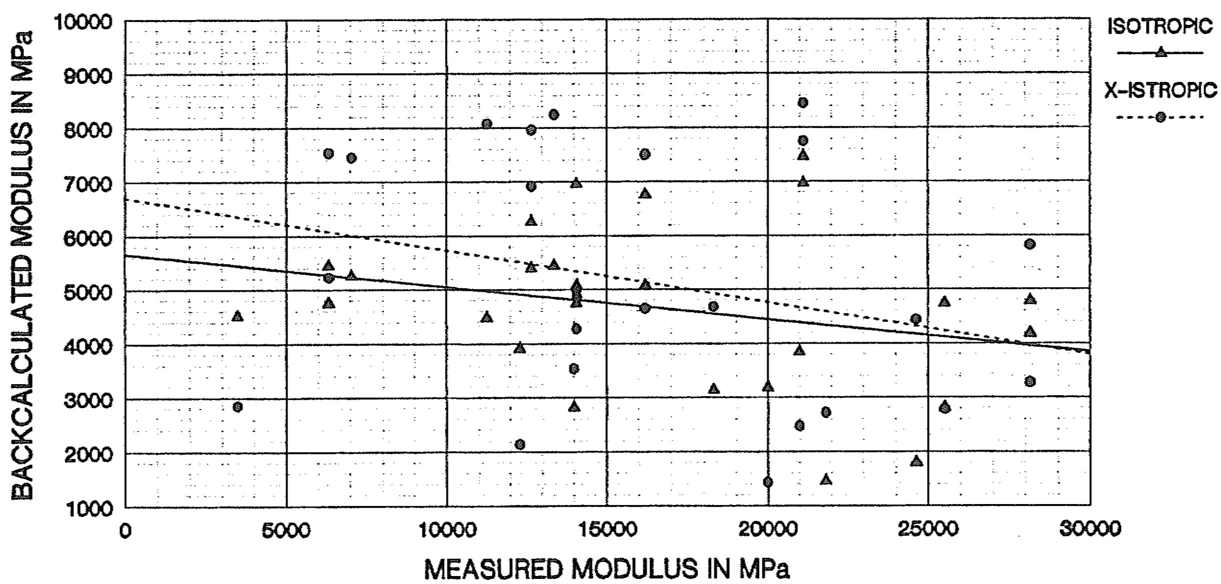

FIG. 6.4.C. CORRELATION BETWEEN MEASURED AND COMPUTED ASPHALTIC CONCRETE MODULI (ST. ANDREWS AND COMBINED DATA)

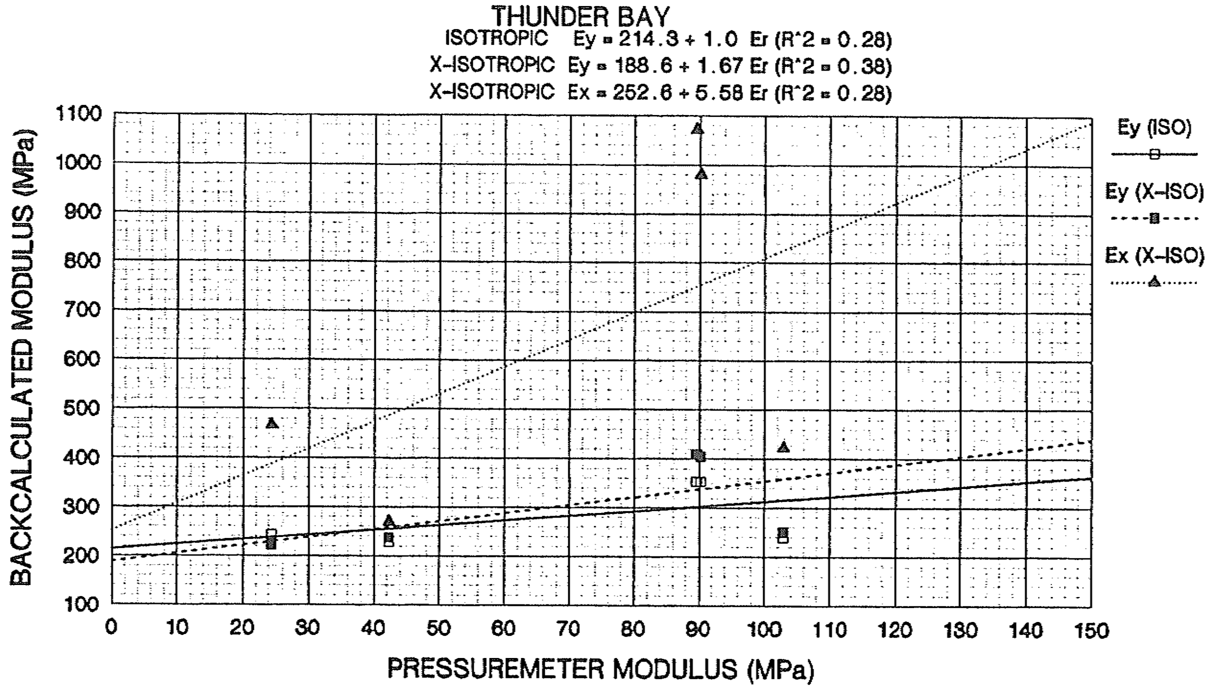

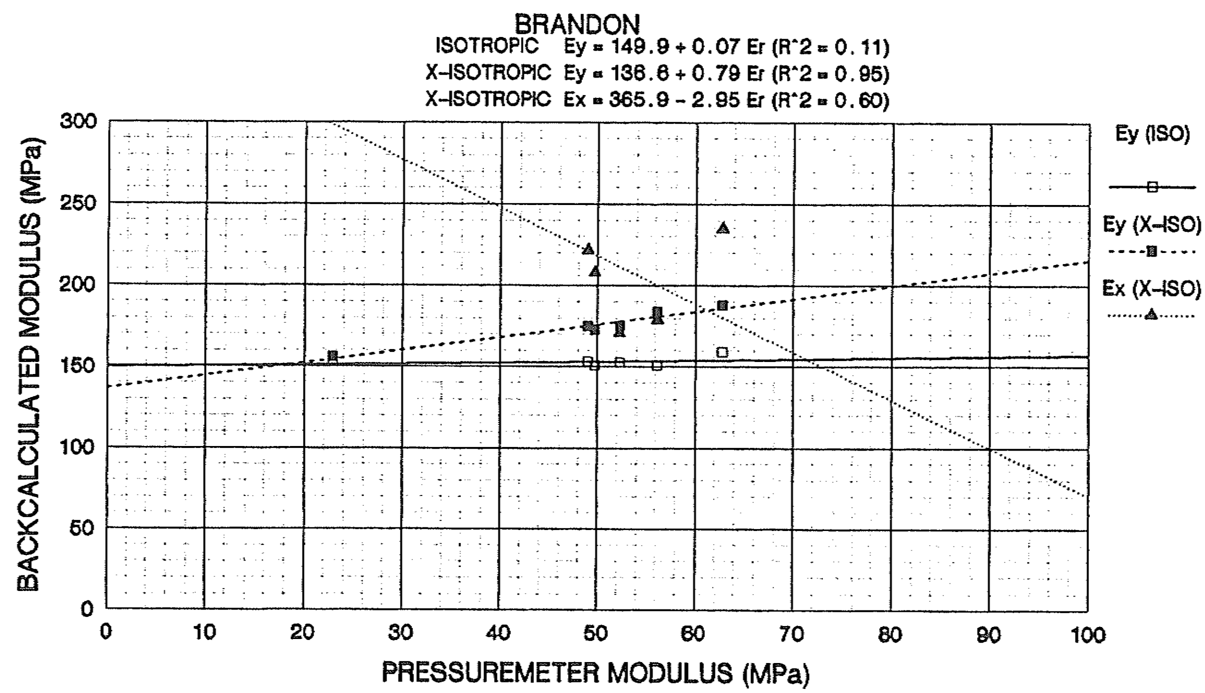

FIG. 6.5.A. CORRELATION BETWEEN MEASURED AND COMPUTED GRANULAR BASE MODULI (THUNDER BAY AND BRANDON)

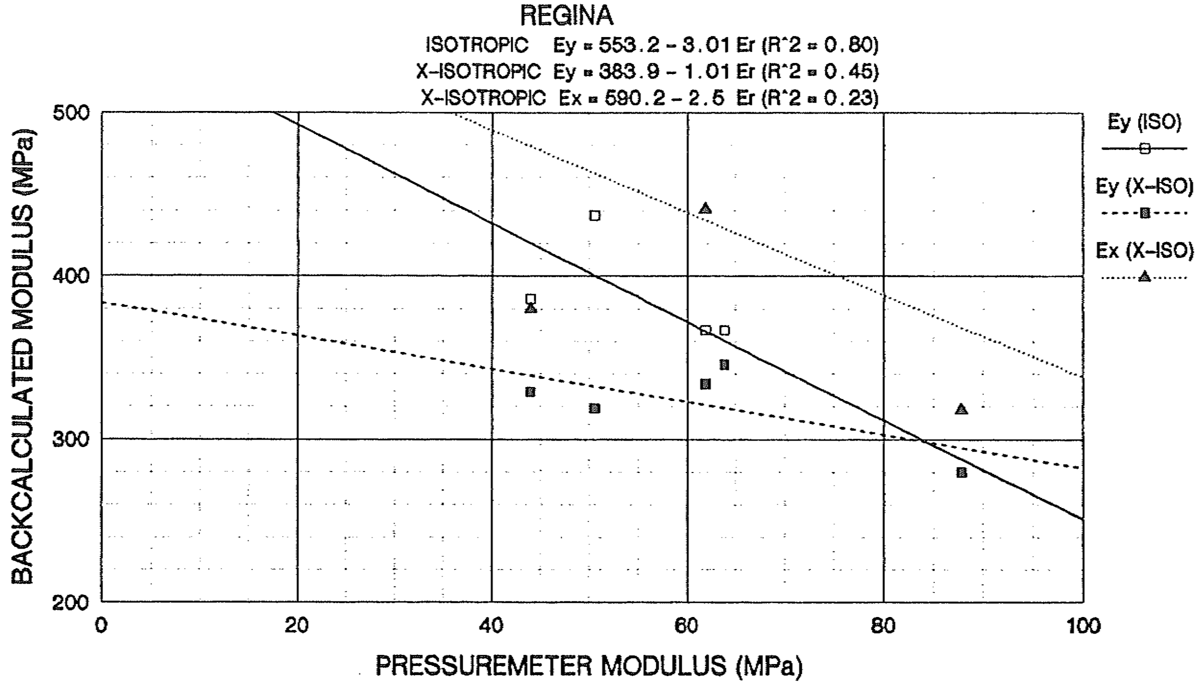

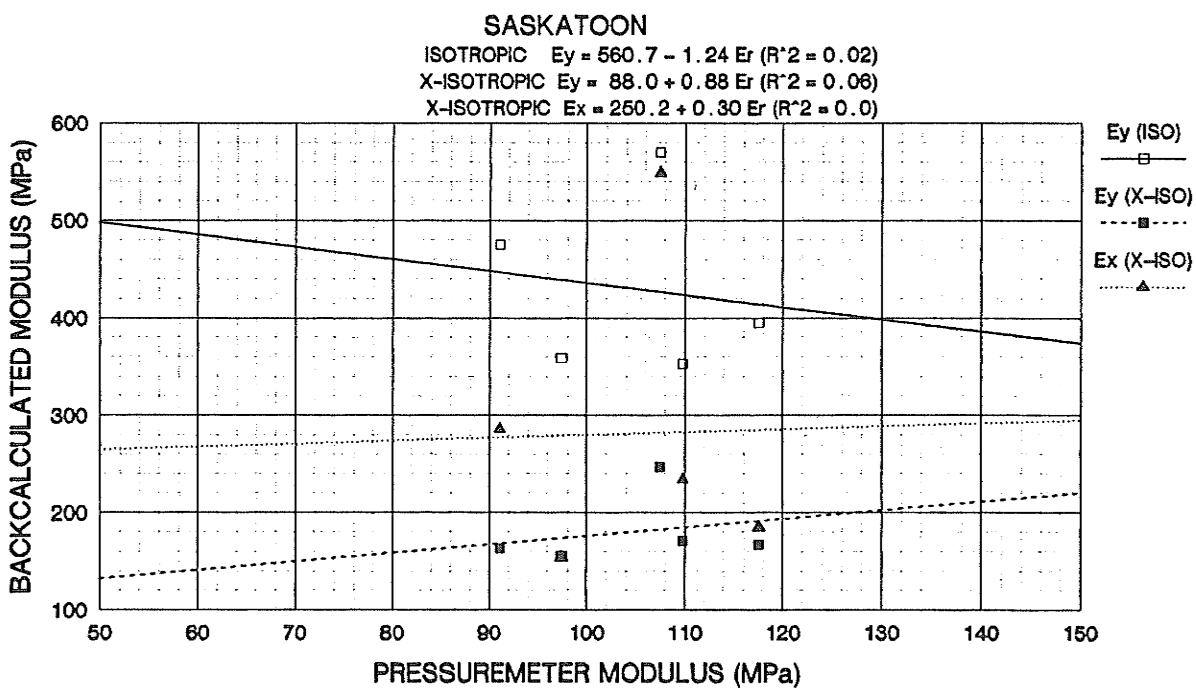

FIG. 6.5.B. CORRELATION BETWEEN MEASURED AND COMPUTED GRANULAR BASE MODULI (REGINA AND SASKATOON)

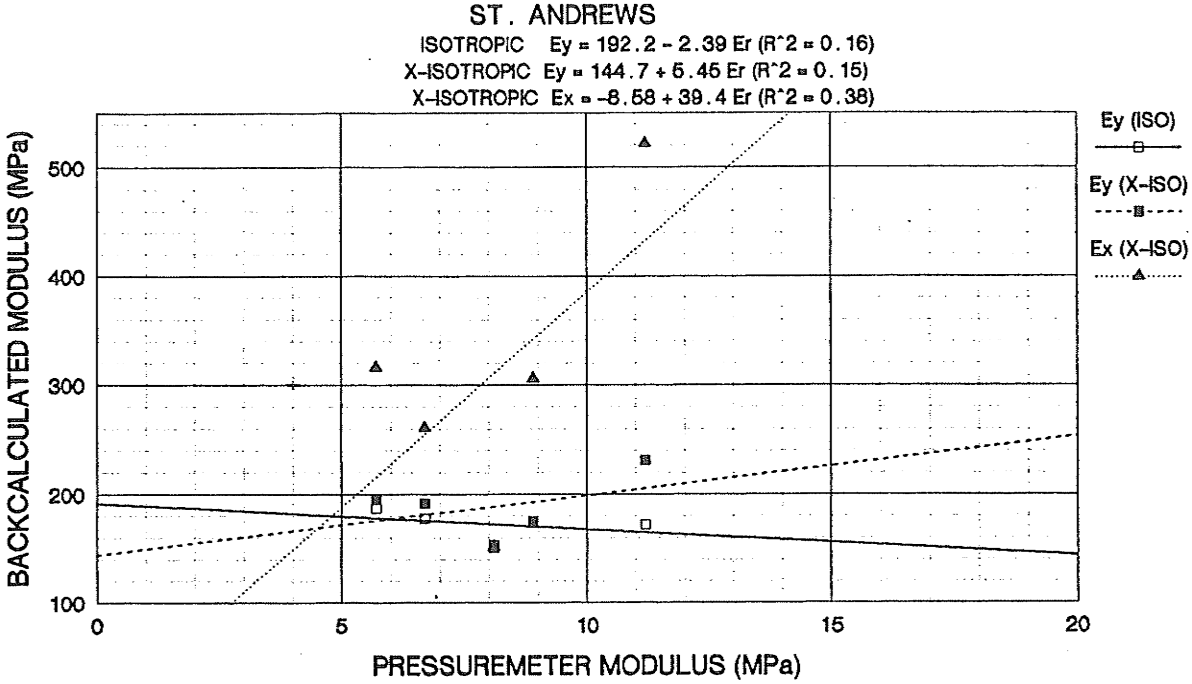

FIG. 6.5.C. CORRELATION BETWEEN MEASURED AND COMPUTED GRANULAR BASE MODULI (ST. ANDREWS)

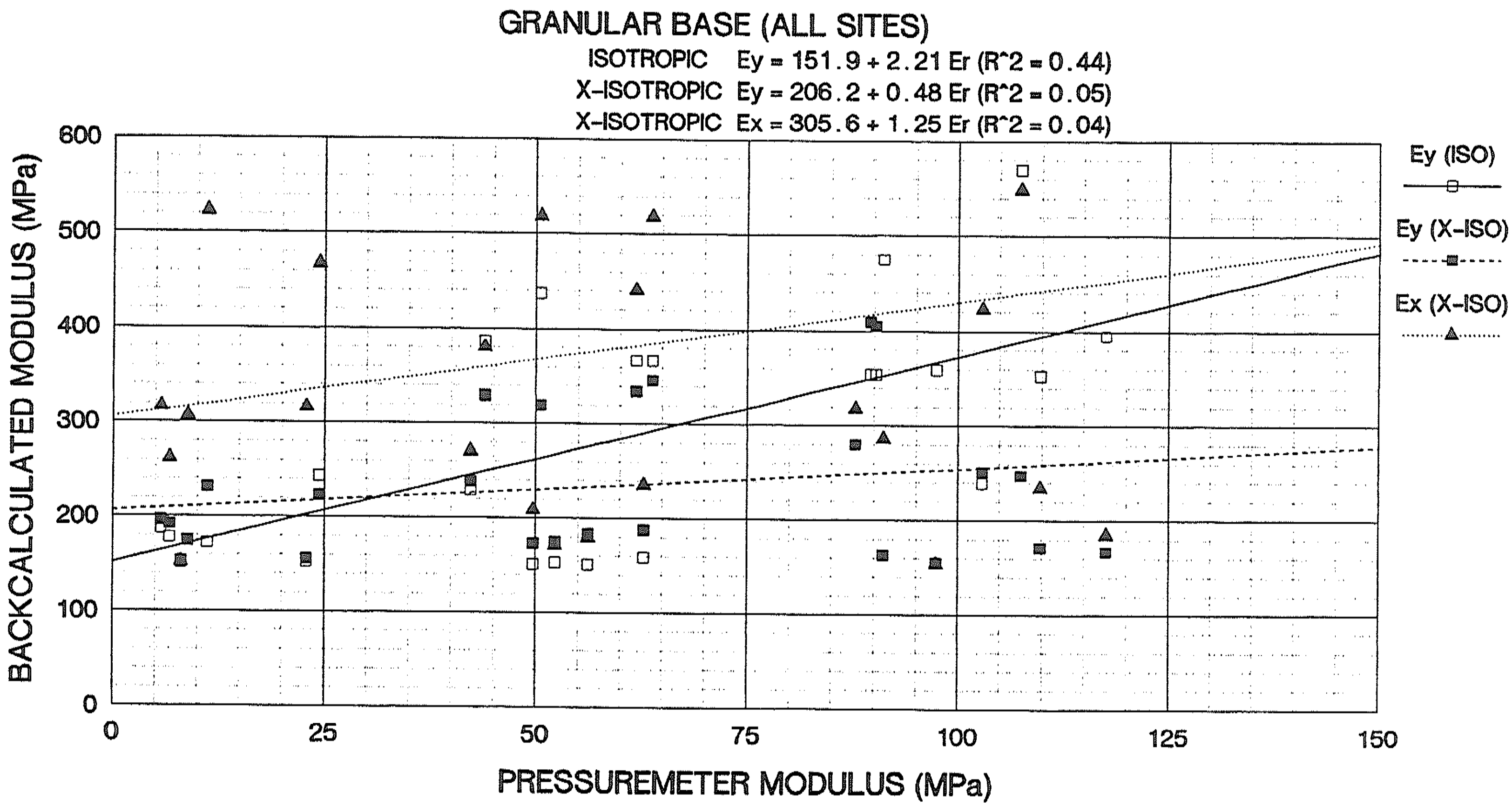

FIG. 6.6. CORRELATION BETWEEN MEASURED AND COMPUTED GRANULAR BASE MODULI (COMBINED DATA - ALL SITES)

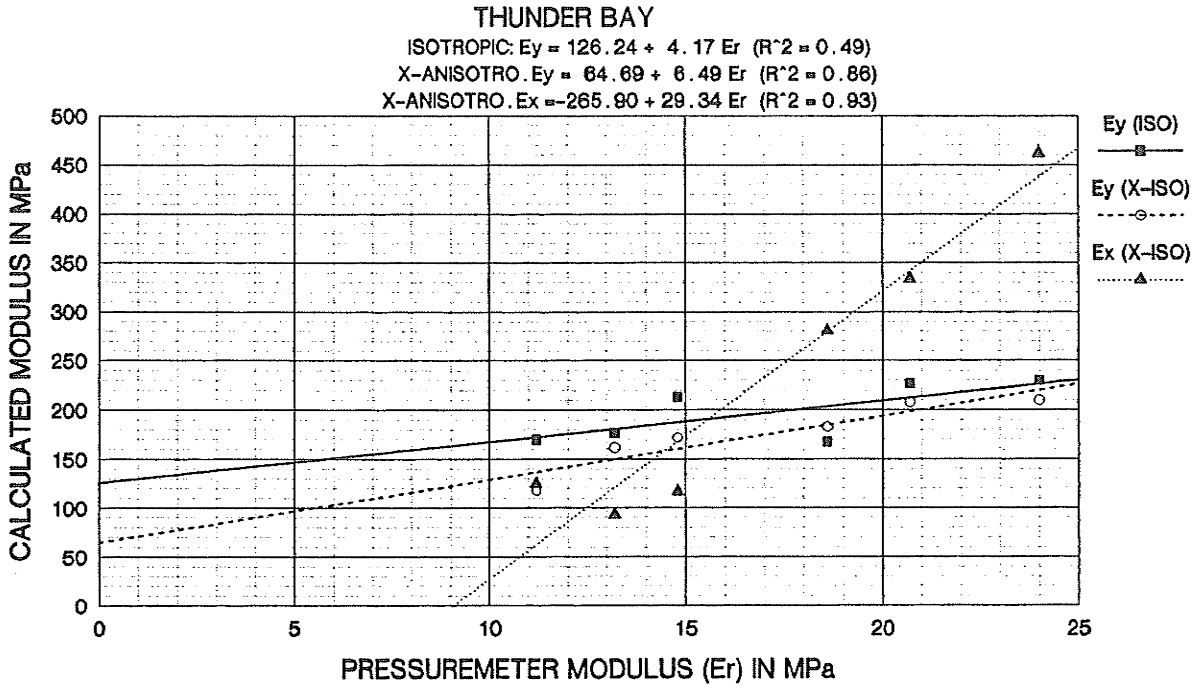

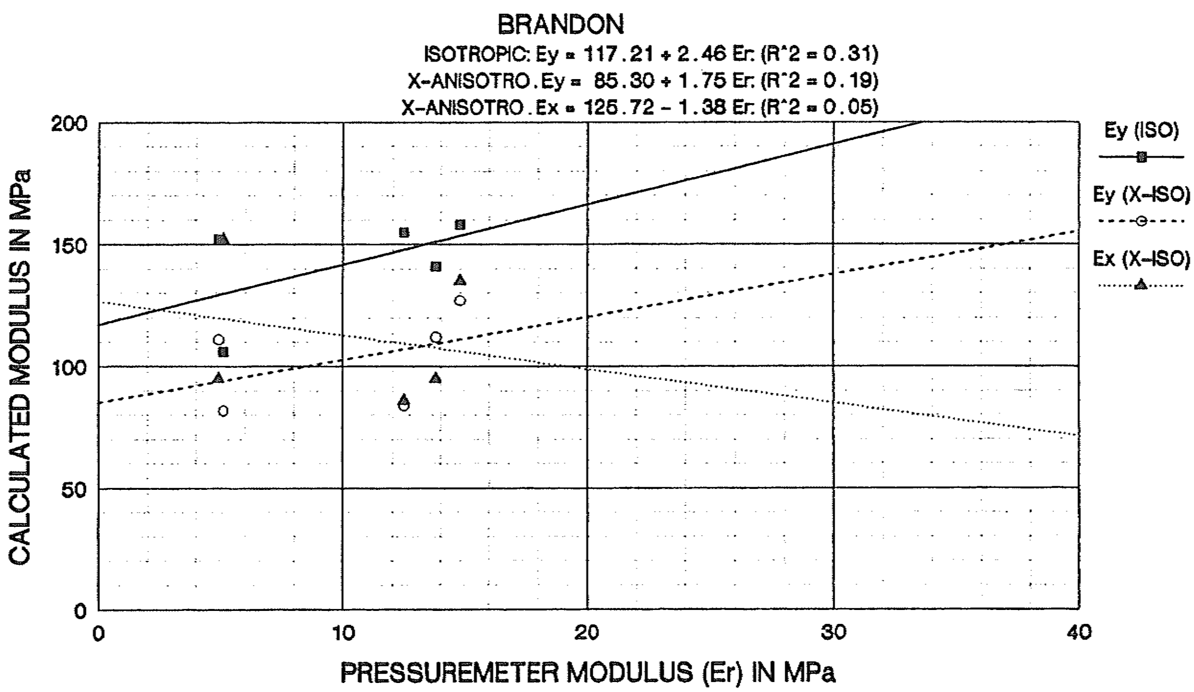

FIG. 6.7.A. CORRELATION BETWEEN MEASURED AND COMPUTED SUBGRADE MODULI (THUNDER BAY AND BRANDON)

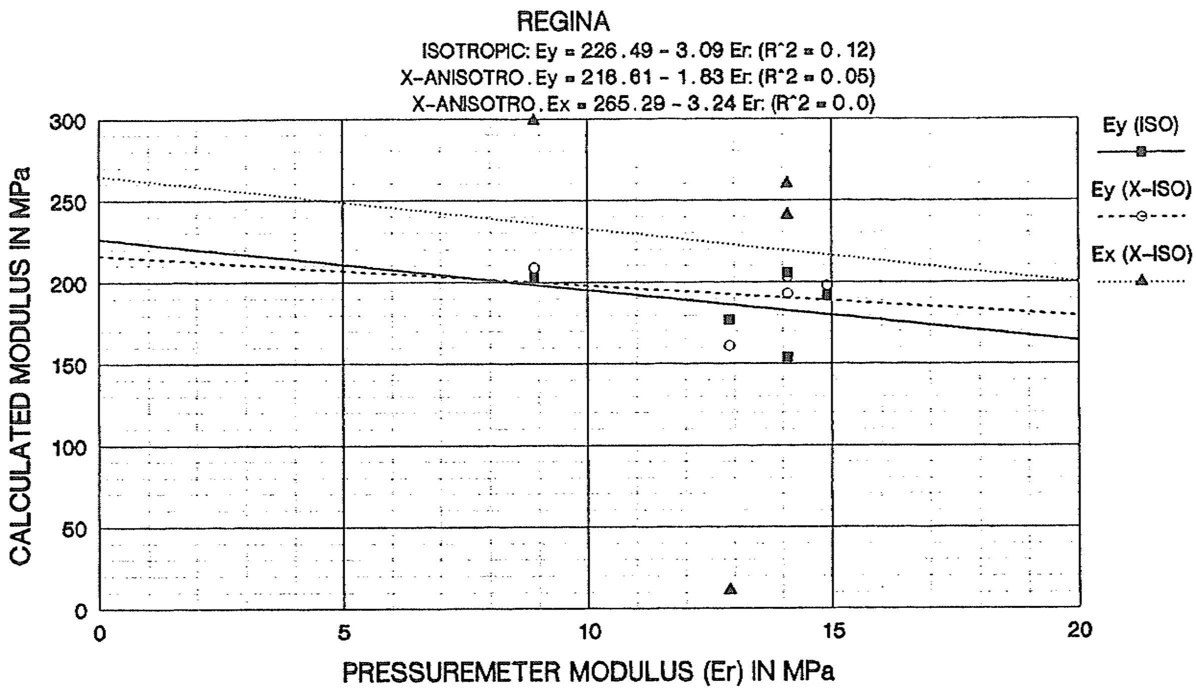

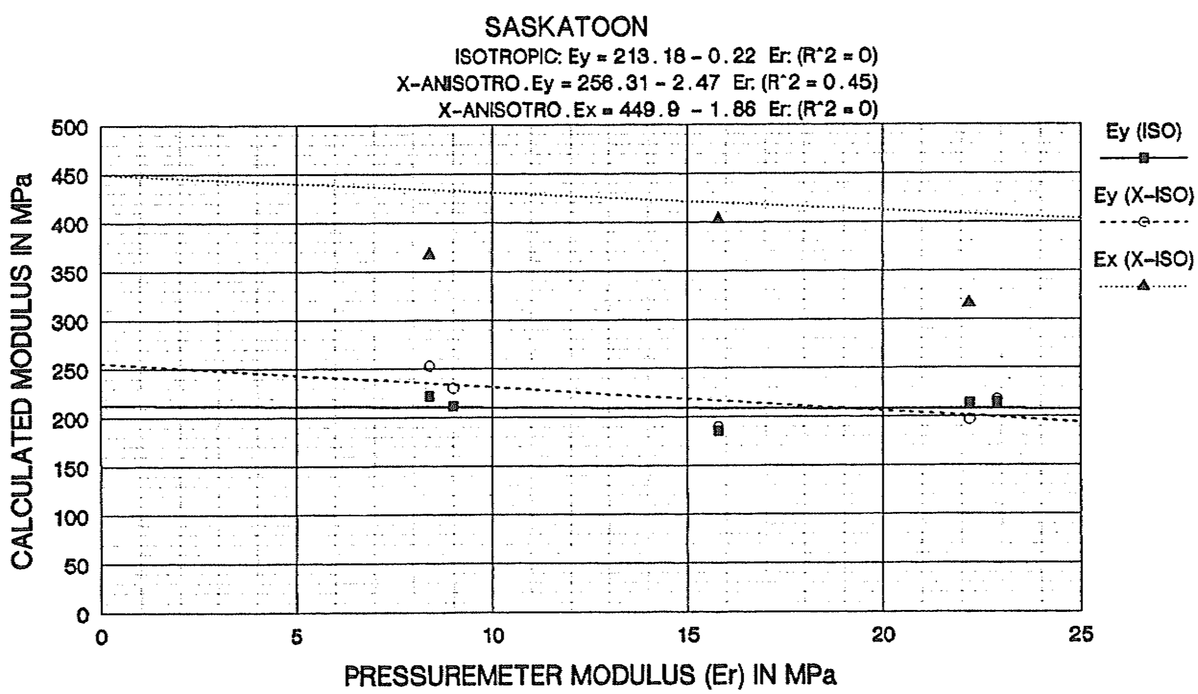

FIG. 6.7.B. CORRELATION BETWEEN MEASURED AND COMPUTED SUBGRADE MODULI (REGINA AND SASKATOON)

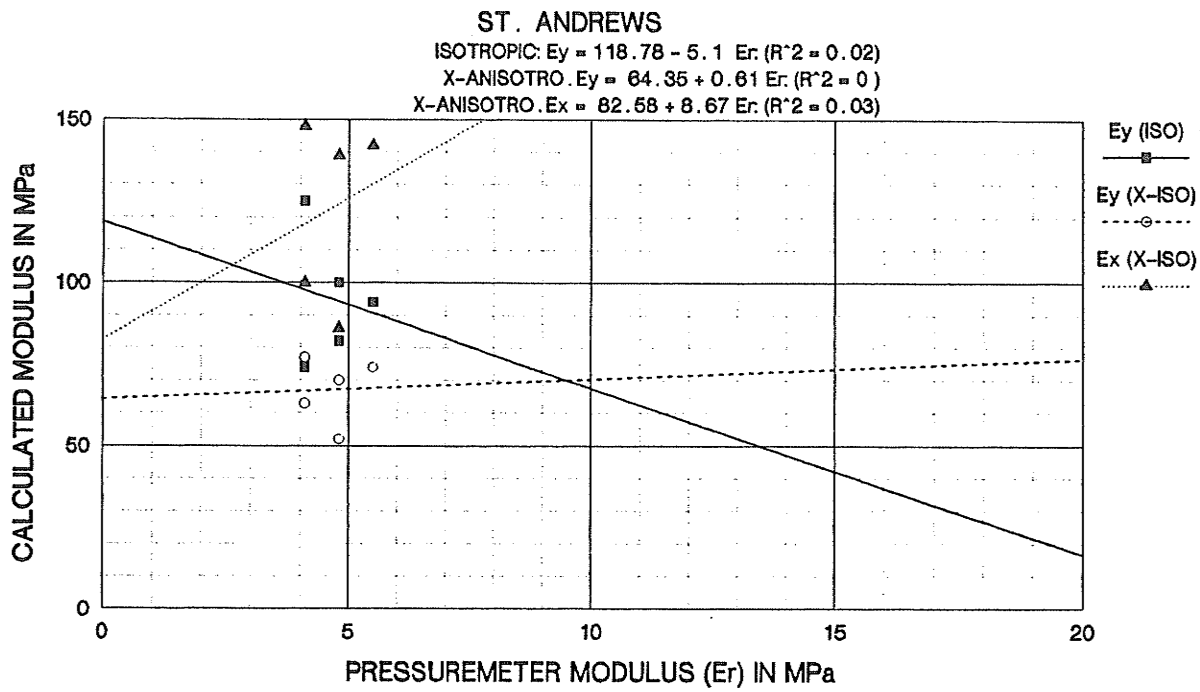

FIG. 6.7.C. CORRELATION BETWEEN MEASURED AND COMPUTED SUBGRADE MODULI (ST. ANDREWS)

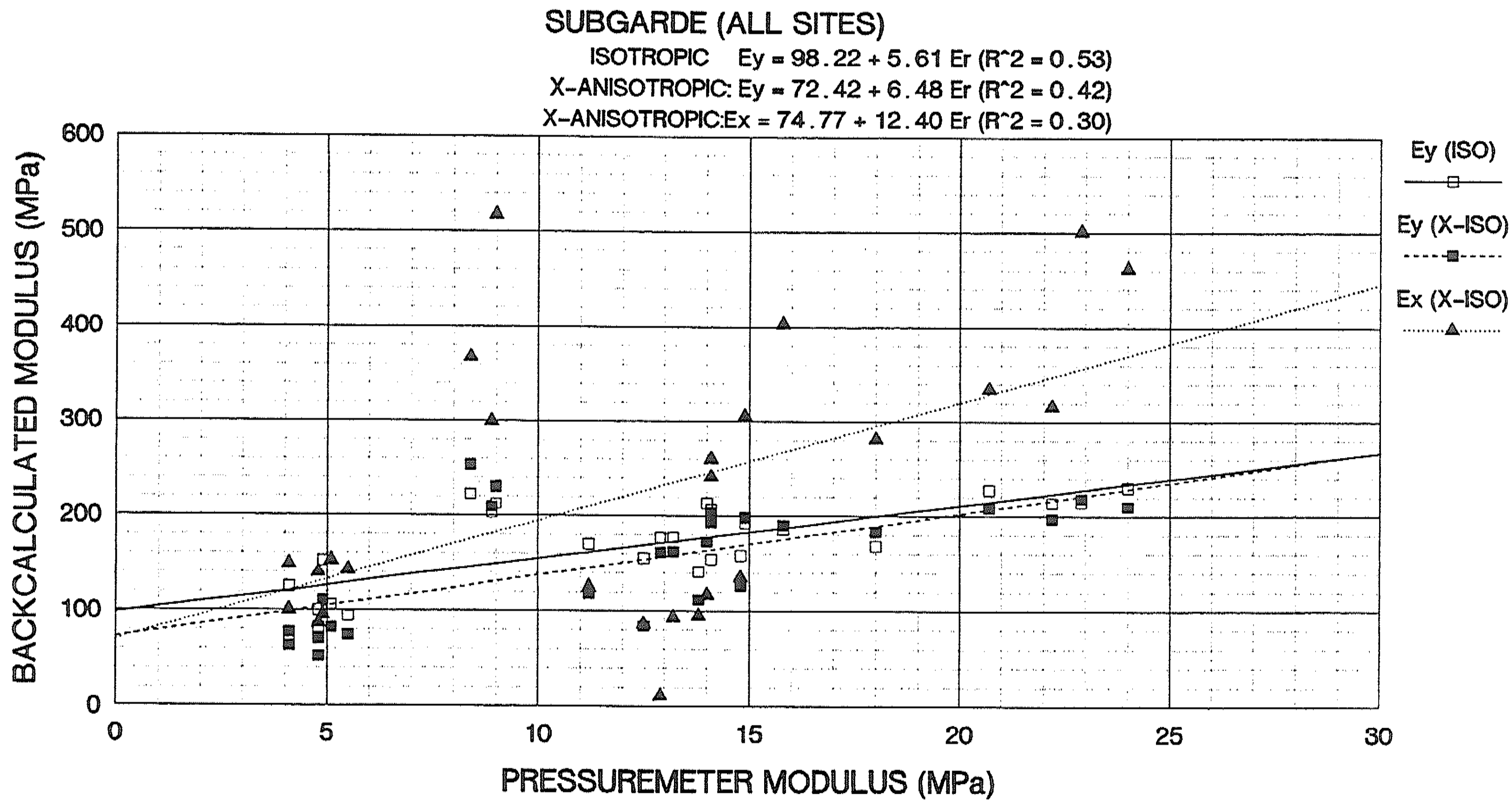

FIG. 6.8. CORRELATION BETWEEN MEASURED AND COMPUTED SUBGRADE MODULI (COMBINED DATA - ALL SITES)

FLINFLON: RUNWAY 18-36: STATION 5+100

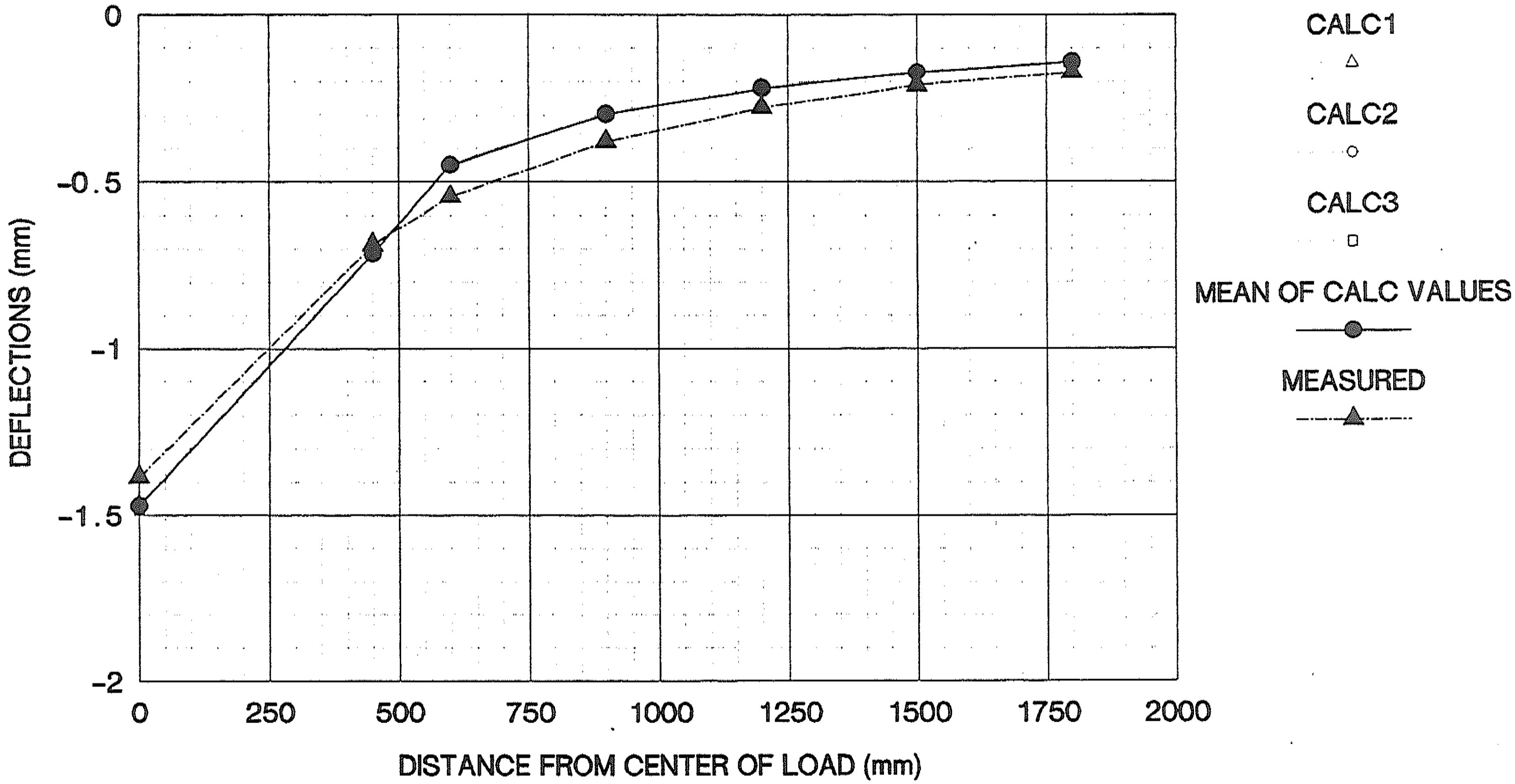

FIG. 6.9. EXAMPLE OF APPLICATION OF ANSYS MODEL TO PRACTICAL DESIGN PROBLEMS

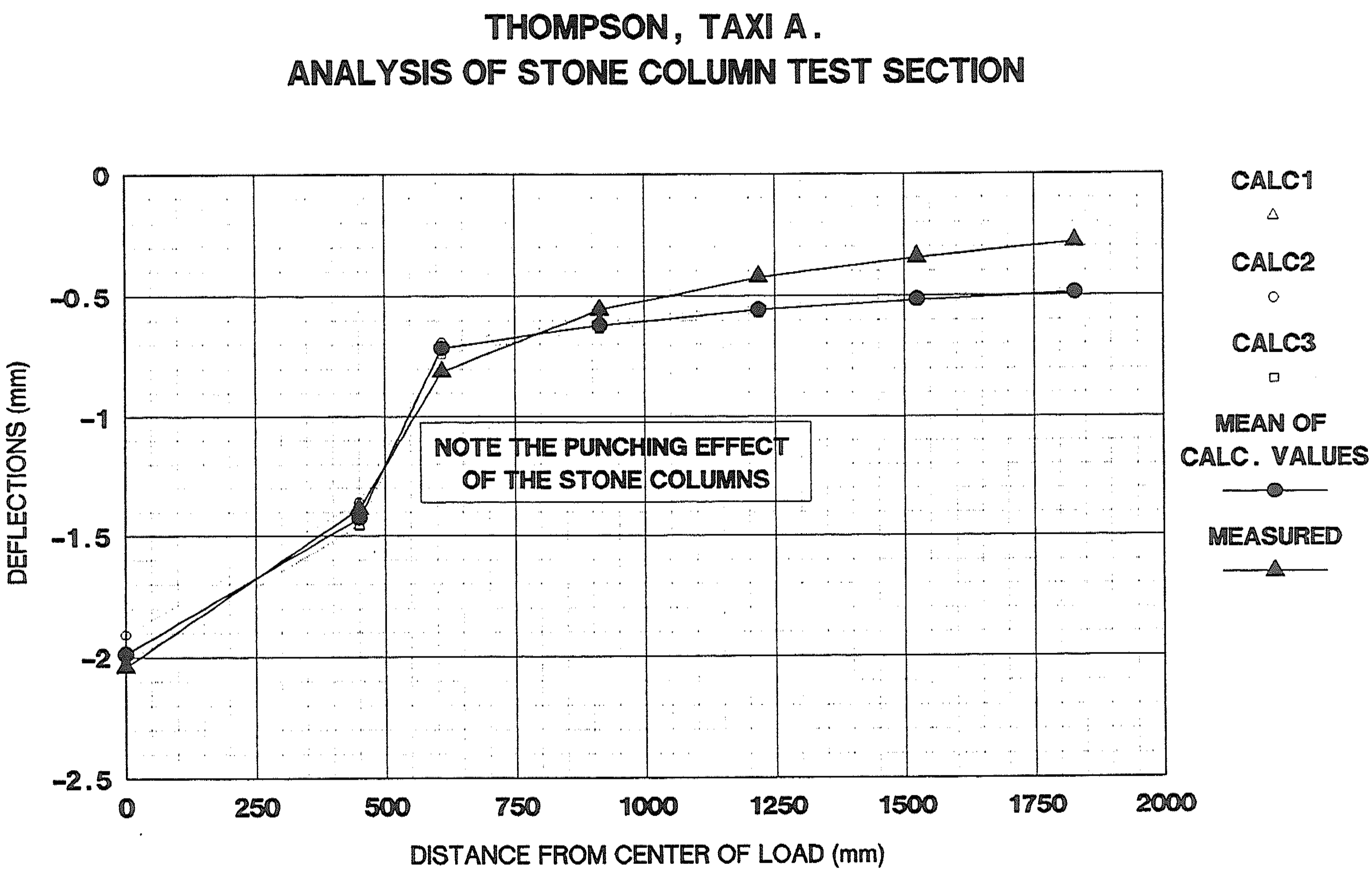

FIG. 6.10: EXAMPLE OF APPLICATION OF ANSYS MODEL TO PRACTICAL DESIGN PROBLEMS

THOMPSON AIRPORT: TAXI A: STONE COLUMN TEST SECTIONS.

DEFLECTION COMPARISON FOR ON- AND OFF-COLUMN LOADINGS

ON COLUMNM (LINE: 87106-S4)

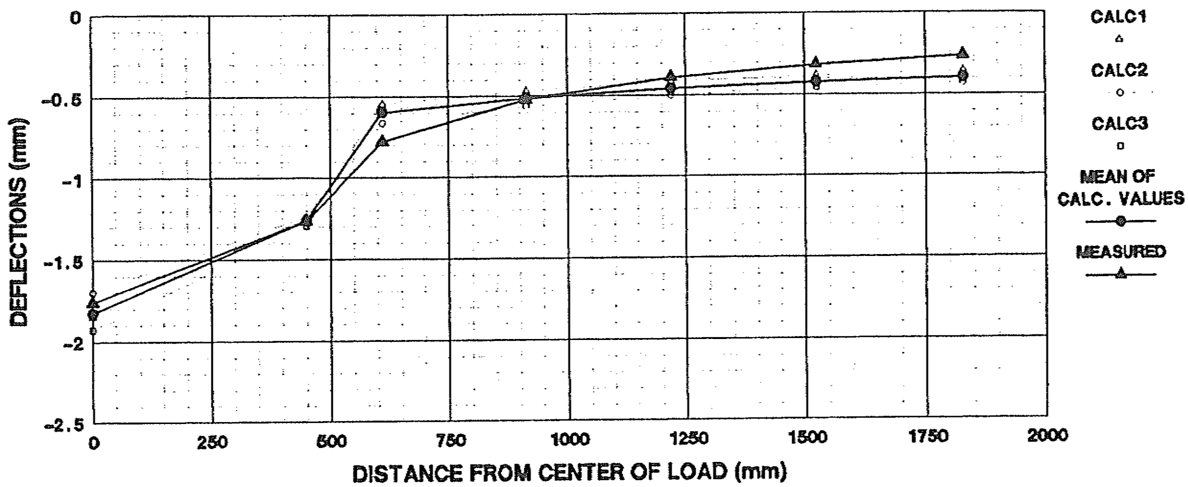

OFF COLUMN (LINE: S4)

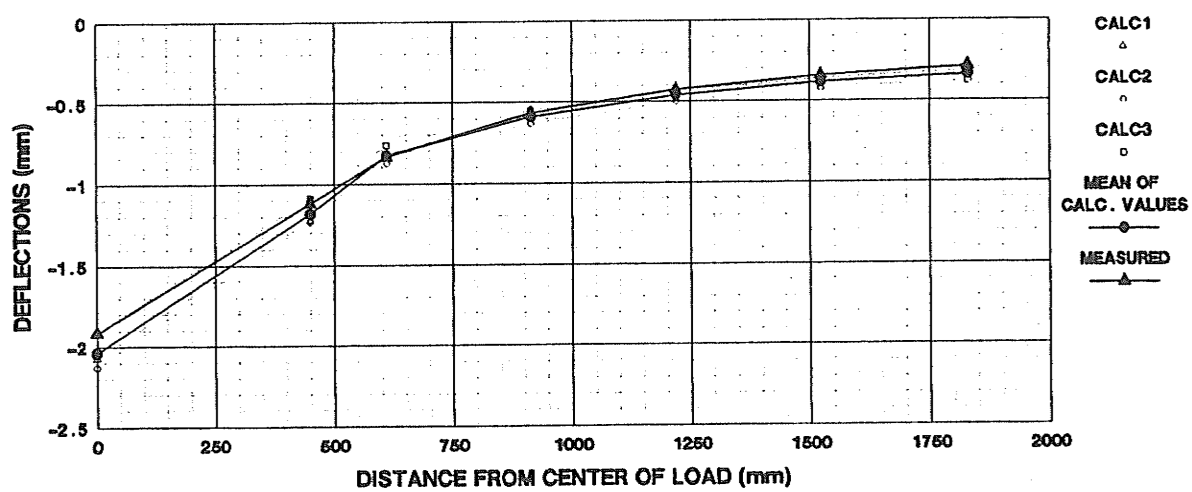

FIG. 6.11-A: EXAMPLE OF APPLICATION OF ANSYS MODEL TO PRACTICAL DESIGN PROBLEMS.

THOMPSON AIRPORT: TAXI A: STONE COLUMN TEST SECTIONS.

DEFLECTION COMPARISON FOR ON-COLUMN AND CONTROL SECTION LOADINGS

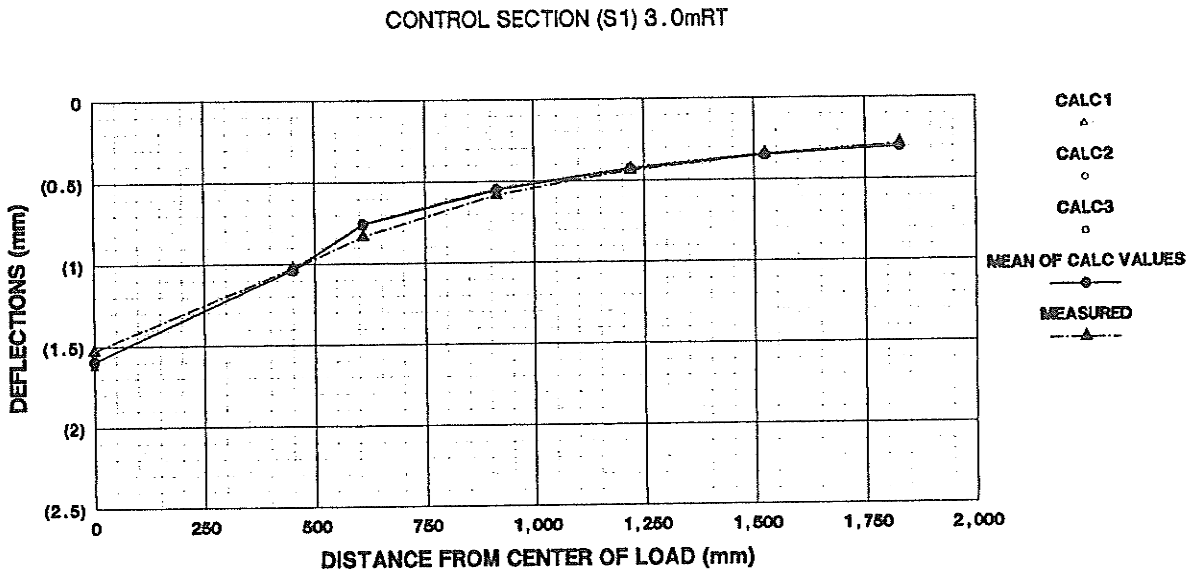

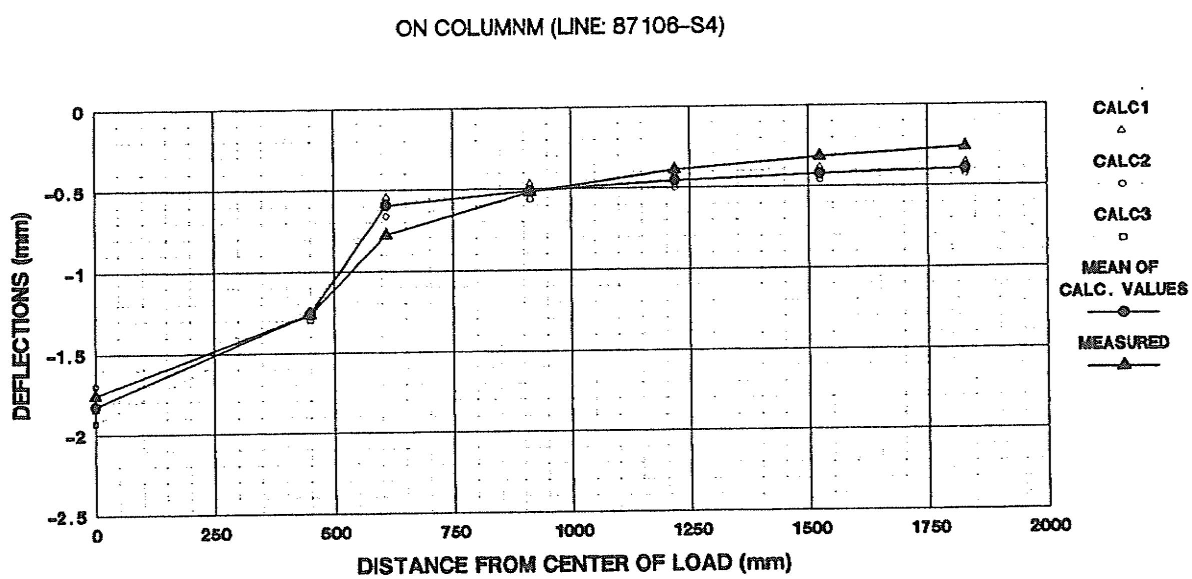

FIG. 6.11-B: EXAMPLE OF APPLICATION OF ANSYS MODEL TO PRACTICAL DESIGN PROBLEMS.

THOMPSON AIRPORT: TAXI A: STONE COLUMN TEST SECTIONS.

DEFLECTION COMPARISON FOR OFF-COLUMN AND CONTROL SECTION LOADINGS

CONTROL SECTION (S1) 3.0mRT

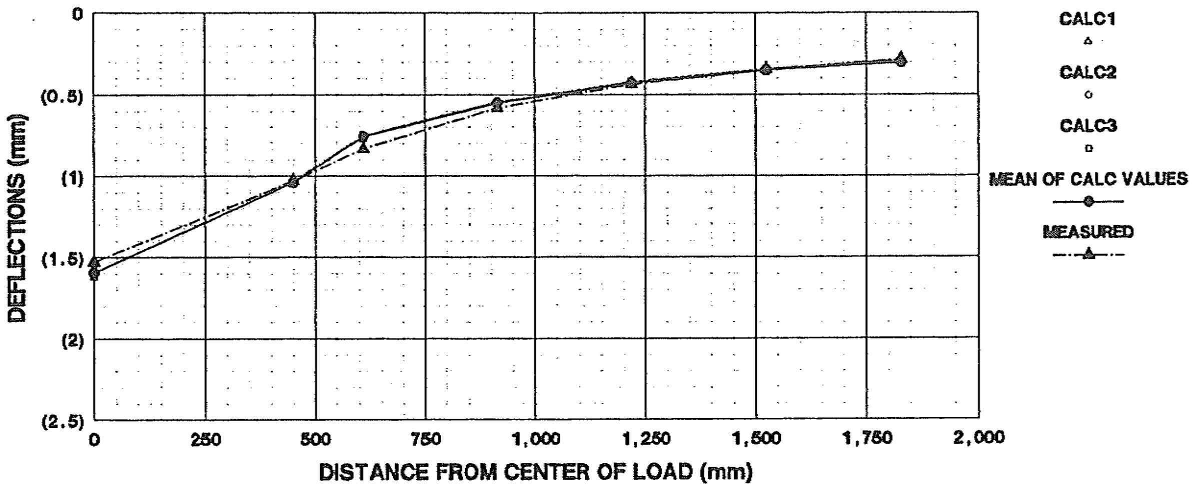

OFF COLUMN (LINE: S4)

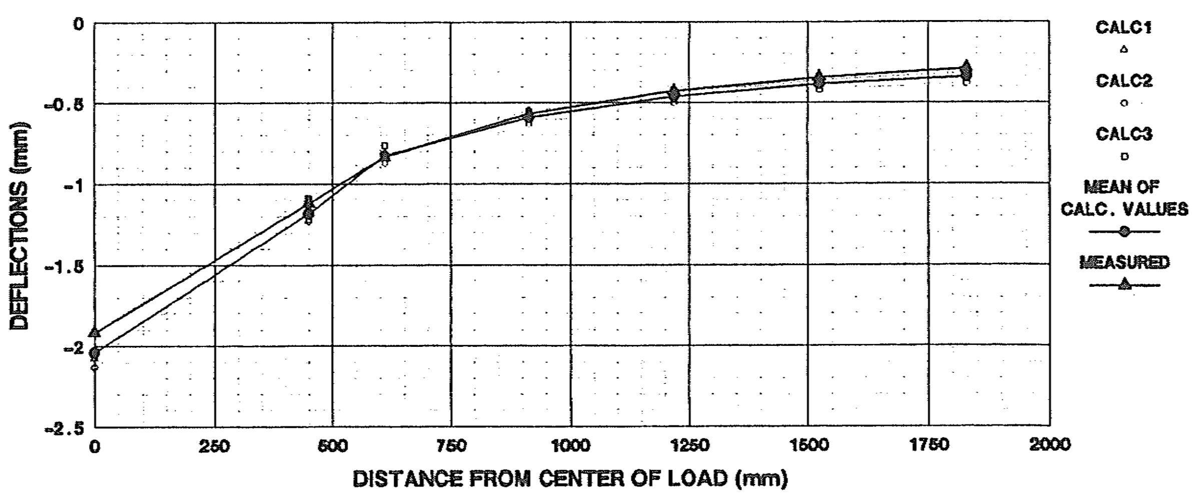

FIG. 6.11-C: EXAMPLE OF APPLICATION OF ANSYS MODEL TO PRACTICAL DESIGN PROBLEMS.

THOMPSON AIRPORT: TAXI A: STONE COLUMN TEST SECTIONS.

COMPARISON OF MEASURED AND COMPUTED VERTICAL STRESSES

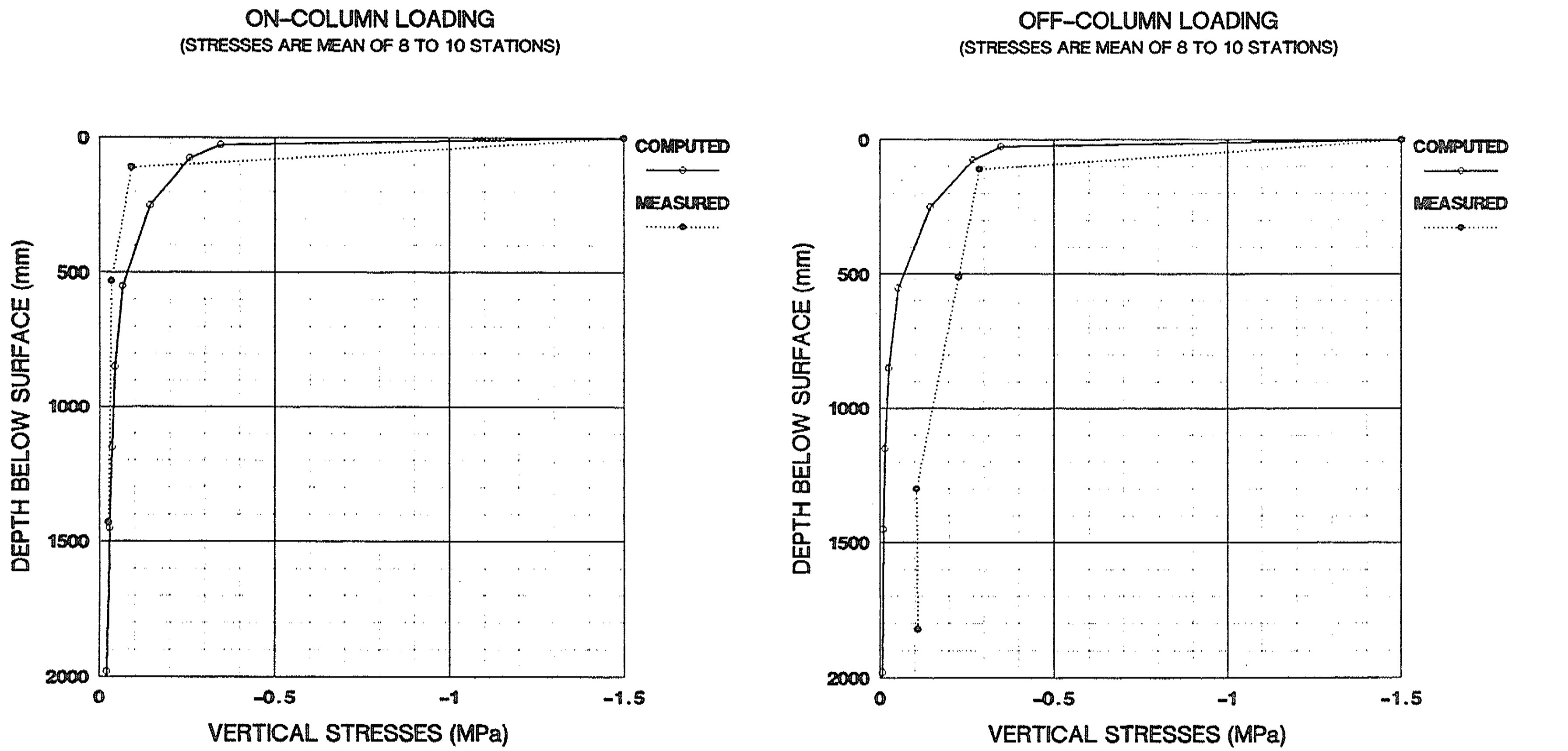

FIG. 6.12–A: EXAMPLE OF APPLICATION OF ANSYS MODEL TO PRACTICAL DESIGN PROBLEMS

THOMPSON AIRPORT: TAXI A: STONE COLUMN TEST SECTIONS.

COMPARISON OF MEASURED AND COMPUTED VERTICAL STRESSES

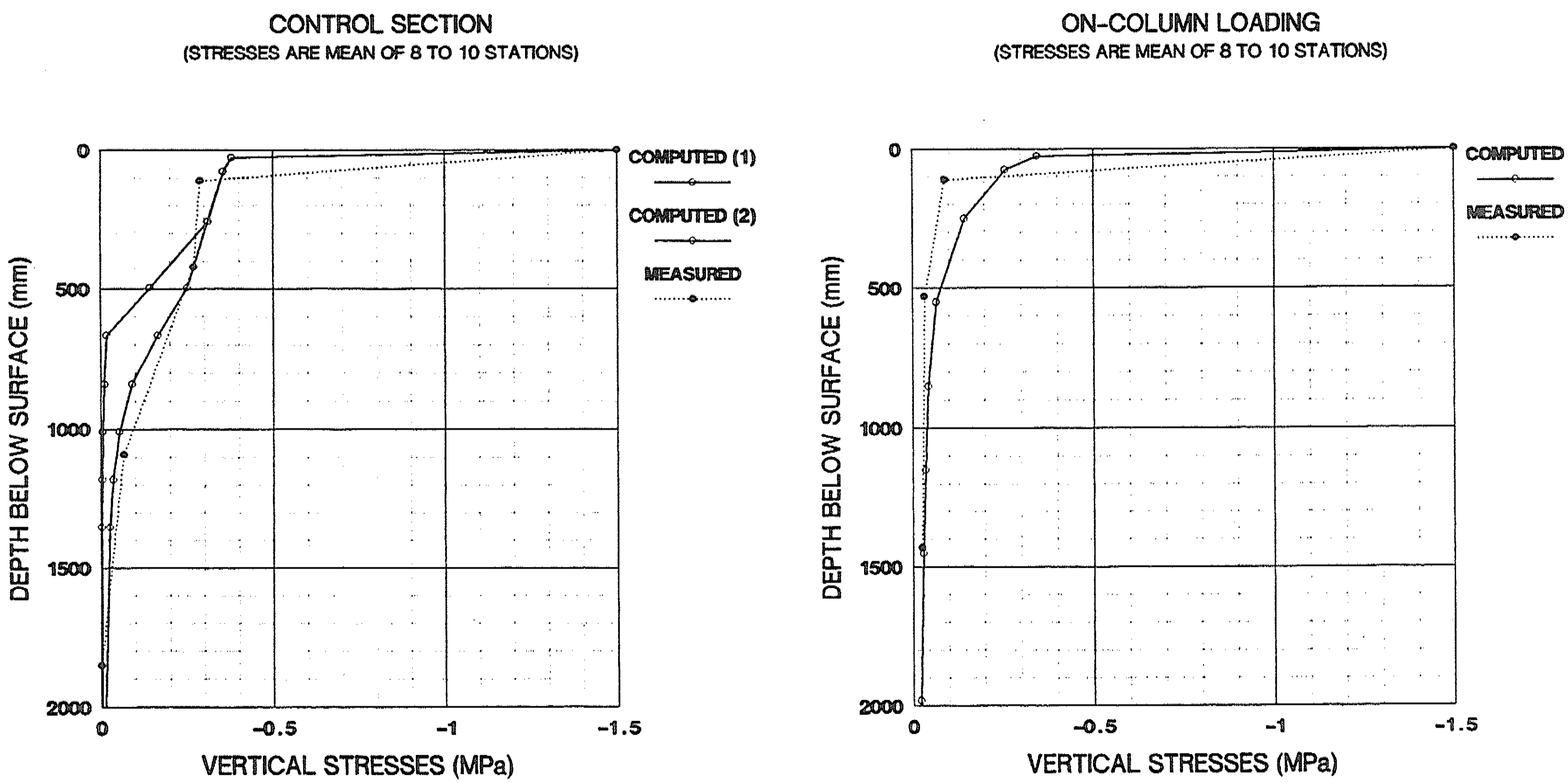

FIG. 6.12-B: EXAMPLE OF APPLICATION OF ANSYS MODEL TO PRACTICAL DESIGN PROBLEMS

THOMPSON AIRPORT: TAXI A: STONE COLUMN TEST SECTIONS.

COMPARISON OF MEASURED AND COMPUTED VERTICAL STRESSES

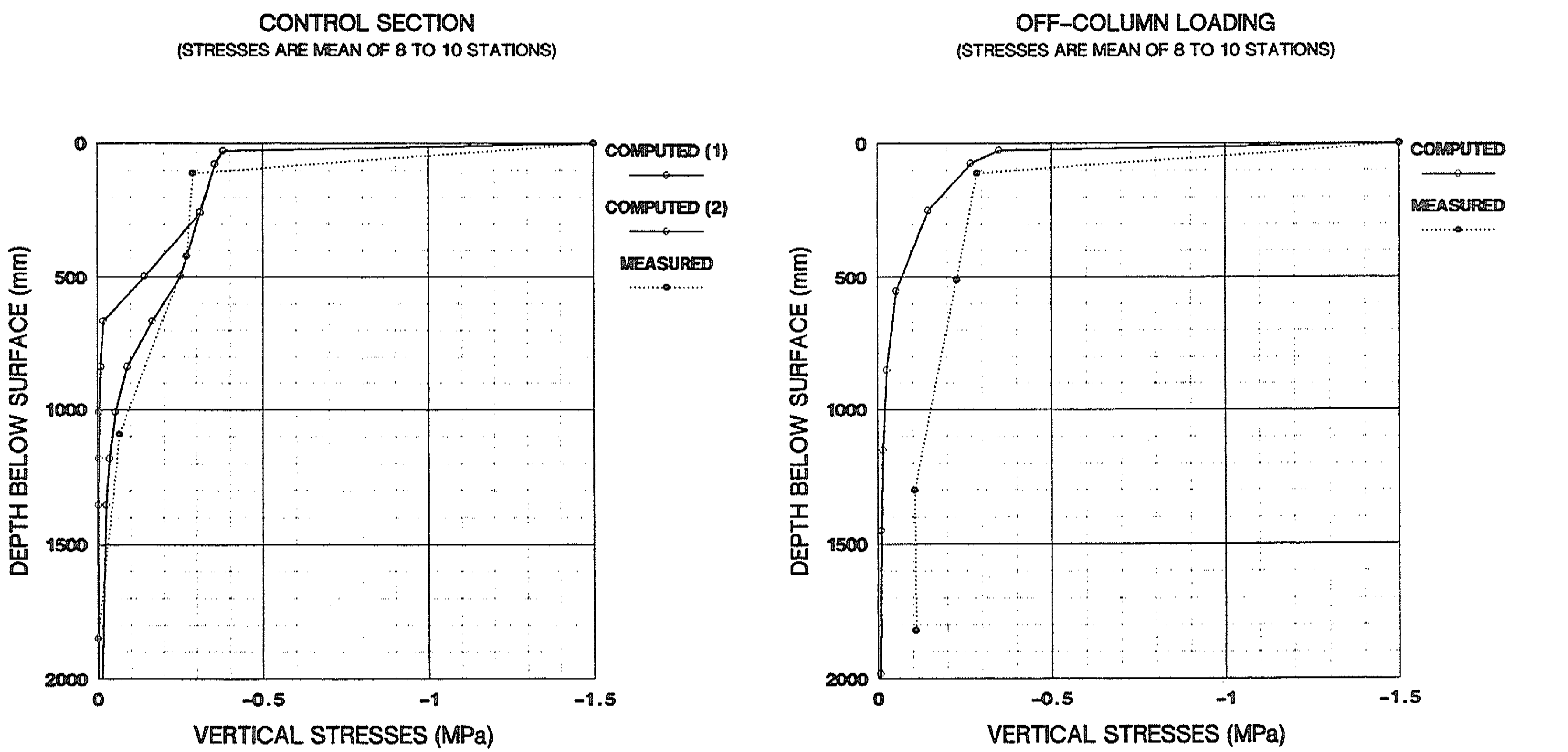

FIG. 6.12-C: EXAMPLE OF APPLICATION OF ANSYS MODEL TO PRACTICAL DESIGN PROBLEMS

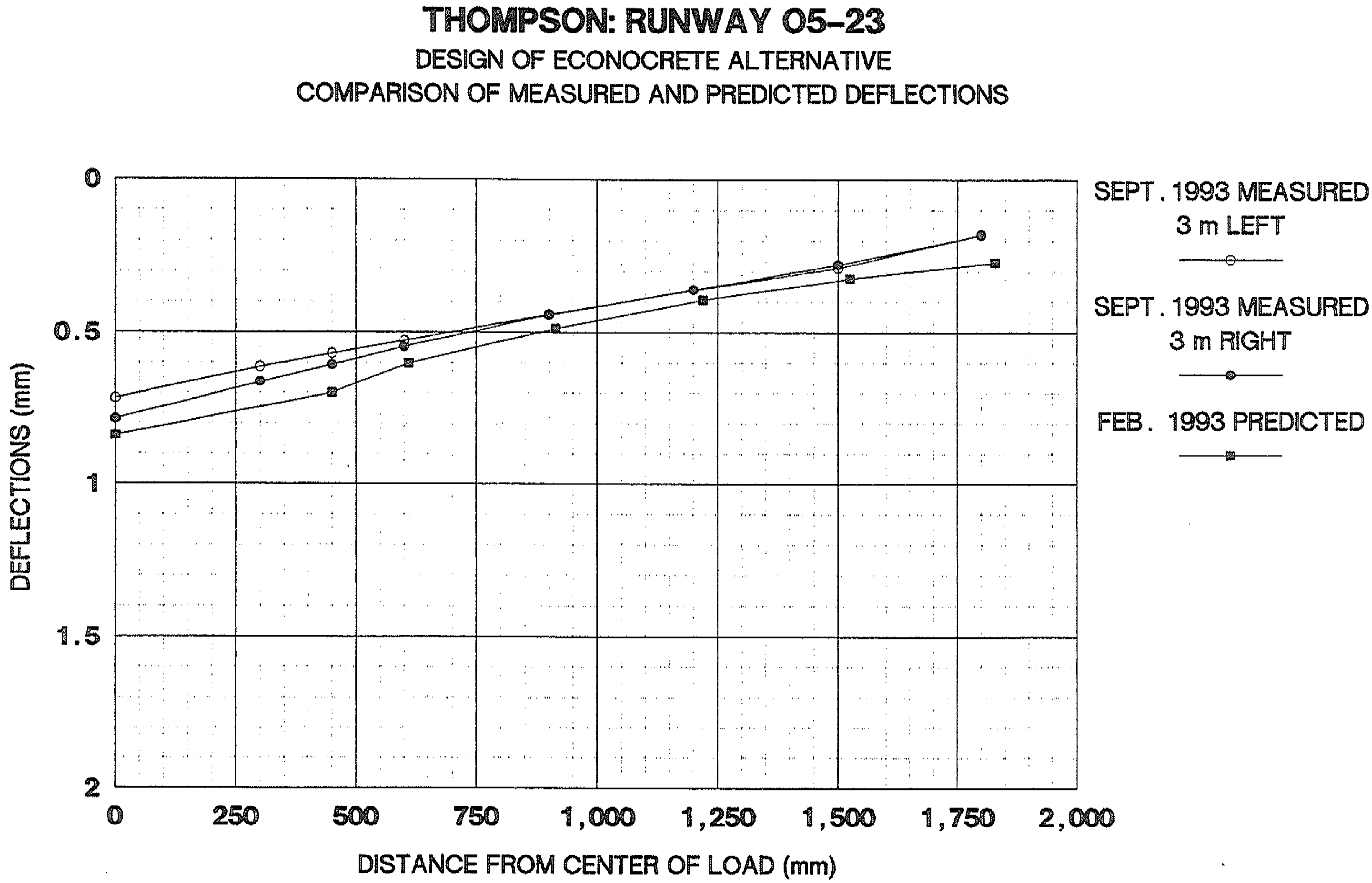

FIG. 6.13. EXAMPLE OF APPLICATION OF ANSYS MODEL TO PRACTICAL DESIGN PROBLEMS

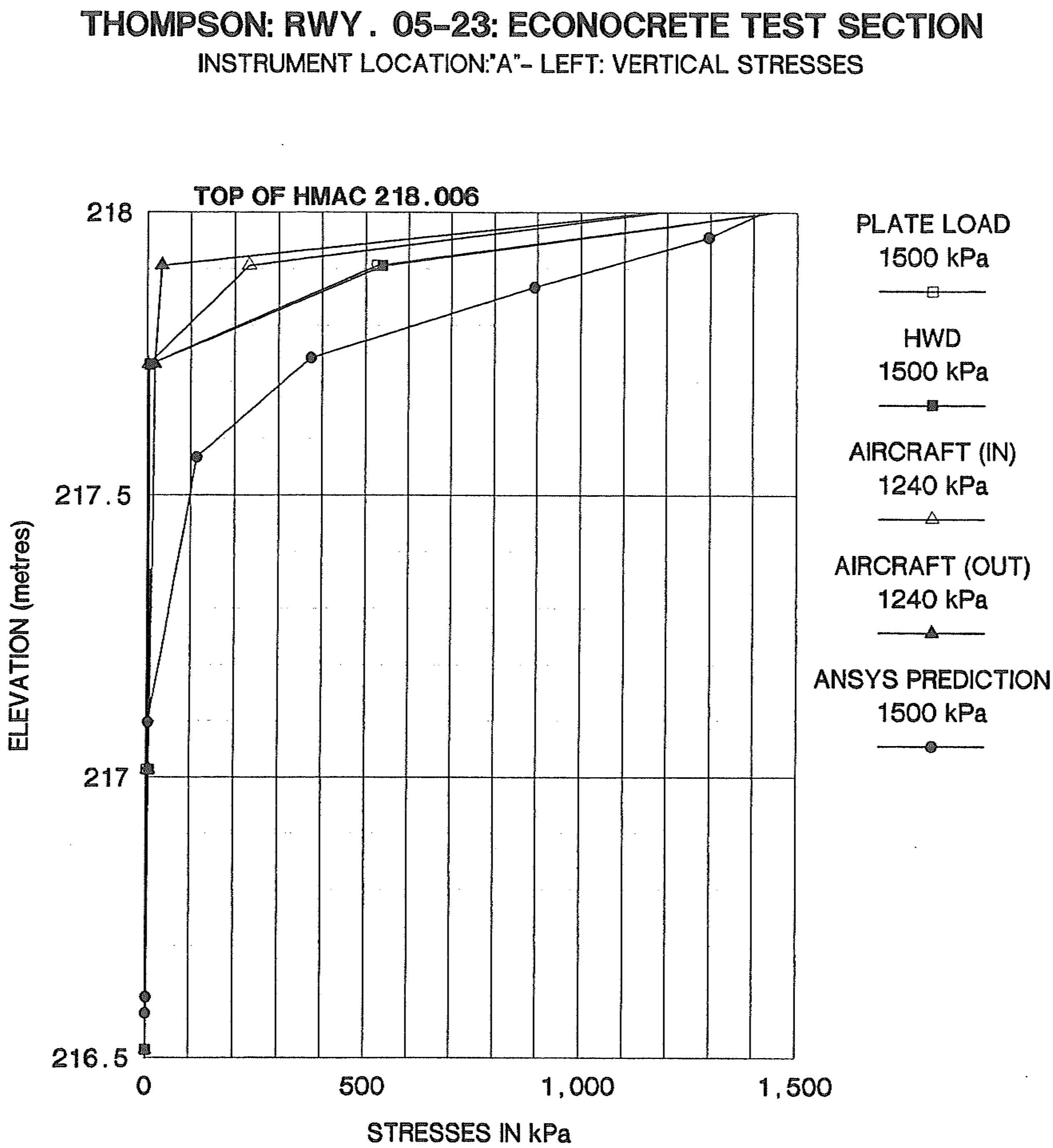

FIG. 6.14: EXAMPLE OF APPLICATION OF ANSYS MODEL TO PRACTICAL DESIGN PROBLEMS

WINNIPEG: RUNWAY 13-31: WHEEL PATH RUTTING

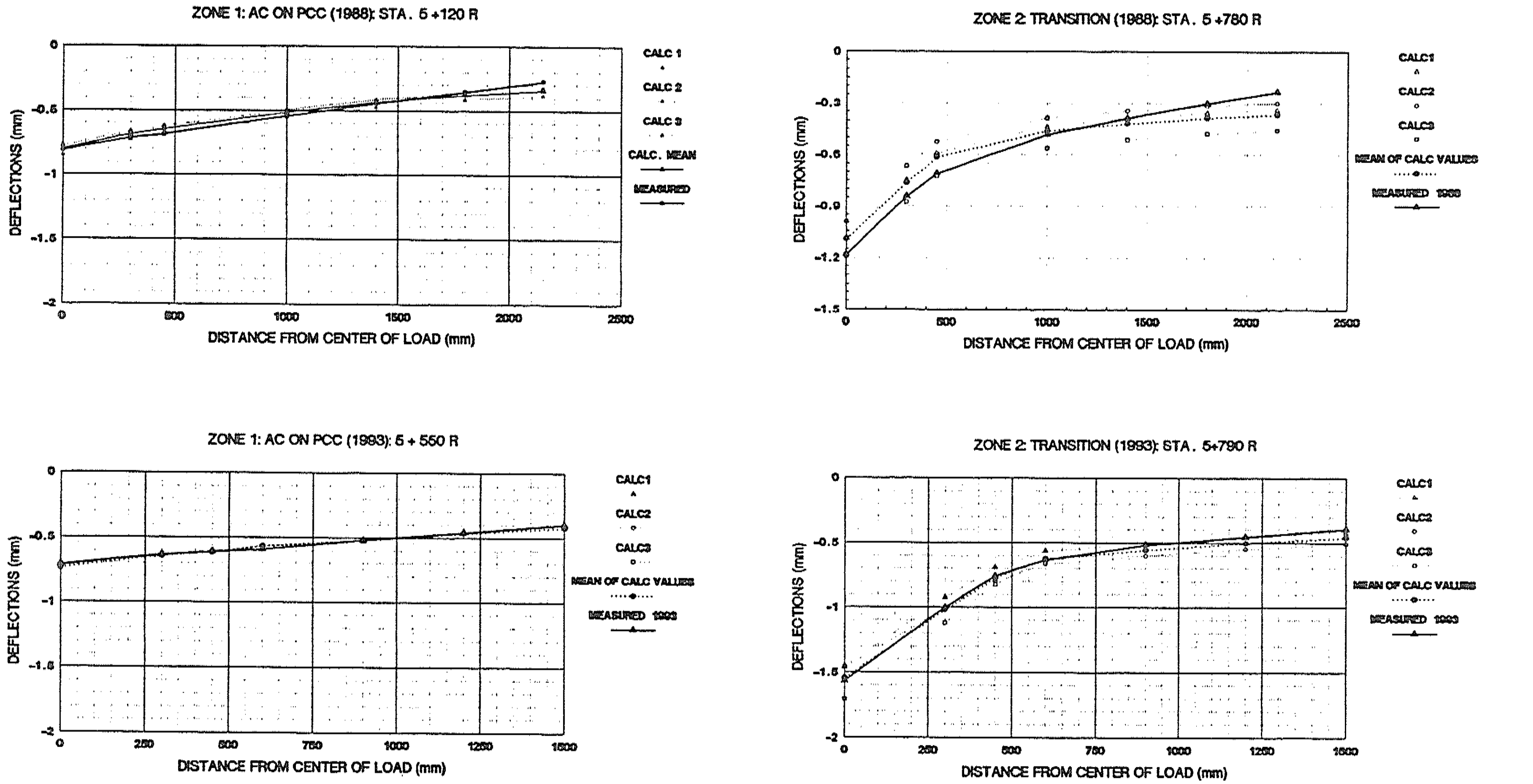

FIG. 6.15.A: EXAMPLE OF APPLICATION OF ANSYS MODEL

TO PRACTICAL DESIGN PROBLEMS

WINNIPEG: RUNWAY 13-31: WHEEL PATH RUTTING

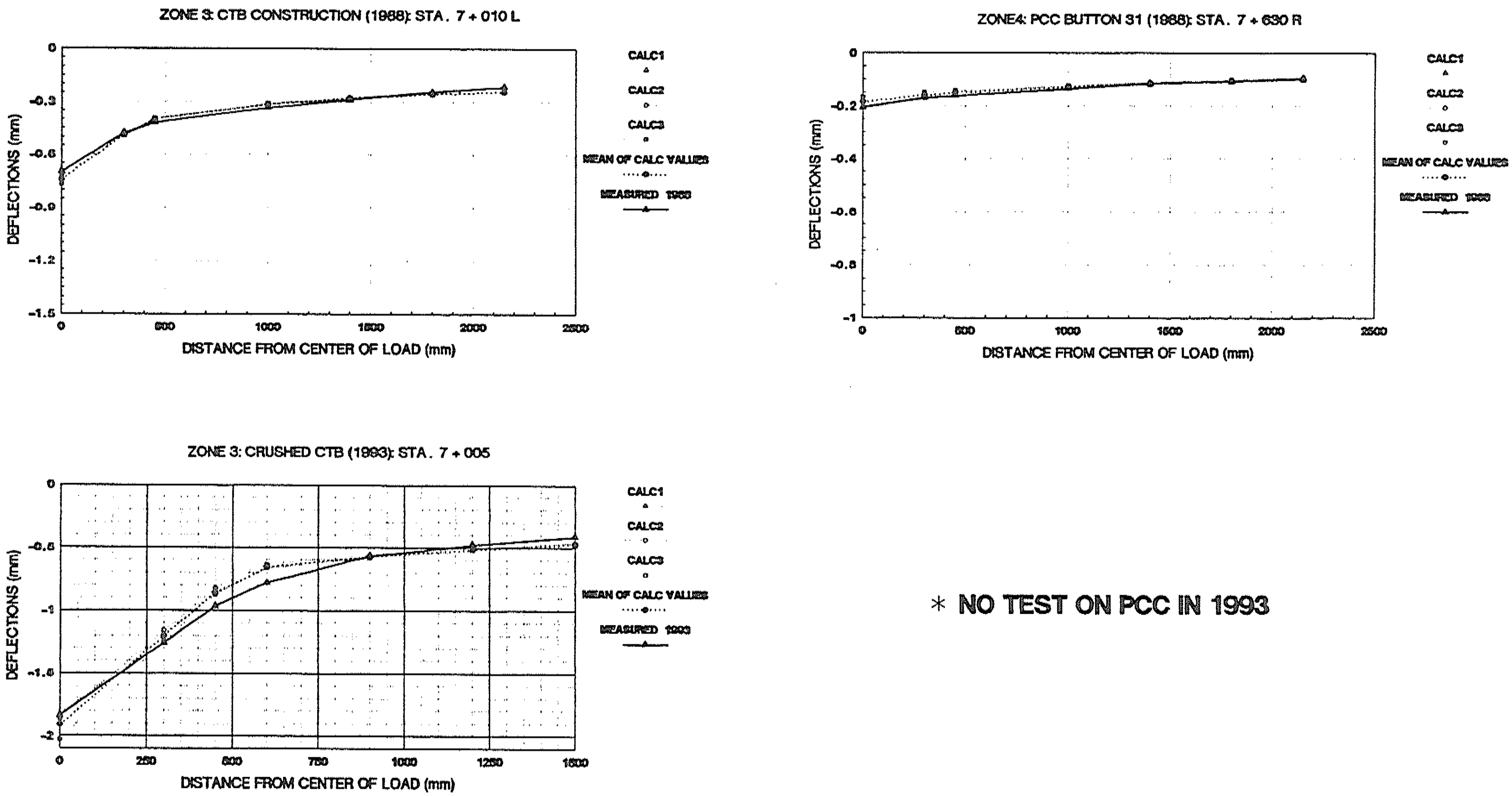

FIG. 6.15.B: EXAMPLE OF APPLICATION OF ANSYS MODEL

TO PRACTICAL DESIGN PROBLEMS

TABLE 6.1.A. TEST LOCATIONS AND PAVEMENT STRUCTURE IN BRANDON AIRPORT.

STATION	PAVEMENT STRUCTURE (mm)	YEAR OF CONSTR.	USC	ANALYSIS SYSTEM
5 + 400	AC 110 BASE 990 SG	1983 1957/83	 SW-SM CL	3L 4P
5 + 600	AC 120 BASE 1100 SG	1983 1957/83	 SW-SM CL	3L 4P
5 + 900	AC 120 BASE 1040 SG	1983 1957/83	 SW-SM CL	3L 4P
6 + 300	AC 120 BASE 980 SG	1983 1957/83	 SW-SM CL	3L 4P
6 + 500	AC 110 BASE 990 SG	1983 1957/83	 SW-SM CL	3L 4P
4 + 950	AC 100 EC 300 SB 350 SG	1983 1983 1983	 SP-SM CL-ML	4L 4P

NOTE: EC IS ECONOCRETE: A LEAN CONCRETE BASE.

TABLE 6.1.B. TEST LOCATIONS AND PAVEMENT STRUCTURE IN ST. ANDREWS AIRPORT.

STATION	PAVEMENT STRUCTURE (mm)	YEAR OF CONSTR.	USC	ANALYSIS SYSTEM
5 + 030	AC 45 BASE 150 [1] SB 300 [1] SG	1968 1968 1968	 SW-SM SW-SM CH	3L 3P
5 + 120	AC 40 BASE/ SB 470[1] SG	1968 1968	 SW-SM CH	3L 3P
5 + 480	AC 50 BASE/ SB 470 SG	1968 1968	 GP-SW SM CH	3L 3P
5 + 660	AC 50 BASE/ SB 550 SG	1968 1968	 SW-SM CH	3L 3P
5 + 840	AC 50 BASE/ SB 460 SG	1968 1968	 SW-SM CH	3L 3P

NOTE 1.: IT WAS DIFFICULT TO DISTINGUISH BETWEEN BASE AND SUB BASE MATERIAL UNDER THIS PAVEMENT, THOUGH CONSTRUCTION RECORDS SHOWED THAT 150 mm OF GRANULAR BASE (GW-GP) WAS PLACED IN 1968.

TABLE 6.1.C. TEST LOCATIONS AND PAVEMENT STRUCTURE IN REGINA AIRPORT.

STATION	PAVEMENT STRUCTURE (mm)	YEAR OF CONSTR.	USC	ANALYSIS SYSTEM
5 + 510	AC 40 AC 120 AC 90 AC 80 BASE[1] SB 1070 SG	1979 U[2] 1979 L[2] 1967 1953 1953 	 SM CH	6L 3P
5 + 990	AC 45 AC 110 AC 115 AC 60 BASE/ SB 710 SG	1979 U 1979 L 1967 1953 1953 	 SW-SM CH	6L 3P
6 + 290	AC 55 AC 110 AC 115 AC 95 BASE/ SB 740 SG	1979 U 1979 L 1967 1953 1953 	 SW-SM CH	6L 3P
6 + 890	AC 40 AC 70 AC 115 AC 120 BASE/ SB 780 SG	1979 U 1979 L 1962 1953 1953 	 SW-SM CH	6L 3P
7 + 310	AC 35 AC 70 AC 95 PCC 265 BASE/ SB 355 SG	1979 U 1979 L 1966 1960 1960 	 SP 	5L 3P

NOTE 1: BASE AND SUB BASE ARE NOT EASILY DISTINGUISHABLE
NOTE 2: U = UPPER COURSE; L = LOWER COURSE.

TABLE 6.1.D. TEST LOCATIONS AND PAVEMENT STRUCTURE IN SASKATOON AIRPORT.

STATION	PAVEMENT STRUCTURE (mm)	YEAR OF CONSTR.	USC	ANALYSIS SYSTEM
5 + 360	AC[1] 30 AC 95 BASE 655 AC[1] 55 BASE/SB 175 SG	1976 1961 1961 1947 1947	 GP-SP SP-SM CLAY TILL	5L 3P
5 + 630	AC 35 AC 115 BASE 550 AC 150 BASE/SB 350 SG	1976 1961 1961 1947 1947	 GP-SP GP-PLASTIC CLAY TILL	5L 3P
5 + 840	AC 40 AC 110 BASE 600 AC 125 BASE/SB 425 SG	1976 1961 1961 1947 1947	 GP-SP SP-PLASTIC CLAY TILL	5L 3P
6 + 140	AC 35 AC 105 BASE 590 AC 70 BASE/SB 600 SG	1976 1961 1961 1947 1947	 GP GP-SP (PL) CH	5L 3P
6 + 470	AC 35 AC 90 BASE 615 AC 95 BASE/SB 465 SG	1976 1961 1961 1947 1947	 GW GP-SP (PL) CH	5L 3P

NOTE: 1) THE 1961 SURFACE WAS BADLY CRACKED. THE THIN OVERLAY IN 1976 REFLECTED ALL THE 1961 CRACKS.

2) THE 1947 AC WAS TOTALLY STRIPPED AND WAS NO MORE THAN GRAVEL

TABLE 6.1.E. TEST LOCATIONS AND PAVEMENT STRUCTURE IN THUNDER BAY AIRPORT.

STATION	PAVEMENT STRUCTURE (mm)	YEAR OF CONST.	USC	ANALYSIS SYST.
5 + 100	AC 70 AC 100 AC 100 BASE 280 SB 600 SG	1984 1965 1954 1954 1954	 GP,GW SW,SM SP,SM	5L 4P
5 + 300	AC 70 AC 100 AC 70 BASE 230 SB 680 SG	1984 1965 1954 1954 1954	 GP,GW SM	5L 4P
5 + 500	AC 70 AC 100 AC 70 PCC 170 SB 110 SG	1984 1965 1954 1942 1942	 SW,SM SP,SM	5L 4P
5 + 650	AC 80 AC 100 AC 70 PCC 190 SB 100 SG	1984 1965 1954 1942 1942	 SM SP,ML	5L 4P
6 + 100	AC 100 AC 100 AC 70 PCC 180 SB 100 SG	1984 1965 1954 1942 1942	 SW SM	5L 4P
TAXI A 10 + 740	AC 135 BASE 300 SB 905 SG	1983 1983 1983	 SW SM ML	3L 4P

TABLE 6.2 - A. SUMMARY OF REGRESSION EQUATIONS FOR CORRELATIONS BETWEEN MEASURED AND BACKCALCULATED A.C. MODULI

SITE	MODEL	REGRESSION EQUATION	R^2
BRANDON	ISOTROPIC	Ecalc = -9001 + 0.48 E meas	0.57
	X-ANISOTROPIC	Ecalc = 2107 + 0.04 Emeas.	0.02
ST. ANDREWS	ISOTROPIC	Ecalc = 4708 - 0.014 Emeas	0.45
	X-ANISOTROPIC	Ecalc = 2520 - 0.482 Emeas	0
REGINA	ISOTROPIC	Ecalc = 6916 - 0.084 Emeas	0.12
	X-ANISOTROPIC	Ecalc = 8984 - 0.083 Emeas	0.05
SASKATOON	ISOTROPIC	Ecalc = 4555 + 0.144 Emeas	0.51
	X-ANISOTROPIC	Ecalc = 6804 + 0.138 Emeas	0.06
THUNDER BAY	ISOTROPIC	Ecalc = 2335 + 0.286 Emeas	0.66
	X-ANISOTROPIC	Ecalc = 4479 + 0.115 Emeas	0.19
ALL DATA	ISOTROPIC	Ecalc = 6706 - 0.097 Emeas	0.09
	X-ANISOTROPIC	Ecalc = 5667 + 0.061 Emeas	0.07

NOTE:

1. Ecalc IS THE CALCULATED RESILIENT MODULI (Ey) FROM BACKCALCULATION OF THE DEFLECTION DATA BASED ON THE "AREA" OF BASIN CRITERION

2. Emeas IS THE STIFFNESS OF THE ASPHALTIC CONCRETE MIX CALCULATED FROM VAN DER POHL AND McLEOD'S NOMOGRAPH USING THE MEASURED VISCOSITY OF ASPHALT CEMENT RECOVERED FROM CORES.

3. NORMALIZED TEMPERATURE IS 21 DEG C.

TABLE 6.2 - B. SUMMARY OF REGRESSION EQUATIONS FOR CORRELATIONS BETWEEN MEASURED AND BACKCALCULATED GRANULAR BASE MODULI

SITE	MODEL	REGRESSION EQUATION	R^2
BRANDON	ISOTROPIC	Ey = 151 + 0.057 Er	0.09
	X-ANISOTROPIC	Ey = 63 + 0.33 Er	0.19
	X-ANISOTROPIC	Ex = 293 - 1.85 Er	0.29
ST. ANDREWS	ISOTROPIC	Ey = 237 - 4.73 Er	0.38
	X-ANISOTROPIC	Ey = 134 + 4.3 Er	0.06
	X-ANISOTROPIC	Ex = -193 + 37.3 Er	0.21
REGINA	ISOTROPIC	Ey = 300 + 0.625 Er	0.39
	X-ANISOTROPIC	Ey = 330 - 0.07 Er	0.02
	X-ANISOTROPIC	Ex = 413 + 0.27 Er	0.02
SASKATOON	ISOTROPIC	Ey = 518 - 0.42 Er	0.52
	X-ANISOTROPIC	Ey = 197 + 0.07 Er	0.11
	X-ANISOTROPIC	Ex = 371 + 0.43 Er	0.19
THUNDER BAY	ISOTROPIC	Ey = 321 - 0.82 Er	0.10
	X-ANISOTROPIC	Ey = 343 - 0.83 Er	0.05
	X-ANISOTROPIC	Ex = 851 - 4.54 Er	0.09
ALL DATA	ISOTROPIC	Ey = 167 + 1.86 Er	0.47
	X-ANISOTROPIC	Ey = 209 + 0.54 Er	0.10
	X-ANISOTROPIC	Ex = 379 + 0.27 Er	0

NOTE:

1. Ey, Ex ARE THE CALCULATED RESILIENT MODULI FROM BACKCALCULATION OF THE DEFLECTION DATA BASED ON THE "AREA" OF BASIN CRITERION

2. Er IS THE UNLOAD-RELOAD MODULUS FROM PRESSUREMETER TESTS.

TABLE 6.2 - C. SUMMARY OF REGRESSION EQUATIONS FOR CORRELATIONS BETWEEN MEASURED AND BACKCALCULATED SUBGRADE MODULI

SITE	MODEL	REGRESSION EQUATION	R^2
BRANDON	ISOTROPIC	Ey = 101.34 + 1.38 Er	0.80
	X-ANISOTROPIC	Ey = 90.61 + 0.42 Er	0.09
	X-ANISOTROPIC	Ex = 156.2 - 1.46 Er	0.49
ST. ANDREWS	ISOTROPIC	Ey = 118.78 - 5.1 Er	0.02
	X-ANISOTROPIC	Ey = 64.35 + 0.61 Er	0
	X-ANISOTROPIC	Ex = 82.58 + 8.67 Er	0.03
REGINA	ISOTROPIC	Ey = 216.1 - 2.37 Er	0.14
	X-ANISOTROPIC	Ey = 214.4 - 1.73 Er	0.10
	X-ANISOTROPIC	Ex = 300.9 - 4.57 Er	0
SASKATOON	ISOTROPIC	Ey = 213.2 - 0.22 Er	0
	X-ANISOTROPIC	Ey = 256.3 -2.47 Er	0.45
	X-ANISOTROPIC	Ex = 449.9 -1.86 Er	0
THUNDER BAY	ISOTROPIC	Ey = 148.4 + 1.38 Er	0.04
	X-ANISOTROPIC	Ey = 161.09 + 0.64 Er	0.03
	X-ANISOTROPIC	Ex = 323.2 + 0.76 Er 3	0.02
ALL DATA	ISOTROPIC	Ey = 90.3 + 5.17 Er	0.54
	X-ANISOTROPIC	Ey = 57.1 + 6.56 Er	0.63
	X-ANISOTROPIC	Ex = 74.3 + 11.2 Er	0.35

NOTE:

1. Ey, Ex ARE THE CALCULATED RESILIENT MODULI FROM BACKCALCULATION OF THE DEFLECTION DATA BASED ON THE "AREA" OF BASIN CRITERION

2. Er IS THE UNLOAD-RELOAD MODULUS FROM PRESSUREMETER TESTS.

CHAPTER SEVEN

CONCLUDING REMARKS AND RECOMMENDATIONS FOR FURTHER RESEARCH

7.1 GENERAL

This chapter summarizes the highlights of the thesis. It synthesizes the various hypotheses and conclusions advanced in the previous chapters. It also points out to the gaps that still exist in the field and suggests topics for further research in this field.

This thesis started with the idea of correlating the back-calculated layer moduli from deflection testing to independently and directly measured moduli. To measure the moduli independently two different approaches had to be taken: one for the surface modulus of asphaltic concrete and another for the unbound layers of granular base and the subgrade. For the surface layer of asphaltic concrete the viscosity and penetration of the asphalt cement, recovered from the cores, were determined in the laboratory between 4°C and 135°C. From this the Shell Bituminous Chart as proposed by Bell (1983) was constructed. This, in turn, was used to determine the moduli of the binder at any temperature. From the binder moduli the mix moduli were calculated using the nomograph of Van der Poel and later modified by McLeod. For the unbound layers the moduli were measured in the field with the PENCEL pressuremeter.

Half-way through the research, doubts were lingering whether the horizontal modulus measured by the pressuremeter would be the appropriate parameter to use in an isotropic model of the layered elastic system which used the vertical modulus. At that time, a survey of the geotechnical literature showed that the subgrade at the test sites exhibited moderate anisotropy. Also many authors suggested that, in many geotechnical problems, anisotropy was an increasingly important consideration. Therefore, it was decided to investigate the effect of anisotropy on the response of the pavement to the applied loads.

As a back-calculation tool, many existing layered elastic models and general finite-element algorithms were evaluated. It became evident that the existing layer elastic models can handle only isotropic cases. They could not be modified because they were mostly commercial proprietary systems. Other public- domain software available at the University of Manitoba would have required extensive modification and writing source codes. Therefore, a commercially available general-purpose finite-element program developed by Swanson Analysis Systems, called ANSYS, was used. To the best of the author's knowledge, this is the first time a cross-anisotropic finite-element model has been applied to a layered elastic system for the evaluation of pavements. In the following sections the results of these analyses are summarized.

7.2 REVIEW OF LITERATURE

Chapter 2 of the thesis provides an extensive literature survey up to the end of 1992. It starts with the application of the theory of elasticity to a homogeneous continuum. Then the application to cross-anisotropic solids is discussed. The application of a cross-anisotropic model, primarily in geotechnical engineering, was reviewed. Finally, some classical works on the application of the cross-anisotropic model to layered elastic system were studied. These authors attempted to solve the problem either by closed-form solutions or by finite-differences method. Only the simplest of the cases were solved by these means. However, they served a very useful purpose by providing accepted solutions for the verification of finite-element models such as that proposed in this thesis.

7.3 FIELD-WORK

Field-work consisted of collecting deflection data on five airports spanning a wide range of geotechnical, pavement-structure and loading conditions. Climate-wise they are all in the wet and cold regions (AASHTO classification); however, there are subtle climatological differences between the sites. The data was collected in two different series once in 1985 and again in 1988. Along with the deflection testing, the pavements were cored to determine the construction thicknesses as well as to obtain asphaltic cores. From the asphalt cores, asphalt cement was extracted to determine penetration and viscosity at 4°C, 25°C, 40°C, 100°C, 135°C and at 145°C. With these data the Shell Bitumen Chart was constructed. From this chart the bitumen stiffness at any other temperature could be determined. By using McLeod's nomograph the mix stiffness was determined. Base and subgrade samples were also recovered for simple geotechnical index tests. Pressuremeter tests were done at the core locations.

7.4 ANALYSIS

Analysis of the deflection data was done using the ANSYS finite-element program. The pavement was modelled both as an isotropic and as a cross-anisotropic layered elastic solid. Stress-dependency of moduli and yield criteria were not considered in the models. However, the model is capable of considering these variations. The number of layers was not limited. In this investigation the maximum number of layers considered was six.

Four load conditions were considered: 500-600 kPa, 800-900 kPa, 1,100-1,200 kPa and 1,400-1,500 kPa. At each site between 15 and 20 stations along the wheel paths and covering the entire runway were investigated with the anisotropic model. Of these, five stations were arbitrarily selected for analysis with the isotropic model. The main reason for not analyzing all the fifteen stations also by the isotropic model was the considerable amount of computer time needed. At each station, for each load three criteria of matching the deflection basins were tried. These were: 1) matching the area of the basin; 2) matching the maximum deflection under the load; and 3) the RMS value of the deflections.

The optimization module in the ANSYS program was used to find the optimum value of moduli which would minimize the differences between computed and measured quantities by the three criteria mentioned above. The number of optimization loops was between 16 and 50, with an average of 20 loops. It is easy to see the amount of data and computer time to generate that data: (15 stations x 4 loads x 3 criteria x 20 optimization loops). After calculation by ANSYS, this data had to be still reworked to prepare the charts and tables presented in this thesis. For this reason, the comparison between isotropic and anisotropic models was restricted to five arbitrarily selected stations at each site. This has the obvious disadvantage of generating a small data-base, particularly when statistical analyses are presented.

From the optimization loops the top five solutions were chosen as the most probable range for moduli. The average of this range was considered the most probable value of the moduli. These were the values used in comparisons and in the various statistical analyses. For comparing the deflection basins and stress distributions, however, all the five top solutions were used. Selected typical data were presented in each chapter for discussions. The complete data and analysis results are presented in Volume 2 of this thesis.

7.5 RESULTS AND CONCLUSIONS

The results have been presented and discussed under various chapters. Based on those discussions, various conclusions and hypotheses were presented. Here these conclusions are summed together and presented as the main findings of this research:

1. A general purpose finite-element method such as ANSYS presents a powerful algorithm to model the pavement under many different assumptions of material properties and layer geometry. Such an algorithm gives practically unrestricted freedom to model the pavement in the most general way.

2. The "AREA"-of-the-basin criterion is by far the most effective method of matching the deflection basins in a back-calculation procedure. Philosophically, it can be defended based on the fact that the deflection basin represents the energy absorbed by the pavement under the falling weight. Thus a match of the shape of volume of the basin should lead to the true material properties. For an axi-symmetrical case, this will reduce to matching the area of the deflection basin. Any method which attempts to match more than one discrete deflection point should also give results approaching the true value of the moduli.

3. Based on the above conclusion, it would be desirable to precede the ANSYS analysis with a curve-fitting program such as is used by ISSEM-4. This will permit closer integration of the basin.

4. Some of the pavements tested in this investigation were aged and badly cracked. Yet, being airfield pavements to carry heavy jet aircraft, they were of substantial construction. Therefore the deflection basins often crossed the cracks. In such cases there is an abrupt deviation of the observed basin from the computed ones. In these

cases the classical models, including the one presented herein, cannot properly analyze the pavement. A more general model should be capable of incorporating a "gap" element across which only partial, or no, load transfer will exist. The ANSYS algorithm is capable of modelling such gap elements. However, it is suggested that a method should be developed to input the pavement condition during deflection testing and to quantify it later during the subsequent analysis.

5. For the pavements tested, the unbound layers exhibited cross-anisotropic ratios ranging between 0.5 and 3. These are the general range reported in the literature for these sites.

6. The stress distribution appeared to be relatively insensitive to the variations in the moduli. This raises a question whether one should be overly concerned with the determination of exact values of moduli. For, in the final analysis, the stresses and strains are the ones which determine the performance of the pavements.

7. Attempts to correlate computed moduli to independently measured moduli met with limited success. It is suggested that using a small data base, and not considering other significant factors, might be the cause for the less-than-spectacular correlations. Yet, the correlations are modest and merit further investigation.

8. In the case of asphalt moduli, three sites gave moderate correlations while the other two showed no correlation at all. When the data were pooled, there was no correlation. On further examination of the pavement history, it would appear that the younger the pavements, the better is the correlation; the older the pavements are, the poorer is the correlation. This leads one back to the conclusion regarding aged and fatigued pavements as discussed (see # 4 above).

9. Isotropic models gave better correlations than cross-anisotropic models. One should, however, remember that the asphaltic concrete layer was always considered isotropic. Taken together with the comments earlier about the insensitivity of stress distribution, it is suggested that the isotropic model for the pavement is adequate.

10. In the regression relationships presented for asphaltic concrete, no physical meaning can be attached to the intercept of the line. However, the slope may be looked upon as the ratio of dynamic to static moduli. For the material tested in this investigation this is approximately two.

11. In comparing the computed moduli for the unbound materials with the pressuremeter-measured moduli, it was found that the data from individual sites showed no correlation at all. This was explained as due to the fact that in any one site, a high uniformity of material could be expected. This results in the data points being clustered around in a narrow region. Thus a regression analysis is not possible nor is not meaningful. However, when the data was pooled, a much better correlation could be seen.

12. In the case of unbound materials, many other factors influence the modulus. These are gradation, moisture content, in-place density to name some. These must be taken into account and a multivariate analysis, instead of a univariate analysis, should be done. It is expected that a better correlation would result.

13. As in the case of asphaltic concrete, the isotropic model gave a much better correlation coefficient than the cross-anisotropic model for unbound materials. This would again indicate that the isotropic model is quite adequate in the analysis of pavements.

14. It is concluded that further tests, and statistical analyses are needed before the pressuremeter can be used to predict reialbly the moduli of unbound layers to be used in a layered elastic analysis.

15. No physical significance for the regression parameters for the unbound layers can be given.

7.6 SUGGESTION FOR FURTHER RESEARCH

The conclusions presented in the previous section would clearly indicate that the back-calculation and evaluation of pavements are far from an exact science despite advanced theories, highly sophisticated and precise measuring equipment, and the availability of fast computing aids. In Chapters 5 and 6 and in the previous sections of this chapter, attention was drawn to many still-outstanding questions in the field. In what follows, these will be discussed to explain why the author thinks they need our attention and what the author's approach would be to these problems.

7.6.1 Field Data Collection

This is an important phase in pavement research. This is why the Strategic Highway Research Program (SHRP) in the USA and its Canadian counterpart (C-SHRP) are spending tens of millions of dollars to obtain reliable data. Good valid results can be obtained only from good quality data. The author must admit that the work in this thesis fell somewhat short of this broad objective. When the research was started, some ten years back, there were no guidelines. Also, the testing was part of Transport Canada's normal design and rehabilitation programs. Therefore, the expenses for collecting data especially for research was not a priority, though Transport Canada did help the author as best as they could within their budgetary constraints. Papers on non-destructive testing were mushrooming. The findings were not always conclusive and were often contradictory. This resulted in everyone devising one's own method of testing and was often directed to the particular topic in which the researcher was interested. Based on the experience gained by the author during this test series, it was determined that at least the following points need investigation:

7.6.1.1 Size of Plate

The size of the plate should be chosen in relation to the pavement thickness and in relation to the surface layer. It was reported, in Chapter 4, that the 1985 test series was done with a 300 mm diameter plate. It was also felt that probably for thick airfield pavements this might not be adequate to mobilize the response of the entire pavement. This study did not, however, analyze this problem and hence it is not possible to present any data linking the effect of plate to the distribution of stress in the pavement. It is, however, suggested that this should be studied in future. A different problem is the effect of confinement that a plate can impose on the surface layer. Some evidence is available to this effect in the literature. It will be realised that these two requirements are contradictory to each other. A thick pavement might require a large rigid plate, but then could introduce confining stresses which could distort the results. Further study is needed in this respect.

7.6.1.2 Sensor Directions and Spacing

In testing thick pavements, such as those in this study, the deflection sensors should reach far enough to define the tapering end of the deflection basin. This was suggested as one of the probable reasons for the large coefficient of variations in the readings of the nearest sensors in the 1985 series of tests. This would be particularly significant if one uses the area-of-the-basin method to back-calculate the moduli. Even though the deflections are small at these distances, the area in the undefined region might be large enough to distort the results significantly.

7.6.1.3 Shape of Deflection Basin in Different Directions

The 1985 series of tests was modelled after Transport Canada's Benkelman Beam test procedures. However, the readings were not taken in radial directions, but always in one direction. This was unfortunate, because the former would have provided one direct evidence of anisotropy. It could have also provided information as to which layers are anisotropic. The back-calculations in this series indicate that the granular base and subgrade of the test pavements show moderate anisotropy. However, there is no direct evidence from the field to show that the pavement response is anisotropic. It is, therefore, suggested that in future testing, deflections should be measured at least orthogonally. This can be done with or without modification of equipment. The modification needed to the equipment is simple and inexpensive.

7.6.1.4 Instrumented Pavements

One of the surprising results from this investigation is the relative insensitivity of the stress distribution to the variations in the moduli. It is conceded that the optimization module prevented a wide variation in the modulus values, in most cases, because such solutions would have been characterized as "infeasible". In some cases, though, there were significant variations. Yet, the stress distributions were practically identical. Therefore, there is a legitimate question as to whether the great efforts being spent to write algorithms to compute the moduli very accurately are warranted. On the other hand it is also legitimate to question whether the stresses calculated are indeed the actual stresses and as to how much confidence one can place on the stress calculations. This is a question that must be answered so that one can, at some future date, recommend a few reliable back-calculation methods with great confidence. However, these questions can be answered only by controlled testing of instrumented pavements. In the past twenty years considerable effort has been spent on the development of analysis systems and computer algorithms. It is now time to check these computational methods against the response of instrumented pavements.

7.6.2 Analysis Methods

7.6.2.1 General

Basically, the analysis method was developed by Burmister in the 1940's and has been enhanced by many since then. Burmister's theory dealt with the isotropic layered system. In the late 1950's and early 1960's, computer algorithms based on Burmister's theory began appearing. As the power of the computers increased dramatically, many of the restrictive assumptions such as linearity, homogeneity, etc. could be dropped. At the present time, most of the computer programs are based on three or four well-known and powerful algorithms. In the mid 1960's to late 1960's, Gerrard and his colleagues developed methods to consider anisotropy. Only the simplest cases could be solved.

However, there is no single program or software package that can consider all these practical restrictions and leave the option of using all or some of the concepts in a generalised pavement model.

In this investigation it was shown that a general-purpose finite-element program, such as ANSYS, could be a very useful computational tool. However, it is suggested that much work or improvements still need to be done.

7.6.2.2 Modelling Capabilities to be Developed

In this thesis the following were not considered explicitly:

1. Non-linearity of the stress-strain function;
2. Stress-dependency of material, particularly of granular base;
3. Temperature-dependency of asphalt materials;
4. Three-dimensional model if true anisotropy were measured in the field;
5. Cracked surfaces (models with gap elements);
6. Yield criteria for materials, particularly for unbound materials;
7. Linear or non-linear dynamic analysis so that the impulse load of the FWD could be truly modelled. Similarly the oscillatory loading of Dynaflect or other loading devices could be also truly modelled; and
8. Slip- and non-slip criteria for composite pavements (very important for overlays, and rehabilitation designs).

It is suggested that all of these capabilities exist with ANSYS and probably with any other similar general-purpose finite-element method. Therefore, one can either attempt to fully utilize the capabilities of a system such as ANSYS, or develop a general-purpose finite-element model that can consider these factors. These programs should be preferably built as independent and interacting modules so that the user has the option of using a simple model or a complex one, depending on the problem on hand. There is considerable scope for further research in this direction.

Since it was suggested earlier that the "AREA"-of-the-basin method yields by far the best correlation between observed and computed deflections, it will be useful to couple a curve-fitting program to a finite-element program. This will result in a tighter control over the objective function in any optimization routine. Also, it would be helpful to examine an energy-based formulation for the deformation basin.

7.6.3 Material Properties

For a computational method to be used with confidence in routine pavement design, evaluation, and research, it should be able to model the real materials in the pavement. Such a model can developed only by correlating computed properties to the actual properties that must be measured by independent means. This matter has been the thrust of this thesis. There are admittedly a few drawbacks in the approach adopted in this thesis. In the case of asphalt surface materials, a nomographic approach was used. Whether a nomographic approach is the most suitable in an advanced research is debatable. The author defends its use for the following reasons;

1. This nomograph is accepted by great many researchers in this field;
2. Nearly 40 years after its publication it still forms the basis of design in many mechanistic design procedures and computer algorithms (e.g. Valkering and Stapel, 1992; Brown and Dawson 1992);
3. The experimental set-up to measure the truly dynamic behaviour of asphalt is very expensive and is available currently only in few laboratories.

However, it would be worthwhile, at least, to measure the resilient modulus as outlined in ASTM and as in the SHRP (Strategic Highway Research Program) protocols. Another drawback of the thesis was the comparison of the nomographic results, which were based on dynamic tests, to the results of a static analysis.

In the case of unbound materials, this thesis used the pressuremeter. The correlation of the pressuremeter moduli with other forms of traditional test methods in pavement engineering (such as plate load tests, resilient moduli from triaxial tests, etc.) has been investigated before by Briaud and his colleagues in Texas A & M University. They have not given any statistics about the correlation but concluded that the pressuremeter modulus is just as reliable as triaxial tests or other tests. In this thesis the pooled results from five different sites with varying soil, moisture, and climatic conditions gave acceptable correlations. It is submitted that this investigation should be pursued further to:

1. Investigate whether a multivariate analysis including other factors such as gradation, moisture content, and in-situ density etc. would improve the correlation;
2. Expand the data-base to include other types of soil and climatic conditions.

7.7 CONCLUDING REMARKS

This thesis analyzed five airfield pavements with a wide range of subgrade conditions, structural make-up, climatic conditions, age, and loading conditions. The analyses were done using a general-purpose finite-element program. It was demonstrated that this program could be used to compute the layer moduli for both anisotropic and isotropic behaviour of the materials. It was also shown that the simpler isotropic model represented the pavement structure quite adequately. An optimization technique was introduced to arrive at the most probable values of the layer moduli. Finally the computed moduli were compared with independently measured moduli. The correlations, while not high, are acceptable and lay a *prima facie* case for further continuing research in this field.

As unique contributions of this thesis the following are cited:

1. Development of an anisotropic model;
2. Incorporation of an optimization technique to arrive at layer moduli.
3. Establishment that the area-of-basin provides the best measure for pavement response and hence should be used in the back-calculation of layer moduli.
4. Establishment of acceptable correlations between computed and measured moduli.

7.7.1 Development of an Anisotropic Mmodel

Pavement structures have been traditionally modelled as elastic, isotropic and homogeneous layered systems. However, geotechnical engineers have found it increasingly necessary to consider anisotropy when analyzing earth structures. Thus there was always the nagging question whether anisotropy would be an important factor in the analyses of pavement structures where the nature of the materials and the methods of construction would likely introduce anisotropy in the layers. With the introduction of the pavement pressuremeter to determine the layer moduli directly *in-situ*, it became important to address this question. To the author's knowledge this thesis is the first research document where not only a model to incorporate anisotropic properties has been suggested but also demonstrates quantitatively that the influence of anisotropy in the layer properties is not significant. Thus the much simpler isotropic model is adequate to characterize the pavement. Furthermore, it also settled the question that the layer moduli measured *in-situ* with simple instruments such as the pavement pressuremeter can be used in the evaluation and analyses of pavement structures.

7.7.2 Incorporation of an Optimization Technique

It is suggested that this thesis is the first research effort to use an optimization technique to back-calculate the layer moduli. No other program is currently available, either commercially developed or developed in the different universities for research purposes, with which practical limits for the material properties *for each of the layers* can be imposed and one can ask the program to seek a feasible solution. What is more, **any or all of the elastic parameters for each layer** (two for isotropic model and five for the anisotropic model) can be varied simultaneously to arrive at the most probable combination of layer moduli for that particular pavement structure responding to a particular loading condition. The lack of such a technique has been the primary reason for the wide divergence of modulus values reported in the literature when different researchers analyzed the same structure and the same deflection data. The technique is transparent in the model suggested in the thesis so that the limits can be set by the users based on their experience or tests. Recent publications (Sivaneswaran et al, 1991) would indicate that some researchers have recognized this problem and are proceeding in the direction suggested by this thesis. However, this thesis has gone even further than suggested by these publications.

7.7.3 Establishment of the Area-of-the Basin Criterion for Back-calculation

Current algorithms for back-calculations attempt to match the maximum deflections (Shell, Chevron, Elsym-5 etc.), deflections at discrete points (ISSEM-4, SENOL) or some other single parameter such as curvature to match the measured deflections to the computed deflections. This thesis suggests, on the other hand, to compare the areas of the measured and computed deflection basins (or the volume of the basins if a three-dimensional model is used). By comparing the results obtained by the "area" method and two other methods it was shown that the "area" method is superior to the other. Conceptually, it should be so because, the area or the volume of the basin represents the energy absorbed by the pavement in deflecting under the imposed load and hence should be the best parameter to compare. Again this thesis is the first research effort to analytically demonstrate this conclusively.

7.7.4 Establishment of Acceptable Correlations Between Measured and Computed Moduli

Often, in the literature, one finds wide divergence between layer moduli measured in the laboratory and the ones back-calculated from deflection data. While, the back-calculated data is often referred to as *in-situ* moduli there has been no reports of correlation between computed moduli and moduli directly measured by in-situ geotechnical tests, except the data published by Briaud et al. (1986, 1987). The relevance of laboratory-measured moduli for pavement analyses has been often questioned. On the other hand, the data published by Briaud and his colleagues (*loc. cit.*) is limited and not conclusive. In this respect this thesis has, not only confirmed Briaud's assertion that the pavement pressuremeter can be used to measure moduli values of earth materials but also has produced acceptable correlations between the measured and computed moduli. Additional work in this direction would be further useful contribution.

It is,therefore, suggested that this thesis has met the objectives it set out to and has made some unique and original contributions to the field of pavement engineering including a powerful general-purpose finite element model with an optimization technique. It addressed some outstanding questions such as the influence of anisotropy, determination of *in-situ* moduli, and the relevance of various type of tests in determining material properties for back-calculation. In the preceding sections many suggestions were made for further research and work in this field.

REFERENCES

ASTM, 1949. Symposium on load tests of bearing capacity of soils. STP 79.

ASTM, 1988. First international symposium on non-destructive testing and back-calculation of moduli. Baltimore, Md.

ASTM/TRB, 1991. Second international symposium on nondestructive testing and back-calculation of moduli. Nashville, Tn. Proceedings published in TRR 1377, 1992.

Acum, W.E.A. and Fox, L. 1951. Computation of load stresses in a three layer elastic system. Geotechnique, v. 2, p. 293.

Ahlvin, R.G. and Ulery, H.H. 1962. Tabulated values for the determination of complete pattern of stresses, strains and deflections beneath a uniform circular load on a homogeneous half space. HRB Bulletin 342, p.1.

Ali, N.A. and Khosla, N.P. 1987. Determination of layer moduli using the falling weight deflectometer. Pre-print copy, TRB Annual meeting 1987.

Allen, J.J. 1973. The effects of stress history on the resilient response of soils, Report No. TR-M-49, U.S. Army Construction Engineering Research Laboratory, Champaign, Illinois.

Allen, J.J. and Thompson, M.R. 1974. Resilient response of granular materials subjected to time-dependent lateral stresses. TRR 510, p. 1.

Anani, B.A. 1979. An evaluation of in-situ elastic moduli from surface deflection basins of multi-layer flexible pavements. Ph.D Thesis in civil engineering, Pennsylvania State University, 173 pp.

Argue, G.H. 1970. The resilient modulus of base and asphalt layers in flexible pavements. M.Sc. Thesis, Carleton University, Ottawa, Canada.

Atkinson, J.H. 1975. Anisotropic elastic deformations in laboratory tests on undisturbed London clay. Geotechnique, v. 25, no. 2, p. 357.

Baguelin, F., Jezequel, J.F. and Shields, D.H. 1978. The pressuremeter and foundation engineering. Trans Tech publications.

Barden, L. 1963. Stresses and displacements in a cross anisotropic soil. Geotechnique, v. 13, p. 198. Discussions: Geotechnique, v. 14:1:59, v. 14:3:278 and v. 15: p.317.

Barker, W.R. 1972. Non-linear finite element analysis of heavily loaded airfield pavements. Proc. Symp. on the Application of the Finite Element Method in Geotech. Eng., U.S. Army WES, Vickburg, Miss., Vol. II, pp. 657, (editor: C.S. Desai).

Barksdale, R.D. 1972. Laboratory evaluation of rutting in base course materials. 3rd Intl. Conf. on Struc. Design of Asphalt Pavements, London, U.K. Vol. 1, pp. 161.

Barksdale, R.D. and Hicks, R.G. 1973. Material characterization and layered theory for use in fatigue analysis. Highway Research Board, Spec. Rept., 140, pp. 20.

Bauer, G.E., Scott, J.D., and Shields, D.H. 1973. The deformation properties of a clay crust. Proc. of the 8th International Conference on Soil Mechanics and Foundation Engineering, Moscow, v. 1. pp. 31-38.

Bauer, G.E. and McRostie, G.C. 1986. Building performance predicted from in-situ and laboratory tests. Proc. 39th Can. Geotech. Conf., Ottawa, Ont., Canada, pp. 329.

Bauer, G.E. and Tanaka, A. 1988. Penetration testing of a desiccated clay crust. Proc. 1st Intl. Symp. on Penetration Testing, ISOPT-1, Orlando, Fla., pp. 477.

Bell, C.W. 1983. Use of the Shell bitumen test data chart in evaluation of asphalt data. Proc. of Assoc. of Asphalt Paving Technilogists, Technical session, Atlanta, Ga. v. 52, pp. 1-31.

Belloti, R., Ghionna, V., Jamiolkowski, M., Robertson, P.K. and Peterson, R.W. 1989. Interpretation of moduli from self-boring pressuremeter tests in sand. Geotechnique, Vol. 39, 2, pp. 269.

Bhattacharya, R.K., 1968, Stresses and displacements in cross-anisotropic half space due to axi-symmetric loading on the top surface. Ph.D. Thesis, University of Wisconsin, Madison, Wis., pp. 162.

Biot, M. 1937. Bending of an infinite beam on an elastic foundation. Proc. ASME, Vol. 59, pp. A-1.

Bowles, J.E. 1988. Foundation analysis and design. 4th Ed., McGraw-Hill, New York.

Boyce, H.R. 1980. A non-linear model for the elastic behaviour of granular materials under repeated loading. Proc. Intl. Symp. on Soils Under Cyclic and Transient Loading. Swansea, England, Jan. 1980, A.A. Balkema, Rotterdam and Boston.

Boyce, H.R. and Brown, S.F. 1976. Measurement of elastic strain in granular materials. Geotechnique, Vol. 26, No. 4, Tech. Notes, pp. 637.

Briaud, J.-L. and Shields, D.H. 1979. A special pressuremeter and pressuremeter test for pavement evaluation and design. Geotech. Test. J., ASTM, Vol. 2, No. 3, pp. 143.

Briaud, J.-L. 1979. The pressuremeter: application to pavement design. Ph.D. Thesis, Univ. of Ottawa, Ottawa, Ont., Canada.

Briaud, J.-L. and Shields, D.H. 1981. Pressuremeter tests at very shallow depths. J. Geotech. Div., Proc. ASCE, Vol. 107, GT 8, pp. 1023.

Briaud, J.-L., Lytton, R.L. and Hung, J.-T. 1983. Obtaining moduli from cyclic pressuremeter tests. J. of Geotech. Eng., Div. Proc. ASCE, Vol. 109, No. 5, pp. 657.

Briaud, J.-L., Tucker, L.M. and Makarim, C.A. 1985. Pressuremeter standards and pressuremeter parameters. 2nd Intl. Symp. on Pressuremeter and its Marine Applications, ASTM STP 950, pp. 330.

Briaud, J.-L., Terry, T.A., Cosentino, P.J., Tucker, L.M. and Lytton, R.L. 1986. Influence of stress, strain, creep and cycles on moduli from preboring and driven pressuremeters. Research Rept. No. 7035-1 prepared for Pailen-Johnson Assoc. and FAA by the Texas A & M Univ.

Briaud, J.-L., Cosentino, P.J. and Terry, T.A. 1987. Pressuremeter moduli for airport pavement design and evaluation" Rept. prepared for FAA, Rept. No. DOT/FAA/PM-87/10.

Briaud, J.-L. and Cosentino, P.J. 1989. The use of pressuremeter in the design of airfield pavements. Symp. on the State-of-the-Art of Pavement Response Monitoring Systems in Roads and Airfields. US Army CRREL, West Lebanon, NH (pre-print copy).

Brinch Hansen, J. 1963. Discussion of Kondner's paper. Proc. ASCE, Vol. 89, SM 4, pp. 241.

Broms, B. 1971. Lateral earth pressures due to compaction of cohesionless soils. Proc. 4th Budapest Conf. on Soil Mechanics, Budapest, pp. 371.

Brooker, E.W. and Ireland, H.O. 1965. Earth pressures at rest related to stress history. Can. Geotech. J., Vol. 2, No. 1, pp. 1-15.

Brown, S.F. 1982. Material characteristics for analytical pavement design. ***In*** Developments in Highway Engineering, Chap. 2 (editor P.S. Pell), Allied Publ. Co., London, U.K.

Brown, S.F. and Snaith, M.S. 1974. The measurement of recoverable and irrecoverable deformations in the repeated load triaxial test. Tech. Note, Geotechnique, Vol. 24, pp. 255.

Brown, S.F., Leshine, A.K.F. and Hyde, A.F.L. 1975. Repeated load triaxial tests on a silty clay. Geotechnique, Vol. 25, pp. 95.

Brown, S.F. and Pappin, J.W. 1981. Analysis of pavements with granular bases. TRR 810, TRB, pp. 17.

Brown, S.F. and Pappin, J.W. 1985. The modelling granular materials in pavements. TRR 1022, TRB, pp. 45.

Brown, S.F., Tam, W. and Brunton, J. 1986. Development of an analytical method for the structural evaluation of pavements. Proc. 2nd Intl. Conf. on Bearing Capacity of Roads and Airfields, Plymouth, U.K. pp. 267.

Brown, S.F. and Dawson, A.R. 1992. Two-stage mechanistic approach to asphalt pavement dssign. Proceedings of the 7th International Conference on Asphalt Pavements, Nottingham, July, 1992. v. 1. pp. 16.

Burmister, D.M. 1943. Theory of stresses and displacements in layered systems and application to design of airport runways. Proc. Highway Research Board, Vol. 22.

Burmister, D.M. 1945. The general theory of stresses and displacement in layered systems. Part 1: Feb. 1945; Part 2: Mar. 1945; Part 3: May 1945; J. of Appl. Physics, Vol. 16.

Burmister, D.M. 1949. Contribution to the general discussion. Symp. on Load Tests on Bearing Capacity of Soils, ASTM STP 79, pp. 139.

Burmister, D.M. 1958. Evaluation of pavement systems of the WASHO Road Test by layered systems methods, HRB Bulletin, 177.

Burmister, D.M. 1962. Application of layered system concepts and principles to the interpretation and evaluation of asphalt pavement performance and to design and construction. Proc. 1st Intl. Conf. on the Struc. design of Asphalt Pavements, Ann Arbor, pp. 441.

Busching, H.W., Goetz, W.H. and Harr, M.E. 1967. Stress-deformation behaviour of anisotropic bituminous mixtures. Proc. AAPT, Vol. 36, pp. 632. Discussions by Finn, F.N. and Nair, K. pp. 663; by Secor, G. and Monismith, C. pp. 668.

Bush III, A.J. 1980. Nondestructive testing for light aircraft pavements. Phase I: evaluation of nondestructive testing devices. Final Rept. prepared for the FAA, Rept. No. FAA-RD-80-9, Jan.1980.

Bush, III, A.J., Alexander, D.R. and Hall Jr., A.W. 1985. Nondestructive airfield rigid pavement evaluation. 3rd Intl. Conf. on the Design and Rehabilitation of Concrete Pavements, Purdue Univ., West Lafayette, Indiana (pre-print copy).

C.G.R.A. 1959. Technical publication no. 11: manual on pavement investigations. Can. Good Roads Assoc. (Transp. Assoc. of Canada - TAC), Ottawa, Canada.

C.G.R.A. 1962. Pavement evaluation studies in Canada. Proc. 1st Intl. Conf. on Structural Design of Asphalt Pavements, Ann Arbor, Mich., pp. 139.

Campanella, R.G., Robertson, P.K. and Gillespie, D. 1986. Seismic cone penetration test. In-Situ 86, Proc. of ASCE Specialty Symp. on the Use of In-Situ Testing in Geotechnical Engineering, Blackburg, VA, pp. 116.

Campanella, R.G. and Robertson, P.K. 1986. Short course on cone penetration testing. Petersburg, Fla., Feb.

Carder, D.R., Pocock, R.G. and Murray, R.T. 1977. Experimental retaining wall facility - lateral stress measurements with sand backfill. TRRL, Lab. Rept. 766, Crowthorne, Berkshire, Eng.

Carder, D.R., Murray, R.T. and Krawczyk, J.V. 1980. Earth pressure against an experimental retaining wall backfilled with silty clay. TRRL Lab. Rept. 946, Crowthorne, Berkshire, Eng.

Carrier, G.F. 1946. Propagation of waves in orthotropic media. Quarterly of Applied Mathematics, 4, pp. 160-165.

Chang, D.W., Roesset, J.M. and Stokoe II, K.H. Nonlinear effects in falling weight deflectometer tests. Research Record 1355, TRB, National Research Council, Washington, D.C., 1992, pp. 1-16.

Cheung, Y.K. 1975. Numerical analysis of pavements. In Soil Mechanics - Recent Developments. Proc. of a Symp. held at the Univ. of New South Wales, Australia (editor S. Valliappan).

Chowdhury, R.N. 1972. Deformation problem in anisotropic soil - application of finite element method. Proc. of the Specialty Conf. on Finite Element Method in Civil Eng., McGill Univ., Que., Canada, pp. 653.

Chowdhury, R.N. 1978. Effective-stress parameters of anisotropic soil. Tech. Note. J. of Geotech. Eng., Div. Proc. ASCE, Vol. 104, GT 1, pp. 125.

Claessen, A.I.M., Edwards, J.M., Sommer, P. and Uge, P. 1977. Asphalt pavement design. Proc. of the 4th Intl. Conf. on Struc. Design of Asphalt Pavements, Ann Arbor, Mich., Vol. 1, pp. 39.

Clayton, Sparks, and Associates. 1980. Pavement deflection testing vehicle: a feasibility study. Rept. prepared for Transport Canada, Transportation Development Centre, Ottawa, Ont., Canada, Oct.

Coetzee, N.F., Mahoney, J.P. and Studstad, R.N. 1988. A performance evaluation of selected state-of-the-art backcalculation computer programs. ASTM: 1st Intl. Symp. on Nondestructive Testing and Backcalculation of Moduli, Baltimore, Md.

Coffman, B.S., Ilves, G. and Edwards, W.F. 1970. Isotropy and asphaltic concrete. Highway Research Record, 329, Transportation Research Brd., Washington, D.C. pp. 65.

Cosentino, P.J. 1987. Pressuremeter moduli for airport pavement design. Ph.D. Thesis, Texas A & M Univ., College Stn., Texas.

D'Amato, P.A. and Witczak, M.W. 1980. Analysis of in-situ granular layer modulus from Dynamic Road Rater Deflection, TRR 755, TRB, pp. 20.

Davidson, R.R. 1979. Interpretation of the pressuremeter test. Tech. Memo. No. 104-78, prepared for the Practice Comm., Woodward-Clyde Consultants, Denver, Col., (revised Dec. 1979).

Deacon, J.A. 1970. Materials characterization - Experimnetal Behaviour. Proceedings, Workshop i\on structural design of asphalt concrete pavement systems, HRB, Special Report 126, Wash., D.C.

Dehlen, G.L. 1969. The effect of nonlinear material response on the behaviour of pavements subjected to traffic loads. Ph.D. Thesis, Univ. of California, Berkeley.

Dempsey, B.J., Herlache, W.A. and Patel, A.J. 1985. A climatic-materials-structural pavement analysis program. TRB Annual Meeting (pre-print copy).

Desai, C.S. 1979. Elementary finite element method. Prentice Hall, N.Y.

Domaschuk, L. and Wade, N.H. 1969. A study of bulk and shear moduli for a sand. J. of Soil Mech. and Found. Div. Proc. ASCE, Vol. 95, SM2, pp. 561.

Dooley, J.C. 1964. Discussion on Pickering's paper. Correspondence, Geotechnique, Vol. 14, No. 3, pp. 278.

Dorman, G.M. and Metcalf, C.T. 1965. Design curves for flexible pavements based on layered elastic system theory. Highway Research Record 71, Highway Research Brd., Washington, D.C. pp. 69.

Douglas, R.A. and Eller, G.L. 1986. Nondestructive pavement testing by wave propagation: advanced methods of analysis and parameter management. TRR 1070, TRB, pp. 53.

Duncan, J.M., Monismith, C.L. and Wilson, E.L. 1968. Finite element analysis for pavements.

HRR 228, HRB, pp. 18.

Duncan, J.M. and Chang, C.Y. 1970. Nonlinear analysis of stress and strain in soils, Journal of Siol Mechanics and Foundation Engineering, ASCE, vol. 96, No. SM 5, 1970, pp. 1629-1653.

Elkins, G.E., Uddin, W. and Hudson, W.R. 1988. Side-by-side field evaluation of deflection testing devices. ASTM: 1st Intl. Symp. on Nondestructive Testing and Backcalculation of Moduli, Baltimore, Md., (preprint copy).

Emery, J.J. 1983. Characterization of flexible pavement components. Unpubl. Rept., Trow Eng. Ltd., Toronto, Canada.

FHWA-TS-87-206, 1986. ELSYM5: Interactive microcomputer version, User's manual: IBM-PC and compatible version.

Feda, J. 1978. Stress in subsoil and methods of final settlement calculation. Elsevier Sc. Publ. Co., N.Y.

Finn, F. and Monismith, C.L. 1984. Asphalt overlay design procedures. NCHRP, Synthesis of Highway Practice, 116.

Foster, C.R. and Fergus, S.M. 1949. Stress distribution in a homogeneous soil. Research Rept. 12-F, presented at the 29th Ann. Meeting of HRB.

Foxworthy, P.T. and Darter, M.I. 1986. Preliminary concepts for FWD testing and evaluation of rigid airfield pavements. TRR 1070, TRB, pp. 77.

Fukagawa, R. and Ohta, H. 1988. Vertical deformation modulus of sand estimated by pressuremeter test and SPT blow count N. Proc. 1st Intl. Symp. on Penetration Testing, ISOPT-1, Orlando, Fla., Vol. 1, pp. 505.

Gazetas, G. 1981. Strip foundation on a cross-anisotropic soil layer subjected to dynamic loading. Geotechnique, Vol. 31, No. 2, pp. 161.

Gazetas, G. 1982. Stresses and displacements in cross-anisotropic soils. J. of Geotech.Div. Proc. ASCE, Vol. 108, GT 4, April, pp. 532.

Gerrard, C.M. and Mulholland, P. 1966. Stress, strain and displacements in a cross-anisotropic and isotropic two layer system. Proc. 3rd Conf. Australian Road Research Brd., Vol. 3, Pt. 2, pp. 1123.

Gerrard, C.M. 1967. Stresses and displacements in layered cross-anisotropic elastic systems. Proc. 5th Australia-New Zealand Conf. on Soil Mech. and Fdn. Eng., Melbourne, Australia, pp. 187.

Gerrard, C.M. 1968. The axi-symmetric deformation of a homogeneous, cross-anisotropic, elastic half space. Highway Research Record 223, HRB, pp. 36.

Gerrard, C.M. and Harrison, W.J. 1971. Analysis of loaded halfspace comprised of anisotropic layers. Commonwealth Sc. and Indus. Research Organization, Australia, Div. of Appl. Geomech., Tech. Paper No. 10.

Gerrard, C.M. 1978. Background to mathematical modelling in geomechanics: the roles of fabric and stress history. In Finite Elements in Geomechanics, (edited by Gudehus), John Wiley & Sons, N.Y. pp. 33.

Gibson, R.E. 1967. Some results concerning displacements and stresses in a non-homogeneous elastic halfspace. Geotechnique, Vol. 17, No. 3, pp. 58: Corrigenda, 1968, Vol. 18, No. 2, pp. 275; 1969, Vol. 19, No. 1, pp. 160.

Gibson, R.E. 1974. The analytical method in soil mechanics. 14th Rankine Lecture, Geotechnique, Vol. 24, No. 2, pp. 115.

Girijavallabhan, C.V. and Reese, L.C. 1968. Finite element method for problems in soil mechanics. J. of the Soil Mechanics Div. Proc. ASCE, Vol. 94, SM 2, pp. 473.

Gomez-Achecar, M. and Thompson, M.R. 1984. Mechanistic design concept for full-depth asphalt concrete pavements. Civil Engineering Studies, Transportation Engineering series No. 41, University of Illinois, Urbana-Champaign.

Gomez-Achecar, M and Thompson, M.R. 1986. ILLI-PAVE based response algorithms for full-depth asphalt concrete flexible pavements. Pre-print copy, Annual meeting of the Transportation Research Board, 1986, Wash., D.C.

Graham, J., Yin, J-H. and Azizi, F. 1989. Prediction of triaxial stress-strain behaviour of Winnipeg clay using anisotropic elasto-plastic model. 42nd Can. Geotech. Conf., Winnipeg, Canada (pre-print copy).

Graham, J. and Houlsby, G.T. 1983. Anisotropic elasticity of natural clays. Geotechnique, Vol. 33, pp. 165.

Hardin, B.O. and Banford, G.E. 1989. Elasticity of particulate materials. J. of Geotech. Eng. Proc. ASCE, Vol. 115, No. 6, pp. 788.

Harris, G.M. 1984(a). Earth pressure measurements behind a 20 m high rigid retaining wall. Proc. 8th Regional Conf. for Africa on Soil Mech. and Fdn. Eng., Harare, Zimbabwe, Vol. 1, pp. 443, A.A. Balkema, Rotterdam, Boston.

Harris, G.M. 1984(b). On the magnitude of residual earth pressures induced by compaction equipment. Proc. 8th Regional Conf. for Africa, Harare, Zimbabwe, Vol. 1, pp. 453.

A.A. Balkema, Rotterdam, Boston.

Heukelom, W. and Foster, C.R. 1960. Dynamic testing of pavements. J. of Soil Mech. Div. Proc. ASCE, Vol. 86, SM1, pp. 1.

Heukelom, W. 1961. Analysis of dynamic deflections of soil and pavements. Geotechnique, Vol. 11, pp. 224.

Heukelom, W. and Klomp, A.J.G. 1964. Road design and dynamic loads. Proc. AAPT, Vol. 33, pp. 92.

Hicks, R.G. and Monismith, C.L. 1971. Factors influencing the resilient response of granular materials. Highway Research Record 345, HRB, pp. 15

Hoffman, M.S. and Thompson, M.R. 1982. Backcalculating nonlinear resilient moduli from deflection data. Transportation Research Record 852, TRB, pp. 42.

Houlsby, G.T. and Withers, N.I. 1988. Analysis of one pressuremeter tests in clay. Geotechnique, Vol. 38, No. 4, pp. 575.

Huang, Y.H. 1971. Deflection and curvature as criteria for flexible pavement design and evaluation. HRB 345, HRB, pp. 1. Discussion By Vaswani, N.K. pp. 12.

Hughes, J.M.O. Bachus, R.C., Benoit, J. and Deshpande, S.C. 1986. The pressuremeter: an in-situ test instrument which provides useful data for geotechnical design. Course Notes for "How To" Session, In-Situ, ASCE Specialty Symp. On The Use Of In-Situ Tests In Geotechnical Eng., Blacksburg, Va.

Hung, J.T., Briaud, J.-L. and Lytton, R.L. 1982. Layer equivalency factors and deformation characteristics of flexible pavements. Research Report No. TTI-2-80-284-3, Texas Transportation Institute, Austin, Texas.

Idriss, I.M., Dobry, R. and Sings, R.D. 1978. Nonlinear behaviour of soft clays during cyclic loading. Journal of Geotechnical Engineering, ASCE, vol. 104, GT 12.

Ingold, T.S. 1979. The effects of compaction on retaining walls. Geotechnique, Vol. 29, No. 3, pp.265.

Ingold, T.S. 1980. Lateral earth pressures - a reconsideration. Ground Engineering Journal, May, pp. 39.

Jaeger, J.C. 1969. Elasticity, fracture and flow. Metheun's Monographs On Physical Subjects, Metheun & Co., London, U.K.

Jones, A. 1962. Tables of stresses in three layer elastic systems. Highway Research Bulletin

342, HRB, pp. 176.

Jones, M.P. and Witczak, M.W. 1977. Subgrade moduli on San Diego test road. TRR 641, TRB, pp. 1

Josselin de Jong, G. 1963. Statics and kinematics of the failable zones of granular materials. U. Waltman, Delft, Holland.

Jung, F.W, and Stolle, D.F.E. 1992. Nondestructive testing with falling weight deflectometer on whole and broken asphalt concrete pavements. Transportation Research Record 1377, pp. 183-192.

Kehdr, S. 1985. Deformation characteristics of granular base course in flexible pavements. TRB Annual Meeting, 1965 (pre-print copy).

Kenis, W.J., Sherwood, J.A. and McMohan, T.F. 1982. Verification and application of the VESYS structural subsystem. Proc. of 5th Intl. Conf. on Struc. Design of Asphalt Pavements, Delft, Holland, Vol. 1. pp. 333.

Kennedy, C.K. 1982. Equipment for assessing the structural strength of road pavements. Proc. Intl. Symp. on Bearing Capacity of Roads and Airfields, Trondheim, Norway, Vol. 1. pp. 421.

Kirwan, R.W., and Snaith, M.S. 1976. A simple chart for the prediction of resilient modulus. Technical Notes, Geotechnique, Vol. 26, pp. 212.

Kondner, R.L. 1963. Hyperbolic stress-strain response: Cohesive soils. Journal Soil Mechanics and Foundation Engineering, ASCE, No. 89-1, pp. 115-143.

Koning, H. 1957. Stress distribution in a homogeneous, anisotropic, elastic semi-infinite solid. Proc. 4th Intl. Conf. on Soil Mechanics and Fndn. Eng., London, Vol. 1, pp. 335.

Lam, A.Y.K.-M. 1982. Resilient moduli of flexible pavement materials. M.Sc. Thesis, McMaster University, Hamilton, Ont., Canada.

Lamb, T.W. and Whitman, R.V. 1969. Soil mechanics. John Wiley and Sons, New York.

Lee, K.M. and Rowe, R.K. 1989. Deformation caused by loading and tunnelling. Geotechnique, Vol. 39, pp. 125.

Lees, G. and Salehi, M. 1969. Orientation of particles with special reference to bituminous paving materials. Highway Research Record, 273, Transportation Research Record, pp. 63.

Lekhnitskii, S.G. 1963. Theory of elasticity of an anisotropic elastic body. Holden Day Inc., San Francisco.

Lo, K.Y., Leonards, G.A. and Yuen, C. 1977. Interpretation and significance of anisotropic behaviour of clays. Norwegian Technical Institute Publication No. 117, pp. 1.

Loh, A.K. and Holt, R.T. 1974. Directional variation in undrained shear strength and fabric of Winnipeg upper brown clay. Canadian Geotechnical Journal, v. 11, pp. 430 - 437.

Lytton, R.L. and Smith, R.E. 1985. Use of nondestructive testing in the design of overlays for flexible pavements. TRR, pp. 11.

Mackerle, J. 1988. A guide to the literature on finite and boundary element techniques and software. Software for Engineering Workstations, Vol. 4, Oct., pp. 170.

Majidsadeh, K. 1982. Dynamic deflection as pavement performance indicator. Proc. Intl. Symp. on Bearing Capacity of Roads and Airfields, Trondheim, Norway, Vol. 1., pp. 97.

Marcuson, W.F. and Townsend, F.C. 1976. Effects of specimen reconstruction on cyclic triaxial results. US Army, WES, Misc. Paper, S-76-5.

May, R. 1981. Interpretting dynamic surface deflections in the granular base layer of the pavement structure . FHWA-RD-80-149, Feb. 1981.

May, R.W. and Witczak, M.W. 1981. Effective granular modulus to model pavement responses. TRR 810, TRB, pp. 1.

Mayne, P.W. and Kuhlaway, F.H. 1982. Ko-OCR relationships in soil. J. of Geotechnical Engineering, Proc. ASCE, Vol. 108, GT 6, pp. 851.

McMohan, T.F. and Yoder, E.J. 1960. Design of pressure sensitive cell and modulus studies of pressures in a flexible pavement. HRB Proc. Vol. 1, pp. 245.

Melvern, J. 1974. Continuum mechanics. Prentice Hall, New York.

Michell, J.H. 1900. The stresses in an aelotropic elastic solid with an infinite plane boundary. Proc. London Math. Soc. vol. 32, pp. 247-258.

Mitchell, J.K. 1988. New developments in penetration tests and equipment. Proc. 1st Intl. Symp. on Penetration Testing, Ispot-1, Orlando, Florida, Vol. 1, pp. 245.

Monismith, C.L. Analytically based asphalt pavement design and rehabilitation: Theory to practice, 1962-1992. Research Record 1354, TRB, National Research Council, Washington, D.C., 1992, pp. 5-26.

Moosazadeh, J. and Witczak, M.W. 1985. Prediction of subgrade moduli for soil that exhibits nonlinear behaviour. TRR 810, TRB, pp. 9.

Nair, K and Chang, C.-Y. 1973. Flexible pavement design and management: material characterization. NCHRP Rept. 140, TRB.

Nayak, M. 1973. Elastic settlement of a cross anisotropic medium under axi-symmetric loading. Soils and Foundation, Vol. 13, No. 2, pp. 83.

Naylor, D.J. 1978. Stress-strain laws for soil. Chapter 2 in Developments in Soil Mechanics, Appl. Sc. Publ., London, U.K., Editor: C.R. Scott.

Nazarian, S. 1989. Applicability of spectral-surface-wave-method in determining moduli of pavements. Symp. on the State-of-the-Art of Pavement Response Monitoring Systems in Roads and Airfields, U.S. Army CRREL, West lebanon, (pre-print copy).

Nazarian, S., Stokoe II, K.H. and Biggs, R.C. 1987. Nondestructively delineating changes in modulus profiles of secondary roads. TRR 1136, TRB, pp. 96.

Odemark, N. 1949. Investigations as to the elastic properties of soils and design of pavements according to the theory of elsticity , Meddelande, No. 77, Vaginstitut.

Ofer, Z. 1982. Lateral pressure developed during compaction. TRR 897, TRB, pp. 71.

Osterberg, J.O. 1949. Contribution to the general discussion. Symp. on Load Tests on the Bearing Capacity of Soils, ASTM, STP 79, pp. 128.

Palmer, L.A. and Barber, E.S. 1940. Soil displacements under a circular loaded area. Proc. HRB, Vol. 20, pp. 279; Discussion pp. 319.

Pappin, J.W. and Brown, S.F. 1980. Resilient stress-strain behaviour of a crushed rock. Proc. Intl. Symp. on Soils Under Cyclic and Transient Loading, Swansea, Vol. 1, pp. 1

Peattie, K.R. 1962. Stress and strain factors for three layer elastic systems. Highway Research Bulletin 342, HRB, pp. 215.

Pickering, D.J. 1970. Anisotropic elastic parameters for soils. Geotechnique, Vol. 20, No. 3, pp. 271; Discussions Geotechnique: 1971, Vol. 21, No. 2, pp. 181; Vol. 21, No. 3, pp. 262; Vol. 22, No. 1, pp. 183; Vol. 22, pp. 533.

Poulos, H.G. and Davis, E.M. 1974. Elastic solutions for soil and rock mechanics. John Wiley & Sons, New York.

Rada, G. and Witczak, M.W. 1981. Comprehensive evaluation of laboratory resilient moduli results for granular materials. TRR 810, TRB, pp. 23.

Radhakrishna, N. and Reese, L.C. 1970. A review of applications of the finite element method of analysis to problems in soil and rock mechanics. Soils and Foundations, Vol. 10, No. 3, pp. 95.

Rauhut, J.B., Roberts, F.L. and Kennedy, T.W. 1979. Response and distress models for pavement studies. TRR 715, TRB, pp. 7.

Raymond, G.P. 1972. Prediction of undrained deformations and pore pressure in weak clays under two embankments. Geotechnique, Vol. 22, No. 3, pp. 381.

Richards, B.G. 1966. The significance of moisture flow and equilibria in unsaturated soils in relation to the design of engineering structures built on shallow foundations in Australia, Symposium on permeability and capillarity, ASTM, Atlantic City, N.J.1

Riggins, M. 1981. Viscoelastic characteristics of marine sediments in large scale simple shear. Ph.D. Dissertation, Texas A & M University.

Robertson, P.K., Campanella, R.G., Brown, P.T., Grof, I. and Hughes, J.M.O. 1985. Design of axially and laterally loaded piles using in-situ tests. Can. Geotechnical J., Vol. 22, No. 4, pp. 518.

RocTest. 1981. PENCEL pressuremeter: instruction manual. RocTest Ltee., Montreal, Quebec, Canada.

Roque, R., Romero, P. and Ruth, Byron E. 1992. Evaluation of a dual plate nondestrucive system to better discriminate near-surface layer moduli. TRR 1355, pp. 52-58, Dec. 1992, Wash. D.C.

Sada, A.S. and Ou, C.-D. 1973. Strain-stress relations and failure of anisotropic clays. J. of Geotechnical Eng., ASCE, Vol. 99, SM 12, pp. 1091.

Sanchez-Salinero, Riesset, J.M., Shao, K.-Y., Stokoe II, K.H. and Rix, G.J. 1987. Analytical evaluation of variables affecting surface wave testing of pavements. TRR 1136, TRB, pp. 86.

Sanders, P.J. and Horak, E. 1992. Use of PENCEL pressuremeter in pavement design. Proceedings of the 7th International Conference on Asphalt Pavements, Nottingham, UK, July, 1992. vol. 1, pp. 259.

Sebastyan, G.Y. 1962. Pavement deflection and rebound measurements and their application to pavement design and evaluation. AAPT, New Orleans.

Seed, H.B., Chan, K. and Monismith, C.L. 1955. Effects of repeated loading on the strength and deformations of compacted clay. Proc. of HRB, Vol. 34, pp. 541.

Seed, H.B. and McNeill, R.L. 1956. Soil deformation characteristics in normal compression and repeated loading tests. Highway Research Bulletin 141, pp. 44.

Seed, H.B. and Chan, C.K. 1958. Effect of stress history and frequency of stress application on the deformation of clay subgrade under repeated loading. Proc. HRB, Vol. 37, pp. 555.

Seed, H.B. and Chan, C.K. 1959. Thixotropic characteristics of clays. Trans. ASCE, Vol. 124, pp. 894.

Seed, H.B., McNeill, R.L. and De Givenin, J. 1960. Clay strength increase caused by repeated loading. Trans. ASCE, Vol. 125, pp. 141.

Seed, H.B., Chan, C.K. and Lee, C.E. 1962. Resilience characteristics of subgrade soils and their relation to fatigue in asphalt pavements. Proc. 1st Intl. Conf. on Struc. Design of Asphalt Pavements, Ann Arbor, Mich., pp. 601.

Seed, H.B. and Chan, C.K. 1959. Thixotropic characteristics of clays. Trans. ASCE, Vol. 124, pp. 894.

Seed, H.B., McNeill, R.L. and De Givenin, J. 1960. Clay strength increase caused by repeated loading. Trans. ASCE, Vol. 125, pp. 141.

Seed, H.B., Chan, C.K. and Lee, C.E. 1962. Resilience characteristics of subgrade soils and their relation to fatigue in asphalt pavements. Proc. 1st Intl. Conf. on Struc. Design of Asphalt Pavements, Ann Arbor, Mich., pp. 601.

Seed, H.B., Mitry, F.G., Monismith, C.L. and Chan, K. 1967. Prediction of flexible pavement deflections from laboratory repeated-load tests. NCHRP Rept. 35, TRB.

Shell Laboratories. 1963. Shell pavement design manual.

Sherif, M.A., Fang, Y-S. and Sherif, R.I. 1984. Ka and Ko behind rotating and non-yielding walls. J. of Geotech. Eng., Proc. ASCE, Vol. 110, No. 1, pp. 41.

Shields, D.H., Ladanyi, B., Murat, J.R. and Clark, J.I. 1986. Stresses in icebergs - will the pressuremeter work? Proc. 39th Can. Geotech. Conf., Ottawa, Ont., Canada, pp. 159.

Shields, D.H. and Bauer, G.E. 1975. Determination of the modulus of deformation of a sensitive clay using laboratory and in situ tests. Proc. of ASCE Specialty Conf. on In-Situ Measurement of Soil Properties, Raleigh, N.C., pp. 395.

Sivaneswaran, N., Kramer, S.L. and Mahoney, J.P. 1991. Advanced backcalculation using a nonlinear least square optimization technique. Research Record 1293, TRB, National Research Council, Washington, D.C., 1991, pp. 93-102.

Skempton, A.W. 1952. The bearing capacity of clays. Tech. Mem. No. 25, National Research Council of Canada, Ottawa, Canada, 1967.

Skempton, A.W. 1964. Long term stability of clay slopes. Geotechnique, vol 4. No. 4., pp. 77-101.

Smith, R.E., Darter, M.I. and Lytton, R.L. 1986. Mechanistic overlay design procedures available to the design engineer. Pre-print copy, TRB Annual Meeting.

Smith, R.G. and Lytton, R.L. 1985. Operating characteristics and user satisfaction of commercially available NDT equipment. TRR 1007, TRB, pp. 1.

Sokolowski, V.V. 1965. Statics of granular media. Pergamon Press, New York.

Sowers, G.F., Robb, A.D., Mullis, C.H. and Glenn, A.J. 1957. The residual lateral pressures produced by compacting soils. Proc. 4th Intl. Conf. on Soil Mech. and Found. Eng., London, Vol. 2, (5/11), pp. 243.

Sowers, G.F. and Vesic, A. S. 1961. Stress distribution beneath pavements of different rigidities. Proc. 5th Intl. Conf. on Soil Mech. and Found. Eng., Paris, Vol. 2, pp. 327.

Spiegel, M.R. 1969. Mathematical handbook of formulas and tables. Schaum Outline Series, McGraw Hill, New York.

Steinbrenner, W. 1947. Tafeln zur setzungs berechnungen (Tables for settlement calculations). Die Strasse, Vol. 1, pp. 121. (Also included in the Lecture Notes at the Technical University of Aachen.)

Steward, R.E., Selig, E.T. and Norman-Gregory, G.M. 1985. Failure criteria and lateral stresses in track foundations. Transp. Research Record 1022, TRB, pp. 59.

Stock, A.F. and Brown, S.F. 1980. Nonlinear characterization of granular materials for asphalt pavement design. Transp. Research Record 755, TRB, pp. 14.

Terzaghi, K. 1942. Theoretical soil mechanics. John Wiley and Sons, New York.

Thenn de Barros, B. 1966. Deflection factor charts for two and three layer systems. Proc. 45th Ann. Meeting of HRB.

Tholen, O., Sharma, J. and Terrel, R.L. 1985. Comparison of falling weight deflectometer with other deflection testing devices. TRR 1007, TRB, pp. 20.

Timoshenko, S. and Goodier, J.N. 1949. Theory of elasticity. Monograph Series, McGraw Hill, New York, 2nd Ed.

Townsend, F.C. 1977. A review of factors affecting cyclic triaxial tests. ASTM Symp. on Dynamic Geotechnical Testing, STP 654, pp. 356.

Turnbull, W.J., Maxwell, A. and Ahlvin, R.G. 1961. Stresses and deflections in homogeneous soil masses. Proc. 5th Intl. Conf. on Soil Mech. and Found. Eng., Paris, Vol. 2, pp. 337.

U.S.A.E, 1991. Second international symposium on pavement response monitoring system for roads and airfields. Hanover, NH.

Uddin, W., Smith, P. and Treybig, H.J. 1985. Discussion of paper by Bush et al., 1985 (REF. Proc. of 3rd Intl. Conf. on the design and rehabilitation of concrete pavements, Purdue University, Lafeyette, Indiana, 1985)

Ueshita, K. and Meyerhof, G.G. 1967. Deflection of multilayer soil systems. J. of the Soil Mechanics Div., Proc. ASCE, Vol. 93, SM 5, pp. 257.

Ueshita, K. and Meyerhof, G.G. 1968. Surface displacement of an elastic layer under uniformly distributed loads. Highway Research Record 228, HRB, pp. 1.

Ullitdtz, P. and Peattie, K.R. 1980. Pavement analysis by programmable calculators. J. of the Transp. Eng. Div., Proc. ASCE, Vol. 106, TE 5, pp. 581.

Ullitdtz, P. and Stubstad, R.N. 1985. Structural evaluation of highway and airfield PCC pavements using the falling weight deflectometer. Undated pre-print at the 1st North American Conf. on Pavement Management Systems.

Uriel, A.O. 1973. Discussion of Raymond's Paper (Geotechnique, v. 22, No. 3, pp. 381-401) Technical Notes: Geotechnique, Vol. 23, pp. 294.

Uriel, A.O. and Canzio, L. 1971. On the elastic anisotropy of soils. Geotechnique, Vol. 21, No. 3, Technical Note, pp. 282.

Uzan, J. 1985. Characterization of granular materials. Transp. Research Record 1022, TRB, pp. 45.

Valkering, C.P. and Stapel, F.D.R. The Shell pavement design method on a personal computer. Proceedings of the 7th international conference on asphalt pavements, Nottingham, U.K., July, 1992, vol. 1, pp. 351-374.

Valliappan, P. 1974. Nonlinear stress-deformation analyses of Lake Agassiz clays using finite element method. Ph.D. Thesis, Univ. of Manitoba, Winnipeg, Man., Canada.

Van Cauwelaert, F. 1977. Coefficients of deformation of an anisotropic body. J. of Eng. Mech. Div., Proc. ASCE, Vol. 103, No. EM5, Oct., pp. 823; Discussions April 1978, EM 2, pp. 513, Oct. 1978, EM 2, pp. 1304 and June 1979, EM 3, pp. 482.

Van der Poel, C. 1954. A general system describing the viscoelastic properties of bitumens and its relation to routine test data. Journal of Applied Chemistry, vol. 4, pp. 221-236.

Vaswani, N.K. 1971. Method for separately evaluating structural performance of subgrades and overlying flexible pavements. HRR 362, HRB (now TRB), pp. 48.

Vesic, A.S. 1962. Validity of layered soild theories for flexible pavements, Proc. International Conference on Structural Design of Asphalt Pavements, Ann Arbor, Mich.

Vesic, A. S. and Domaschuk, L. 1964. Theoretical analysis of the structural behaviour of test flexible pavements. NCHRP Rept. No. 10, HRB.

Wang, M.C. and Anani, B.A. 1981. Evaluation of in-situ elastic moduli from road rater deflection basin. TRR 810, TRB, pp. 54.

Warren, S.J. 1982. The pressuremeter test in a homogeneous linearly elastic cross anisotropic soil. Tech. Note, Geotechnique, Vol. 32, pp. 157.

Westergaard, H.M. 1939. A problem in elasticity suggested by a problem in soil mechanics: soft material reinforced with numerous strong horizontal sheets. Timoshenko 60th Anniv. Vol., McMillan, New York.

Whiffin, A.C. 1954. The pressures generated in soil by compaction equipment, ASTM symposium on dynamic testing, pp. 186.

Wolf, K. 1935. Ausbreitung der Kraft in der Halbebene und im Halbraum bei anisotropem Material, Zeitung der Angew. Mech., Berlin, v. 15, No. 5, pp. 249-254.

Wood, D.M. 1982. Laboratory investigation of the behaviour of soils under cyclic loading. - A review. *In* Soil Mechanics: Transient and Cyclic Loads: Constitutive Relations and Numerical Treatment, Editors: G.N. Pande and O.C. Zienkiewicz, John Wiley and Sons, New York. pp. 513.

Wroth, C.P. 1984. The interpretation of in-situ soil tests. 24th Rankine Lecture, Geotechnique, Vol. 34, No. 4, pp. 449.

Wroth, C.P. and Houlsby, G.T. 1985. Soil mechanics: property characterization and analysis procedures. Proc. 11th Intl. Conf. on Soil Mech. and Found. Eng., San Francisco, Vol. 3, pp. 1-54.

Yoder, E.J. and Witczack, M.W. 1974. Principles of pavement design. John Wiley & Sons, New York, 2nd Ed.

Yuen, C.M-K. 1976. Cross-anisotropic deformation of leda clay. M.Sc. Thesis, Univ. of Western Ontario, London, Ont., Canada, 1975.

APPENDIX 4-I

RESULTS OF PRESSUREMETER TESTS AT VARIOUS SITES

(TABLES)

Note: Pressuremeter results in the form of charts are included in Vol. 2.

BRANDON: RWY 08-26: PMT RESULTS 1985.

(MODULI AND PRESSURES ARE IN kPa)

FACILITY	STATION	HOLE #	DEPTH (m)	LAYER	Eo	Er	Pl	Po	Pl*	Eo/Pl*
RWY 08-26	5 + 183	2	0.60	BASE	39939	112465	0	6.3	0	
			1.50	SG	4570	9488	470	17.1	452.9	10.1
	5 + 488	3	0.60	BASE	63625	0	0	6.3	0	
			1.50	SG	2465	0	0	17.3	0	
	5 + 787	4	0.60	BASE	53777	109682	0	6.3	0	
			1.50	SG	7474	18877	0	15.7	0	
	6 + 108	5	0.60	BASE	52324	0	0	6.3	0	
			1.50	SG	3404	0	480	15.7	464.3	7.3
	6 + 435	6	0.60	BASE	24092	56231	0	6.3	0	
			1.50	SG	1343	4928	280	15.7	264.3	5.1
	5 + 090	8	0.60	BASE	30360	0	2300	6.3	2293.7	13.2
			1.50	SG	2804	0	0	15.7	0	
	5 + 278	9	0.60	BASE	57042	0	0	6.3	0	
			1.50	SG	7581	0	820	15.7	804.3	9.4
	5 + 384	10	0.60	BASE	9167	0	720	6.3	713.7	12.8
			1.50	SG	1395	0	150	15.7	134.3	10.4
	5 + 588	11	0.60	BASE	11378	29537	0	6.3	0	
			1.50	SG	6193	0	610	15.7	594.3	10.4
	5 + 691	12	0.60	BASE	55600	0	0	6.3	0	
			1.50	SG	3737	0	500	15.7	484.3	7.7
	5 + 895	13	1.50	SG	6402	0	600	15.7	584.3	11.0
	5 + 978	14	0.60	BASE	58790	0	0	6.3	0	
			1.50	SG	5971	0	490	15.7	474.3	12.6
		15	0.60	BASE	32576	0	0	6.3	0	
			1.50	SG	6058	0	650	15.7	634.3	9.6
		16	0.60	BASE	45059	0	0	6.3	0	
			1.50	SG	4686	0	500	15.7	484.3	9.7
		17			30365	0	1400	6.3	1393.7	21.8
		18			20987	0	0	15.7	0	
		19			32683	0	1800	6.3	1793.7	18.2
					12728	0	0	15.7	0	

REGINA: 1985: PMT MODULI.

FACILITY	STATION	HOLE #	DEPTH (m)	LAYER	Eo	Er	Pl	Pl*	Po	Eo/PL*
					(MODULUS AND PRESSURES ARE IN kPa)					
TAXI B	5 + 300	1	1.20	BASE	48262	0	2300	2289.4	10.6	21.1
		1	2.25	SG	15161	0	900	876.5	23.5	17.3
TAXI B	5 + 691	2	1.20	BASE	26464	64122	0	0	10.6	
		2	2.25	SG	7083	12506	650	626.5	23.5	11.3
TAXI A	6 + 700	4	1.20	BASE	26275	0	1350	1339.4	10.6	19.6
		4	2.25	SG	34644	0	1600	1576.5	23.5	22.0
TAXI A	7 + 090	5	1.20	BASE	29547	63487	1800	1789.5	10.6	16.5
		5	2.25	SG	9488	17842	630	604.3	25.7	15.7
TAXI C		7	2.50	SG	24506	40179	1200	1171.5	28.5	20.9
RWY. 12-30	5 + 504	8	0.75	BASE	83117	126795	0	0	7.9	
		8	2.25	SG	6491	10526	450	424.3	25.7	15.3
	5 + 595	9	0.75	BASE	38299	0	0	0	7.9	
		9	2.25	SG	7403	0	500	474.3	25.7	15.6
	5 + 700	10	0.75	BASE	48228	0	0	0	7.9	
		10	2.25	SG	7319	0	600	574.3	25.7	12.7
	5 + 800	11	0.70	BASE	34150	0	0	0	7.9	
		11	2.20	SG	6085	0	540	514.3	25.7	11.8
	5 + 907	12	0.70	BASE	144993	0	0	0	7.9	
		12	2.20	SG	3889	0	0	0	25.7	
	6 + 106	14	0.70	BASE	54039	0	0	0	7.9	
		14	2.20	SG	5057	0	520	494.3	25.7	10.2
	6 + 208	15	0.70	BASE	67336	136031	0	0	7.9	
		15	2.20	SG	7039	13121	620	594.3	25.7	11.8
	6 + 306	16	0.70	BASE	14634	0	500	492.1	7.9	29.7
		16	2.20	SG	24238	0	550	524.3	25.7	46.2
	6 + 409	17	0.70	BASE	56525	0	0	0	7.9	
		17	2.20	SG	9884	0	650	624.3	25.7	15.8
	6 + 513	18	0.70	BASE	58554	0	0	0	7.9	
		18	2.20	SG	10169	0	720	694.3	25.7	14.6
	6 + 857	19	0.70	BASE	56313	0	0	0	7.9	
		19	2.20	SG	16964	0	620	594.3	25.7	28.5
	6 + 961	20	0.70	BASE	88957	0	0	0	7.9	
		20	2.20	SG	6406	0	540	514.3	25.7	12.5
	7 + 054	21	0.70	BASE	90009	0	0	0	7.9	
		21	2.20	SG	5357	0	0	0	25.7	

ST. ANDREWS: RWY 13-31: PMT RESULTS 1988.										
					(MODULI AND PRESSURES ARE IN kPa)					
FACILITY	STATION	HOLE #	DEPTH (m)	LAYER	Eo	Er	Pl	Po	Pl*	Eo/Pl*
RWY.13-31	5 + 030	1	0.7	BASE	7373	8851	285	7.6	277.4	26.6
			1.70	SUBGRADE	4603	4121	145	18.4	126.6	36.4
	5 + 120	2	0.26	BASE	6915	0	620	2.7	617.3	11.2
			0.75	STAB.CLAY	9522	8852	270	8.1	261.9	36.4
			1.75	SUBGRADE	4007	4831	152.5	18.9	133.6	30.0
	5 + 210	3	0.25	BASE	8335	0	770	2.6	767.4	10.9
			0.75	STAB.CLAY	7803	9609	230	8.1	221.9	35.2
			1.75	SUBGRADE	3778	4831	167.5	18.9	148.6	25.4
	5 + 300	4	0.23	BASE	5166	0	410	2.4	407.6	12.7
			0.70	STAB.CLAY	8799	9234	225	7.6	217.4	40.5
			1.7	SUBGRADE	4603	3916	117.5	18.4	99.1	46.4
	5 + 390	5	0.23	BASE	7087	0	630	2.4	627.6	11.3
			0.70	STAB.CLAY	10990	0	290	7.6	282.4	38.9
			1.7	SUBGRADE	7373	0	185	18.4	166.6	44.3
	5 + 480	6	0.25	BASE	4696	0	600	2.6	597.4	7.9
			0.75	STAB.CLAY	5339	8546	162.5	8.1	154.4	34.6
			1.75	SUBGRADE	4603	4832	132.5	18.9	113.6	40.5
	5 + 570	7	0.22	BASE	7709	0	620	2.3	617.7	12.5
			0.73	STAB.CLAY	4307	8485	270	7.9	262.1	16.4
			1.75	SUBGRADE	3290	4475	147.5	18.9	128.6	25.6
	5 + 660	8	0.28	BASE	9945	0	975	2.9	972.1	10.2
			0.80	STAB.CLAY	10253	10751	325	8.6	316.4	32.4
			1.8	SUBGRADE	2954	4122	147.5	19.4	128.1	23.1
	5 + 750	9	0.23	BASE	8376	0	950	2.9	947.1	8.8
			0.70	STAB.CLAY	6671	11141	345	7.6	337.4	19.8
			1.7	SUBGRADE	5286	5188	157.5	18.4	139.1	38.0
	5 + 840	10	0.23	BASE	4330	0	0	2.4	0	
			0.70	STAB.CLAY	6737	10753	300	7.6	292.4	23.0
			1.7	SUBGRADE	4603	5547	147.5	18.4	129.1	35.7
	5 + 900	11	0.23	BASE	4342	0	550	2.4	547.6	7.9
			0.70	STAB.CLAY	8082	10376	250	7.6	242.4	33.3
			1.7	SUBGRADE	2620	4122	132.5	18.4	114.1	23.0

THUNDER BAY: RWY 12-30: PMT RESULTS 1985.										
					(MODULI AND PRESSURES ARE IN kPa)					
FACILITY	STATION	HOLE #	DEPTH (m)	LAYER	Eo	Er	Pl	Po	Pl*	Eo/Pl*
RWY. 12-30	5 + 100	10	0.75	BASE	177985	0	0	6.3	0	
			1.50	SUBBASE	44140	0	0	14.9	0	
			2.50	SUBGRADE	13166	0	0	27	0	
	5 + 204	1	0.60	BASE	119476	0	0	6.3	0	
			1.50	SUBBASE	30530	73457	2400	14.9	2385.1	12.8
			2.50	SUBGRADE	7472	16458	920	27	893	8.4
	5 + 298	11	1.50	SUBBASE	48110	0	0	14.9	0	
			2.50	SUBGRADE	10991	0	0	27	0	
	5 + 395	12	1.50	SUBGRADE	34358	0	2500	14.9	2485.1	13.8
	5 + 496	2	1.50	SUBGRADE	20462	0	1420	14.9	1405.1	14.6
			2.50	SUBGRADE	6257	0	0	27	0	
	5 + 597	13	1.50	SUBGRADE	8363	0	0	14.9	0	
			2.50	SUBGRADE	4857	0	520	27	493	9.9
	5 + 654	14	1.50	SUBGRADE	10730	24417	1200	14.9	1185.1	9.1
			2.50	SUBGRADE	9374	14751	740	27	713	13.1
	5 + 912	15	1.50	SUBGRADE	9342	0	1350	14.9	1335.1	7.0
			2.50	SUBGRADE	4587	0	620	27	593	7.7
	6 + 067	3	1.50	SUBGRADE	6843	0	0	14.9	0	
			2.50	SUBGRADE	7508	0	0	27	0	
	6 + 298	4	1.50	SUBGRADE	8893	0	0	14.9	0	
			2.50	SUBGRADE	6214	0	740	27	713	8.7
TAXI A	10 + 340	7	0.75	BASE	158421	0	0	7.9	0	
			2.00	SUBGRADE	8001	18549	980	19.8	960.2	8.3
	10 + 730	8	0.75	BASE	102868	0	0	7.9	0	
			2.00	SUBGRADE	8729	0	0	19.8	0	
TAXI D	10 + 495	9	0.75	BASE	117347	0	0	7.9	0	
			2.00	SUBGRADE	8147	20632	1030	19.8	1010.2	8.1

REGINA: RWY 12-30: PMT RESULTS 1988.										
					(MODULI AND PRESSURES ARE IN kPa)					
FACILITY	STATION	HOLE #	DEPTH (m)	LAYER	Eo	Er	Pl	Pl*	Po	Eo/Pl*
RWY. 12-30	5 + 055	1	0.60	BASE	123469	0	0	0	6.3	
			1.15	SUBGRADE	4029	0	260	247.6	12.4	16.3
			2.15	SUBGRADE	4337	0	295	271.8	23.2	16.0
	5 + 100	2	0.60	BASE	57859	0	0	0	6.3	
			1.15	SUBGRADE	9324	8044	275	262.6	12.4	35.5
			2.15	SUBGRADE	4548	4853	220	196.8	23.2	23.1
	5 + 330	3	0.70	BASE	42465	0	0	0	7.4	
			1.10	SUBGRADE	10026	10782	325	313.1	11.9	32.0
			2.10	SUBGRADE	8627	8995	340	317.3	22.7	27.2
	5 + 498	4	0.70	BASE	50646	0	0	0	7.1	
			1.20	SUBGRADE	11920	14888	460	447	13	26.7
			2.20	SUBGRADE	4548	5122	230	206.2	23.8	22.1
	5 + 700	5	0.70	BASE	35655	0	0	0	7.5	
			1.30	SUBGRADE	10026	9381	370	356	14	28.2
			2.30	SUBGRADE	5460	6954	240	215.2	24.8	25.4
	5 + 800	6	0.70	BASE	41535	0	0	0	7.6	
			1.30	SUBGRADE	12163	9524	335	321	14	37.9
			2.30	SUBGRADE	6002	7133	265	240.2	24.8	25.0
	6 + 000	7	0.70	BASE	44019	0	0	0	7	
			1.20	SUBGRADE	13613	14118	380	367	13	37.1
			2.20	SUBGRADE	4656	7204	275	251.2	23.8	18.5
	6 + 100	8	0.75	BASE	52923	0	0	0	7.8	
			1.30	SUBGRADE	13613	10280	320	306	14	44.5
			2.30	SUBGRADE	4491	6221	285	260.2	24.8	17.3
	6 + 300	9	0.70	BASE	61876	0	0	0	7.5	
			1.25	SUBGRADE	15085	14114	310	296.5	13.5	50.9
			2.25	SUBGRADE	7248	8458	190	165.7	24.3	43.7
	6 + 400	10	0.76	BASE	63000	0	0	0	8	
			1.35	SUBGRADE	16578	18049	420	405.4	14.6	40.9
			2.35	SUBGRADE	10026	7409	210	184.6	25.4	54.3
	6 + 850	11	0.64	BASE	63749	0	0	0	6.7	
			1.15	SUBGRADE	10026	8826	195	182.6	12.4	54.9
			2.15	SUBGRADE	8627	6399	157.5	134.3	23.2	64.2
	7 + 050	12	0.76	BASE	34541	0	1425	1417	8	24.4
			1.35	SUBGRADE	15085	12336	365	350.4	14.6	43.1
			2.35	SUBGRADE	6566	7726	177.5	152.1	25.4	43.2
	7 + 190	13	0.75	BASE	30073	0	0	0	7.9	
			1.20	SUBGRADE	11446	11053	310	297	13	38.5
			2.20	SUBGRADE	6566	4849	130	106.2	23.8	61.8
	7 + 220	14	0.73	BASE	18908	0	1275	1267.3	7.7	14.9
			1.20	SUBGRADE	9324	8455	210	197	13	47.3
			2.20	SUBGRADE	7248	6638	170	146.2	23.8	49.6
	7 + 310	15	0.65	BASE	87814	0	0	0	6.8	
			1.05	SUBGRADE	13613	12948	335	323.7	11.3	42.1
			2.05	SUBGRADE	4681	5611	190	167.9	22.1	27.9
	7 + 370	16	0.59	BASE	79671	0	0	0	6.2	
			1.00	SUBGRADE	7048	11084	430	419.2	10.8	16.8
			2.00	SUBGRADE	6566	6278	150	128.4	21.6	51.1
	5 + 390	17	0.70	BASE	23293		1625	1617.7	7.3	
			1.20	SUBGRADE	4931	9748	270	257	13	19.2
			2.20	SUBGRADE	5089	13063	325	301.2	23.8	16.9

REGINA: RWY 12-30: PMT RESULTS 1988.										
					(MODULI AND PRESSURES ARE IN kPa)					
FACILITY	STATION	HOLE #	DEPTH (m)	LAYER	Eo	Er	Pl	Pl*	Po	Eo/Pl*
	5 + 570	18	0.67	BASE	27267				7	
			1.25	SUBGRADE	9324	10026	315	301.5	13.5	30.9
			2.25	SUBGRADE	3575	6462	190	165.7	24.3	21.6
	6 + 890	19	0.72	BASE	36642				7.6	
			1.30	SUBGRADE	4595	6637	155	141	14	32.6
			2.30	SUBGRADE	10026	8538	180	155.2	24.8	64.6
	5 + 024R	23	0.60	BASE	30573				6.3	
	5 + 024L	24	0.60	BASE	61090				6.3	
	5 + 061R	25	0.60	BASE	24990				6.3	
	5 + 064R	25	0.60	BASE	40808				6.3	
	5 + 097L	27	0.60	BASE	21655				6.3	
	5 + 134R	28	0.60	BASE	25844				6.3	

SASKATOON: RWY 15-33: PMT RESULTS 1988.

(MODULI VALUES AND PRESSURES ARE IN kPa)

FACILITY	STATION	HOLE #	DEPTH (m)	LAYER	Eo	Er	Pl	Pl*	Po	Eo/Pl*
RWY. 15-33	5 + 100	1	0.50	BASE	61208	0	0	0.0	5.3	
			1.20	SUBGRADE	5767	11281	600	587.5	12.5	9.8
			2.10	SUBGRADE	9548	9508	420	398.1	21.9	24.0
	5 + 150	2	0.50	BASE	180475	0	0	0.0	5.3	
			1.20	SUBGRADE	34402	40141	1150	1137.5	12.5	30.2
			2.20	SUBGRADE	4073	6551	410	387.0	23.0	10.5
	5 + 360	3	0.50	BASE	109820	0	0	0.0	5.3	
			1.30	SUBGRADE	22273	22228	720	706.4	13.6	31.5
			2.30	SUBGRADE	5295	7489	320	297.2	22.8	17.8
	5 + 450	4	0.50	BASE	57322	0	0	0.0	5.3	
			1.00	1961 BASE	53705	0	0	0.0	10.5	
			1.50	SUBGRADE	13296	12655	470	455.1	14.9	29.2
			2.10	SUBGRADE	3972	7101	410	388.1	21.9	10.2
	5 + 540	5	0.50	BASE	37202	0	0	0.0	5.3	
			1.00	1961 BASE	65732	0	0	0.0	10.5	
			1.50	SUBGRADE	5986	8984	300	285.1	14.9	21.0
			2.20	SUBGRADE	5909	9799	550	527.0	23.0	11.2
	5 + 630	6	0.50	BASE	97408	0	0	0.0	5.3	
			1.00	1961 BASE	29352	0	0	0.0	10.5	
			1.50	SUBGRADE	21855	12915	490	474.3	15.7	46.1
			2.10	SUBGRADE	4493	7760	430	408.1	21.9	11.0
	5 + 660	7	0.50	BASE	89780	0	0	0.0	5.3	
			1.00	1961 BASE	65070	0	0	0.0	10.5	
			1.50	SUBGRADE	10283	10307	400	384.3	15.7	26.8
			2.20	SUBGRADE	3932	5801	330	307.0	23.0	12.8
	5 + 680	8	0.50	BASE	55664	0	0	0.0	5.3	
			0.94	1961 BASE	36454	0	0	0.0	9.9	
			1.50	SUBGRADE	5986	8533	400	385.1	14.9	15.5
			2.10	SUBGRADE	4610	5563	205	183.1	21.9	25.2
	5 + 690	9	0.50	BASE	54948	0	0	0.0	5.3	
			1.00	1961 BASE	31543	0	0	0.0	10.5	
			1.50	SUBGRADE	10283	9540	490	475.1	14.9	21.6
			2.10	SUBGRADE	3516	6298	390	369.2	20.8	9.5
	5 + 750	10	0.50	BASE	37842	0	0	0.0	5.3	
			1.00	1961 BASE	56328	0	0	0.0	10.5	
			1.50	SUBGRADE	4610	6542	400	384.3	15.7	12.0
			2.20	SUBGRADE	1299	3199	250	227.6	22.4	5.7
	5 + 840	11	0.50	BASE	117594	0	0	0.0	5.3	
			1.10	1961 BASE	30495	0	0	0.0	11.5	
			1.50	SUBGRADE	14070	15751	420	405.1	14.9	34.7
			2.10	SUBGRADE	2497	7105	290	268.1	21.9	9.3
	5 + 930	12	0.50	BASE	99567	0	0	0.0	5.3	
			1.00	1961 BASE	35108	0	0	0.0	10.5	
			1.40	SUBGRADE	8102	8281	300	284.9	15.1	28.4
			2.00	SUBGRADE	7390	10530	450	429.1	20.9	17.2
	6 + 020	13	0.40	BASE	220460	0	0	0.0	4.2	
			0.90	1961 BASE	94244	0	0	0.0	9.4	
			1.50	SUBGRADE	12531	11699	345	329.3	15.7	38.1
			2.10	SUBGRADE	5295	6671	240	218.1	21.9	24.3

SASKATOON: RWY 15-33: PMT RESULTS 1988.										
					(MODULI VALUES AND PRESSURES ARE IN kPa)					
FACILITY	STATION	HOLE #	DEPTH (m)	LAYER	Eo	Er	Pl	Pl*	Po	Eo/Pl*
	6 + 140	14	0.50	BASE	91079	0	0	0.0	5.3	
			1.20	1961 BASE	109194	0	0	0.0	12.6	
			1.80	SUBGRADE	5986	0	350	332.2	17.8	18.0
			2.80	SUBGRADE	639	0	40	10.7	29.3	59.7
	6 + 260	15	0.50	BASE	57038	0	0	0.0	5.3	
			1.20	1961 BASE	31120	0	0	0.0	12.6	
			1.60	SUBGRADE	10283	9967	360	344.2	15.8	29.9
			2.80	SUBGRADE	3261	4533	290	259.8	30.2	12.6
	6 + 380	16	0.50	BASE	81828	0	0	0.0	5.3	
			1.20	1961 BASE	32564	0	0	0.0	12.6	
			1.60	SUBGRADE	7390	7525	280	264.2	15.8	28.0
			2.60	SUBGRADE	5986	6306	350	322.8	27.2	18.5
	6 + 470	17	0.50	BASE	107528	0	0	0.0	5.3	
			1.00	1961 BASE	131708	0	0	0.0	10.5	
			1.60	SUBGRADE	6684	8990	250	234.2	15.8	28.5
			2.50	SUBGRADE	9548	9483	305	280.2	24.8	34.1
	6 + 590	18	0.40	BASE	63435	0	0	0.0	4.2	
			1.50	SUBGRADE	14070	12924	380	365.1	14.9	38.5
			2.00	SUBGRADE	2059	3466	0	0.0	19.8	
	6 + 680	19	0.50	BASE	28734	0	0	0.0	5.3	
			1.50	SUBGRADE	13296	12111	375	360.1	14.9	36.9
			2.00	SUBGRADE	1514	2970	115	93.4	21.6	16.2

APPENDIX 5 - I

THEORY OF STIF 42 ISOPARAMETRIC ELASTIC SOILD

(SOURCE: ANSYS THEORETICAL MANUAL)

2.42 STIF42 - TWO-DIMENSIONAL ISOPARAMETRIC SOLID ELEMENT

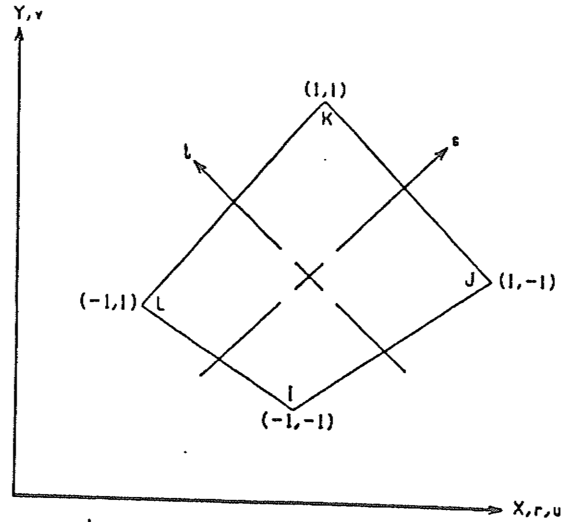

	SHAPE FUNCTIONS	INTEGRATION POINTS
Stiffness Matrix	$u = \frac{1}{4}(u_I(1-s)(1-t)$ $+ u_J(1+s)(1-t)$ $+ u_K(1+s)(1+t)$ $+ u_L(1-s)(1+t))$ (and, if modified extra shapes are included (KEYOPT(2) $\neq$ 1) and element has 4 unique nodes $+ u_1(1-s^2)$ $+ u_2(1-t^2)$ $v = \frac{1}{4}(v_I(1-s)$ - - - (similar to u) (u_1 or u_2 motions normal to the edge along the centerline are suppressed for axisymmetric elements near the centerline)	2 x 2

	SHAPE FUNCTIONS	INTEGRATION POINTS
Mass Matrix	Same as stiffness matrix without modified extra displacement shapes	2 x 2
Stress Stiffness Matrix	Same as stiffness matrix without modified extra displacement shapes	2 x 2
Thermal and Newton-Raphson Load Vector	Same as stiffness matrix	2 x 2
Load Vector for Pressure	Same as stiffness matrix, without modified extra displacement shapes, specialized to the edge	2

Element Temperature Distribution: Bilinear across element, constant thru thickness or around circumference

Nodal Temperature Distribution: Same as element temperature distribution

Pressure Distribution: Uniform along each side

References: Wilson(*38*), Taylor(*49*)

Derivation of Element by Virtual Work:

A complete derivation of the element matrices and load vector are developed for this element. The principle of virtual work is used in the derivation below:

$$\delta U = \delta V \tag{2.42.1}$$

where: δU = virtual strain energy

δV = virtual external work

The virtual strain energy may be expressed as:

$$\delta U = \int_{vol} \{\delta\epsilon\}^T \{\sigma\} \, d(vol) \tag{2.42.2}$$

where:

$$\{\epsilon\} = \begin{Bmatrix} \epsilon_x \\ \epsilon_y \\ \gamma_{xy} \\ \epsilon_z \end{Bmatrix} = \text{strain vector}$$

$$\{\sigma\} = \begin{Bmatrix} \sigma_x \\ \sigma_y \\ \tau_{xy} \\ \sigma_z \end{Bmatrix} = \text{stress vector}$$

These two vectors, both in the element coordinate system, are related by:

$$\{\sigma\} = [D](\{\epsilon\} - \{\epsilon^{th}\}) \tag{2.42.3}$$

where:

$$[D]^{-1} = \begin{bmatrix} \frac{1}{EX} & -\frac{NUXY}{EY} & 0 & -\frac{NUXZ}{EZ} \\ -\frac{NUXY}{EY} & \frac{1}{EY} & 0 & -\frac{NUYZ}{EZ} \\ 0 & 0 & \frac{1}{GXY} & 0 \\ -\frac{NUXZ}{EZ} & -\frac{NUYZ}{EZ} & 0 & \frac{1}{EZ} \end{bmatrix}$$

$$\{\epsilon^{th}\} = \begin{Bmatrix} ALPX\ \Delta T \\ ALPY\ \Delta T \\ 0 \\ ALPZ\ \Delta T \end{Bmatrix}$$

where EX, EY, EZ, NUXY, NUYZ, NUXZ, ALPX, ALPY, ALPZ, GXY are input quantities (GXY may be determined from EX, EY, and NUXY) and ΔT is the difference between the actual temperature at the integration point and the reference temperature (T_{ref}). If a plane stress analysis is requested (KEYOPT(3) = 0 or 3), the variables ALPZ, NUXZ, and NUYZ are internally set to 0.0. Combining equation (2.42.2) and (2.42.3):

$$\delta U = \int_{vol} (\{\delta\epsilon\}^T[D]\{\epsilon\} - \{\delta\epsilon\}^T[D]\{\epsilon^{th}\})\, d(vol) \tag{2.42.4}$$

Next, consider the element orientation in Figure 2.42.1. If KEYOPT(1) = 1 is selected, the element x-axis is not parallel to the global x-axis but rather is parallel to side I-J.

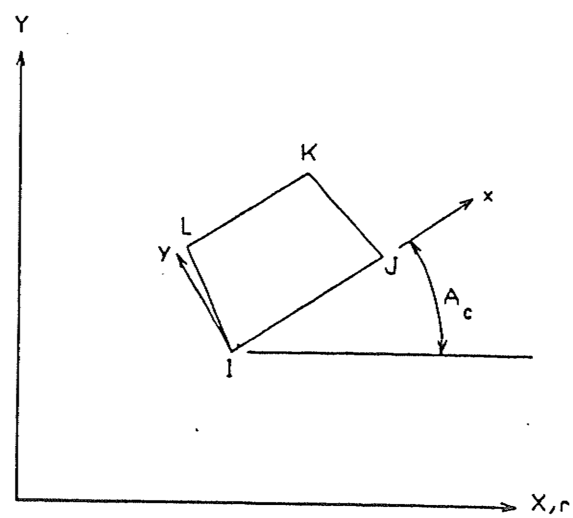

Figure 2.42.1 Element Coordinate Systems

The element and global axes are related by the tensor transformation:

$$\{\epsilon\} = [T_m]\{e\} \tag{2.42.5}$$

$$[T_m] = \begin{bmatrix} C^2 & S^2 & SC & 0 \\ S^2 & C^2 & -SC & 0 \\ -2\beta SC & 2\beta SC & \beta(C^2-S^2) & 0 \\ 0 & 0 & 0 & 1 \end{bmatrix}$$

$$\{e\} = \begin{Bmatrix} \epsilon_X \\ \epsilon_Y \\ \gamma_{XY} \\ \epsilon_Z \end{Bmatrix}$$

and:

$$C = \cos (A_c)$$

$$S = \sin (A_c)$$

$$\beta = \begin{cases} +1 \text{ if nodes ordered counter clockwise} \\ -1 \text{ if nodes ordered clockwise} \end{cases}$$

This tensor transformation has been derived by Lekhnitskii(*24*). Combining equation (2.42.4) and (2.42.5):

$$\delta U = \int_{vol} (\{\delta\epsilon\}^T [T_m]^T [D][T_m]\{\epsilon\} - \{\delta\epsilon\}^T [T_m]^T [D]\{\epsilon^{th}\}) \; d(vol) \qquad (2.42.6)$$

Note that if $A_c = 0.$, $[T_m]$ reduces down to an identity matrix.

Next, the strains must be related to the shape functions. It is known from basic elasticity theory that:

$$\epsilon_x = \frac{\partial u}{\partial X} \qquad (2.42.7)$$

$$\epsilon_y = \frac{\partial v}{\partial Y} \qquad (2.42.8)$$

$$\gamma_{xy} = \frac{\partial u}{\partial Y} + \frac{\partial v}{\partial X} \qquad (2.42.9)$$

$$\epsilon_z = \frac{u}{r} \qquad (2.42.10)$$

where r is the radial coordinate of the integration point and where all variables are in the global coordinate system. Equation (2.42.10) is included only if the problem is axisymmetric (KEYOPT(3) = 1). u and v are defined thru the displacement functions. These are repeated here, including the extra displacement functions (KEYOPT(2) = 0):

$$u = \frac{1}{4}(u_I(1-s)(1-t) + u_J(1+s)(1-t) + u_K(1+s)(1+t) + u_L(1-s)(1+t)) + u_1(1-s^2) + u_2(1-t^2) \qquad (2.42.11)$$

and

$$v = \frac{1}{4}(v_I(1-s)(1-t) + v_J(1+s)(1-t) + v_K(1+s)(1+t) + v_L(1-s)(1+t)) + v_1(1-s^2) + v_2(1-t^2) \qquad (2.42.12)$$

or

$$u = h_I u_I + h_J u_J + h_K u_K + h_L u_L + h_1 u_1 + h_2 u_2 \qquad (2.42.13)$$

and

$$v = h_I v_I + h_J v_J + h_K v_K + h_L v_L + h_1 v_1 + h_2 v_2 \qquad (2.42.14)$$

where: u_I = u-displacement (in x-direction) of node I, etc.

u_1 = value of first extra shape function in x-direction (nodeless variable), etc.

$h_I = \frac{1}{4}(1-s)(1-t)$, etc.

Note that the extra shape functions (as shown in Figure 2.42.2) permit a parabolic deformation along an element edge. Normally this is helpful in modeling a structure, but occasionally it may cause a problem because of the incompatibility at the adjoining edges of two different elements, i.e., a gap develops along the interelement boundaries. Because of this problem, ANSYS uses a modified form of the extra displacement shapes. For completeness of theoretical development, a detailed development of the element stiffness matrix formulation with the standard extra shape functions is carried out. Later discussion is presented regarding the modification of the effect of the extra shapes (Taylor, et al(*49*)).

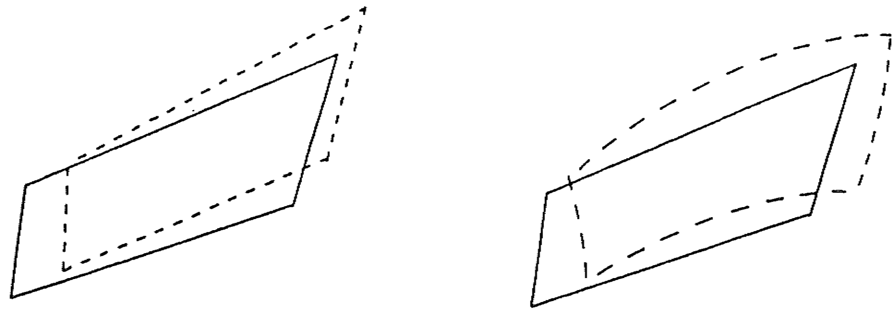

Figure 2.42.2 Effect of Extra Shape Functions

The shape functions, which define both u and v, are now combined with equations (2.42.7) thru (2.42.10) in order to relate the strains to the nodal displacements as:

$$\begin{Bmatrix} \varepsilon_X \\ \varepsilon_Y \\ \gamma_{XY} \\ \varepsilon_Z \end{Bmatrix} = \begin{bmatrix} \frac{\partial h_I}{\partial X} & 0 & \frac{\partial h_J}{\partial X} & 0 & \frac{\partial h_K}{\partial X} & 0 & \frac{\partial h_L}{\partial X} & 0 \\ 0 & \frac{\partial h_I}{\partial Y} & 0 & \frac{\partial h_J}{\partial Y} & 0 & \frac{\partial h_K}{\partial Y} & 0 & \frac{\partial h_L}{\partial Y} \\ \frac{\partial h_I}{\partial Y} & \frac{\partial h_I}{\partial X} & \frac{\partial h_J}{\partial Y} & \frac{\partial h_J}{\partial X} & \frac{\partial h_K}{\partial Y} & \frac{\partial h_K}{\partial X} & \frac{\partial h_L}{\partial Y} & \frac{\partial h_L}{\partial X} \\ \frac{h_I}{R} & 0 & \frac{h_J}{R} & 0 & \frac{h_K}{R} & 0 & \frac{h_L}{R} & 0 \end{bmatrix} \begin{Bmatrix} u_I \\ v_I \\ u_J \\ v_J \\ u_K \\ v_K \\ u_L \\ v_L \end{Bmatrix} + \begin{bmatrix} \frac{\partial h_1}{\partial X} & 0 & \frac{\partial h_2}{\partial X} & 0 \\ 0 & \frac{\partial h_1}{\partial Y} & 0 & \frac{\partial h_2}{\partial Y} \\ \frac{\partial h_1}{\partial Y} & \frac{\partial h_1}{\partial X} & \frac{\partial h_2}{\partial Y} & \frac{\partial h_2}{\partial X} \\ \frac{h_1}{R} & 0 & \frac{h_2}{R} & 0 \end{bmatrix} \begin{Bmatrix} u_1 \\ v_1 \\ u_2 \\ v_2 \end{Bmatrix} \quad (2.42.15$$

where h_i, $\frac{\partial h_i}{\partial X}$, $\frac{\partial h_i}{\partial Y}$, and R are specialized to the integration point being studied.

Equation (2.42.15) can be reduced in matrix form as,

$$\underset{}{\{\epsilon\}} = \underset{4\times8}{[B_n]}\ \underset{8\times1}{\{u_n\}} + \underset{4\times4}{[G]}\ \underset{4\times1}{\{u_e\}} \quad (2.42.16)$$

$$= [B_n]\ [G] \begin{Bmatrix} \{u_n\} \\ ---- \\ \{u_e\} \end{Bmatrix} \tag{2.42.17}$$

$$= \underset{4x12}{[B]} \ \underset{12x1}{\{u\}} \tag{2.42.18}$$

In equation (2.42.15) we see that the derivatives of the shape functions ($h_I, \ldots h_4$) are with respect to X and Y, while these shape functions are functions of s and t (see equations (2.42.11) and (2.42.12)). For a two-dimensional quadrilateral element, the s - t coordinates are related to the X - Y coordinates as:

$$X = \frac{1}{4}\left[h_I X_I + h_J X_J + h_K X_K + h_L X_L\right] \tag{2.42.19}$$

and

$$Y = \frac{1}{4}\left[h_I Y_I + h_J Y_J + h_K Y_K + h_L Y_L\right] \tag{2.42.20}$$

where:

$h_I, \ldots h_L$ = shape functions (equations (2.42.11) thru (2.42.12))

X_I = X coordinate of node I, etc.

The transition of equation (2.42.15) from one set of variables to the other is handled with the help of "chain rule". The derivatives of h_I with respect to s and t may be expresed as:

$$\frac{\partial h_I}{\partial s} = \frac{\partial h_I}{\partial X}\frac{\partial X}{\partial s} + \frac{\partial h_I}{\partial Y}\frac{\partial Y}{\partial s} \tag{2.42.21}$$

$$\frac{\partial h_I}{\partial t} = \frac{\partial h_I}{\partial X}\frac{\partial X}{\partial t} + \frac{\partial h_I}{\partial Y}\frac{\partial Y}{\partial t} \tag{2.42.22}$$

In matrix form equation (2.42.21) and (2.42.22)) can be written as:

$$\begin{Bmatrix} \dfrac{\partial h_I}{\partial s} \\ \dfrac{\partial h_I}{\partial t} \end{Bmatrix} = \begin{bmatrix} \dfrac{\partial X}{\partial s} & \dfrac{\partial Y}{\partial s} \\ \dfrac{\partial X}{\partial t} & \dfrac{\partial Y}{\partial t} \end{bmatrix} \begin{Bmatrix} \dfrac{\partial h_I}{\partial X} \\ \dfrac{\partial h_I}{\partial Y} \end{Bmatrix} \tag{2.42.23}$$

The 2 x 2 matrix in equation (2.42.23) relating shape function derivatives with respect to local (s - t) and global (X - Y) coordinate system is known as the Jacobian matrix. Inverting equation (2.42.23):

$$\begin{Bmatrix} \dfrac{\partial h_I}{\partial X} \\ \dfrac{\partial h_I}{\partial Y} \end{Bmatrix} = \begin{bmatrix} \dfrac{\partial X}{\partial s} & \dfrac{\partial Y}{\partial s} \\ \dfrac{\partial X}{\partial t} & \dfrac{\partial Y}{\partial t} \end{bmatrix}^{-1} \begin{Bmatrix} \dfrac{\partial h_I}{\partial s} \\ \dfrac{\partial h_I}{\partial t} \end{Bmatrix} \qquad (2.42.24)$$

For later convenience, the inverse of the (2 x 2) Jacobian matrix as used in equation (2.42.23) will be defined as,

$$\begin{bmatrix} Q_{11} & Q_{12} \\ Q_{21} & Q_{22} \end{bmatrix} = \begin{bmatrix} \dfrac{\partial X}{\partial s} & \dfrac{\partial Y}{\partial s} \\ \dfrac{\partial X}{\partial t} & \dfrac{\partial Y}{\partial t} \end{bmatrix}^{-1} \qquad (2.42.25)$$

where:

$$Q_{11} = \frac{\dfrac{\partial Y}{\partial t}}{\Delta}$$

$$Q_{12} = \frac{-\dfrac{\partial Y}{\partial s}}{\Delta}$$

$$Q_{21} = \frac{-\dfrac{\partial X}{\partial s}}{\Delta}$$

$$Q_{22} = \frac{\dfrac{\partial X}{\partial s}}{\Delta}$$

$$\Delta = \frac{\partial X}{\partial s}\frac{\partial Y}{\partial t} - \frac{\partial Y}{\partial s}\frac{\partial X}{\partial t}$$

Δ is defined as the determinant of the Jacobian matrix, and is simply referred to as the Jacobian. The Jacobian is the mapping factor relating the s - t and X - Y coordinate systems. For a parallelogram, the Jacobian is the ratio of the element area in X - Y space divided by 4.0 (the element area in s - t space). Thus, equation (2.42.24) can be written as:

$$\frac{\partial h_I}{\partial X} = (+ \frac{\partial Y}{\partial t}\frac{\partial h_I}{\partial s} - \frac{\partial Y}{\partial s}\frac{\partial h_I}{\partial t})/\Delta \qquad (2.42.25a)$$

$$\frac{\partial h_I}{\partial Y} = (+ \frac{\partial X}{\partial t}\frac{\partial h_I}{\partial s} - \frac{\partial X}{\partial s}\frac{\partial h_I}{\partial t})/\Delta \qquad (2.42.25b)$$

Combining equation (2.42.6) and (2.42.18)

$$\delta U = \int_{vol} (\{\delta u\}^T [B]^T [T_m]^T [D]\ [T_m][B]\{u\} - \{\delta u\}^T [B]^T [T_m]^T [D]\{\epsilon^{th}\})\ d(vol) \qquad (2.42.26)$$

This results in:

$$[K_e] = \int_{vol} [B]^T [T_m]^T [D][T_m][B]\ d(vol) \qquad (2.42.27)$$

and

$$\{F_e^{th}\} = \int_{vol} [B]^T [T_m]^T [D]\{\epsilon^{th}\}\ d(vol) \qquad (2.42.28)$$

Using equation (2.42.17), the results in equation (2.42.27) can be further expanded as:

$$[K_e] = \int_{vol} \Big[\ [B_n][G]\ \Big]^T [T_m][D][T_m] \Big[\ [B_n][G]\ \Big]\ d(vol) \qquad (2.42.29)$$

or

$$= \int_{vol} \begin{bmatrix} \Big[\ [B_n]^T [T_m]^T [D][T_m][B_n]\ \Big] & \Big[\ [B_n]^T [T_m]^T [D][T_m][G]\ \Big] \\ \Big[\ [G]^T [T_m]^T [D][T_m][B_n]\ \Big] & \Big[\ [G]^T [T_m]^T [D][T_m][G]\ \Big] \end{bmatrix} d(vol) \qquad (2.42.30)$$

or

$$= \begin{bmatrix} [K_{nn}] & [K_{ne}] \\ [K_{en}] & [K_{ee}] \end{bmatrix} \tag{2.42.31}$$

where, $[K_{nn}]$ and $[K_{ee}]$ are the stiffnesses involving nodal and extra degrees of freedoms, respectively, and

$$\underset{8x8}{[K_{nn}]} = \int_{vol} [B_n]^T [T_m]^T [D][T_m][B_n] \; d(vol) \tag{2.42.32}$$

$$\underset{4x8}{[K_{en}]} = \int_{vol} [G]^T [T_m]^T [D][T_m][B_n] \; d(vol) \tag{2.42.33}$$

$$\underset{8x4}{[K_{ne}]} = [K_{en}]^T \tag{2.42.34}$$

$$\underset{4x4}{[K_{ee}]} = \int_{vol} [G]^T [T_m]^T [D][T_m][G] \; d(vol) \tag{2.42.35}$$

Similarly, the load vector is expanded to be:

$$\{F_e^{th}\} = \int_{vol} \Big[[B_n][G] \Big]^T [T_m]^T [D]\{\epsilon^{th}\} \; d(vol) \tag{2.42.36}$$

or

$$= \int_{vol} \left\{ \begin{array}{c} [B_m]^T [T_m]^T [D]\{\epsilon^{th}\} \\ \\ [G]^T [T_m]^T [D]\{\epsilon^{th}\} \end{array} \right\} d(vol) \tag{2.42.37}$$

or

$$= \left\{ \begin{array}{c} \{F_{nn}^{th}\} \\ \{F_{ee}^{th}\} \end{array} \right\} \tag{2.42.38}$$

so that:

$$\{F_{nn}^{th}\} = \int_{vol} [B_n]^T [T_m]^T [D]\{\epsilon^{th}\} \; d(vol) \tag{2.42.39}$$

$$\{F_{ee}^{th}\} = \int_{vol} [G]^T [T_m]^T [D] \{\epsilon^{th}\} \, d(vol) \qquad (2.42.40)$$

From equations (2.42.31) and (2.42.38) it is clear that when the extra shapes are dropped, the element stiffness and load vector computation becomes simplified as,

$$[K_e] = [K_{nn}] \qquad (2.42.41)$$

and

$$\{F_e^{th}\} = \{F_{nn}^{th}\} \qquad (2.42.42)$$

When the extra shape functions are used, a 12 by 12 stiffness matrix is generated. This matrix must then be condensed by an 8 by 8 matrix, because there are only 8 degrees of freedom to connect to the rest of the structure. The condensation is analogous to that associated with superelement generation (equation (1.10.8)). The load vector may also be generated with 12 terms and is then also condensed to 8 (like equation (1.10.9)).

Modified Extra Displacement Shapes

This section comments on the ramifications and possible modifications of extra displacement shapes for both the plane stress/plane strain case and the axisymmetric case. Extra shapes allow the element to move more flexibly. This flexibility is especially needed in bending environments. However, extra shapes can cause the element to be "incompatible" and lead to poor results. For the plane stress/plain strain case, the element with extra shapes will not pass the patch test unless the element geometry is that of a parallelogram (Taylor, et al(*49*)). For the axisymmetric case, the satisfaction of patch test is not in general possible, even when the elements are rectangular, and no proposed modification has been found that uniformly improves the results. However, a scheme (referred to as the modified extra shape option) is presented below, which ensures satisfaction of the patch test for the plane stress/plane strain case (and the same procedure is also offered for the axisymmetric case).

For this element to pass the patch test it is required that $\{u_e\}$ (displacements involving the extra shapes) be zero, whenever $\{u_n\}$ (nodal displacements) corresponds to rigid body motion or constant stress state. Now define $\{u_n\} = \{v_o\}$ as the set of nodal displacements which corresponds to an arbitrary constant stress state. Then, the element equilibrium equations become:

$$\begin{bmatrix} [K_{nn}] & [K_{ne}] \\ [K_{en}] & [K_{ee}] \end{bmatrix} \begin{Bmatrix} \{v_o\} \\ \{u_e\} \end{Bmatrix} = \begin{Bmatrix} \{F_n\} \\ \{0\} \end{Bmatrix} \tag{2.42.43}$$

The bottom part of these equations give:

$$\{u_e\} = -[K_{ee}]^{-1}[K_{en}]\{v_o\} \tag{2.42.44}$$

Since $\{u_e\} = \{0\}$, equation (2.42.44) becomes:

$$[K_{ee}]^{-1}[K_{en}]\{v_o\} = \{0\} \tag{2.42.45}$$

$[K_{ee}]^{-1}$ is positive definite and, therefore, can never of itself make the left hand side of equation (2.42.45) equal to zero, so that it can be dropped:

$$[K_{en}]\{v_o\} = \{0\} \tag{2.45.46}$$

Substituting equation (2.42.33) in for $[K_{en}]$, and moving $\{v_o\}$ into the integral,

$$\int_{vol} [G]^T[T_m]^T[D][T_m][B_n]\{v_o\}\, d(vol) = \{0\} \tag{2.42.47}$$

From the assumption on $\{v_o\}$ it is observed that the term $([T_m]^T[D][T_m][B_n]\{v_o\})$ is in fact the arbitrary constant stress state $\{\sigma\}$, so that it can be separated from equation (2.42.47) as,

$$\int_{vol} [G]^T\, d(vol)\ \{\sigma\} = \{0\} \tag{2.42.48}$$

or

$$\lfloor \sigma \rfloor \int_{vol} [G]\, d(vol) = \lfloor 0 \rfloor \tag{2.42.49}$$

Now, since stress vector $\{\sigma\}$ is, in general, not equal to zero, equation (2.42.49) reduces to:

$$\int_{vol} [G]\, d(vol) = [0] \tag{2.42.50}$$

From equations (2.42.15) and (2.42.16), matrix [G] for plane stress/plane strain case can be expressed as,

$$[G] = \begin{bmatrix} \frac{\partial h_1}{\partial X} & 0 & \frac{\partial h_2}{\partial X} & 0 \\ 0 & \frac{\partial h_1}{\partial Y} & 0 & \frac{\partial h_2}{\partial Y} \\ \frac{\partial h_1}{\partial Y} & \frac{\partial h_1}{\partial X} & \frac{\partial h_2}{\partial Y} & \frac{\partial h_2}{\partial X} \\ 0 & 0 & 0 & 0 \end{bmatrix} \qquad (2.42.51)$$

Replacing $\frac{\partial h_i}{\partial x}$ and $\frac{\partial h_i}{\partial y}$ from equations (2.42.24), (2.42.25) and (2.42.51)

$$[G] = \begin{bmatrix} Q_{11} & Q_{12} & 0 & 0 \\ 0 & 0 & Q_{21} & Q_{22} \\ Q_{21} & Q_{22} & Q_{11} & Q_{12} \\ 0 & 0 & 0 & 0 \end{bmatrix} \begin{bmatrix} \frac{\partial h_1}{\partial s} & 0 & \frac{\partial h_2}{\partial s} & 0 \\ \frac{\partial h_1}{\partial t} & 0 & \frac{\partial h_2}{\partial t} & 0 \\ 0 & \frac{\partial h_1}{\partial s} & 0 & \frac{\partial h_2}{\partial t} \\ 0 & \frac{\partial h_1}{\partial t} & 0 & \frac{\partial h_2}{\partial t} \end{bmatrix} \qquad (2.42.52)$$

Letting

$$[Q] = \begin{bmatrix} Q_{11} & Q_{12} & 0 & 0 \\ 0 & 0 & Q_{21} & Q_{22} \\ Q_{21} & Q_{22} & Q_{11} & Q_{12} \\ 0 & 0 & 0 & 0 \end{bmatrix} \qquad (2.42.53)$$

and

$$[D_h] = \begin{bmatrix} \frac{\partial h_1}{\partial s} & 0 & \frac{\partial h_2}{\partial s} & 0 \\ \frac{\partial h_1}{\partial t} & 0 & \frac{\partial h_2}{\partial t} & 0 \\ 0 & \frac{\partial h_1}{\partial s} & 0 & \frac{\partial h_2}{\partial s} \\ 0 & \frac{\partial h_1}{\partial t} & 0 & \frac{\partial h_2}{\partial t} \end{bmatrix} \qquad (2.42.54)$$

equation (2.42.52) can be written as:

$$[G] = [Q][D_h] \tag{2.42.55}$$

Now to enforce the satisfaction of equation (2.42.50), the procedure suggested by the reference (Taylor, et al(*49*)) is to compute [Q] in equation (2.42.53) at the centroid (origin) of the element:

$$[Q_c] = [Q]\Big|_{s=t=0} \tag{2.42.56}$$

and replace matrix [Q] in equation (2.42.55) by $[Q_c]$, creating a modified [G] matrix:

$$[G_m] = [Q_c][D_h] \tag{2.42.57}$$

Finally to compute the stiffness matrix for the modified extra shape function option the [G] matrix in equations (2.42.33) thru (2.42.35) and equation (2.42.40) is replaced by $[G_m]$ from equation (2.42.57).

APPENDIX 5 - II

USER DEFINED CODES AND MACROS USED IN THIS THESIS

```
/COM, THIS MODEL CAN BE ALTERED TO ANY DESIRED WIDTH
/COM, SPECIFY TO VARIABLE "EDGE" AS THE WIDTH OF THE MODEL

/COM, WINNIPEG AIRPORT.
/COM, RUNWAY 13-31 :ANALYSIS OF FWD DATA (1988)
/COM, ANSYS FINITE ELEMENT ANALYSIS USING
/COM, LAYERED ELASTIC MODEL.

/COM, USER DEFINED CODES FOR MODEL GEOMETRY AND ANALYSIS
/COM, GEOMETRY FOR STATION  5+870 3mL
/COM, DEFLECTIONS FOR STATION 5+870 3mL
/COM,=====================================================
=======

/show,VGA

/TITLE, WIA 13-31 5+870 3mL

/COM, PARAMETERS

*SET,STA,5870          * STATION ID:
*SET,N,4               * NUMBER OF LAYERS
*SET,H1,100            * AC
*SET,H2,500            * CTB
*SET,H3,160            * PCC
*SET,H4,15000          * CLAY SUBGRADE

*SET,NSL1,2            * number of sublayers in layer 1
*SET,NSL2,3            * number of sublayers in layer 2
*SET,NSL3,1            * number of sublayers in layer 3
*SET,NSL4,15           * number of sublayers in layer 4

*SET,SEN1,0            * Location of the HWD sensors
*SET,SEN2,300
*SET,SEN3,450
*SET,SEN4,1000
*SET,SEN5,1400
*SET,SEN6,1800
*SET,SEN7,2150

*SET,NNOD,25           * Definition of lateral extent
*SET,NELE,(NNOD-1)
*SET,EDGE,3000
```

/COM, MEASURED DISPLACEMENTS

```
*SET,m1,(-1.165)          * Measured deflections at the
*SET,m2,(-0.770)          * sensor locations
*SET,m3,(-0.652)
*SET,m4,(-0.422)
*SET,m5,(-0.344)
*SET,m6,(-0.285)
*SET,m7,(-0.234)
```

/COM, MEASURED STRESSES (If stresses were measured)

```
*SET,STR1,
*SET,STR2,
*SET,STR3,
*SET,STR4,
```

/COM, LOADS

```
*SET,DIA,450.000000       * diameter of wheel or HWD load (mm)
*SET,MPA1,1.40            * tire pressure  (MPa)
*SET,PTLD,0.0000000       * point load if applicable
```

/COM, INITIAL MATERIAL PROPERTIES

```
*SET,EY1,3000.000000      * vertical modulus of AC in layer 1 (MPa)
*SET,EX1,EY1              * EX1 = EY1 : ISOTROPIC MATERIAL
*SET,NUV1,0.20000E+00     * vertical Poisson's ratio of AC in layer 1
*SET,DEN1,0.23500E-05     * density of asphalt in layer 1 (kg/m^3)
*SET,EY2,300.0000         * vertical modulus of CTB
*SET,EX2,EY2              * ISOTROPIC MATERIAL
*SET,NUV2,0.25000E+00     * vertical Poisson's ratio of CTB
*SET,DEN2,0.24500E-05     * density of layer 2 (kg/cm^3)
*SET,EY3,10000.0000       * vertical modulus of PCC
*SET,EX3,EY3              * ISOTROPIC MATERIAL
*SET,NUV3,0.15000         * vertical Poisson's ratio of PCC
*SET,DEN3,0.245000E-05    * density of layer 3 (kg/cm^3)
*SET,EY4,70.00000         * vertical modulus of subgrade (MPa)
*SET,EX4,EY4              * ISOTROPIC MATERIAL
*SET,NUV4,0.440000        * vertical Poisson's ratio of subgrade
*SET,DEN4,0.245000E-05    * density of layer 4 (kg/cm^3)
```

/COM, LIMITS FOR MATERIAL PROPERTIES

```
*SET,LOE1,2000              * MODULI LIMITS FOR THE LAYERS
*SET,HIE1,5000
*SET,LOE2,200
*SET,HIE2,600
*SET,LOE3,8000
*SET,HIE3,15000
*SET,LOE4,40
*SET,HIE4,120

*SET,NUH1,.25               * POISSON'S RATIO LIMITS
*SET,NUL1,.15
*SET,NUH2,.3
*SET,NUL2,.20
*SET,NUH3,.2
*SET,NUL3,.12
*SET,NUH4,.48
*SET,NUL4,.42

*SET,TH1,(MPA1)             * TENSION LIMITS
*SET,TL1,(-MPA1)
*SET,TH2,(0.30)
*SET,TL2,(-MPA1)
*SET,TH3,(0.7)
*SET,TL3,(-MPA1)
*SET,TH4,(0)
*SET,TL4,(-MPA1)
```

/COM, NODE GENERATION

```
/PREP7
px1= DIA/2
NDELETE,ALL
EDELETE,ALL

N,1
N,9,SEN3
FILL
N,14,SEN4
FILL
N,18,SEN6
FILL
N,19,SEN7
N,NNOD,EDGE
FILL
```

```
SUM1=NSL1+1
T1=H1/NSL1
NGEN,SUM1,NNOD,1,NNOD,1,,-T1
BEG2=((NSL1*NNOD)+1)
FNOD=BEG2
*IF,H2,EQ,0,:NOD
SUM2=NSL2+1
END2=BEG2+(NSL2*NNOD)-1
T2=H2/NSL2
NGEN,SUM2,NNOD,BEG2,END2,1,,-T2
BEG3=BEG2+(NSL2*NNOD)
FNOD=BEG3
*IF,H3,EQ,0,:NOD
SUM3=NSL3+1
END3=END2+(NSL3*NNOD)
T3=H3/NSL3
NGEN,SUM3,NNOD,BEG3,END3,1,,-T3
BEG4=BEG3+(NSL3*NNOD)
FNOD=BEG4
*IF,H4,EQ,0,:NOD
SUM4=NSL4+1
END4=END3+(NSL4*NNOD)
T4=H4/NSL4
NGEN,SUM4,NNOD,BEG4,END4,1,,-T4
BEG5=BEG4+(NSL4*NNOD)
FNOD=BEG5
*IF,H5,EQ,0,:NOD
SUM5=NSL5+1
END5=END4+(NSL5*NNOD)
T5=H5/NSL5
NGEN,SUM5,NNOD,BEG5,END5,1,,-T5
BEG6=BEG5+(NSL5*NNOD)
FNOD=BEG6
*IF,H6,EQ,0,:NOD
SUM6=NSL6+1
END6=END5+(NSL6*NNOD)
T6=H6/NSL6
NGEN,SUM6,NNOD,BEG6,END6,1,,-T6
BEG7=BEG6+(NSL6*NNOD)
FNOD=BEG7
*IF,H7,EQ,0,:NOD
SUM7=NSL7+1
END7=END6+(NSL7*NNOD)
T7=H7/NSL7
NGEN,SUM7,NNOD,BEG7,END7,1,,-T7
FNOD=BEG7+(NSL7*NNOD)
```

```
:NOD
NPLOT                          * View the node pattern
```

/COM, GENERATE ELEMENTS

```
ET,1,42,,,1
MAT,1
EY,1,EY1
EX,1,EX1
NUXY,1,NUV1
E,1,2,(NNOD+2),(NNOD+1)
EGEN,NELE,1,1
EGEN,NSL1,NNOD,1,NELE,1
BEL2=(NSL1*NELE)+1
ENDE=BEL2-NELE
*IF,H2,EQ,0,:ELE
MAT,2
EY,2,EY2
EX,2,EX2
NUXY,2,NUV2
EEL2=(NSL1+1)*NELE
E,BEG2,(BEG2+1),(BEG2+(NNOD+1)),(BEG2+NNOD)
EGEN,NELE,1,BEL2
EGEN,NSL2,NNOD,BEL2,EEL2,1
BEL3=(BEL2+(NSL2*NELE))
ENDE=BEL3-NELE
*IF,H3,EQ,0,:ELE
MAT,3
EY,3,EY3
EX,3,EX3
NUXY,3,NUV3
EEL3=EEL2+(NSL3*NELE)
E,BEG3,(BEG3+1),(BEG3+(NNOD+1)),(BEG3+NNOD)
EGEN,NELE,1,BEL3
EGEN,NSL3,NNOD,BEL3,EEL3,1
BEL4=(BEL3+(NSL3*NELE))
ENDE=BEL4-NELE
*IF,H4,EQ,0,:ELE
MAT,4
EY,4,EY4
EX,4,EX4
NUXY,4,NUV4
EEL4=EEL3+(NSL4*NELE)
E,BEG4,(BEG4+1),(BEG4+(NNOD+1)),(BEG4+NNOD)
EGEN,NELE,1,BEL4
EGEN,NSL4,NNOD,BEL4,EEL4,1
```

```
BEL5=(BEL4+(NSL4*NELE))
ENDE=BEL5-NELE
*IF,H5,EQ,0,:ELE
MAT,5
EY,5,EY5
EX,5,EX5
NUXY,5,NUV5
EEL5=EEL4+(NSL5*NELE)
E,BEG5,(BEG5+1),(BEG5+(NNOD+1)),(BEG5+NNOD)
EGEN,NELE,1,BEL5
EGEN,NSL5,NNOD,BEL5,EEL5,1
BEL6=(BEL5+(NSL5*NELE))
ENDE=BEL6-NELE
*IF,H6,EQ,0,:ELE
MAT,6
EY,6,EY6
EX,6,EX6
NUXY,6,NUV6
EEL6=EEL5+(NSL6*NELE)
E,BEG6,(BEG6+1),(BEG6+(NNOD+1)),(BEG6+NNOD)
EGEN,NELE,1,BEL6
EGEN,NSL6,NNOD,BEL6,EEL6,1
BEL7=(BEL6+(NSL6*NELE))
ENDE=BEL7-NELE
*IF,H7,EQ,0,:ELE
MAT,7
EY,7,EY7
EX,7,EX7
NUXY,7,NUV7
EEL7=EEL6+(NSL7*NELE)
E,BEG7,(BEG7+1),(BEG7+(NNOD+1)),(BEG7+NNOD)
EGEN,NELE,1,BEL7
EGEN,NSL7,NNOD,BEL7,EEL7,1
BEL8=(BEL7+(NSL7*NELE))
ENDE=BEL8-NELE
:ELE
EPLOT                          * View the elemets
```

/COM, DEFINE BOUNDARY CONDITIONS

```
SYMBC,0,1,0
NSEL,X,EDGE
D,ALL,UX
NALL
D,FNOD,ALL,0,,(FNOD+NELE),1
```

```
/PBC,ALL,1
/PNUM,ELEM,1
/PNUM,MAT,1
NSEL,NODE,1,4
PSF,ALL,,,MPA1
NALL
SAVE                              * Save the geometry of the model
```

/COM, SOLUTION PHASE

```
RESUME,,,,1
MAT,1
EX,1,EY1
MAT,2
EX,2,EY2
MAT,3
EX,3,EY3
MAT,4
EX,4,EY4
MAT,5
EX,5,EY5
MAT,6
EX,6,EY6
MAT,7
EX,7,EY7
SFWRITE
FINISH
/SOLVE
FINISH
```

/COM, POST PROCESSING

```
/POST1
STRESS,TENS,42,1                  * Define the stress parameters
STRESS,VERT,42,2
SET

*GET,UY1,UY,1                     * Store deflections at sensor points
*GET,UY2,UY,6
*GET,UY3,UY,9
*GET,UY4,UY,14
*GET,UY5,UY,16
*GET,UY6,UY,18
*GET,UY7,UY,19
*GET,UY8,UY,EDGE
```

```
ESEL,MAT,1,N,1
ESORT,TENS
*GET,TENS,MAX
TEN1 = TENS
EALL
ESEL,MAT,2,N,1
ESORT,TENS
*GET,TENS,MAX
TEN2 = TENS
EALL
ESEL,MAT,3,N,1
ESORT,TENS
*GET,TENS,MAX
TEN3 = TENS
EALL
ESEL,MAT,4,N,1
ESORT,TENS
*GET,TENS,MAX
TEN4 = TENS
EALL
ESEL,MAT,5,N,1
ESORT,TENS
*GET,TENS,MAX
TEN5 = TENS
EALL
ESEL,ELEM,1,ENDE,NELE

/COM, GET VERTICAL STRESSES

*GET,V1,VERT,1
*GET,V21,VERT,NNOD                  * bottom of A.C.
*GET,V41,VERT,(NNOD+NELE)
*GET,V61,VERT,(NNOD+(2*NELE))
*GET,V81,VERT,(NNOD+(3*NELE))       * bottom of crushed CTB
*GET,V101,VERT,(NNOD+(4*NELE))      * PCC
*GET,V121,VERT,(NNOD+(5*NELE))      * top of subgrade
*GET,V141,VERT,(NNOD+(6*NELE))
*GET,V161,VERT,(NNOD+(7*NELE))
*GET,V181,VERT,(NNOD+(8*NELE))
*GET,V201,VERT,(NNOD+(9*NELE))
*GET,V221,VERT,(NNOD+(10*NELE))
*GET,V241,VERT,(NNOD+(11*NELE))
*GET,V261,VERT,(NNOD+(12*NELE))
*GET,V301,VERT,(NNOD+(13*NELE))
*GET,V341,VERT,(NNOD+(14*NELE))
*GET,V381,VERT,(NNOD+(15*NELE))
```

```
*GET,V421,VERT,(NNOD+(16*NELE))
*GET,V461,VERT,(NNOD+(17*NELE))
EALL
STORE
```

/COM, CALCULATE THE OBJECTIVE FUNCTION (Here area of Basin)

```
a1 = (m1+m2)/2
d1 = (SEN2-SEN1)
ma1= a1*d1
a2 = (m2+m3)/2
d2 = (SEN3-SEN2)
ma2= a2*d2
a3 = (m3+m4)/2
d3 = (SEN4-SEN3)
ma3= a3*d3
a4 = (m4+m5)/2
d4 = (SEN5-SEN4)
ma4= a4*d4
a5 = (m5+m6)/2
d5 = (SEN6-SEN5)
ma5= a5*d5
a6 = (m6+m7)/2
d6 = (SEN7-SEN6)
ma6= a6*d6
ca1 = ((UY1+UY2)/2)*d1
ca2 = ((UY2+UY3)/2)*d2
ca3 = ((UY3+UY4)/2)*d3
ca4 = ((UY4+UY5)/2)*d4
ca5 = ((UY5+UY6)/2)*d5
ca6 = ((UY6+UY7)/2)*d6
err1 = (ca1-ma1)*(ca1-ma1)
err2 = (ca2-ma2)*(ca2-ma2)
area = err1 + err2
err3 = (ca3-ma3)*(ca3-ma3)
area = area + err3
err4 = (ca4-ma4)*(ca4-ma4)
err4 = err4
area = area + err4
err5 = (ca5-ma5)*(ca5-ma5)
area = area + err5
err6 = (ca6-ma6)*(ca6-ma6)
AREA = (area + err6)            * Objective function
FINISH
```

/COM, OPTIMIZATION PROCESS

```
/OPT                          * Call the optimization routine
opvar,EY1,dv,LOE1,HIE1        * Define design variables
opvar,EY2,dv,LOE2,HIE2
opvar,EY3,dv,LOE3,HIE3
opvar,EY4,dv,LOE4,HIE4
opvar,NUV1,dv,NUL1,NUH1
opvar,NUV2,dv,NUL2,NUH2
opvar,NUV3,dv,NUL3,NUH3
opvar,NUV4,dv,NUL4,NUH4
opvar,TEN1,sv,TL1,TH1         * Define state variables
opvar,TEN2,sv,TL2,TH2
opvar,TEN3,sv,TL3,TH3
opvar,TEN4,sv,TL4,TH4
opvar,AREA,obj                * Define objective function
opeqn,0,3,3,0,0
opcopy,,1
oprun,50                      * Run 50 loops of optimazation
FINISH
/OPT
RESUME
OPSEL,15                      * Select the best 15 solutions and rank them
OPSORT,AREA,0
/OUTPUT,WIA587O,OUT           * Write results to user-defined file
OPLIST,ALL
```

/COM, DEFINE THE PARAMETERS TO BE PRINTED OUT

```
PRVAR,OBJ,EY1,EY2,EY3,EY4
PRVAR,OBJ,UY1,UY2,UY3,UY4,UY5,UY6,UY7,UY8
PRVAR,OBJ,V1,V21,V41,V61,V81,V101,V121,V141,V161,V181
PRVAR,OBJ,V201,V221,V241,V261,V301,V341,V381,V421,V461
PRVAR,OBJ,TEN1,TEN2,TEN3,TEN4
FINISH
```

APPENDIX 6-I

TYPICAL RESULTS OF ANALYSES FOR EACH SITE (TABLES)

Note: The tables on the following pages show the results for one station at each site for the maximum load. The results include comparison of deflections and moduli, and computations of stresses. The complete set of results for all stations at all sites are included in another volume.

ANSYS FEM ANALYSIS: ISOTROPIC MODEL

BRANDON: RWY 08-26: STA. 5 + 900 R: LOAD 1360 kPa

OPTIMIZATION CRITERION: "AREA" OF DEFLECTION BASIN.

CALCULATED MODULI (MPa)

SET	12	15	8	14	7	MIN	AVG	MAX
EY1	4007	4197	3765	4174	3768	3765	3982	4197
EY2	151	151	151	151	151	151	151	151
EY3	134	125	152	133	153	125	139	153

CALCULATED AND OBSERVED DEFLECTIONS (mm)

						OBSERVED DEFL.(mm)	SENSOR DISTANCE(mm)
UY1	-0.957705	-0.960424	-0.968034	-0.943629	-0.966645	-0.947	0
UY2	-0.599350	-0.611414	-0.598156	-0.593670	-0.596417	-0.605	300
UY3	-0.317227	-0.331788	-0.313732	-0.314272	-0.311827	-0.344	614
UY4	-0.199192	-0.212520	-0.197319	-0.195922	-0.195766	-0.206	914
UY5	-0.145869	-0.157777	-0.145720	-0.142214	-0.144629	-0.138	1219
UY6	-0.116836	-0.127598	-0.118204	-0.112998	-0.117506	-0.112	1524
UY7	-0.098376	-0.108212	-0.101087	-0.094439	-0.100684	-0.092	1829

OPTIMIZATION CRITERION: MAXIMUM DEFLECTION

CALCULATED MODULI (MPa)

SET	7	1	12	3	4	MIN	AVG	MAX
EY1	4310.17	3000.00	8447.64	8630.63	7256.32	3000.00	6328.95	8630.63
EY2	162.09	200.00	153.85	151.83	188.50	151.83	171.25	200.00
EY3	140.63	100.00	74.70	143.82	119.46	74.70	115.72	143.82

CALCULATED AND OBSERVED DEFLECTIONS (mm)

						OBSERVED DEFL.(mm)	SENSOR DISTANCE(mm)
UY1	-0.930919	-0.913101	-0.888839	-0.800859	-0.731936	-0.947	0
UY2	-0.599836	-0.540406	-0.662389	-0.575267	-0.497979	-0.605	300
UY3	-0.339366	-0.297187	-0.434915	-0.351684	-0.289518	-0.344	614
UY4	-0.228773	-0.203915	-0.310742	-0.235356	-0.189435	-0.206	914
UY5	-0.177611	-0.157114	-0.242593	-0.177419	-0.139209	-0.138	1219
UY6	-0.149247	-0.127059	-0.201356	-0.146787	-0.110062	-0.112	1524
UY7	-0.131080	-0.105636	-0.173522	-0.128626	-0.090735	-0.092	1829

ANSYS FEM ANALYSIS: ISOTROPIC MODEL

BRANDON: RWY 08-26: STA. 5 + 900 R: LOAD 1360 kPa

OPTIMIZATION CRITERION: RMS VALUE OF DEFLECTIONS.

CALCULATED MODULI (MPa)

SET	7	1	10	9	3	MIN	AVG	MAX
EY1	4310.17	3000.00	5523.45	3566.60	8630.63	3000.00	5006.17	8630.63
EY2	162.09	200.00	153.74	153.81	151.83	151.83	164.29	200.00
EY3	140.63	100.00	219.65	205.46	143.82	100.00	161.91	219.65

CALCULATED AND OBSERVED DEFLECTIONS (mm)

						OBSERVED DEFL.(mm)	SENSOR DISTANCE(mm)
UY1	-0.930919	-0.913101	-0.844099	-0.911096	-0.800859	-0.947	0
UY2	-0.599836	-0.540406	-0.552338	-0.532115	-0.575267	-0.605	300
UY3	-0.339366	-0.297187	-0.301750	-0.250213	-0.351684	-0.344	614
UY4	-0.228773	-0.203915	-0.191130	-0.140460	-0.235356	-0.206	914
UY5	-0.177611	-0.157114	-0.143620	-0.094839	-0.177419	-0.138	1219
UY6	-0.149247	-0.127059	-0.121264	-0.072183	-0.146787	-0.112	1524
UY7	-0.131080	-0.105636	-0.109065	-0.058945	-0.128626	-0.092	1829

ANSYS FEM ANALYSIS: ISOTROPIC MODEL

BRANDON: RWY 08-26: STA. 5 + 900 R

DISTRIBUTION OF VERTICAL STRESSES

"AREA" OF BASIN

DEPTH (mm)	DEPTH RATIO z/ao	LOAD 1: 588 kPa 2	12	4	1	5	AVG.	STRESS RATIO p/po	LOAD 2: 844 kPa 9	5	8	13	16	AVG.	STRESS RATIO p/po
30	0.20	-0.493	-0.492	-0.492	-0.490	-0.491	-0.492	0.837	-0.706	-0.714	-0.717	-0.698	-0.698	-0.707	0.837
90	0.60	-0.267	-0.264	-0.263	-0.258	-0.260	-0.262	0.446	-0.375	-0.399	-0.408	-0.355	-0.351	-0.378	0.448
224	1.49	-0.107	-0.105	-0.103	-0.100	-0.101	-0.103	0.175	-0.142	-0.161	-0.167	-0.127	-0.125	-0.145	0.171
432	2.88	-0.055	-0.055	-0.053	-0.052	-0.052	-0.053	0.091	-0.070	-0.077	-0.079	-0.064	-0.064	-0.071	0.084
640	4.27	-0.033	-0.033	-0.031	-0.031	-0.031	-0.032	0.054	-0.040	-0.044	-0.045	-0.038	-0.038	-0.041	0.049
848	5.65	-0.022	-0.022	-0.021	-0.020	-0.021	-0.021	0.036	-0.026	-0.029	-0.029	-0.025	-0.025	-0.027	0.031
1056	7.04	-0.015	-0.015	-0.015	-0.014	-0.015	-0.015	0.025	-0.018	-0.020	-0.020	-0.017	-0.017	-0.018	0.022
1660	11.07	-0.007	-0.007	-0.007	-0.007	-0.007	-0.007	0.012	-0.009	-0.009	-0.010	-0.009	-0.008	-0.009	0.011
2660	17.73	-0.003	-0.003	-0.003	-0.003	-0.003	-0.003	0.004	-0.003	-0.004	-0.004	-0.003	-0.003	-0.004	0.004

DEPTH (mm)	DEPTH RATIO z/ao	LOAD 3: 1192 kPa 16	4	7	9	10	AVG.	STRESS RATIO p/po	LOAD 4: 1360 kPa 12	15	8	14	7	AVG.	STRESS RATIO p/po
30	0.20	-0.997	-0.996	-0.991	-0.988	-0.988	-0.992	0.832	-1.137	-1.134	-1.140	-1.135	-1.140	-1.137	0.836
90	0.60	-0.534	-0.538	-0.520	-0.514	-0.509	-0.523	0.439	-0.603	-0.597	-0.612	-0.597	-0.611	-0.604	0.444
224	1.49	-0.211	-0.210	-0.196	-0.194	-0.191	-0.200	0.168	-0.237	-0.232	-0.241	-0.233	-0.242	-0.237	0.174
432	2.88	-0.110	-0.109	-0.100	-0.104	-0.104	-0.105	0.088	-0.124	-0.122	-0.122	-0.123	-0.124	-0.123	0.090
640	4.27	-0.064	-0.064	-0.059	-0.063	-0.063	-0.063	0.053	-0.073	-0.072	-0.072	-0.072	-0.073	-0.072	0.053
848	5.65	-0.042	-0.042	-0.039	-0.042	-0.042	-0.041	0.035	-0.047	-0.046	-0.047	-0.047	-0.048	-0.047	0.035
1056	7.04	-0.028	-0.030	-0.028	-0.030	-0.030	-0.029	0.024	-0.032	-0.032	-0.033	-0.032	-0.033	-0.032	0.024
1660	11.07	-0.013	-0.014	-0.013	-0.014	-0.014	-0.014	0.012	-0.015	-0.015	-0.016	-0.015	-0.016	-0.015	0.011
2660	17.73	-0.005	-0.005	-0.005	-0.005	-0.005	-0.005	0.004	-0.006	-0.006	-0.006	-0.006	-0.006	-0.006	0.004

MAXIMUM DEFLECTION

DEPTH (mm)	DEPTH RATIO z/ao	7	1	3	4	11	AVG.	STRESS RATIO p/po	7	1	3	12	4	AVG.	STRESS RATIO p/po
30	0.20	-0.492	-0.504	-0.478	-0.484	-0.479	-0.487	0.829	-0.706	-0.723	-0.686	-0.687	-0.695	-0.699	0.829
90	0.60	-0.262	-0.297	-0.226	-0.245	-0.224	-0.251	0.427	-0.377	-0.426	-0.325	-0.325	-0.352	-0.361	0.427
224	1.49	-0.101	-0.126	-0.074	-0.087	-0.074	-0.092	0.157	-0.145	-0.181	-0.106	-0.107	-0.125	-0.133	0.157
432	2.88	-0.050	-0.058	-0.042	-0.045	-0.043	-0.048	0.081	-0.072	-0.084	-0.060	-0.061	-0.065	-0.068	0.081
640	4.27	-0.029	-0.031	-0.026	-0.027	-0.028	-0.028	0.048	-0.041	-0.045	-0.038	-0.039	-0.038	-0.040	0.048
848	5.65	-0.019	-0.019	-0.018	-0.017	-0.019	-0.018	0.031	-0.027	-0.027	-0.026	-0.026	-0.024	-0.026	0.031
1056	7.04	-0.013	-0.012	-0.013	-0.011	-0.014	-0.013	0.021	-0.018	-0.017	-0.018	-0.019	-0.016	-0.018	0.021
1660	11.07	-0.006	-0.005	-0.006	-0.005	-0.007	-0.006	0.010	-0.009	-0.008	-0.009	-0.009	-0.008	-0.009	0.010
2660	17.73	-0.002	-0.002	-0.002	-0.002	-0.003	-0.002	0.004	-0.003	-0.003	-0.004	-0.004	-0.003	-0.003	0.004

DEPTH (mm)	DEPTH RATIO z/ao	7	1	12	3	4	AVG.	STRESS RATIO p/po	7	1	12	3	4	AVG.	STRESS RATIO p/po
30	0.20	-0.997	-1.022	-0.971	-0.969	-0.981	-0.988	0.829	-1.138	-1.166	-1.108	-1.105	-1.120	-1.127	0.829
90	0.60	-0.532	-0.601	-0.458	-0.458	-0.497	-0.509	0.427	-0.607	-0.686	-0.522	-0.523	-0.567	-0.581	0.427
224	1.49	-0.204	-0.256	-0.148	-0.149	-0.176	-0.187	0.157	-0.233	-0.292	-0.168	-0.170	-0.201	-0.213	0.157
432	2.88	-0.101	-0.118	-0.080	-0.085	-0.092	-0.095	0.080	-0.115	-0.135	-0.092	-0.097	-0.105	-0.109	0.080
640	4.27	-0.059	-0.064	-0.048	-0.053	-0.054	-0.055	0.047	-0.067	-0.073	-0.054	-0.061	-0.062	-0.063	0.047
848	5.65	-0.038	-0.038	-0.030	-0.036	-0.034	-0.035	0.030	-0.043	-0.043	-0.034	-0.041	-0.039	-0.040	0.030
1056	7.04	-0.026	-0.024	-0.020	-0.026	-0.023	-0.024	0.020	-0.029	-0.027	-0.022	-0.029	-0.026	-0.027	0.020
1660	11.07	-0.012	-0.011	-0.010	-0.013	-0.011	-0.011	0.010	-0.014	-0.012	-0.011	-0.015	-0.013	-0.013	0.010
2660	17.73	-0.005	-0.004	-0.004	-0.005	-0.005	-0.005	0.004	-0.006	-0.005	-0.005	-0.006	-0.005	-0.005	0.004

RMS VALUE OF DEFLECTION

DEPTH (mm)	DEPTH RATIO z/ao	7	1	9	3	4	AVG.	STRESS RATIO p/po	12	7	1	3	10	AVG.	STRESS RATIO p/po
30	0.20	-0.492	-0.504	-0.498	-0.478	-0.484	-0.491	0.835	-0.700	-0.706	-0.723	-0.686	-0.687	-0.701	0.830
90	0.60	-0.262	-0.297	-0.280	-0.226	-0.245	-0.262	0.445	-0.362	-0.377	-0.426	-0.325	-0.322	-0.362	0.429
224	1.49	-0.101	-0.126	-0.116	-0.074	-0.087	-0.101	0.171	-0.132	-0.145	-0.181	-0.106	-0.105	-0.134	0.158
432	2.88	-0.050	-0.058	-0.058	-0.042	-0.045	-0.051	0.086	-0.066	-0.072	-0.084	-0.060	-0.059	-0.068	0.081
640	4.27	-0.029	-0.031	-0.034	-0.026	-0.027	-0.029	0.050	-0.038	-0.041	-0.045	-0.038	-0.035	-0.040	0.047
848	5.65	-0.019	-0.019	-0.023	-0.018	-0.017	-0.019	0.032	-0.025	-0.027	-0.027	-0.026	-0.022	-0.025	0.030
1056	7.04	-0.013	-0.012	-0.016	-0.013	-0.011	-0.013	0.022	-0.017	-0.018	-0.017	-0.018	-0.015	-0.017	0.020
1660	11.07	-0.006	-0.005	-0.008	-0.006	-0.005	-0.006	0.011	-0.008	-0.009	-0.008	-0.009	-0.007	-0.008	0.010
2660	17.73	-0.002	-0.002	-0.003	-0.002	-0.002	-0.002	0.004	-0.003	-0.003	-0.003	-0.004	-0.003	-0.003	0.004

DEPTH (mm)	DEPTH RATIO z/ao	7	1	14	3	10	AVG.	STRESS RATIO p/po	7	1	10	9	3	AVG.	STRESS RATIO p/po
30	0.20	-0.997	-1.022	-0.982	-0.969	-0.971	-0.988	0.829	-1.138	-1.166	-1.124	-1.143	-1.105	-1.135	0.835
90	0.60	-0.532	-0.601	-0.491	-0.458	-0.455	-0.507	0.426	-0.607	-0.686	-0.566	-0.622	-0.523	-0.601	0.442
224	1.49	-0.204	-0.256	-0.172	-0.149	-0.149	-0.186	0.156	-0.233	-0.292	-0.208	-0.250	-0.170	-0.231	0.170
432	2.88	-0.101	-0.118	-0.089	-0.085	-0.083	-0.095	0.080	-0.115	-0.135	-0.114	-0.128	-0.097	-0.118	0.087
640	4.27	-0.059	-0.064	-0.053	-0.053	-0.050	-0.056	0.047	-0.067	-0.073	-0.071	-0.076	-0.061	-0.069	0.051
848	5.65	-0.038	-0.038	-0.035	-0.036	-0.032	-0.036	0.030	-0.043	-0.043	-0.049	-0.051	-0.041	-0.045	0.033
1056	7.04	-0.026	-0.024	-0.024	-0.026	-0.021	-0.024	0.020	-0.029	-0.027	-0.035	-0.036	-0.029	-0.031	0.023
1660	11.07	-0.012	-0.011	-0.012	-0.013	-0.010	-0.012	0.010	-0.014	-0.012	-0.017	-0.017	-0.015	-0.015	0.011
2660	17.73	-0.005	-0.004	-0.005	-0.005	-0.004	-0.005	0.004	-0.006	-0.005	-0.006	-0.006	-0.006	-0.006	0.004

ANSYS FEM ANALYSIS: X-ANISOTROPIC MODEL

BRANDON: RWY 08-26: STA. 5 + 900 R: LOAD 1360 kPa

OPTIMIZATION CRITERION: "AREA" OF DEFLECTION BASIN.

CALCULATED MODULI (MPa)

SET	16	15	14	11	6	MIN	AVG	MAX
EY1	4728	4761	4669	4585	4361	4361	4621	4761
EY2	154	153	159	163	167	153	159	167
EX2	92	94	146	185	169	92	137	185
EY3	158	157	139	131	119	119	141	158
EX3	166	210	120	99	107	99	140	210
R2	0.60	0.61	0.92	1.13	1.01	0.60	0.85	1.13
R3	1.05	1.34	0.86	0.76	0.90	0.76	0.98	1.34

CALCULATED AND OBSERVED DEFLECTIONS (mm)

						OBSERVED DEFL.(mm)	SENSOR DISTANCE(mm)
UY1	-0.945652	-0.939634	-0.912547	-0.894481	-0.930686	-0.947	0
UY2	-0.603158	-0.598953	-0.587551	-0.575118	-0.600663	-0.605	300
UY3	-0.313365	-0.311436	-0.321733	-0.320045	-0.341566	-0.344	614
UY4	-0.186698	-0.187141	-0.205389	-0.210085	-0.231163	-0.206	914
UY5	-0.131195	-0.133887	-0.151069	-0.158020	-0.178677	-0.138	1219
UY6	-0.103467	-0.108009	-0.121056	-0.128190	-0.148219	-0.112	1524
UY7	-0.087151	-0.093074	-0.101884	-0.108465	-0.127876	-0.092	1829

OPTIMIZATION CRITERION: MAXIMUM DEFLECTION

CALCULATED MODULI (MPa)

SET	1	7	12	13	11	MIN	AVG	MAX
EY1	3000	4452	1517	1523	8172	1517	3733	8172
EY2	200	183	162	162	162	162	174	200
EX2	200	304	338	233	104	104	236	338
EY3	100	54	64	213	65	54	99	213
EX3	100	87	135	182	42	42	109	182
R2	1.00	1.66	2.08	1.44	0.64	0.64	1.36	2.08
R3	1.00	1.60	2.10	0.86	0.65	0.65	1.24	2.10

CALCULATED AND OBSERVED DEFLECTIONS (mm)

						OBSERVED DEFL.(mm)	SENSOR DISTANCE(mm)
UY1	-0.913101	-1.015370	-1.057160	-1.095570	-1.141040	-0.947	0
UY2	-0.540406	-0.722174	-0.537217	-0.557635	-0.898787	-0.605	300
UY3	-0.297187	-0.502744	-0.267786	-0.278786	-0.653408	-0.344	614
UY4	-0.203915	-0.407653	-0.177145	-0.188177	-0.516723	-0.206	914
UY5	-0.157114	-0.357546	-0.130539	-0.147524	-0.438879	-0.138	1219
UY6	-0.127059	-0.324563	-0.099248	-0.124585	-0.389778	-0.112	1524
UY7	-0.105636	-0.300229	-0.076328	-0.110184	-0.355645	-0.092	1829

ANSYS FEM ANALYSIS: X-ANISOTROPIC MODEL

BRANDON: RWY 08-26: STA. 5 + 900 R: LOAD 1360 kPa

OPTIMIZATION CRITERION: RMS VALUE OF DEFLECTIONS.

CALCULATED MODULI (MPa)

SET	1	15	16	13	12	MIN	AVG	MAX
EY1	3000	3348	1609	1540	1517	1517	2203	3348
EY2	200	194	161	164	162	161	176	200
EX2	200	323	391	103	402	103	284	402
EY3	100	114	133	138	208	100	139	208
EX3	100	99	155	296	436	99	217	436
R2	1.00	1.67	2.42	0.63	2.48	0.63	1.64	2.48
R3	1.00	0.87	1.17	2.15	2.10	0.87	1.46	2.15

CALCULATED AND OBSERVED DEFLECTIONS (mm)

						OBSERVED DEFL.(mm)	SENSOR DISTANCE(mm)
UY1	-0.913101	-0.814625	-1.089280	-1.193460	-0.915117	-0.947	0
UY2	-0.540406	-0.483625	-0.604211	-0.567217	-0.419450	-0.605	300
UY3	-0.297187	-0.262874	-0.349970	-0.227640	-0.169372	-0.344	614
UY4	-0.203915	-0.177796	-0.264137	-0.119989	-0.090007	-0.206	914
UY5	-0.157114	-0.135905	-0.223065	-0.073904	-0.055200	-0.138	1219
UY6	-0.127059	-0.109382	-0.197987	-0.048480	-0.035971	-0.112	1524
UY7	-0.105636	-0.090517	-0.181002	-0.032561	-0.024149	-0.092	1829

ANSYS FEM ANALYSIS: X-ANISOTROPIC MODEL

BRANDON: RWY 08-26: STA. 5 + 900 R

DISTRIBUTION OF VERTICAL STRESSES

"AREA OF BASIN"

		LOAD 1: 588 kPa							LOAD 2: 844 kPa							LOAD 3: 1192 kPa						LOAD 4: 1360 kPa					
DEPTH (mm)	DEPTH RATIO (z/ro)	3	16	15	9	8	AVG	STRESS RATIO (p/po)	8	15	12	1	3	AVG	STRESS RATIO (p/po)	8	5	4	2	AVG	STRESS RATIO (p/po)	15	14	11	6	AVG	STRESS RATIO (p/po)
30	0.20	-0.508	-0.496	-0.510	-0.514	-0.497	-0.505	0.859	-0.733	-0.730	-0.735	-0.723	-0.728	-0.730	0.865	-1.002	-1.039	-0.997	-1.016	-1.013	0.850	-1.117	-1.130	-1.137	-1.137	-1.130	0.831
90	0.60	-0.309	-0.274	-0.314	-0.324	-0.278	-0.300	0.510	-0.453	-0.446	-0.464	-0.426	-0.439	-0.445	0.528	-0.544	-0.644	-0.531	-0.587	-0.576	0.483	-0.552	-0.590	-0.608	-0.610	-0.590	0.434
224	1.49	-0.134	-0.110	-0.137	-0.143	-0.115	-0.128	0.217	-0.197	-0.195	-0.208	-0.181	-0.190	-0.194	0.230	-0.209	-0.270	-0.206	-0.247	-0.233	0.196	-0.202	-0.223	-0.235	-0.238	-0.225	0.165
432	2.88	-0.060	-0.053	-0.061	-0.062	-0.055	-0.058	0.099	-0.087	-0.086	-0.091	-0.084	-0.088	-0.087	0.103	-0.100	-0.114	-0.103	-0.117	-0.109	0.091	-0.111	-0.114	-0.122	-0.121	-0.117	0.086
640	4.27	-0.032	-0.030	-0.033	-0.034	-0.031	-0.032	0.055	-0.046	-0.045	-0.047	-0.045	-0.047	-0.046	0.054	-0.057	-0.061	-0.058	-0.065	-0.060	0.051	-0.068	-0.067	-0.071	-0.070	-0.069	0.051
848	5.65	-0.020	-0.019	-0.021	-0.021	-0.020	-0.020	0.034	-0.027	-0.025	-0.028	-0.027	-0.029	-0.027	0.032	-0.036	-0.037	-0.036	-0.040	-0.037	0.031	-0.046	-0.043	-0.045	-0.044	-0.045	0.033
1056	7.04	-0.013	-0.013	-0.014	-0.014	-0.014	-0.014	0.023	-0.017	-0.015	-0.017	-0.017	-0.018	-0.017	0.020	-0.025	-0.024	-0.023	-0.026	-0.024	0.020	-0.034	-0.030	-0.029	-0.029	-0.030	0.022
1660	11.07	-0.006	-0.006	-0.006	-0.006	-0.007	-0.006	0.011	-0.007	-0.006	-0.008	-0.008	-0.008	-0.007	0.009	-0.014	-0.013	-0.010	-0.012	-0.012	0.010	-0.020	-0.014	-0.013	-0.013	-0.015	0.011
2160	14.40	-0.002	-0.002	-0.002	-0.002	-0.003	-0.002	0.004	-0.003	-0.002	-0.004	-0.003	-0.003	-0.003	0.004	-0.007	-0.006	-0.004	-0.005	-0.005	0.004	-0.008	-0.005	-0.004	-0.005	-0.006	0.004

MAXIMUM DEFLECTION

DEPTH (mm)	DEPTH RATIO (z/ro)	1	13	12	7	11	AVG	STRESS RATIO (p/po)	1	7	13	11	5	AVG	STRESS RATIO (p/po)	13	7	11	12	AVG	STRESS RATIO (p/po)	7	12	13	11	AVG	STRESS RATIO (p/po)
30	0.20	-0.504	-0.512	-0.477	-0.499	-0.475	-0.493	0.839	-0.723	-0.716	-0.694	-0.684	-0.707	-0.705	0.835	-1.038	-1.012	-0.966	-1.035	-1.013	0.849	-1.154	-1.216	-1.205	-1.102	-1.169	0.860
90	0.60	-0.297	-0.315	-0.220	-0.282	-0.221	-0.267	0.454	-0.426	-0.405	-0.339	-0.322	-0.375	-0.373	0.442	-0.640	-0.571	-0.454	-0.648	-0.578	0.485	-0.652	-0.818	-0.789	-0.517	-0.694	0.510
224	1.49	-0.126	-0.136	-0.072	-0.106	-0.070	-0.102	0.174	-0.181	-0.153	-0.118	-0.106	-0.135	-0.139	0.164	-0.273	-0.215	-0.148	-0.299	-0.234	0.196	-0.246	-0.388	-0.343	-0.167	-0.286	0.210
432	2.88	-0.058	-0.063	-0.041	-0.048	-0.040	-0.050	0.085	-0.084	-0.068	-0.067	-0.061	-0.071	-0.070	0.083	-0.122	-0.096	-0.083	-0.137	-0.110	0.092	-0.110	-0.183	-0.141	-0.092	-0.132	0.097
640	4.27	-0.031	-0.034	-0.026	-0.026	-0.024	-0.028	0.048	-0.045	-0.037	-0.041	-0.039	-0.043	-0.041	0.049	-0.066	-0.052	-0.050	-0.075	-0.061	0.051	-0.060	-0.098	-0.077	-0.054	-0.072	0.053
848	5.65	-0.019	-0.020	-0.018	-0.015	-0.016	-0.017	0.030	-0.027	-0.021	-0.027	-0.028	-0.029	-0.026	0.031	-0.039	-0.030	-0.033	-0.049	-0.038	0.032	-0.034	-0.058	-0.049	-0.034	-0.044	0.032
1056	7.04	-0.012	-0.012	-0.013	-0.009	-0.011	-0.011	0.019	-0.017	-0.013	-0.018	-0.021	-0.020	-0.018	0.021	-0.024	-0.018	-0.023	-0.034	-0.025	0.021	-0.020	-0.036	-0.034	-0.021	-0.028	0.020
1660	11.07	-0.005	-0.006	-0.006	-0.005	-0.009	-0.006	0.010	-0.008	-0.007	-0.008	-0.013	-0.009	-0.009	0.010	-0.013	-0.009	-0.017	-0.016	-0.014	0.012	-0.010	-0.020	-0.015	-0.010	-0.014	0.010
2160	14.40	-0.002	-0.003	-0.003	-0.002	-0.005	-0.003	0.005	-0.003	-0.003	-0.003	-0.006	-0.004	-0.004	0.005	-0.006	-0.005	-0.009	-0.006	-0.007	0.006	-0.006	-0.010	-0.006	-0.004	-0.006	0.005

RMS VALUE OF DEFLECTIONS

DEPTH (mm)	DEPTH RATIO (z/ro)	1	12	11	5	7	AVG	STRESS RATIO (p/po)	1	16	10	12	7	AVG	STRESS RATIO (p/po)	13	14	12	5	AVG	STRESS RATIO (p/po)	15	16	13	12	AVG	STRESS RATIO (p/po)
30	0.20	-0.504	-0.528	-0.477	-0.493	-0.499	-0.500	0.851	-0.723	-0.717	-0.751	-0.701	-0.743	-0.727	0.861	-1.054	-1.073	-1.049	-0.998	-1.044	0.876	-1.173	-1.215	-1.179	-1.219	-1.197	0.880
90	0.60	-0.297	-0.361	-0.221	-0.262	-0.282	-0.284	0.483	-0.426	-0.408	-0.505	-0.362	-0.483	-0.437	0.517	-0.698	-0.731	-0.682	-0.530	-0.661	0.554	-0.697	-0.804	-0.739	-0.817	-0.764	0.562
224	1.49	-0.126	-0.177	-0.073	-0.094	-0.106	-0.115	0.196	-0.181	-0.170	-0.235	-0.138	-0.222	-0.189	0.224	-0.314	-0.324	-0.313	-0.191	-0.285	0.239	-0.295	-0.342	-0.340	-0.355	-0.333	0.245
432	2.88	-0.058	-0.086	-0.042	-0.050	-0.048	-0.057	0.097	-0.084	-0.082	-0.104	-0.072	-0.099	-0.088	0.104	-0.131	-0.137	-0.137	-0.100	-0.126	0.106	-0.142	-0.142	-0.156	-0.151	-0.148	0.109
640	4.27	-0.031	-0.046	-0.027	-0.030	-0.026	-0.032	0.055	-0.045	-0.045	-0.054	-0.042	-0.052	-0.048	0.056	-0.068	-0.073	-0.073	-0.061	-0.069	0.058	-0.079	-0.078	-0.085	-0.085	-0.082	0.060
848	5.65	-0.019	-0.028	-0.019	-0.020	-0.015	-0.020	0.034	-0.027	-0.027	-0.032	-0.026	-0.032	-0.029	0.034	-0.040	-0.044	-0.045	-0.040	-0.042	0.036	-0.047	-0.047	-0.055	-0.055	-0.051	0.038
1056	7.04	-0.012	-0.017	-0.014	-0.014	-0.009	-0.013	0.022	-0.017	-0.017	-0.019	-0.017	-0.022	-0.018	0.022	-0.025	-0.028	-0.030	-0.028	-0.028	0.023	-0.029	-0.031	-0.039	-0.039	-0.034	0.025
1660	11.07	-0.005	-0.009	-0.010	-0.006	-0.005	-0.007	0.012	-0.008	-0.008	-0.007	-0.008	-0.015	-0.009	0.011	-0.009	-0.012	-0.021	-0.013	-0.014	0.012	-0.012	-0.014	-0.029	-0.028	-0.021	0.015
2160	14.40	-0.002	-0.004	-0.005	-0.003	-0.002	-0.003	0.006	-0.003	-0.003	-0.002	-0.003	-0.008	-0.004	0.005	-0.003	-0.005	-0.011	-0.005	-0.006	0.005	-0.004	-0.006	-0.015	-0.013	-0.009	0.007

ANSYS FEM ANALYSIS: ISOTROPIC MODEL

ST.ANDREWS: RWY 13-31: STA. 5 + 840 L: LOAD 972 kPa

OPTIMIZATION CRITERION: "AREA" OF DEFLECTION BASIN.

CALCULATED MODULI (MPa)

SET	9	8	6	7	10	MIN	AVG	MAX
EY1	4794	3989	4693	4704	4905	3989	4617	4905
EY2	261	244	238	226	305	226	255	305
EY3	130	140	139	139	158	130	141	158

CALCULATED AND OBSERVED DEFLECTIONS (mm)

						OBSERVED DEFL.(mm)	SENSOR DISTANCE(mm)
UY1	-0.950827	-0.995046	-0.984193	-1.018620	-0.827253	-2.093	0
UY2	-0.471135	-0.473872	-0.471331	-0.486281	-0.406966	-1.123	300
UY3	-0.364141	-0.362898	-0.357077	-0.366487	-0.316659	-0.754	450
UY4	-0.311774	-0.310028	-0.303394	-0.311004	-0.272671	-0.552	600
UY5	-0.251643	-0.251375	-0.244616	-0.251570	-0.222530	-0.344	900
UY6	-0.216245	-0.217796	-0.211031	-0.218028	-0.193257	-0.252	1200
UY7	-0.194079	-0.196997	-0.190294	-0.197400	-0.174957	-0.204	1500

OPTIMIZATION CRITERION: MAXIMUM DEFLECTION

CALCULATED MODULI (MPa)

SET	11	10	2	5	9	MIN	AVG	MAX
EY1	4943	4795	4389	3527	4861	3527	4503	4943
EY2	267	265	310	203	161	161	241	310
EY3	197	189	108	166	191	108	170	197

CALCULATED AND OBSERVED DEFLECTIONS (mm)

						OBSERVED DEFL.(mm)	SENSOR DISTANCE(mm)
UY1	-0.784771	-0.785136	-0.886369	-0.988761	-1.060340	-2.093	0
UY2	-0.323738	-0.317573	-0.457145	-0.380860	-0.408113	-1.123	300
UY3	-0.226847	-0.218833	-0.361151	-0.252893	-0.249013	-0.754	450
UY4	-0.183690	-0.174199	-0.309189	-0.195858	-0.182371	-0.552	600
UY5	-0.138864	-0.127144	-0.243370	-0.138111	-0.125351	-0.344	900
UY6	-0.114312	-0.101197	-0.201888	-0.107408	-0.098243	-0.252	1200
UY7	-0.099515	-0.085553	-0.174805	-0.089145	-0.082604	-0.204	1500

OPTIMIZATION CRITERION: RMS VALUE OF DEFLECTIONS.

CALCULATED MODULI (MPa)

SET	16	11	7	14	15	MIN	AVG	MAX
EY1	4623	4990	4982	3840	4991	3840	4685	4991
EY2	498	496	488	499	497	488	496	499
EY3	51	51	55	51	61	51	54	61

CALCULATED AND OBSERVED DEFLECTIONS (mm)

						OBSERVED DEFL.(mm)	SENSOR DISTANCE(mm)
UY1	-0.880019	-0.869673	-0.825886	-0.866307	-0.779569	-2.093	0
UY2	-0.580097	-0.568434	-0.521112	-0.551616	-0.482978	-1.123	300
UY3	-0.505864	-0.493486	-0.446036	-0.476461	-0.410506	-0.754	450
UY4	-0.454779	-0.442324	-0.395380	-0.423945	-0.362148	-0.552	600
UY5	-0.374648	-0.362428	-0.317128	-0.341134	-0.288151	-0.344	900
UY6	-0.313624	-0.301963	-0.258522	-0.278196	-0.233240	-0.252	1200
UY7	-0.267615	-0.256572	-0.214921	-0.230912	-0.192704	-0.204	1500

ANSYS FEM ANALYSIS: ISOTROPIC MODEL

ST.ANDREWS: RWY 13-31: STA. 5 + 840 L

DISTRIBUTION OF VERTICAL STRESSES

"AREA" OF BASIN

LOAD 1: 498 kPa

DEPTH (mm)	DEPTH RATIO (z/ro)	13	11	8	15	14	AVG.	STRESS RATIO (p/po)
12	0.08	-0.453	-0.453	-0.454	-0.454	-0.460	-0.455	0.913
37	0.25	-0.345	-0.344	-0.352	-0.351	-0.369	-0.352	0.707
126	0.84	-0.227	-0.223	-0.231	-0.233	-0.249	-0.232	0.467
280	1.87	-0.113	-0.108	-0.111	-0.116	-0.124	-0.114	0.229
433	2.89	-0.053	-0.051	-0.051	-0.055	-0.061	-0.054	0.109
1010	6.73	-0.012	-0.012	-0.012	-0.013	-0.014	-0.013	0.026
2010	13.40	-0.002	-0.002	-0.002	-0.002	-0.002	-0.002	0.005
3010	20.07	-0.002	-0.002	-0.002	-0.002	-0.002	-0.002	0.004
4010	26.73	-0.001	-0.001	-0.001	-0.001	-0.001	-0.001	0.003

LOAD 2: 703 kPa

DEPTH (mm)	11	8	16	14	5	AVG.	STRESS RATIO (p/po)
12	-0.640	-0.640	-0.652	-0.645	-0.643	-0.644	0.916
37	-0.492	-0.492	-0.534	-0.510	-0.501	-0.506	0.720
126	-0.325	-0.324	-0.362	-0.340	-0.334	-0.337	0.479
280	-0.162	-0.161	-0.173	-0.168	-0.166	-0.166	0.236
433	-0.077	-0.078	-0.080	-0.083	-0.079	-0.079	0.113
1010	-0.018	-0.019	-0.018	-0.020	-0.019	-0.019	0.027
2010	-0.003	-0.003	-0.003	-0.003	-0.003	-0.003	0.005
3010	-0.003	-0.003	-0.003	-0.003	-0.003	-0.003	0.004
4010	-0.002	-0.002	-0.002	-0.002	-0.002	-0.002	0.003

LOAD 3: 972 kPa

DEPTH (mm)	9	8	6	7	10	AVG.	STRESS RATIO (p/po)
12	-0.906	-0.910	-0.904	-0.901	-0.910	-0.906	0.932
37	-0.752	-0.764	-0.744	-0.737	-0.766	-0.753	0.774
126	-0.511	-0.516	-0.505	-0.498	-0.518	-0.510	0.524
280	-0.245	-0.244	-0.247	-0.244	-0.244	-0.245	0.252
433	-0.116	-0.118	-0.120	-0.121	-0.116	-0.118	0.122
1010	-0.027	-0.028	-0.029	-0.029	-0.027	-0.028	0.029
2010	-0.005	-0.005	-0.005	-0.005	-0.005	-0.005	0.005
3010	-0.004	-0.004	-0.004	-0.004	-0.004	-0.004	0.004
4010	-0.003	-0.003	-0.003	-0.003	-0.003	-0.003	0.003

MAXIMUM DEFLECTION

LOAD 1: 498 kPa

DEPTH (mm)	DEPTH RATIO (z/ro)	9	10	11	7	3	AVG.	STRESS RATIO (p/po)
12	0.08	-0.473	-0.470	-0.471	-0.467	-0.455	-0.467	0.938
37	0.25	-0.415	-0.406	-0.410	-0.392	-0.356	-0.396	0.795
126	0.84	-0.290	-0.284	-0.288	-0.262	-0.237	-0.272	0.546
280	1.87	-0.137	-0.141	-0.144	-0.123	-0.121	-0.133	0.267
433	2.89	-0.064	-0.073	-0.075	-0.061	-0.063	-0.067	0.135
1010	6.73	-0.015	-0.018	-0.018	-0.015	-0.016	-0.016	0.033
2010	13.40	-0.002	-0.003	-0.003	-0.003	-0.003	-0.003	0.005
3010	20.07	-0.002	-0.002	-0.002	-0.002	-0.002	-0.002	0.004
4010	26.73	-0.001	-0.001	-0.001	-0.001	-0.001	-0.001	0.003

LOAD 2: 703 kPa

DEPTH (mm)	14	12	6	9	8	AVG.	STRESS RATIO (p/po)
12	-0.664	-0.677	-0.677	-0.675	-0.674	-0.673	0.958
37	-0.572	-0.618	-0.619	-0.612	-0.610	-0.606	0.863
126	-0.395	-0.439	-0.438	-0.435	-0.428	-0.427	0.608
280	-0.185	-0.201	-0.198	-0.204	-0.200	-0.197	0.281
433	-0.083	-0.088	-0.084	-0.096	-0.096	-0.089	0.127
1010	-0.019	-0.020	-0.019	-0.022	-0.023	-0.020	0.029
2010	-0.003	-0.004	-0.004	-0.004	-0.004	-0.004	0.005
3010	-0.003	-0.003	-0.003	-0.003	-0.003	-0.003	0.004
4010	-0.002	-0.002	-0.002	-0.002	-0.002	-0.002	0.003

LOAD 3: 972 kPa

DEPTH (mm)	11	10	2	5	9	AVG.	STRESS RATIO (p/po)
12	-0.906	-0.907	-0.915	-0.908	-0.888	-0.905	0.931
37	-0.755	-0.756	-0.776	-0.755	-0.685	-0.746	0.767
126	-0.520	-0.519	-0.520	-0.507	-0.448	-0.503	0.517
280	-0.259	-0.256	-0.233	-0.243	-0.227	-0.244	0.251
433	-0.130	-0.128	-0.100	-0.123	-0.125	-0.121	0.125
1010	-0.031	-0.031	-0.023	-0.031	-0.034	-0.030	0.031
2010	-0.005	-0.005	-0.005	-0.005	-0.005	-0.005	0.005
3010	-0.004	-0.004	-0.004	-0.004	-0.004	-0.004	0.004
4010	-0.003	-0.003	-0.003	-0.003	-0.003	-0.003	0.003

RMS VALUE OF DEFLECTIONS

LOAD 1: 498 kPa

DEPTH (mm)	DEPTH RATIO (z/ro)	8	11	9	13	14	AVG.	STRESS RATIO (p/po)
12	0.08	-0.471	-0.454	-0.458	-0.476	-0.460	-0.464	0.932
37	0.25	-0.407	-0.353	-0.362	-0.427	-0.371	-0.384	0.770
126	0.84	-0.276	-0.234	-0.243	-0.299	-0.246	-0.259	0.521
280	1.87	-0.126	-0.115	-0.120	-0.134	-0.118	-0.123	0.246
433	2.89	-0.057	-0.053	-0.057	-0.056	-0.058	-0.056	0.112
1010	6.73	-0.013	-0.012	-0.013	-0.012	-0.014	-0.013	0.026
2010	13.40	-0.002	-0.002	-0.002	-0.002	-0.002	-0.002	0.005
3010	20.07	-0.002	-0.002	-0.002	-0.002	-0.002	-0.001	0.004
4010	26.73	-0.001	-0.001	-0.001	-0.001	-0.001	-0.001	0.003

LOAD 2: 703 kPa

DEPTH (mm)	10	9	11	12	7	AVG.	STRESS RATIO (p/po)
12	-0.664	-0.643	-0.673	-0.654	-0.659	-0.659	0.937
37	-0.572	-0.495	-0.599	-0.538	-0.553	-0.552	0.785
126	-0.391	-0.316	-0.403	-0.363	-0.369	-0.368	0.524
280	-0.179	-0.147	-0.174	-0.171	-0.173	-0.169	0.240
433	-0.078	-0.070	-0.074	-0.075	-0.086	-0.077	0.109
1010	-0.018	-0.017	-0.017	-0.017	-0.022	-0.018	0.026
2010	-0.003	-0.003	-0.004	-0.003	-0.004	-0.003	0.005
3010	-0.003	-0.003	-0.003	-0.003	-0.003	-0.003	0.004
4010	-0.002	-0.002	-0.002	-0.002	-0.002	-0.002	0.003

LOAD 3: 972 kPa

DEPTH (mm)	16	11	7	14	15	AVG.	STRESS RATIO (p/po)
12	-0.927	-0.925	-0.924	-0.931	-0.925	-0.926	0.953
37	-0.815	-0.809	-0.808	-0.834	-0.808	-0.815	0.839
126	-0.535	-0.537	-0.536	-0.559	-0.535	-0.540	0.556
280	-0.210	-0.215	-0.216	-0.222	-0.216	-0.216	0.222
433	-0.068	-0.069	-0.071	-0.071	-0.072	-0.070	0.072
1010	-0.013	-0.013	-0.014	-0.013	-0.014	-0.013	0.014
2010	-0.005	-0.005	-0.005	-0.005	-0.005	-0.005	0.005
3010	-0.003	-0.003	-0.003	-0.003	-0.003	-0.003	0.003
4010	-0.003	-0.003	-0.003	-0.003	-0.003	-0.003	0.003

ANSYS FEM ANALYSIS: X-ANISOTROPIC MODEL

ST.ANDREWS: RWY 13-31: STA. 5 + 840 L: LOAD 972 kPa

OPTIMIZATION CRITERION: "AREA" OF DEFLECTION BASIN.

CALCULATED MODULI (MPa)

SET	1	13	4	9	16	MIN	AVG	MAX
EY1	4389	4850	4793	4864	4138	4138	4607	4864
EY2	310	284	272	328	233	233	285	328
EX2	692	605	729	838	554	554	683	838
EY3	108	116	115	117	115	108	114	117
EX3	170	173	195	192	157	157	177	195
R2	2.23	2.13	2.68	2.56	2.38	2.13	2.39	2.68
R3	1.58	1.50	1.69	1.64	1.36	1.36	1.55	1.69

CALCULATED AND OBSERVED DEFLECTIONS (mm)

						OBSERVED DEFL.(mm)	SENSOR DISTANCE(mm)
UY1	-0.831262	-0.840636	-0.826595	-0.758814	-0.938167	-2.093	0
UY2	-0.471574	-0.462738	-0.454218	-0.432209	-0.492649	-1.123	300
UY3	-0.394517	-0.377556	-0.371229	-0.361377	-0.394653	-0.754	450
UY4	-0.354489	-0.334600	-0.330400	-0.324932	-0.347328	-0.552	600
UY5	-0.303577	-0.282696	-0.281238	-0.278853	-0.291798	-0.344	900
UY6	-0.270579	-0.250088	-0.250324	-0.248952	-0.257817	-0.252	1200
UY7	-0.248377	-0.228485	-0.229828	-0.228761	-0.235742	-0.204	1500

OPTIMIZATION CRITERION: MAXIMUM DEFLECTION

CALCULATED MODULI (MPa)

SET	12	11	4	9	6	MIN	AVG	MAX
EY1	2657	1106	3119	2065	2813	1106	2352	3119
EY2	494	476	496	467	445	445	476	496
EX2	758	1256	435	801	906	435	831	1256
EY3	196	186	145	97	98	97	144	196
EX3	485	449	296	185	200	185	323	485
R2	1.54	2.64	0.88	1.71	2.04	0.88	1.76	2.64
R3	2.47	2.41	2.04	1.91	2.05	1.91	2.18	2.47

CALCULATED AND OBSERVED DEFLECTIONS (mm)

						OBSERVED DEFL.(mm)	SENSOR DISTANCE(mm)
UY1	-0.539505	-0.546795	-0.567499	-0.610549	-0.656146	-2.093	0
UY2	-0.253671	-0.253150	-0.250151	-0.299508	-0.363402	-1.123	300
UY3	-0.207206	-0.211085	-0.191946	-0.242001	-0.305130	-0.754	450
UY4	-0.182926	-0.187900	-0.159238	-0.206330	-0.270507	-0.552	600
UY5	-0.153281	-0.158458	-0.117109	-0.155429	-0.222406	-0.344	900
UY6	-0.135018	-0.139724	-0.090484	-0.119929	-0.188926	-0.252	1200
UY7	-0.123187	-0.127318	-0.073152	-0.095083	-0.165263	-0.204	1500

ANSYS FEM ANALYSIS: X-ANISOTROPIC MODEL

ST.ANDREWS: RWY 13-31: STA. 5 + 840 L: LOAD 498 kPa

OPTIMIZATION CRITERION: RMS VALUE OF DEFLECTIONS.

CALCULATED MODULI (MPa)

SET	11	2	14	6	16	MIN	AVG	MAX
EY1	2557	4389	4739	2813	3949	2557	3689	4739
EY2	473	310	419	445	376	310	405	473
EX2	594	692	1108	906	906	594	841	1108
EY3	77	108	139	98	136	77	112	139
EX3	73	170	275	200	251	73	194	275
R2	1.25	2.23	2.64	2.04	2.41	1.25	2.11	2.64
R3	0.94	1.58	1.98	2.05	1.84	0.94	1.68	2.05

CALCULATED AND OBSERVED DEFLECTIONS (mm)

						OBSERVED DEFL.(mm)	SENSOR DISTANCE(mm)
UY1	-0.950906	-0.831262	-0.609375	-0.656146	-0.672374	-2.093	0
UY2	-0.621617	-0.471574	-0.344144	-0.363402	-0.366598	-1.123	300
UY3	-0.554137	-0.394517	-0.290246	-0.305130	-0.306383	-0.754	450
UY4	-0.509236	-0.354489	-0.262009	-0.270507	-0.275076	-0.552	600
UY5	-0.441971	-0.303577	-0.225554	-0.222406	-0.235225	-0.344	900
UY6	-0.393570	-0.270579	-0.201648	-0.188926	-0.209542	-0.252	1200
UY7	-0.358848	-0.248377	-0.185400	-0.165263	-0.192322	-0.204	1500

ANSYS FEM ANALYSIS: X-ANISOTROPIC MODEL

ST.ANDREWS: RWY 13-31: STA. 5 + 840 L

DISTRIBUTION OF VERTICAL STRESSES

"AREA" OF BASIN

		LOAD 1: 498 kPa							LOAD 2: 703 kPa							LOAD 3: 972 kPa						
DEPTH (mm)	DEPTH RATIO (z/ro)	12	14	13	9	4	AVG.	STRESS RATIO (p/po)	15	13	16	14	12	AVG.	STRESS RATIO (p/po)	1	13	4	9	16	AVG.	STRESS RATIO (p/po)
12	0.08	-0.469	-0.478	-0.464	-0.455	-0.453	-0.464	0.932	-0.674	-0.676	-0.672	-0.658	-0.678	-0.672	0.955	-0.935	-0.924	-0.933	-0.936	-0.930	-0.931	0.958
37	0.25	-0.404	-0.433	-0.383	-0.354	-0.351	-0.385	0.773	-0.609	-0.613	-0.605	-0.552	-0.617	-0.599	0.852	-0.830	-0.789	-0.816	-0.830	-0.812	-0.815	0.839
126	0.84	-0.284	-0.305	-0.259	-0.236	-0.240	-0.265	0.532	-0.426	-0.425	-0.427	-0.373	-0.431	-0.417	0.593	-0.582	-0.521	-0.567	-0.580	-0.567	-0.563	0.580
280	1.87	-0.138	-0.141	-0.125	-0.118	-0.124	-0.129	0.259	-0.197	-0.191	-0.206	-0.175	-0.195	-0.193	0.274	-0.274	-0.236	-0.275	-0.274	-0.277	-0.267	0.275
433	2.89	-0.064	-0.063	-0.058	-0.056	-0.061	-0.061	0.122	-0.090	-0.086	-0.099	-0.081	-0.087	-0.089	0.126	-0.120	-0.107	-0.127	-0.121	-0.130	-0.121	0.124
1010	6.73	-0.017	-0.015	-0.015	-0.014	-0.015	-0.015	0.031	-0.025	-0.023	-0.025	-0.022	-0.024	-0.024	0.034	-0.023	-0.024	-0.025	-0.023	-0.026	-0.024	0.025
2010	13.40	-0.005	-0.004	-0.004	-0.004	-0.003	-0.004	0.008	-0.007	-0.007	-0.005	-0.006	-0.007	-0.006	0.009	-0.005	-0.005	-0.005	-0.005	-0.005	-0.005	0.005
3010	20.07	-0.003	-0.003	-0.003	-0.003	-0.003	-0.003	0.006	-0.005	-0.004	-0.003	-0.004	-0.005	-0.004	0.006	-0.004	-0.004	-0.004	-0.004	-0.004	-0.004	0.004
4010	26.73	-0.003	-0.002	-0.002	-0.002	-0.002	-0.002	0.005	-0.004	-0.004	-0.003	-0.004	-0.004	-0.004	0.005	-0.003	-0.003	-0.003	-0.003	-0.003	-0.003	0.003

MAXIMUM DEFLECTION

DEPTH (mm)	DEPTH RATIO (z/ro)	11	15	16	8	9	AVG.	STRESS RATIO (p/po)	13	14	15	12	11	AVG.	STRESS RATIO (p/po)	12	11	4	9	6	AVG.	STRESS RATIO (p/po)
12	0.08	-0.469	-0.463	-0.462	-0.454	-0.454	-0.460	0.924	-0.668	-0.649	-0.651	-0.648	-0.684	-0.660	0.939	-0.948	-0.965	-0.935	-0.950	-0.942	-0.948	0.976
37	0.25	-0.403	-0.373	-0.370	-0.352	-0.350	-0.369	0.742	-0.585	-0.529	-0.534	-0.523	-0.636	-0.562	0.799	-0.893	-0.960	-0.851	-0.898	-0.861	-0.893	0.918
126	0.84	-0.273	-0.250	-0.248	-0.225	-0.231	-0.245	0.493	-0.408	-0.363	-0.364	-0.357	-0.456	-0.389	0.554	-0.650	-0.766	-0.590	-0.638	-0.569	-0.643	0.661
280	1.87	-0.127	-0.123	-0.123	-0.106	-0.116	-0.119	0.239	-0.190	-0.179	-0.176	-0.176	-0.207	-0.186	0.264	-0.299	-0.359	-0.263	-0.271	-0.228	-0.284	0.292
433	2.89	-0.060	-0.059	-0.058	-0.051	-0.058	-0.057	0.115	-0.084	-0.084	-0.082	-0.083	-0.091	-0.085	0.121	-0.134	-0.154	-0.113	-0.103	-0.089	-0.119	0.122
1010	6.73	-0.015	-0.013	-0.014	-0.013	-0.014	-0.014	0.028	-0.018	-0.020	-0.019	-0.019	-0.019	-0.019	0.027	-0.030	-0.030	-0.032	-0.027	-0.024	-0.028	0.029
2010	13.40	-0.004	-0.003	-0.004	-0.002	-0.003	-0.003	0.006	-0.004	-0.004	-0.004	-0.004	-0.005	-0.004	0.006	-0.007	-0.007	-0.010	-0.010	-0.008	-0.008	0.009
3010	20.07	-0.002	-0.002	-0.003	-0.002	-0.002	-0.002	0.005	-0.003	-0.003	-0.003	-0.003	-0.003	-0.003	0.005	-0.005	-0.005	-0.007	-0.006	-0.006	-0.006	0.006
4010	26.73	-0.002	-0.002	-0.002	-0.001	-0.002	-0.002	0.004	-0.002	-0.003	-0.003	-0.003	-0.003	-0.003	0.004	-0.004	-0.004	-0.006	-0.005	-0.005	-0.005	0.005

RMS VALUE OF DEFLECTIONS

DEPTH (mm)	DEPTH RATIO (z/ro)	13	10	14	3	12	AVG.	STRESS RATIO (p/po)	8	12	7	5	16	AVG.	STRESS RATIO (p/po)	11	2	14	6	16	AVG.	STRESS RATIO (p/po)
17	0.08	-0.475	-0.470	-0.474	-0.472	-0.476	-0.473	0.950	-0.666	-0.668	-0.641	-0.665	-0.663	-0.660	0.939	-0.943	-0.935	-0.944	-0.942	-0.944	-0.942	0.969
37	0.25	-0.423	-0.403	-0.411	-0.408	-0.416	-0.412	0.828	-0.576	-0.578	-0.496	-0.567	-0.551	-0.554	0.788	-0.877	-0.830	-0.862	-0.861	-0.865	-0.859	0.884
126	0.84	-0.297	-0.270	-0.268	-0.272	-0.274	-0.276	0.555	-0.384	-0.386	-0.318	-0.362	-0.348	-0.360	0.512	-0.615	-0.582	-0.618	-0.569	-0.623	-0.601	0.619
280	1.87	-0.139	-0.122	-0.115	-0.121	-0.119	-0.123	0.248	-0.171	-0.171	-0.150	-0.151	-0.154	-0.159	0.227	-0.255	-0.274	-0.291	-0.228	-0.293	-0.268	0.276
433	2.89	-0.063	-0.056	-0.051	-0.056	-0.054	-0.056	0.113	-0.079	-0.074	-0.073	-0.064	-0.073	-0.073	0.103	-0.088	-0.120	-0.127	-0.089	-0.129	-0.111	0.114
1010	6.73	-0.014	-0.014	-0.014	-0.014	-0.014	-0.014	0.028	-0.019	-0.017	-0.018	-0.017	-0.018	-0.018	0.025	-0.018	-0.023	-0.024	-0.024	-0.025	-0.023	0.023
2010	13.40	-0.002	-0.003	-0.004	-0.002	-0.004	-0.003	0.007	-0.003	-0.003	-0.003	-0.005	-0.004	-0.004	0.006	-0.005	-0.005	-0.006	-0.008	-0.006	-0.006	0.006
3010	20.07	-0.002	-0.002	-0.003	-0.002	-0.003	-0.002	0.005	-0.003	-0.003	-0.002	-0.003	-0.003	-0.003	0.004	-0.003	-0.004	-0.004	-0.006	-0.004	-0.004	0.004
4010	26.73	-0.001	-0.002	-0.003	-0.001	-0.002	-0.002	0.004	-0.002	-0.002	-0.002	-0.003	-0.003	-0.002	0.003	-0.003	-0.003	-0.004	-0.005	-0.003	-0.004	0.004

ANSYS FEM ANALYSIS: ISOTROPIC MODEL

REGINA: RWY 12-30: STA. 5 + 990 L: LOAD 1485 kPa

OPTIMIZATION CRITERION: "AREA" OF DEFLECTION BASIN.

CALCULATED MODULI (MPa)

SET	6	10	8	5	9	MIN	AVG	MAX
EY1	6264	3370	6939	2768	5612	2768	4991	6939
EY2	2765	6325	2906	2270	5381	2270	3929	6325
EY3	1532	2660	2960	2265	2072	1532	2298	2960
EY4	477	495	434	429	391	391	445	495
EY5	167	141	236	178	216	141	188	236
EY6	138	187	152	170	178	138	165	187

CALCULATED AND OBSERVED DEFLECTIONS (mm)

						OBSERVED DEFL.(mm)	SENSOR DISTANCE(mm)
UY1	-0.747052	-0.734105	-0.736490	-0.818981	-0.693485	-0.691	0
UY2	-0.612430	-0.590175	-0.615209	-0.620479	-0.569576	-0.599	300
UY3	-0.541451	-0.525589	-0.550939	-0.535531	-0.504738	-0.560	450
UY4	-0.376636	-0.362489	-0.397592	-0.353592	-0.340513	-0.406	1000
UY5	-0.307348	-0.290041	-0.333244	-0.280976	-0.270473	-0.314	1400
UY6	-0.259615	-0.240338	-0.290625	-0.232755	-0.224918	-0.248	1800
UY7	-0.221832	-0.201879	-0.258279	-0.195935	-0.191289	-0.190	2250

OPTIMIZATION CRITERION: MAXIMUM DEFLECTION

CALCULATED MODULI (MPa)

SET	9	10	13	7	12	MIN	AVG	MAX
EY1	5612	9136	9487	9256	9736	5612	8645	9736
EY2	5381	2197	2137	2532	2048	2048	2859	5381
EY3	2072	1125	1505	2381	2527	1125	1922	2527
EY4	391	495	496	422	498	391	461	498
EY5	216	141	236	187	136	136	183	236
EY6	178	179	186	183	194	178	184	194

CALCULATED AND OBSERVED DEFLECTIONS (mm)

						OBSERVED DEFL.(mm)	SENSOR DISTANCE(mm)
UY1	-0.693485	-0.679409	-0.668939	-0.663441	-0.647978	-0.691	0
UY2	-0.569576	-0.559318	-0.551009	-0.548762	-0.536309	-0.599	300
UY3	-0.504738	-0.490533	-0.484385	-0.483599	-0.473277	-0.560	450
UY4	-0.340513	-0.327819	-0.334072	-0.326674	-0.324584	-0.406	1000
UY5	-0.270473	-0.259412	-0.275537	-0.260556	-0.260307	-0.314	1400
UY6	-0.224918	-0.212360	-0.237381	-0.216441	-0.215322	-0.248	1800
UY7	-0.191289	-0.175402	-0.208482	-0.182895	-0.179612	-0.190	2250

OPTIMIZATION CRITERION: RMS VALUE OF DEFLECTIONS.

CALCULATED MODULI (MPa)

SET	6	12	10	8	9	MIN	AVG	MAX
EY1	6264	8770	9136	6939	5612	5612	7344	9136
EY2	2765	2227	2322	2906	5381	2227	3120	5381
EY3	1532	1845	2660	2960	2072	1532	2214	2960
EY4	477	494	495	434	391	391	458	495
EY5	167	228	141	236	216	141	198	236
EY6	138	113	187	152	178	113	154	187

CALCULATED AND OBSERVED DEFLECTIONS (mm)

						OBSERVED DEFL.(mm)	SENSOR DISTANCE(mm)
UY1	-0.747052	-0.691583	-0.674831	-0.736490	-0.693485	-0.691	0
UY2	-0.612430	-0.571336	-0.564226	-0.615209	-0.569576	-0.599	300
UY3	-0.541451	-0.504380	-0.502136	-0.550939	-0.504738	-0.560	450
UY4	-0.376636	-0.349962	-0.351428	-0.397592	-0.340513	-0.406	1000
UY5	-0.307348	-0.286238	-0.285063	-0.333244	-0.270473	-0.314	1400
UY6	-0.259615	-0.242589	-0.238851	-0.290625	-0.224918	-0.248	1800
UY7	-0.221832	-0.207852	-0.202490	-0.258279	-0.191289	-0.190	2250

ANSYS FEM ANALYSIS: ISOTROPIC MODEL

REGINA: RWY 12-30: STA. 5 + 990 L

DISTRIBUTION OF VERTICAL STRESSES

"AREA" OF BASIN

DEPTH (mm)	DEPTH RATIO (z/ro)	LOAD 1: 733 kPa 2	12	14	11	1	AVG.	STRESS RATIO (p/po)	LOAD 2: 1166 kPa 3	13	15	6	8	AVG.	STRESS RATIO (p/po)	LOAD 3: 1485 kPa 6	10	8	5	9	AVG.	STRESS RATIO (p/po)
20	0.09	-0.715	-0.702	-0.704	-0.710	-0.710	-0.708	0.966	-1.129	-1.137	-1.141	-1.129	-1.130	-1.133	0.972	-1.438	-1.462	-1.439	-1.455	-1.448	-1.448	0.975
59	0.26	-0.675	-0.629	-0.636	-0.659	-0.658	-0.652	0.889	-1.044	-1.074	-1.091	-1.044	-1.047	-1.060	0.909	-1.329	-1.418	-1.334	-1.395	-1.369	-1.369	0.922
98	0.44	-0.608	-0.521	-0.535	-0.576	-0.578	-0.564	0.769	-0.907	-0.967	-0.999	-0.911	-0.919	-0.941	0.807	-1.160	-1.329	-1.170	-1.285	-1.234	-1.236	0.832
137	0.61	-0.510	-0.394	-0.413	-0.462	-0.472	-0.450	0.614	-0.723	-0.811	-0.857	-0.739	-0.750	-0.776	0.666	-0.941	-1.174	-0.955	-1.116	-1.035	-1.044	0.703
174	0.77	-0.402	-0.294	-0.312	-0.346	-0.374	-0.346	0.471	-0.541	-0.640	-0.682	-0.584	-0.595	-0.608	0.522	-0.743	-0.959	-0.758	-0.926	-0.812	-0.840	0.565
212	0.94	-0.301	-0.223	-0.239	-0.244	-0.295	-0.260	0.355	-0.386	-0.479	-0.504	-0.460	-0.468	-0.459	0.394	-0.585	-0.719	-0.597	-0.742	-0.599	-0.649	0.437
250	1.11	-0.215	-0.164	-0.175	-0.160	-0.223	-0.187	0.256	-0.262	-0.342	-0.353	-0.352	-0.355	-0.333	0.286	-0.448	-0.507	-0.453	-0.576	-0.419	-0.480	0.324
285	1.27	-0.161	-0.125	-0.127	-0.111	-0.170	-0.139	0.189	-0.196	-0.256	-0.265	-0.279	-0.270	-0.253	0.217	-0.355	-0.371	-0.344	-0.448	-0.308	-0.365	0.246
315	1.40	-0.133	-0.103	-0.097	-0.090	-0.134	-0.112	0.152	-0.169	-0.212	-0.224	-0.236	-0.213	-0.211	0.181	-0.300	-0.301	-0.272	-0.360	-0.254	-0.297	0.200
414	1.84	-0.064	-0.054	-0.053	-0.051	-0.062	-0.057	0.077	-0.080	-0.102	-0.108	-0.103	-0.099	-0.098	0.084	-0.131	-0.135	-0.126	-0.152	-0.122	-0.133	0.090
582	2.59	-0.043	-0.039	-0.039	-0.038	-0.042	-0.040	0.055	-0.053	-0.069	-0.073	-0.064	-0.066	-0.065	0.056	-0.081	-0.085	-0.084	-0.095	-0.083	-0.086	0.058
750	3.33	-0.031	-0.030	-0.031	-0.030	-0.029	-0.030	0.041	-0.037	-0.049	-0.051	-0.042	-0.046	-0.045	0.039	-0.053	-0.055	-0.059	-0.063	-0.059	-0.058	0.039
918	4.08	-0.023	-0.023	-0.023	-0.023	-0.021	-0.023	0.031	-0.027	-0.036	-0.037	-0.029	-0.033	-0.033	0.028	-0.038	-0.039	-0.042	-0.045	-0.044	-0.042	0.028
1500	6.67	-0.017	-0.017	-0.018	-0.018	-0.016	-0.017	0.023	-0.022	-0.027	-0.028	-0.023	-0.025	-0.025	0.021	-0.029	-0.031	-0.032	-0.034	-0.033	-0.032	0.021
2500	11.11	-0.013	-0.013	-0.014	-0.014	-0.012	-0.013	0.018	-0.018	-0.021	-0.021	-0.018	-0.019	-0.019	0.017	-0.023	-0.025	-0.024	-0.027	-0.026	-0.025	0.017
3500	15.56	-0.011	-0.011	-0.011	-0.011	-0.009	-0.011	0.014	-0.014	-0.017	-0.017	-0.014	-0.015	-0.015	0.013	-0.018	-0.020	-0.019	-0.022	-0.021	-0.020	0.013

MAXIMUM DEFLECTION

DEPTH (mm)	DEPTH RATIO (z/ro)						AVG.	STRESS RATIO (p/po)	8	6	9	11	7	AVG.	STRESS RATIO (p/po)	9	10	13	7	12	AVG.	STRESS RATIO (p/po)
20	0.09	-0.718	-0.714	-0.716	-0.719	-0.722	-0.718	0.979	-1.130	-1.129	-1.137	-1.126	-1.121	-1.129	0.968	-1.448	-1.425	-1.423	-1.427	-1.425	-1.430	0.963
59	0.26	-0.664	-0.648	-0.655	-0.666	0.908	1.690	-2.305	-1.047	-1.044	-1.075	-1.035	-1.015	-1.043	0.895	-1.369	-1.281	-1.276	-1.293	-1.280	-1.300	0.875
98	0.44	-0.581	-0.549	-0.563	-0.581	0.793	1.476	-2.013	-0.919	-0.911	-0.969	-0.895	-0.859	-0.910	0.781	-1.234	-1.070	-1.064	-1.094	-1.070	-1.107	0.745
137	0.61	-0.473	-0.429	-0.447	-0.469	0.640	1.191	-1.624	-0.750	-0.739	-0.813	-0.718	-0.673	-0.739	0.633	-1.035	-0.827	-0.821	-0.858	-0.831	-0.874	0.589
174	0.77	-0.372	-0.329	-0.347	-0.361	0.492	0.916	-1.249	-0.595	-0.584	-0.637	-0.564	-0.524	-0.581	0.498	-0.812	-0.641	-0.640	-0.667	-0.655	-0.683	0.460
212	0.94	-0.289	-0.256	-0.270	-0.270	0.368	0.685	-0.934	-0.468	-0.460	-0.471	-0.446	-0.418	-0.452	0.388	-0.599	-0.513	-0.520	-0.532	-0.536	-0.540	0.364
250	1.11	-0.217	-0.193	-0.201	-0.193	0.263	0.490	-0.668	-0.355	-0.352	-0.329	-0.343	-0.323	-0.340	0.292	-0.419	-0.403	-0.414	-0.411	-0.428	-0.415	0.280
285	1.27	-0.168	-0.152	-0.150	-0.145	0.198	0.368	-0.503	-0.270	-0.279	-0.242	-0.273	-0.252	-0.263	0.226	-0.308	-0.328	-0.338	-0.320	-0.341	-0.327	0.220
315	1.40	-0.139	-0.128	-0.117	-0.121	0.164	0.306	-0.418	-0.213	-0.236	-0.199	-0.231	-0.204	-0.217	0.186	-0.254	-0.283	-0.288	-0.260	-0.278	-0.273	0.184
414	1.84	-0.065	-0.060	-0.058	-0.058	0.080	0.148	-0.202	-0.099	-0.103	-0.096	-0.102	-0.093	-0.099	0.085	-0.122	-0.124	-0.132	-0.119	-0.119	-0.123	0.083
582	2.59	-0.042	-0.040	-0.041	-0.040	0.054	0.101	-0.137	-0.066	-0.064	-0.065	-0.065	-0.061	-0.064	0.055	-0.083	-0.076	-0.086	-0.078	-0.073	-0.079	0.053
750	3.33	-0.029	-0.029	-0.030	-0.028	0.039	0.072	-0.098	-0.046	-0.042	-0.046	-0.043	-0.042	-0.044	0.038	-0.059	-0.049	-0.058	-0.053	-0.047	-0.053	0.036
918	4.08	-0.021	-0.021	-0.022	-0.021	0.029	0.053	-0.073	-0.033	-0.029	-0.034	-0.031	-0.031	-0.032	0.027	-0.044	-0.036	-0.042	-0.039	-0.034	-0.039	0.026
1500	6.67	-0.015	-0.016	-0.017	-0.016	0.022	0.041	-0.056	-0.025	-0.023	-0.026	-0.023	-0.023	-0.024	0.021	-0.033	-0.029	-0.032	-0.030	-0.027	-0.030	0.020
2500	11.11	-0.012	-0.013	-0.013	-0.013	0.017	0.032	-0.044	-0.019	-0.018	-0.020	-0.018	-0.019	-0.019	0.016	-0.026	-0.024	-0.025	-0.024	-0.022	-0.024	0.016
3500	15.56	-0.009	-0.010	-0.010	-0.010	0.014	0.026	-0.035	-0.015	-0.014	-0.016	-0.014	-0.015	-0.015	0.013	-0.021	-0.020	-0.020	-0.019	-0.018	-0.020	0.013

ANSYS FEM ANALYSIS: ISOTROPIC MODEL

REGINA: RWY 12-30: STA. 5 + 990 L

DISTRIBUTION OF VERTICAL STRESSES

RMS VALUE OF DEFLECTIO

LOAD 1: 733 kPa

DEPTH (mm)	DEPTH RATIO (z/ro)	12	11	8	6	2	AVG.	STRESS RATIO (p/po)
20	0.09	-0.705	-0.708	-0.710	-0.710	-0.717	-0.710	0.968
59	0.26	-0.638	-0.651	-0.658	-0.656	-0.683	-0.657	0.897
98	0.44	-0.540	-0.563	-0.578	-0.572	-0.624	-0.576	0.785
137	0.61	-0.425	-0.453	-0.472	-0.464	-0.532	-0.469	0.640
174	0.77	-0.334	-0.357	-0.374	-0.367	-0.421	-0.370	0.505
212	0.94	-0.270	-0.283	-0.295	-0.289	-0.309	-0.289	0.394
250	1.11	-0.213	-0.218	-0.223	-0.221	-0.213	-0.218	0.297
285	1.27	-0.171	-0.175	-0.170	-0.175	-0.156	-0.169	0.231
315	1.40	-0.143	-0.149	-0.134	-0.148	-0.128	-0.140	0.191
414	1.84	-0.064	-0.065	-0.062	-0.064	-0.058	-0.063	0.086
582	2.59	-0.041	-0.041	-0.042	-0.040	-0.037	-0.040	0.055
750	3.33	-0.027	-0.027	-0.029	-0.026	-0.024	-0.027	0.036
918	4.08	-0.018	-0.019	-0.021	-0.019	-0.018	-0.019	0.026
1500	6.67	-0.013	-0.015	-0.016	-0.014	-0.014	-0.014	0.020
2500	11.11	-0.010	-0.011	-0.012	-0.011	-0.011	-0.011	0.015
3500	15.56	-0.007	-0.009	-0.009	-0.009	-0.009	-0.009	0.012

LOAD 2: 1166 kPa

DEPTH (mm)	DEPTH RATIO (z/ro)	6	12	8	11	13	AVG.	STRESS RATIO (p/po)
20	0.09	-1.129	-1.120	-1.130	-1.127	-1.122	-1.125	0.965
59	0.26	-1.044	-1.013	-1.047	-1.036	-1.020	-1.032	0.885
98	0.44	-0.911	-0.855	-0.919	-0.896	-0.869	-0.890	0.763
137	0.61	-0.739	-0.670	-0.750	-0.721	-0.689	-0.714	0.612
174	0.77	-0.584	-0.525	-0.595	-0.568	-0.544	-0.563	0.483
212	0.94	-0.460	-0.425	-0.468	-0.450	-0.441	-0.449	0.385
250	1.11	-0.352	-0.336	-0.355	-0.347	-0.348	-0.348	0.298
285	1.27	-0.279	-0.269	-0.270	-0.278	-0.279	-0.275	0.236
315	1.40	-0.236	-0.225	-0.213	-0.237	-0.232	-0.228	0.196
414	1.84	-0.103	-0.101	-0.099	-0.104	-0.103	-0.102	0.087
582	2.59	-0.064	-0.064	-0.066	-0.065	-0.065	-0.065	0.056
750	3.33	-0.042	-0.043	-0.046	-0.043	-0.043	-0.043	0.037
918	4.08	-0.029	-0.029	-0.033	-0.031	-0.029	-0.030	0.026
1500	6.67	-0.023	-0.021	-0.025	-0.023	-0.021	-0.023	0.019
2500	11.11	-0.018	-0.016	-0.019	-0.018	-0.015	-0.017	0.015
3500	15.56	-0.014	-0.012	-0.015	-0.015	-0.012	-0.013	0.012

LOAD 3: 1485 kPa

DEPTH (mm)	DEPTH RATIO (z/ro)	6	12	10	8	9	AVG.	STRESS RATIO (p/po)
20	0.09	-1.438	-1.427	-1.429	-1.439	-1.448	-1.436	0.967
59	0.26	-1.329	-1.291	-1.296	-1.334	-1.369	-1.324	0.891
98	0.44	-1.160	-1.091	-1.099	-1.170	-1.234	-1.151	0.775
137	0.61	-0.941	-0.856	-0.866	-0.955	-1.035	-0.931	0.627
174	0.77	-0.743	-0.672	-0.680	-0.758	-0.812	-0.733	0.494
212	0.94	-0.585	-0.543	-0.547	-0.597	-0.599	-0.574	0.387
250	1.11	-0.448	-0.429	-0.427	-0.453	-0.419	-0.435	0.293
285	1.27	-0.355	-0.344	-0.334	-0.344	-0.308	-0.337	0.227
315	1.40	-0.300	-0.288	-0.268	-0.272	-0.254	-0.276	0.186
414	1.84	-0.131	-0.130	-0.119	-0.126	-0.122	-0.126	0.085
582	2.59	-0.081	-0.083	-0.074	-0.084	-0.083	-0.081	0.055
750	3.33	-0.053	-0.055	-0.048	-0.059	-0.059	-0.055	0.037
918	4.08	-0.038	-0.039	-0.035	-0.042	-0.044	-0.039	0.027
1500	6.67	-0.029	-0.028	-0.027	-0.032	-0.033	-0.030	0.020
2500	11.11	-0.023	-0.021	-0.022	-0.024	-0.026	-0.023	0.016
3500	15.56	-0.018	-0.016	-0.018	-0.019	-0.021	-0.019	0.012

ANSYS FEM ANALYSIS: ISOTROPIC MODEL

SASKATOON: RWY 15-33: STA. 5 + 630 R: LOAD 1415 kPa

OPTIMIZATION CRITERION: "AREA" OF DEFLECTION BASIN.

CALCULATED MODULI (MPa)

SET	1	6	2	15	5	MIN	AVG	MAX
EY1	3000	5376	8854	2610	8773	2610	5723	8854
EY2	2000	1709	3100	1628	1914	1628	2070	3100
EY3	200	162	363	648	567	162	388	648
EY4	150	220	254	296	257	150	235	296
EY5	150	210	208	216	218	150	200	218

CALCULATED AND OBSERVED DEFLECTIONS (mm)

						OBSERVED DEFL.(mm)	SENSOR DISTANCE(mm)
UY1	-1.817540	-1.892360	-1.158950	-1.004620	-0.978399	-1.517	0
UY2	-1.142200	-1.179700	-0.787951	-0.632550	-0.643479	-0.975	300
UY3	-0.803102	-0.816219	-0.602610	-0.494924	-0.503795	-0.704	450
UY4	-0.323893	-0.308343	-0.333612	-0.318173	-0.314665	-0.309	1000
UY5	-0.213914	-0.212217	-0.266742	-0.260854	-0.256645	-0.211	1400
UY6	-0.150722	-0.164200	-0.226613	-0.222644	-0.218758	-0.158	1800
UY7	-0.106793	-0.132379	-0.197737	-0.193707	-0.190383	-0.119	2250

OPTIMIZATION CRITERION: MAXIMUM DEFLECTION

CALCULATED MODULI (MPa)

SET	1	12	16	11	15	MIN	AVG	MAX
EY1	3000	2835	2545	2923	2553	2545	2771	3000
EY2	2000	1522	1508	1527	1508	1508	1613	2000
EY3	200	640	658	632	668	200	560	668
EY4	150	297	278	297	300	150	264	300
EY5	150	107	104	109	106	104	115	150

CALCULATED AND OBSERVED DEFLECTIONS (mm)

						OBSERVED DEFL.(mm)	SENSOR DISTANCE(mm)
UY1	-1.817540	-1.308910	-1.304940	-1.299390	-1.285420	-1.517	0
UY2	-1.142200	-0.922812	-0.925583	-0.912355	-0.911180	-0.975	300
UY3	-0.803102	-0.778138	-0.785060	-0.766654	-0.773087	-0.704	450
UY4	-0.323893	-0.576605	-0.585048	-0.564508	-0.575868	-0.309	1000
UY5	-0.213914	-0.498439	-0.505872	-0.486972	-0.497495	-0.211	1400
UY6	-0.150722	-0.440386	-0.446617	-0.429669	-0.438804	-0.158	1800
UY7	-0.106793	-0.392321	-0.397177	-0.382406	-0.389815	-0.119	2250

OPTIMIZATION CRITERION: RMS VALUE OF DEFLECTIONS.

CALCULATED MODULI (MPa)

SET	15	16	10	9	11	MIN	AVG	MAX
EY1	3874	3834	5489	2660	4671	2660	4106	5489
EY2	3711	3513	3972	4005	3176	3176	3675	4005
EY3	174	233	171	218	305	171	220	305
EY4	164	161	150	150	150	150	155	164
EY5	274	265	189	177	179	177	217	274

CALCULATED AND OBSERVED DEFLECTIONS (mm)

						OBSERVED DEFL.(mm)	SENSOR DISTANCE(mm)
UY1	-1.604850	-1.435280	-1.659660	-1.663010	-1.308000	-1.517	0
UY2	-1.039790	-0.919206	-1.132390	-1.127950	-0.853700	-0.975	300
UY3	-0.718751	-0.645089	-0.822259	-0.835469	-0.622542	-0.704	450
UY4	-0.228241	-0.246086	-0.306108	-0.393019	-0.278149	-0.309	1000
UY5	-0.144030	-0.166276	-0.199316	-0.296402	-0.188387	-0.211	1400
UY6	-0.108374	-0.126532	-0.148147	-0.243435	-0.134783	-0.158	1800
UY7	-0.087242	-0.101764	-0.115373	-0.207529	-0.097411	-0.119	2250

ANSYS FEM ANALYSIS: ISOTROPIC MODEL

SASKATOON: RWY 15-33: STA. 5 + 630 R

DISTRIBUTION OF VERTICAL STRESSES

"AREA" OF BASIN

LOAD 1: 732 kPa

DEPTH (mm)	DEPTH RATIO (z/ro)	7	1	2	14	15	AVG.	STRESS RATIO (p/po)
17	0.08	-0.686	-0.702	-0.692	-0.718	-0.719	-0.703	0.961
64	0.28	-0.560	-0.593	-0.575	-0.668	-0.671	-0.614	0.838
122	0.54	-0.416	-0.450	-0.439	-0.591	-0.593	-0.498	0.680
218	0.97	-0.279	-0.308	-0.301	-0.427	-0.426	-0.348	0.476
355	1.58	-0.168	-0.186	-0.181	-0.235	-0.233	-0.201	0.274
492	2.19	-0.107	-0.114	-0.110	-0.121	-0.120	-0.114	0.156
630	2.80	-0.074	-0.074	-0.070	-0.063	-0.062	-0.069	0.094
823	3.66	-0.054	-0.052	-0.048	-0.039	-0.039	-0.047	0.064
1068	4.75	-0.041	-0.039	-0.036	-0.030	-0.031	-0.035	0.048
2690	11.96	-0.007	-0.007	-0.006	-0.006	-0.006	-0.007	0.009
3690	16.40	-0.004	-0.004	-0.004	-0.004	-0.004	-0.004	0.005

LOAD 2: 1075 kPa

DEPTH (mm)	DEPTH RATIO (z/ro)	1	7	2	6	15	AVG.	STRESS RATIO (p/po)
17	0.08	-1.038	-1.015	-1.023	-1.037	-1.040	-1.031	0.959
64	0.28	-0.878	-0.829	-0.851	-0.861	-0.920	-0.868	0.807
122	0.54	-0.666	-0.615	-0.649	-0.627	-0.769	-0.665	0.619
218	0.97	-0.456	-0.412	-0.445	-0.414	-0.536	-0.453	0.421
355	1.58	-0.276	-0.248	-0.268	-0.248	-0.302	-0.268	0.250
492	2.19	-0.168	-0.158	-0.162	-0.152	-0.173	-0.163	0.151
630	2.80	-0.109	-0.110	-0.103	-0.100	-0.106	-0.106	0.098
823	3.66	-0.077	-0.080	-0.072	-0.071	-0.073	-0.075	0.069
1068	4.75	-0.058	-0.061	-0.053	-0.055	-0.056	-0.056	0.053
2690	11.96	-0.010	-0.011	-0.009	-0.010	-0.010	-0.010	0.009
3690	16.40	-0.006	-0.006	-0.005	-0.006	-0.006	-0.006	0.005

LOAD 3: 1415 kPa

DEPTH (mm)	DEPTH RATIO (z/ro)	1	6	2	15	5	AVG.	STRESS RATIO (p/po)
17	0.08	-1.347	-1.318	-1.328	-1.379	-1.351	-1.345	0.950
64	0.28	-1.139	-1.076	-1.105	-1.288	-1.200	-1.162	0.821
122	0.54	-0.865	-0.799	-0.842	-1.140	-1.006	-0.930	0.658
218	0.97	-0.592	-0.535	-0.578	-0.816	-0.695	-0.643	0.454
355	1.58	-0.358	-0.322	-0.348	-0.451	-0.381	-0.372	0.263
492	2.19	-0.218	-0.206	-0.210	-0.244	-0.210	-0.218	0.154
630	2.80	-0.142	-0.143	-0.134	-0.138	-0.122	-0.136	0.096
823	3.66	-0.100	-0.104	-0.093	-0.089	-0.081	-0.093	0.066
1068	4.75	-0.075	-0.079	-0.069	-0.065	-0.061	-0.070	0.049
2690	11.96	-0.014	-0.014	-0.012	-0.012	-0.011	-0.013	0.009
3690	16.40	-0.008	-0.008	-0.007	-0.007	-0.007	-0.007	0.005

MAXIMUM DEFLECTION

DEPTH (mm)	DEPTH RATIO (z/ro)						AVG.	STRESS RATIO (p/po)
17	0.08	-0.686	-0.702	-0.704	-0.717	-0.718	-0.705	0.956
64	0.28	-0.560	-0.593	-0.618	-0.666	-0.668	-0.621	0.841
122	0.54	-0.416	-0.450	-0.506	-0.586	-0.590	-0.510	0.691
218	0.97	-0.279	-0.308	-0.352	-0.423	-0.425	-0.357	0.484
355	1.58	-0.168	-0.186	-0.199	-0.235	-0.234	-0.204	0.277
492	2.19	-0.107	-0.114	-0.111	-0.122	-0.121	-0.115	0.156
630	2.80	-0.074	-0.074	-0.065	-0.063	-0.062	-0.068	0.092
823	3.66	-0.054	-0.052	-0.042	-0.038	-0.038	-0.045	0.061
1068	4.75	-0.041	-0.039	-0.031	-0.028	-0.029	-0.034	0.046
2690	11.96	-0.007	-0.007	-0.006	-0.006	-0.006	-0.006	0.009
3690	16.40	-0.004	-0.004	-0.004	-0.004	-0.004	-0.004	0.005

DEPTH (mm)	DEPTH RATIO (z/ro)	1	7	14	13	12	AVG.	STRESS RATIO (p/po)
17	0.08	-1.038	-1.015	-1.056	-1.062	-1.060	-1.046	0.973
64	0.28	-0.878	-0.829	-0.966	-0.991	-0.984	-0.929	0.865
122	0.54	-0.666	-0.615	-0.831	-0.877	-0.866	-0.771	0.717
218	0.97	-0.456	-0.412	-0.585	-0.624	-0.614	-0.538	0.501
355	1.58	-0.276	-0.248	-0.324	-0.339	-0.335	-0.304	0.283
492	2.19	-0.168	-0.158	-0.177	-0.177	-0.177	-0.171	0.159
630	2.80	-0.109	-0.110	-0.100	-0.093	-0.094	-0.101	0.094
823	3.66	-0.077	-0.080	-0.061	-0.055	-0.056	-0.066	0.061
1068	4.75	-0.058	-0.061	-0.041	-0.037	-0.038	-0.047	0.044
2690	11.96	-0.010	-0.011	-0.008	-0.007	-0.008	-0.009	0.008
3690	16.40	-0.006	-0.006	-0.005	-0.005	-0.005	-0.005	0.005

DEPTH (mm)	DEPTH RATIO (z/ro)	1	12	16	11	15	AVG.	STRESS RATIO (p/po)
17	0.08	-1.347	-1.378	-1.380	-1.377	-1.381	---	---
64	0.28	-1.139	-1.286	-1.293	-1.283	-1.294	-1.259	0.890
122	0.54	-0.865	-1.141	-1.149	-1.136	-1.151	-1.089	0.769
218	0.97	-0.592	-0.825	-0.817	-0.821	-0.817	-0.774	0.547
355	1.58	-0.358	-0.459	-0.442	-0.457	-0.440	-0.431	0.305
492	2.19	-0.218	-0.242	-0.231	-0.242	-0.229	-0.233	0.164
630	2.80	-0.142	-0.128	-0.122	-0.129	-0.122	-0.128	0.091
823	3.66	-0.100	-0.075	-0.071	-0.075	-0.071	-0.078	0.055
1068	4.75	-0.075	-0.050	-0.048	-0.051	-0.048	-0.054	0.038
2690	11.96	-0.014	-0.010	-0.010	-0.010	-0.010	-0.010	0.007
3690	16.40	-0.008	-0.006	-0.006	-0.006	-0.006	-0.007	0.005

RMS VALUE OF DEFLECTIONS

DEPTH (mm)	DEPTH RATIO (z/ro)	7	1	16	12	13	AVG.	STRESS RATIO (p/po)
17	0.08	-0.686	-0.702	-0.715	-0.716	-0.717	-0.707	0.966
64	0.28	-0.560	-0.593	-0.660	-0.663	-0.666	-0.628	0.858
122	0.54	-0.416	-0.450	-0.574	-0.581	-0.586	-0.522	0.713
218	0.97	-0.279	-0.308	-0.403	-0.419	-0.423	-0.366	0.501
355	1.58	-0.168	-0.186	-0.217	-0.234	-0.235	-0.208	0.284
492	2.19	-0.107	-0.114	-0.113	-0.122	-0.121	-0.115	0.158
630	2.80	-0.074	-0.074	-0.060	-0.063	-0.062	-0.067	0.091
823	3.66	-0.054	-0.052	-0.036	-0.037	-0.037	-0.043	0.059
1068	4.75	-0.041	-0.039	-0.026	-0.027	-0.027	-0.032	0.044
2690	11.96	-0.007	-0.007	-0.005	-0.005	-0.005	-0.006	0.008
3690	16.40	-0.004	-0.004	-0.003	-0.003	-0.003	-0.004	0.005

DEPTH (mm)	DEPTH RATIO (z/ro)	1	14	7	13	2	AVG.	STRESS RATIO (p/po)
17	0.08	-1.038	-1.039	-1.015	-1.008	-1.023	-1.025	0.953
64	0.28	-0.878	-0.866	-0.829	-0.780	-0.851	-0.841	0.782
122	0.54	-0.666	-0.629	-0.615	-0.523	-0.649	-0.617	0.574
218	0.97	-0.456	-0.422	-0.412	-0.343	-0.445	-0.416	0.387
355	1.58	-0.276	-0.262	-0.248	-0.227	-0.268	-0.256	0.238
492	2.19	-0.168	-0.170	-0.158	-0.153	-0.162	-0.162	0.151
630	2.80	-0.109	-0.120	-0.110	-0.107	-0.103	-0.110	0.102
823	3.66	-0.077	-0.090	-0.080	-0.074	-0.072	-0.079	0.073
1068	4.75	-0.058	-0.069	-0.061	-0.052	-0.053	-0.058	0.054
2690	11.96	-0.010	-0.012	-0.011	-0.010	-0.009	-0.010	0.010
3690	16.40	-0.006	-0.007	-0.006	-0.006	-0.005	-0.006	0.006

DEPTH (mm)	DEPTH RATIO (z/ro)	15	16	10	9	11	AVG.	STRESS RATIO (p/po)
17	0.08	-1.345	-1.347	-1.330	-1.365	-1.345	-1.346	0.952
64	0.28	-1.089	-1.122	-1.050	-1.146	-1.136	-1.109	0.784
122	0.54	-0.746	-0.817	-0.700	-0.819	-0.864	-0.789	0.558
218	0.97	-0.496	-0.553	-0.458	-0.549	-0.595	-0.530	0.375
355	1.58	-0.329	-0.347	-0.304	-0.349	-0.361	-0.338	0.239
492	2.19	-0.220	-0.218	-0.202	-0.219	-0.213	-0.215	0.152
630	2.80	-0.156	-0.147	-0.142	-0.144	-0.132	-0.144	0.102
823	3.66	-0.118	-0.109	-0.106	-0.102	-0.092	-0.105	0.075
1068	4.75	-0.094	-0.087	-0.083	-0.078	-0.072	-0.083	0.058
2690	11.96	-0.016	-0.015	-0.014	-0.013	-0.013	-0.014	0.010
3690	16.40	-0.009	-0.008	-0.008	-0.008	-0.008	-0.008	0.006

ANSYS FEM ANALYSIS: X-ANISOTROPIC MODEL

SASKATOON: RWY 15-33: STA. 5 + 630 R: LOAD 1415 kPa

OPTIMIZATION CRITERION: "AREA" OF DEFLECTION BASIN.

CALCULATED MODULI (MPa)

SET	6	8	3	10	14	MIN	AVG	MAX
EY1	8313	8375	8685	7557	9498	7557	8486	9498
EY2	1652	1627	1681	1535	3967	1535	2092	3967
EY3	154	153	155	152	152	152	153	155
EX3	120	157	127	202	106	106	142	202
EY4	292	292	288	298	276	276	289	298
EX4	541	682	666	623	645	541	632	682
EY5	264	291	288	297	297	264	287	297
EX5	202	219	240	489	167	167	263	489
R3	0.78	1.02	0.82	1.33	0.70	0.70	0.93	1.33
R4	1.85	2.34	2.31	2.09	2.34	1.85	2.19	2.34
R5	0.77	0.75	0.83	1.65	0.56	0.56	0.91	1.65

CALCULATED AND OBSERVED DEFLECTIONS (mm)

						OBSERVED DEFL.(mm)	SENSOR DISTANCE(mm)
UY1	-1.640140	-1.542450	-1.548830	-1.521500	-1.321881	-1.517	0
UY2	-1.056480	-0.983382	-0.988874	-0.962220	-0.936744	-0.975	300
UY3	-0.743759	-0.685025	-0.687150	-0.669072	-0.698607	-0.704	450
UY4	-0.271957	-0.238779	-0.236544	-0.235866	-0.261353	-0.309	1000
UY5	-0.192891	-0.166223	-0.166953	-0.165762	-0.177189	-0.212	1400
UY6	-0.159283	-0.136357	-0.139155	-0.139104	-0.145098	-0.158	1800
						-0.119	2250

OPTIMIZATION CRITERION: MAXIMUM DEFLECTION

CALCULATED MODULI (MPa)

SET	13	16	5	15	1	MIN	AVG	MAX
EY1	8396	7270	6608	9536	3000	3000	6962	9536
EY2	1540	2222	1625	1515	2000	1515	1780	2222
EY3	159	159	177	153	200	153	170	200
EX3	126	125	265	86	200	86	160	265
EY4	229	231	245	272	150	150	225	272
EX4	540	552	489	662	150	150	478	662
EY5	286	291	243	208	150	150	236	291
EX5	525	495	543	379	150	150	419	543
R3	0.79	0.79	1.50	0.56	1.00	0.56	0.93	1.50
R4	2.36	2.38	2.00	2.43	1.00	1.00	2.03	2.43
R5	1.83	1.70	2.23	1.82	1.00	1.00	1.72	2.23

CALCULATED AND OBSERVED DEFLECTIONS (mm)

						OBSERVED DEFL.(mm)	SENSOR DISTANCE(mm)
UY1	-1.499420	-1.418390	-1.397660	-1.639610	-1.662220	-1.517	0
UY2	-0.919567	-0.902177	-0.878929	-1.024280	-1.103330	-0.975	300
UY3	-0.611686	-0.615176	-0.612189	-0.698513	-0.808655	-0.704	450
UY4	-0.158501	-0.165035	-0.220492	-0.232508	-0.333204	-0.309	1000
UY5	-0.088970	-0.093294	-0.150207	-0.165040	-0.216627	-0.212	1400
UY6	-0.062595	-0.067423	-0.119052	-0.135611	-0.152050	-0.158	1800
UY7	-0.046060	-0.051769	-0.098984	-0.113402	-0.107896	-0.119	2250

ANSYS FEM ANALYSIS: X-ANISOTROPIC MODEL

SASKATOON: RWY 15-33: STA. 5 + 630 R: LOAD 1415 kPa

OPTIMIZATION CRITERION: RMS VALUE OF DEFLECTIONS.

CALCULATED MODULI (MPa)

SET	16	10	4	1	12	MIN	AVG	MAX
EY1	3119	5415	6608	6866	8509	3119	6103	8509
EY2	4517	3031	1625	3933	2816	1625	3184	4517
EY3	193	159	177	189	153	153	174	193
EX3	289	191	265	344	112	112	240	344
EY4	204	288	245	202	179	179	224	288
EX4	305	534	489	501	123	123	390	534
EY5	173	132	243	122	241	122	183	243
EX5	430	322	543	216	598	216	422	598
R3	1.50	1.20	1.50	1.82	0.73	0.73	1.35	1.82
R4	1.49	1.85	2.00	2.48	0.68	0.68	1.70	2.48
R5	2.48	2.44	2.23	1.76	2.48	1.76	2.28	2.48

CALCULATED AND OBSERVED DEFLECTIONS (mm)

						OBSERVED DEFL.(mm)	SENSOR DISTANCE(mm)
UY1	-1.361350	-1.393640	-1.397660	-1.346160	-1.406380	-1.517	0
UY2	-0.961688	-0.935550	-0.878929	-0.992052	-0.939883	-0.975	300
UY3	-0.729122	-0.671754	-0.612189	-0.782254	-0.660573	-0.704	450
UY4	-0.325618	-0.230307	-0.220492	-0.397244	-0.160283	-0.309	1000
UY5	-0.238621	-0.144660	-0.150207	-0.301609	-0.062905	-0.212	1400
UY6	-0.196973	-0.103593	-0.119052	-0.250354	-0.028440	-0.158	1800
UY7	-0.169919	-0.073008	-0.098984	-0.213344	-0.011092	-0.119	2250

ANSYS FEM ANALYSIS: X-ANISOTROPIC MODEL

SASKATOON: RWY 15-33: STA. 5 + 630 R

DISTRIBUTION OF VERTICAL STRESSES

"AREA" OF BASIN

DEPTH (mm)	DEPTH RATIO (z/ro)	LOAD 1: 732 kPa							LOAD 2: 1075 kPa							LOAD 3: 1415 kPa						
		6	9	11	8	3	AVG.	STRESS RATIO (p/po)	9	4	15	6	12	AVG.	STRESS RATIO (p/po)	6	8	3	10	14	AVG.	STRESS RATIO (p/po)
17	0.08	-0.673	-0.677	-0.679	-0.676	-0.676	-0.676	0.924	-1.007	-1.008	-1.005	-1.024	-1.013	-1.012	0.941	-1.297	-1.304	-1.299	-1.312	-1.299	-1.302	0.920
64	0.28	-0.484	-0.498	-0.499	-0.495	-0.494	-0.494	0.675	-0.778	-0.785	-0.771	-0.793	-0.806	-0.787	0.732	-0.994	-1.013	-0.996	-1.038	-0.948	-0.998	0.705
122	0.54	-0.260	-0.281	-0.280	-0.277	-0.278	-0.275	0.376	-0.483	-0.498	-0.472	-0.467	-0.531	-0.490	0.456	-0.659	-0.682	-0.658	-0.712	-0.543	-0.651	0.460
218	0.97	-0.149	-0.166	-0.164	-0.165	-0.164	-0.162	0.221	-0.303	-0.316	-0.292	-0.281	-0.340	-0.307	0.285	-0.438	-0.451	-0.437	-0.465	-0.330	-0.424	0.300
355	1.58	-0.118	-0.125	-0.124	-0.128	-0.126	-0.124	0.169	-0.222	-0.229	-0.212	-0.211	-0.241	-0.223	0.207	-0.314	-0.320	-0.318	-0.318	-0.259	-0.306	0.216
492	2.19	-0.093	-0.094	-0.094	-0.099	-0.097	-0.095	0.130	-0.165	-0.168	-0.157	-0.160	-0.175	-0.165	0.153	-0.232	-0.236	-0.239	-0.231	-0.205	-0.229	0.162
630	2.80	-0.075	-0.073	-0.073	-0.079	-0.077	-0.075	0.103	-0.128	-0.128	-0.122	-0.125	-0.132	-0.127	0.118	-0.181	-0.184	-0.190	-0.179	-0.169	-0.181	0.128
823	3.66	-0.063	-0.053	-0.056	-0.065	-0.063	-0.060	0.082	-0.099	-0.097	-0.097	-0.095	-0.099	-0.097	0.090	-0.139	-0.138	-0.154	-0.137	-0.144	-0.142	0.101
1068	4.75	-0.044	-0.034	-0.038	-0.045	-0.043	-0.041	0.056	-0.068	-0.067	-0.068	-0.065	-0.067	-0.067	0.063	-0.095	-0.091	-0.108	-0.094	-0.104	-0.099	0.070
2690	11.96	-0.005	-0.008	-0.008	-0.006	-0.006	-0.007	0.009	-0.018	-0.019	-0.017	-0.022	-0.019	-0.019	0.018	-0.013	-0.013	-0.013	-0.015	-0.013	-0.014	0.010
3690	16.40	-0.003	-0.005	-0.005	-0.004	-0.003	-0.004	0.006	-0.011	-0.013	-0.011	-0.014	-0.012	-0.012	0.011	-0.007	-0.007	-0.008	-0.009	-0.007	-0.008	0.006

MAXIMUM DEFLECTION

DEPTH (mm)	DEPTH RATIO (z/ro)	LOAD 1: 732 kPa							LOAD 2: 1075 kPa							LOAD 3: 1415 kPa						
							AVG.	STRESS RATIO (p/po)	11	16	12	15	13	AVG.	STRESS RATIO (p/po)	13	16	5	15	1	AVG.	STRESS RATIO (p/po)
17	0.08	-0.698	-0.697	-0.695	-0.696	-0.693	-0.696	0.950	-1.000	-0.989	-0.987	-0.994	-0.994	-0.993	0.923	-1.301	-1.302	-1.322	-1.287	-1.345	-1.312	0.927
64	0.28	-0.538	-0.529	-0.536	-0.529	-0.527	-0.532	0.727	-0.770	-0.745	-0.748	-0.759	-0.753	-0.755	0.703	-1.004	-0.991	-1.069	-0.963	-1.105	-1.026	0.725
122	0.54	-0.336	-0.314	-0.341	-0.320	-0.327	-0.328	0.448	-0.492	-0.464	-0.480	-0.483	-0.467	-0.477	0.444	-0.670	-0.635	-0.753	-0.622	-0.772	-0.690	0.488
218	0.97	-0.211	-0.192	-0.215	-0.198	-0.204	-0.204	0.279	-0.317	-0.292	-0.317	-0.314	-0.299	-0.308	0.286	-0.446	-0.418	-0.498	-0.417	-0.513	-0.458	0.324
355	1.58	-0.150	-0.142	-0.152	-0.146	-0.148	-0.148	0.202	-0.231	-0.210	-0.237	-0.231	-0.222	-0.226	0.210	-0.321	-0.308	-0.337	-0.314	-0.341	-0.324	0.229
492	2.19	-0.107	-0.106	-0.111	-0.109	-0.110	-0.109	0.148	-0.172	-0.156	-0.180	-0.174	-0.168	-0.170	0.158	-0.239	-0.233	-0.239	-0.242	-0.227	-0.236	0.167
630	2.80	-0.080	-0.082	-0.084	-0.083	-0.085	-0.083	0.113	-0.134	-0.121	-0.141	-0.136	-0.132	-0.133	0.124	-0.187	-0.187	-0.178	-0.194	-0.157	-0.181	0.128
823	3.66	-0.059	-0.056	-0.061	-0.062	-0.066	-0.061	0.083	-0.107	-0.092	-0.108	-0.109	-0.102	-0.104	0.096	-0.147	-0.158	-0.121	-0.162	-0.104	-0.138	0.098
1068	4.75	-0.040	-0.035	-0.040	-0.040	-0.045	-0.040	0.055	-0.075	-0.061	-0.068	-0.079	-0.072	-0.071	0.066	-0.107	-0.121	-0.079	-0.117	-0.068	-0.098	0.070
2690	11.96	-0.006	-0.008	-0.009	-0.007	-0.008	-0.008	0.011	-0.013	-0.011	-0.012	-0.014	-0.013	-0.013	0.012	-0.023	-0.021	-0.020	-0.019	-0.013	-0.019	0.014
3690	16.40	-0.004	-0.005	-0.006	-0.004	-0.005	-0.005	0.006	-0.008	-0.007	-0.008	-0.008	-0.008	-0.008	0.007	-0.013	-0.012	-0.012	-0.011	-0.008	-0.011	0.008

RMS VALUE OF DEFLECTIONS

DEPTH (mm)	DEPTH RATIO (z/ro)	LOAD 1: 732 kPa							LOAD 2: 1075 kPa							LOAD 3: 1415 kPa						
		1	14	6	3	15	AVG.	STRESS RATIO (p/po)	1	6	14	3	10	AVG.	STRESS RATIO (p/po)	16	10	4	1	12	AVG.	STRESS RATIO (p/po)
17	0.08	-0.696	-0.690	-0.684	-0.687	-0.682	-0.688	0.940	-1.022	-1.005	-1.015	-1.010	-1.005	-1.011	0.941	-1.360	-1.324	-1.322	-1.329	-1.297	-1.326	0.937
64	0.28	-0.572	-0.539	-0.553	-0.542	-0.540	-0.549	0.750	-0.839	-0.812	-0.793	-0.796	-0.783	-0.805	0.748	-1.109	-1.033	-1.069	-1.048	-0.961	-1.044	0.738
122	0.54	-0.399	-0.336	-0.390	-0.351	-0.364	-0.368	0.503	-0.586	-0.572	-0.492	-0.516	-0.508	-0.535	0.498	-0.723	-0.665	-0.753	-0.679	-0.577	-0.679	0.480
218	0.97	-0.265	-0.210	-0.258	-0.223	-0.237	-0.239	0.326	-0.389	-0.378	-0.309	-0.328	-0.333	-0.348	0.323	-0.454	-0.431	-0.498	-0.432	-0.359	-0.435	0.307
355	1.58	-0.176	-0.154	-0.174	-0.158	-0.165	-0.165	0.226	-0.259	-0.256	-0.227	-0.232	-0.238	-0.243	0.226	-0.317	-0.314	-0.337	-0.306	-0.267	-0.308	0.218
492	2.19	-0.117	-0.114	-0.124	-0.114	-0.119	-0.118	0.161	-0.172	-0.181	-0.169	-0.167	-0.169	-0.172	0.160	-0.226	-0.234	-0.239	-0.220	-0.199	-0.224	0.158
630	2.80	-0.081	-0.087	-0.092	-0.084	-0.090	-0.087	0.119	-0.119	-0.136	-0.130	-0.124	-0.124	-0.127	0.118	-0.168	-0.181	-0.178	-0.163	-0.155	-0.169	0.120
823	3.66	-0.054	-0.057	-0.063	-0.056	-0.066	-0.059	0.081	-0.079	-0.092	-0.088	-0.082	-0.090	-0.086	0.080	-0.121	-0.125	-0.121	-0.109	-0.115	-0.118	0.083
1068	4.75	-0.035	-0.034	-0.041	-0.035	-0.046	-0.038	0.052	-0.052	-0.060	-0.056	-0.051	-0.057	-0.055	0.051	-0.082	-0.079	-0.079	-0.067	-0.084	-0.078	0.055
2690	11.96	-0.007	-0.008	-0.010	-0.008	-0.011	-0.009	0.012	-0.010	-0.015	-0.020	-0.011	-0.008	-0.013	0.012	-0.018	-0.026	-0.020	-0.015	-0.038	-0.023	0.017
3690	16.40	-0.004	-0.005	-0.006	-0.005	-0.006	-0.005	0.007	-0.006	-0.009	-0.012	-0.007	-0.005	-0.008	0.007	-0.011	-0.016	-0.012	-0.009	-0.020	-0.014	0.010

ANSYS FEM ANALYSIS: ISOTROPIC MODEL

THUNDER BAY: RWY. 12-30: STA. 5 + 300 R: LOAD 1479 kPa

OPTIMIZATION CRITERION: "AREA" OF DEFLECTION BASIN.

CALCULATED MODULI (MPa)

SET	3	9	4	11	7	MIN	AVG	MAX
EY1	6763	6884	7817	7042	7206	6763	7143	7817
EY2	2039	2553	4869	2032	2040	2032	2707	4869
EY3	2704	3646	2164	3565	3717	2164	3159	3717
EY4	451	303	255	258	258	255	305	451
EY5	299	299	299	299	298	298	299	299
EY6	248	245	232	241	244	232	242	248

CALCULATED AND OBSERVED DEFLECTIONS (mm)

						OBSERVED DEFL.(mm)	SENSOR DISTANCE(mm)
UY1	-0.408303	-0.414723	-0.404357	-0.420614	-0.423016	-0.317	0
UY2	-0.260202	-0.277918	-0.287478	-0.272054	-0.273049	-0.253	300
UY3	-0.172346	-0.186684	-0.191647	-0.174814	-0.175565	-0.186	614
UY4	-0.123402	-0.133122	-0.133572	-0.118472	-0.119396	-0.133	914
UY5	-0.094077	-0.101146	-0.099309	-0.085099	-0.086230	-0.097	1219
UY6	-0.075616	-0.081536	-0.078705	-0.064737	-0.066074	-0.075	1524
UY7	-0.063588	-0.069145	-0.065856	-0.051901	-0.053432	-0.060	1829

OPTIMIZATION CRITERION: MAXIMUM DEFLECTION

CALCULATED MODULI (MPa)

SET	12	13	4	11	9	MIN	AVG	MAX
EY1	7527	7854	6158	5075	7504	5075	6824	7854
EY2	5171	2920	2604	4459	2387	2387	3508	5171
EY3	3981	3287	3316	2608	3072	2608	3253	3981
EY4	288	260	389	391	422	260	350	422
EY5	294	298	211	252	211	211	253	298
EY6	237	246	221	223	228	221	231	246

CALCULATED AND OBSERVED DEFLECTIONS (mm)

						OBSERVED DEFL.(mm)	SENSOR DISTANCE(mm)
UY1	-0.384872	-0.416851	-0.426377	-0.446679	-0.455240	-0.317	0
UY2	-0.283099	-0.285374	-0.289697	-0.317955	-0.315180	-0.251	300
UY3	-0.199759	-0.191370	-0.196062	-0.224014	-0.222436	-0.186	614
UY4	-0.146400	-0.136350	-0.137307	-0.167110	-0.165955	-0.133	914
UY5	-0.113607	-0.104127	-0.099931	-0.132594	-0.130206	-0.097	1219
UY6	-0.093392	-0.084684	-0.075937	-0.111091	-0.107154	-0.075	1524
UY7	-0.080678	-0.072470	-0.060457	-0.097322	-0.092160	-0.060	1829

ANSYS FEM ANALYSIS: ISOTROPIC MODEL

THUNDER BAY: RWY. 12-30: STA. 5 + 300 R: LOAD 1479 kPa

OPTIMIZATION CRITERION: RMS VALUE OF DEFLECTIONS.

CALCULATED MODULI (MPa)

SET	14	12	4	11	9	MIN	AVG	MAX
EY1	6301	7527	6158	5075	7504	5075	6513	7527
EY2	5758	5171	2604	4459	2387	2387	4076	5758
EY3	3991	3981	3316	2608	3072	2608	3394	3991
EY4	293	319	389	391	422	293	363	422
EY5	298	294	211	252	211	211	253	298
EY6	247	237	221	223	228	221	231	247

CALCULATED AND OBSERVED DEFLECTIONS (mm)

						OBSERVED DEFL.(mm)	SENSOR DISTANCE(mm)
UY1	-0.389308	-0.392438	-0.426377	-0.446679	-0.455240	-0.317	0
UY2	-0.282398	-0.292344	-0.289697	-0.317955	-0.315180	-0.253	300
UY3	-0.197359	-0.212028	-0.196062	-0.224014	-0.222436	-0.186	614
UY4	-0.144345	-0.160972	-0.137307	-0.167110	-0.165955	-0.133	914
UY5	-0.112477	-0.129452	-0.099931	-0.132594	-0.130206	-0.097	1219
UY6	-0.093022	-0.109744	-0.075937	-0.111091	-0.107154	-0.075	1524
UY7	-0.080752	-0.097110	-0.060457	-0.097322	-0.092160	-0.060	1829

ANSYS FEM ANALYSIS: ISOTROPIC MODEL

THUNDER BAY: RWY. 12-30: STA. 5 + 300 R

DISTRIBUTION OF VERTICAL STRESSES

"AREA" OF BASIN

LOAD 1: 730 kPa

DEPTH (mm)	DEPTH RATIO 15	13	9	11	16	15	AVG.	STRES RATIO p/po
17	0.11	-0.706	-0.702	-0.703	-0.698	-0.698	-0.630	0.960
52	0.35	-0.645	-0.634	-0.633	-0.619	-0.618	-0.630	0.862
95	0.63	-0.506	-0.490	-0.479	-0.471	-0.468	-0.483	0.661
145	0.97	-0.322	-0.304	-0.284	-0.292	-0.285	-0.298	0.408
188	1.25	-0.197	-0.182	-0.175	-0.177	-0.168	-0.180	0.246
223	1.49	-0.133	-0.122	-0.134	-0.121	-0.112	-0.124	0.170
385	2.57	-0.067	-0.064	-0.073	-0.066	-0.063	-0.067	0.091
683	4.55	-0.028	-0.029	-0.032	-0.031	-0.031	-0.030	0.042
910	6.07	-0.017	-0.018	-0.019	-0.019	-0.019	-0.018	0.025
1137	7.58	-0.006	-0.006	-0.006	-0.006	-0.006	-0.006	0.009
1650	11.00	-0.003	-0.003	-0.003	-0.003	-0.003	-0.003	0.004
2650	17.67	-0.002	-0.002	-0.002	-0.002	-0.002	-0.002	0.002

LOAD 2: 1001 kPa

DEPTH (mm)	DEPTH RATIO 15	2	1	13	10	15	AVG.	STRES RATIO p/po
17	0.11	-0.969	-0.965	-0.962	-0.961	-0.963	-0.964	0.963
52	0.35	-0.889	-0.875	-0.869	-0.864	-0.870	-0.873	0.872
95	0.63	-0.700	-0.683	-0.678	-0.672	-0.673	-0.681	0.680
145	0.97	-0.443	-0.435	-0.432	-0.431	-0.418	-0.432	0.431
188	1.25	-0.268	-0.266	-0.260	-0.262	-0.244	-0.260	0.260
223	1.49	-0.176	-0.176	-0.167	-0.165	-0.155	-0.168	0.168
385	2.57	-0.090	-0.089	-0.084	-0.085	-0.082	-0.086	0.086
683	4.55	-0.039	-0.038	-0.037	-0.039	-0.039	-0.039	0.039
910	6.07	-0.024	-0.024	-0.023	-0.024	-0.025	-0.024	0.024
1137	7.58	-0.008	-0.009	-0.008	-0.008	-0.009	-0.008	0.008
1650	11.00	-0.004	-0.004	-0.004	-0.004	-0.004	-0.004	0.004
2650	17.67	-0.002	-0.003	-0.002	-0.002	-0.003	-0.002	0.002

LOAD 3: 1305 kPa

DEPTH (mm)	DEPTH RATIO 15	10	14	13	15	16	AVG.	STRES RATIO p/po
17	0.11	-1.255	-1.263	-1.265	-1.258	-1.266	-1.261	0.966
52	0.35	-1.130	-1.157	-1.164	-1.142	-1.168	-1.152	0.883
95	0.63	-0.871	-0.903	-0.909	-0.893	-0.914	-0.898	0.688
145	0.97	-0.536	-0.556	-0.555	-0.569	-0.560	-0.555	0.425
188	1.25	-0.316	-0.317	-0.314	-0.360	-0.321	-0.326	0.250
223	1.49	-0.209	-0.194	-0.195	-0.258	-0.202	-0.212	0.162
385	2.57	-0.111	-0.104	-0.105	-0.136	-0.109	-0.113	0.087
683	4.55	-0.052	-0.054	-0.054	-0.059	-0.056	-0.055	0.042
910	6.07	-0.033	-0.034	-0.034	-0.036	-0.036	-0.035	0.027
1137	7.58	-0.012	-0.012	-0.012	-0.012	-0.013	-0.012	0.009
1650	11.00	-0.005	-0.005	-0.005	-0.005	-0.005	-0.005	0.004
2650	17.67	-0.003	-0.003	-0.003	-0.003	-0.003	-0.003	0.003

LOAD 4: 1479 kPa

DEPTH (mm)	DEPTH RATIO 15	3	9	4	11	7	AVG.	STRES RATIO p/po
17	0.11	-1.405	-1.410	-1.412	-1.402	-1.401	-1.406	0.951
52	0.35	-1.229	-1.245	-1.245	-1.219	-1.217	-1.231	0.832
95	0.63	-0.966	-0.976	-0.926	-0.946	-0.948	-0.953	0.644
145	0.97	-0.672	-0.658	-0.543	-0.640	-0.649	-0.633	0.428
188	1.25	-0.449	-0.412	-0.308	-0.403	-0.410	-0.397	0.268
223	1.49	-0.302	-0.252	-0.206	-0.244	-0.246	-0.250	0.169
385	2.57	-0.154	-0.131	-0.118	-0.129	-0.129	-0.132	0.089
683	4.55	-0.069	-0.067	-0.064	-0.068	-0.069	-0.067	0.045
910	6.07	-0.042	-0.043	-0.041	-0.043	-0.044	-0.043	0.029
1137	7.58	-0.014	-0.015	-0.014	-0.015	-0.015	-0.015	0.010
1650	11.00	-0.006	-0.006	-0.006	-0.006	-0.006	-0.006	0.004
2650	17.67	-0.004	-0.004	-0.004	-0.004	-0.004	-0.004	0.003

MAXMUM DEFLECTION

LOAD 1

DEPTH (mm)	DEPTH RATIO z/ao						AVG.	STRES RATIO p/po
17	0.11	-0.718	-0.720	-0.717	-0.715	-0.714	-0.717	0.982
52	0.35	-0.651	-0.657	-0.648	-0.642	-0.638	-0.647	0.887
95	0.63	-0.506	-0.512	-0.501	-0.497	-0.485	-0.500	0.685
145	0.97	-0.317	-0.314	-0.314	-0.316	-0.292	-0.311	0.425
188	1.25	-0.191	-0.182	-0.194	-0.194	-0.166	-0.185	0.254
223	1.49	-0.127	-0.116	-0.136	-0.130	-0.136	-0.129	0.177
385	2.57	-0.066	-0.062	-0.073	-0.068	-0.059	-0.066	0.090
683	4.55	-0.029	-0.030	-0.033	-0.031	-0.030	-0.031	0.042
910	6.07	0.018	-0.018	-0.020	-0.019	-0.018	-0.011	0.016
1137	7.58	-0.006	-0.006	-0.007	-0.007	-0.006	-0.006	0.009
1650	11.00	-0.003	-0.003	-0.003	-0.003	-0.003	-0.003	0.004
2650	17.67	-0.002	-0.002	-0.002	-0.002	-0.002	-0.002	0.003

LOAD 2

DEPTH (mm)	DEPTH RATIO z/ao	9	7	6	16	13	AVG.	STRES RATIO p/po
17	0.11	-0.962	-0.965	-0.965	-0.973	-0.958	-0.965	0.964
52	0.35	-0.867	-0.877	-0.875	-0.901	-0.854	-0.875	0.874
95	0.63	-0.668	-0.691	-0.692	-0.705	-0.669	-0.685	0.684
145	0.97	-0.411	-0.449	-0.455	-0.426	-0.443	-0.437	0.436
188	1.25	-0.243	-0.279	-0.282	-0.239	-0.272	-0.263	0.263
223	1.49	-0.160	-0.184	-0.181	-0.148	-0.165	-0.168	0.168
385	2.57	-0.085	-0.092	-0.096	-0.081	-0.085	-0.088	0.088
683	4.55	-0.040	-0.040	-0.046	-0.041	-0.040	-0.041	0.041
910	6.07	-0.025	-0.025	-0.028	-0.025	-0.022	-0.025	0.025
1137	7.58	-0.009	-0.009	-0.009	-0.008	-0.007	-0.008	0.008
1650	11.00	-0.004	-0.004	-0.004	-0.004	-0.003	-0.004	0.004
2650	17.67	-0.003	-0.003	-0.003	-0.002	-0.002	-0.002	0.002

LOAD 3

DEPTH (mm)	DEPTH RATIO z/ao	8	15	16	6	5	AVG.	STRES RATIO p/po
17	0.11	-1.255	-1.268	-1.258	-1.258	-1.258	-1.259	0.965
52	0.35	-1.130	-1.175	-1.138	-1.143	-1.141	-1.146	0.878
95	0.63	-0.871	-0.919	-0.873	-0.900	-0.902	-0.893	0.684
145	0.97	-0.536	-0.556	-0.525	-0.586	-0.593	-0.559	0.429
188	1.25	-0.317	-0.312	-0.290	-0.364	-0.368	-0.330	0.253
223	1.49	-0.209	-0.194	-0.175	-0.240	-0.236	-0.211	0.162
385	2.57	-0.111	-0.106	-0.095	-0.121	-0.125	-0.111	0.085
683	4.55	-0.052	-0.056	-0.051	-0.052	-0.060	-0.054	0.041
910	6.07	-0.033	-0.035	-0.032	-0.033	-0.036	-0.034	0.026
1137	7.58	-0.012	-0.012	-0.011	-0.012	-0.012	-0.012	0.009
1650	11.00	-0.005	-0.005	-0.005	-0.005	-0.005	-0.005	0.004
2650	17.67	-0.003	-0.003	-0.003	-0.003	-0.003	-0.003	0.003

LOAD 4: NO COMPUTATIONS (AVG. / STRES RATIO p/po)

RMS VALUE OF DEFLECTIONS

LOAD 1

DEPTH (mm)	DEPTH RATIO z/ao	12	14	9	10	15	AVG.	STRES RATIO p/po
17	0.11	-0.702	-0.709	-0.704	-0.704	-0.703	-0.704	0.965
52	0.35	-0.632	-0.656	-0.638	-0.639	-0.634	-0.640	0.877
95	0.63	-0.487	-0.513	-0.505	-0.504	-0.483	-0.498	0.683
145	0.97	-0.300	-0.312	-0.332	-0.328	-0.286	-0.311	0.427
188	1.25	-0.177	-0.174	-0.206	-0.204	-0.158	-0.184	0.252
223	1.49	-0.117	-0.106	-0.132	-0.134	-0.097	-0.117	0.161
385	2.57	-0.062	-0.057	-0.070	-0.067	-0.053	-0.062	0.085
683	4.55	-0.029	-0.030	-0.033	-0.029	-0.027	-0.030	0.041
910	6.07	-0.018	-0.018	-0.020	-0.018	-0.016	-0.018	0.025
1137	7.58	-0.007	-0.006	-0.007	-0.007	-0.005	-0.006	0.008
1650	11.00	-0.003	-0.003	-0.003	-0.003	-0.002	-0.003	0.004
2650	17.67	-0.002	-0.002	-0.002	-0.002	-0.002	-0.002	0.002

LOAD 2

DEPTH (mm)	DEPTH RATIO z/ao	12	9	10	13	14	AVG.	STRES RATIO p/po
17	0.11	-0.962	-0.965	-0.965	-0.979	-0.979	-0.970	0.969
52	0.35	-0.867	-0.875	-0.877	-0.924	-0.926	-0.894	0.893
95	0.63	-0.668	-0.692	-0.691	-0.738	-0.752	-0.708	0.707
145	0.97	-0.411	-0.455	-0.449	-0.455	-0.484	-0.451	0.450
188	1.25	-0.243	-0.282	-0.279	-0.258	-0.283	-0.269	0.269
223	1.49	-0.160	-0.181	-0.184	-0.161	-0.169	-0.171	0.171
385	2.57	-0.085	-0.096	-0.092	-0.087	-0.089	-0.090	0.090
683	4.55	-0.040	-0.046	-0.040	-0.044	-0.045	-0.043	0.043
910	6.07	-0.025	-0.028	-0.025	-0.026	-0.026	-0.026	0.026
1137	7.58	-0.009	-0.009	-0.009	-0.008	-0.008	-0.009	0.009
1650	11.00	-0.004	-0.004	-0.004	-0.004	-0.004	-0.004	0.004
2650	17.67	-0.003	-0.003	-0.003	-0.002	-0.002	-0.002	0.002

LOAD 3

DEPTH (mm)	DEPTH RATIO z/ao	12	13	9	10	2	AVG.	STRES RATIO p/po
17	0.11	-1.255	-1.269	-1.258	-1.258	-1.248	-1.258	0.964
52	0.35	-1.130	-1.181	-1.141	-1.143	-1.107	-1.140	0.874
95	0.63	-0.871	-0.920	-0.902	-0.900	-0.850	-0.889	0.681
145	0.97	-0.536	-0.554	-0.593	-0.586	-0.541	-0.562	0.431
188	1.25	-0.317	-0.334	-0.368	-0.364	-0.340	-0.344	0.264
223	1.49	-0.209	-0.246	-0.236	-0.240	-0.238	-0.234	0.179
385	2.57	-0.111	-0.125	-0.125	-0.121	-0.121	-0.120	0.092
683	4.55	-0.052	-0.050	-0.060	-0.052	-0.049	-0.053	0.040
910	6.07	-0.033	-0.032	-0.036	-0.033	-0.031	-0.033	0.025
1137	7.58	-0.012	-0.013	-0.012	-0.012	-0.011	-0.012	0.009
1650	11.00	-0.005	-0.006	-0.005	-0.005	-0.005	-0.005	0.004
2650	17.67	-0.003	-0.003	-0.003	-0.003	-0.003	-0.003	0.003

LOAD 4

DEPTH (mm)	DEPTH RATIO z/ao	14	12	4	11	9	AVG.	STRES RATIO p/po
17	0.11	-1.431	-1.424	-1.416	-1.431	-1.404	-1.421	0.961
52	0.35	-1.312	-1.286	-1.264	-1.313	-1.230	-1.281	0.866
95	0.63	-1.025	-0.993	-0.995	-1.032	-0.963	-1.001	0.677
145	0.97	-0.630	-0.613	-0.667	-0.651	-0.658	-0.644	0.435
188	1.25	-0.356	-0.351	-0.422	-0.393	-0.427	-0.390	0.264
223	1.49	-0.216	-0.213	-0.267	-0.261	-0.277	-0.247	0.167
385	2.57	-0.118	-0.115	-0.132	-0.136	-0.136	-0.127	0.086
683	4.55	-0.065	-0.062	-0.059	-0.064	-0.059	-0.062	0.042
910	6.07	-0.041	-0.039	-0.039	-0.041	-0.037	-0.039	0.027
1137	7.58	-0.014	-0.014	-0.015	-0.014	-0.014	-0.014	0.010
1650	11.00	-0.006	-0.006	-0.006	-0.006	-0.006	-0.006	0.004
2650	17.67	-0.004	-0.004	-0.004	-0.004	-0.004	-0.004	0.003

ANSYS FEM ANALYSIS: X-ANISOTROPIC MODEL

THUNDER BAY: RWY 12-30: STA. 5 + 300 R: LOAD 1479 kPa

OPTIMIZATION CRITERION: "AREA" OF DEFLECTION BASIN.

CALCULATED MODULI (MPa)

SET	13	9	1	6	10	MIN	AVG	MAX
EY1	7937	7724	6350	7571	7921	6350	7500	7937
EY2	5987	5972	5645	5896	5988	5645	5897	5988
EY3	3954	3989	3919	3975	3993	3919	3966	3993
EY4	493	467	331	270	494	270	411	494
EX4	1275	778	989	808	1293	778	1028	1293
EY5	300	299	289	297	295	289	296	300
EX5	191	303	434	675	406	191	402	675
EY6	211	219	222	217	242	211	222	242
EX6	525	547	553	503	460	460	518	553
R4	2.59	1.67	2.99	2.99	2.62	1.67	2.57	2.99
R5	0.64	1.01	1.50	2.28	1.37	0.64	1.36	2.28
R6	2.50	2.50	2.49	2.32	1.90	1.90	2.34	2.50

CALCULATED AND OBSERVED DEFLECTIONS (mm)

						OBSERVED DEFL.(mm)	SENSOR DISTANCE(mm)
UY1	-0.290393	-0.292926	-0.301465	-0.303078	-0.282043	-0.317	0
UY2	-0.212458	-0.211671	-0.214495	-0.219339	-0.205800	-0.253	300
UY3	-0.156403	-0.152765	-0.152289	-0.156400	-0.152566	-0.186	614
UY4	-0.118607	-0.114035	-0.111643	-0.115440	-0.117497	-0.133	914
UY5	-0.092887	-0.088602	-0.085602	-0.089677	-0.094003	-0.097	1219
UY6	-0.075272	-0.071777	-0.068894	-0.073541	-0.078058	-0.075	1524
UY7	-0.063245	-0.060596	-0.058102	-0.063324	-0.067212	-0.060	1829

OPTIMIZATION CRITERION: MAXIMUM DEFLECTION

CALCULATED MODULI (MPa)

SET	15	16	9	12	10	MIN	AVG	MAX
EY1	7881	7714	7553	5187	5090	5090	6685	7881
EY2	3186	5152	5887	5553	2207	2207	4397	5887
EY3	3399	2223	1838	1288	1696	1288	2089	3399
EY4	437	327	290	355	425	290	367	437
EX4	347	680	457	846	857	347	637	857
EY5	275	235	200	199	298	199	241	298
EX5	492	479	379	132	452	132	387	492
EY6	244	217	228	239	238	217	233	244
EX6	607	537	562	480	135	135	464	607
R4	0.79	2.08	1.57	2.38	2.01	0.79	1.77	2.38
R5	1.79	2.03	1.89	0.66	1.52	0.66	1.58	2.03
R6	2.49	2.47	2.46	2.01	0.57	0.57	2.00	2.49

CALCULATED AND OBSERVED DEFLECTIONS (mm)

						OBSERVED DEFL.(mm)	SENSOR DISTANCE(mm)
UY1	-0.285816	-0.303137	-0.346328	-0.377371	-0.391421	-0.317	0
UY2	-0.183404	-0.210280	-0.246384	-0.264538	-0.251572	-0.253	300
UY3	-0.114791	-0.139436	-0.164635	-0.180779	-0.171799	-0.186	614
UY4	-0.073672	-0.094043	-0.111459	-0.126845	-0.127462	-0.133	914
UY5	-0.048109	-0.065001	-0.077710	-0.091755	-0.099785	-0.097	1219
UY6	-0.031791	-0.046260	-0.056426	-0.068816	-0.081321	-0.075	1524
UY7	-0.021176	-0.034114	-0.043082	-0.053969	-0.068567	-0.060	1829

ANSYS FEM ANALYSIS: X-ANISOTROPIC MODEL

THUNDER BAY: RWY 12-30: STA. 5 + 300 R: LOAD 1479 kPa

OPTIMIZATION CRITERION: RMS VALUE OF DEFLECTIONS.

CALCULATED MODULI (MPa)

SET	16	9	15	12	10	MIN	AVG	MAX
EY1	7714	7553	7881	5187	5090	5090	6685	7881
EY2	5152	5887	4284	5553	2207	2207	4617	5887
EY3	2223	1838	3399	1288	1696	1288	2089	3399
EY4	281	290	447	355	425	281	360	447
EX4	586	457	356	846	857	356	620	857
EY5	235	200	275	199	298	199	241	298
EX5	479	379	250	132	452	132	338	479
EY6	221	228	244	239	238	221	234	244
EX6	546	562	602	480	135	135	465	602
R4	2.08	1.57	0.79	2.38	2.01	0.79	1.77	2.38
R5	2.03	1.89	0.91	0.66	1.52	0.66	1.40	2.03
R6	2.47	2.46	2.47	2.01	0.57	0.57	2.00	2.47

CALCULATED AND OBSERVED DEFLECTIONS (mm)

						OBSERVED DEFL.(mm)	SENSOR DISTANCE(mm)
UY1	-0.312872	-0.346462	-0.288195	-0.378689	-0.391868	-0.317	0
UY2	-0.217753	-0.246433	-0.193255	-0.265492	-0.251832	-0.253	300
UY3	-0.142941	-0.164535	-0.124189	-0.181073	-0.171771	-0.186	614
UY4	-0.094741	-0.111271	-0.080163	-0.126694	-0.127297	-0.133	914
UY5	-0.064265	-0.077501	-0.052003	-0.091406	-0.099593	-0.097	1219
UY6	-0.045010	-0.056237	-0.033885	-0.068423	-0.081149	-0.075	1524
UY7	-0.032824	-0.042928	-0.022186	-0.053608	-0.068427	-0.060	1829

ANSYS FEM ANALYSIS: X-ANISOTROPIC MODEL

THUNDER BAY: RWY 12-30: STA. 5+300 R

DISTRIBUTION OF VERTICAL STRESSES

AREA" OF BASIN

DEPTH (mm)	DEPTH RATIO z/ao	LOAD 1: 730 kPa 9	6	5	10	4	AVG.	STRESS RATIO p/po	LOAD 2: 1001 kPa 11	16	7	4	5	AVG.	STRESS RATIO p/po
				0.000											
17	0.11	-0.719	-0.719	-0.718	-0.722	-0.720	-0.720	0.986	-0.990	-0.990	-0.987	-0.982	-0.983	-0.986	0.985
52	0.35	-0.622	-0.622	-0.619	-0.630	-0.624	-0.623	0.854	-0.847	-0.845	-0.835	-0.819	-0.822	-0.834	0.833
95	0.63	-0.455	-0.456	-0.443	-0.464	-0.451	-0.454	0.622	-0.620	-0.609	-0.587	-0.568	-0.577	-0.592	0.591
145	0.97	-0.287	-0.290	-0.270	-0.292	-0.276	-0.283	0.388	-0.402	-0.376	-0.351	-0.338	-0.351	-0.363	0.363
188	1.25	-0.181	-0.185	-0.175	-0.182	-0.170	-0.179	0.245	-0.263	-0.225	-0.218	-0.213	-0.220	-0.228	0.228
223	1.49	-0.125	-0.130	-0.136	-0.124	-0.118	-0.127	0.174	-0.188	-0.145	-0.160	-0.161	-0.159	-0.163	0.163
385	2.57	-0.083	-0.088	-0.099	-0.083	-0.076	-0.086	0.118	-0.129	-0.089	-0.110	-0.108	-0.104	-0.108	0.108
683	4.55	-0.052	-0.056	-0.064	-0.054	-0.048	-0.055	0.075	-0.081	-0.054	-0.069	-0.067	-0.064	-0.067	0.067
910	6.07	-0.027	-0.032	-0.034	-0.029	-0.027	-0.030	0.041	-0.036	-0.031	-0.033	-0.041	-0.040	-0.036	0.036
1137	7.58	-0.012	-0.014	-0.014	-0.012	-0.012	-0.013	0.018	-0.013	-0.012	-0.013	-0.015	-0.014	-0.013	0.013
1650	11.00	-0.010	-0.010	-0.010	-0.010	-0.010	-0.010	0.013	-0.008	-0.010	-0.008	-0.007	-0.006	-0.008	0.008
2650	17.67	-0.006	-0.006	-0.006	-0.006	-0.006	-0.006	0.008	-0.004	-0.007	-0.004	-0.003	-0.003	-0.004	0.004
3650	24.33	-0.005	-0.005	-0.004	-0.005	-0.005	-0.005	0.007	-0.003	-0.005	-0.003	-0.002	-0.002	-0.003	0.003

DEPTH (mm)	DEPTH RATIO z/ao	LOAD 3: 1305 kPa 8	13	4	7	6	AVG.	STRESS RATIO p/po	LOAD 4: 1479 kPa 13	9	1	6	10	AVG.	STRESS RATIO p/po
17	0.11	-1.266	-1.256	-1.265	-1.265	-1.269	-1.264	0.969	-1.457	-1.456	-1.464	-1.456	-1.457	-1.458	0.986
52	0.35	-1.055	-1.035	-1.049	-1.051	-1.060	-1.050	0.805	-1.258	-1.254	-1.281	-1.254	-1.259	-1.261	0.853
95	0.63	-0.743	-0.758	-0.716	-0.737	-0.730	-0.737	0.565	-0.919	-0.911	-0.942	-0.908	-0.922	-0.920	0.622
145	0.97	-0.463	-0.527	-0.410	-0.453	-0.426	-0.456	0.349	-0.580	-0.566	-0.590	-0.562	-0.584	-0.577	0.390
188	1.25	-0.302	-0.358	-0.244	-0.288	-0.259	-0.290	0.222	-0.361	-0.343	-0.364	-0.343	-0.365	-0.355	0.240
223	1.49	-0.227	-0.241	-0.178	-0.208	-0.191	-0.209	0.160	-0.241	-0.224	-0.243	-0.229	-0.243	-0.236	0.159
385	2.57	-0.150	-0.140	-0.117	-0.142	-0.139	-0.137	0.105	-0.151	-0.138	-0.164	-0.160	-0.149	-0.153	0.103
683	4.55	-0.086	-0.076	-0.074	-0.098	-0.097	-0.086	0.066	-0.086	-0.084	-0.112	-0.119	-0.089	-0.098	0.066
910	6.07	-0.042	-0.042	-0.055	-0.073	-0.048	-0.052	0.040	-0.043	-0.047	-0.057	-0.063	-0.051	-0.052	0.035
1137	7.58	-0.014	-0.014	-0.020	-0.029	-0.015	-0.019	0.014	-0.019	-0.020	-0.023	-0.025	-0.023	-0.022	0.015
1650	11.00	-0.006	-0.005	-0.007	-0.011	-0.006	-0.007	0.005	-0.017	-0.017	-0.018	-0.017	-0.014	-0.017	0.011
2650	17.67	-0.002	-0.002	-0.003	-0.005	-0.002	-0.003	0.002	-0.011	-0.011	-0.011	-0.010	-0.008	-0.010	0.007
3650	24.33	-0.002	-0.001	-0.002	-0.003	-0.002	-0.002	0.002	-0.008	-0.008	-0.008	-0.007	-0.006	-0.007	0.005

MAXIMUM DEFLECTIONS

DEPTH (mm)	DEPTH RATIO z/ao						AVG.	STRESS RATIO p/po	15	16	9	12	10	AVG.	STRESS RATIO p/po
17	0.11	-0.712	-0.715	-0.715	-0.721	-0.714	-0.715	0.980	-0.971	-0.984	-0.983	-0.996	-0.979	-0.983	0.982
52	0.35	-0.600	-0.619	-0.606	-0.627	-0.607	-0.612	0.838	-0.793	-0.827	-0.821	-0.863	-0.815	-0.824	0.823
95	0.63	-0.434	-0.436	-0.425	-0.452	-0.441	-0.438	0.599	-0.564	-0.579	-0.563	-0.609	-0.595	-0.582	0.581
145	0.97	-0.278	-0.268	-0.250	-0.272	-0.284	-0.270	0.370	-0.369	-0.347	-0.319	-0.350	-0.403	-0.357	0.357
188	1.25	-0.176	-0.165	-0.154	-0.167	-0.185	-0.169	0.232	-0.232	-0.210	-0.184	-0.210	-0.276	-0.222	0.222
223	1.49	-0.118	-0.115	-0.115	-0.118	-0.131	-0.119	0.164	-0.149	-0.145	-0.130	-0.155	-0.200	-0.156	0.156
385	2.57	-0.077	-0.076	-0.081	-0.077	-0.085	-0.079	0.108	-0.095	-0.093	-0.087	-0.097	-0.128	-0.100	0.100
683	4.55	-0.048	-0.050	-0.053	-0.046	-0.051	-0.050	0.068	-0.060	-0.061	-0.058	-0.052	-0.075	-0.061	0.061
910	6.07	-0.027	-0.033	-0.032	-0.025	-0.029	-0.029	0.040	-0.037	-0.045	-0.042	-0.029	-0.044	-0.039	0.039
1137	7.58	-0.012	-0.015	-0.015	-0.011	-0.011	-0.013	0.018	-0.016	-0.023	-0.022	-0.014	-0.015	-0.018	0.018
1650	11.00	-0.010	-0.010	-0.010	-0.009	-0.007	-0.009	0.013	-0.015	-0.015	-0.015	-0.013	-0.006	-0.013	0.013
2650	17.67	-0.006	-0.006	-0.006	-0.006	-0.004	-0.006	0.008	-0.009	-0.009	-0.009	-0.008	-0.002	-0.007	0.007
3650	24.33	-0.005	-0.005	-0.004	-0.004	-0.003	-0.004	0.006	-0.007	-0.006	-0.006	-0.005	-0.002	-0.005	0.005

DEPTH (mm)	DEPTH RATIO z/ao	15	16	9	12	10	AVG.	STRESS RATIO p/po						AVG.	STRESS RATIO p/po
17	0.11	-1.255	-1.270	-1.269	-1.285	-1.263	-1.269	0.972	-1.450	-1.449	-1.451	-1.458	-1.446	-1.451	0.981
52	0.35	-1.028	-1.067	-1.060	-1.113	-1.052	-1.064	0.815	-1.233	-1.229	-1.240	-1.259	-1.228	-1.238	0.837
95	0.63	-0.733	-0.747	-0.726	-0.785	-0.767	-0.752	0.576	-0.880	-0.868	-0.898	-0.900	-0.897	-0.889	0.601
145	0.97	-0.480	-0.447	-0.411	-0.451	-0.520	-0.462	0.354	-0.539	-0.517	-0.563	-0.538	-0.587	-0.549	0.371
188	1.25	-0.303	-0.271	-0.238	-0.271	-0.356	-0.288	0.220	-0.328	-0.307	-0.344	-0.325	-0.385	-0.338	0.228
223	1.49	-0.197	-0.187	-0.168	-0.200	-0.258	-0.202	0.155	-0.222	-0.207	-0.226	-0.228	-0.268	-0.230	0.156
385	2.57	-0.125	-0.120	-0.112	-0.125	-0.165	-0.130	0.099	-0.141	-0.133	-0.147	-0.151	-0.169	-0.148	0.100
683	4.55	-0.079	-0.078	-0.075	-0.067	-0.097	-0.079	0.061	-0.087	-0.084	-0.096	-0.097	-0.100	-0.093	0.063
910	6.07	-0.048	-0.058	-0.054	-0.037	-0.057	-0.051	0.039	-0.055	-0.054	-0.053	-0.053	-0.058	-0.054	0.037
1137	7.58	-0.021	-0.029	-0.028	-0.018	-0.019	-0.023	0.018	-0.027	-0.026	-0.022	-0.023	-0.022	-0.024	0.016
1650	11.00	-0.020	-0.020	-0.019	-0.016	-0.008	-0.017	0.013	-0.020	-0.020	-0.020	-0.018	-0.012	-0.018	0.012
2650	17.67	-0.012	-0.011	-0.011	-0.010	-0.003	-0.010	0.007	-0.012	-0.012	-0.013	-0.011	-0.006	-0.011	0.007
3650	24.33	-0.009	-0.008	-0.008	-0.006	-0.002	-0.007	0.005	-0.009	-0.008	-0.009	-0.007	-0.004	-0.008	0.005

RMS VALUE OF DEFLECTIONS

DEPTH (mm)	DEPTH RATIO z/ao	15	16	9	12	10	AVG.	STRESS RATIO p/po	16	15	9	12	10	AVG.	STRESS RATIO p/po
17	0.11	-0.704	-0.711	-0.711	-0.720	-0.708	-0.711	0.974	-0.984	-0.976	-0.983	-0.996	-0.979	-0.984	0.983
52	0.35	-0.578	-0.596	-0.594	-0.624	-0.590	-0.596	0.817	-0.824	-0.806	-0.821	-0.863	-0.815	-0.826	0.825
95	0.63	-0.413	-0.415	-0.407	-0.440	-0.430	-0.421	0.577	-0.574	-0.575	-0.563	-0.609	-0.595	-0.583	0.582
145	0.97	-0.269	-0.246	-0.231	-0.253	-0.291	-0.258	0.353	-0.340	-0.371	-0.319	-0.350	-0.403	-0.356	0.356
188	1.25	-0.170	-0.146	-0.133	-0.152	-0.199	-0.160	0.219	-0.202	-0.231	-0.184	-0.210	-0.276	-0.221	0.221
223	1.49	-0.111	-0.100	-0.094	-0.112	-0.145	-0.112	0.154	-0.138	-0.151	-0.130	-0.155	-0.200	-0.155	0.155
385	2.57	-0.070	-0.064	-0.063	-0.070	-0.093	-0.072	0.099	-0.089	-0.096	-0.087	-0.097	-0.128	-0.099	0.099
683	4.55	-0.044	-0.043	-0.042	-0.038	-0.054	-0.044	0.061	-0.060	-0.060	-0.058	-0.052	-0.075	-0.061	0.061
910	6.07	-0.027	-0.033	-0.030	-0.021	-0.032	-0.028	0.039	-0.045	-0.037	-0.042	-0.029	-0.044	-0.039	0.039
1137	7.58	-0.012	-0.017	-0.016	-0.010	-0.011	-0.013	0.018	-0.023	-0.016	-0.022	-0.014	-0.015	-0.018	0.018
1650	11.00	-0.011	-0.011	-0.011	-0.009	-0.004	-0.009	0.013	-0.016	-0.015	-0.015	-0.013	-0.006	-0.013	0.013
2650	17.67	-0.007	-0.006	-0.006	-0.006	-0.002	-0.005	0.007	-0.009	-0.010	-0.009	-0.008	-0.002	-0.007	0.007
3650	24.33	-0.005	-0.005	-0.004	-0.004	-0.001	-0.004	0.005	-0.006	-0.007	-0.006	-0.005	-0.002	-0.005	0.005

DEPTH (mm)	DEPTH RATIO z/ao	16	9	15	12	10	AVG.	STRESS RATIO p/po	16	9	15	12	10	AVG.	STRESS RATIO p/po
17	0.11	-1.269	-1.269	-1.263	-1.285	-1.263	-1.270	0.973	-1.442	-1.442	-1.438	-1.461	-1.435	-1.444	0.976
52	0.35	-1.063	-1.060	-1.050	-1.113	-1.052	-1.068	0.818	-1.208	-1.205	-1.200	-1.265	-1.196	-1.215	0.821
95	0.63	-0.741	-0.726	-0.749	-0.785	-0.767	-0.754	0.577	-0.842	-0.825	-0.853	-0.893	-0.872	-0.857	0.579
145	0.97	-0.438	-0.411	-0.476	-0.451	-0.520	-0.459	0.352	-0.498	-0.468	-0.535	-0.513	-0.590	-0.521	0.352
188	1.25	-0.261	-0.238	-0.292	-0.271	-0.356	-0.284	0.217	-0.296	-0.270	-0.324	-0.308	-0.405	-0.321	0.217
223	1.49	-0.178	-0.168	-0.190	-0.200	-0.258	-0.199	0.152	-0.202	-0.191	-0.209	-0.227	-0.293	-0.225	0.152
385	2.57	-0.115	-0.112	-0.121	-0.125	-0.165	-0.128	0.098	-0.131	-0.127	-0.131	-0.142	-0.188	-0.144	0.097
683	4.55	-0.078	-0.075	-0.076	-0.067	-0.097	-0.078	0.060	-0.088	-0.085	-0.081	-0.076	-0.110	-0.088	0.060
910	6.07	-0.059	-0.054	-0.046	-0.037	-0.057	-0.050	0.039	-0.067	-0.061	-0.049	-0.042	-0.064	-0.057	0.038
1137	7.58	-0.030	-0.028	-0.020	-0.018	-0.019	-0.023	0.018	-0.034	-0.032	-0.022	-0.021	-0.022	-0.026	0.018
1650	11.00	-0.020	-0.019	-0.019	-0.016	-0.008	-0.017	0.013	-0.023	-0.022	-0.022	-0.019	-0.009	-0.019	0.013
2650	17.67	-0.012	-0.011	-0.012	-0.010	-0.003	-0.010	0.007	-0.013	-0.013	-0.015	-0.011	-0.003	-0.011	0.007
3650	24.33	-0.008	-0.008	-0.009	-0.006	-0.002	-0.007	0.005	-0.010	-0.009	-0.010	-0.007	-0.002	-0.008	0.005

APPENDIX 6-II

TYPICAL RESULTS OF ANALYSES FOR EACH SITE (CHARTS)

Note: The charts on the following pages show the results for one station at each site for the maximum load. The results include comparison of deflections and moduli, and computations of stresses. The complete set of results for all stations at all sites are included in another volume.

OPTIMIZING CRITERION: "AREA" OF DEFLECTION BASIN

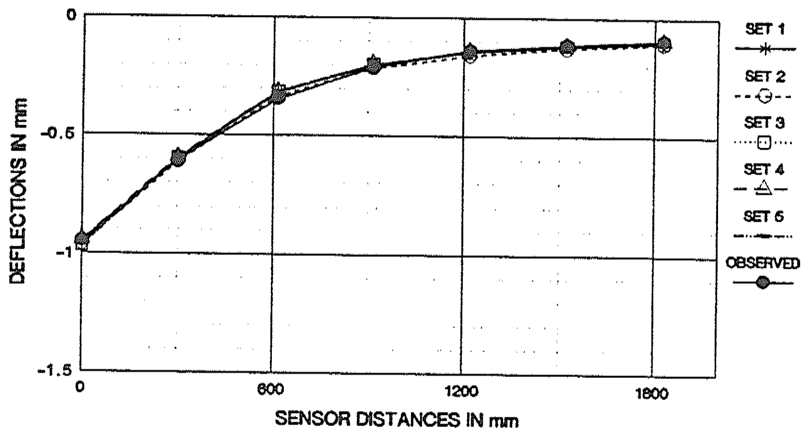

OPTIMIZING CRITERION: MAXIMUM DEFLECTION

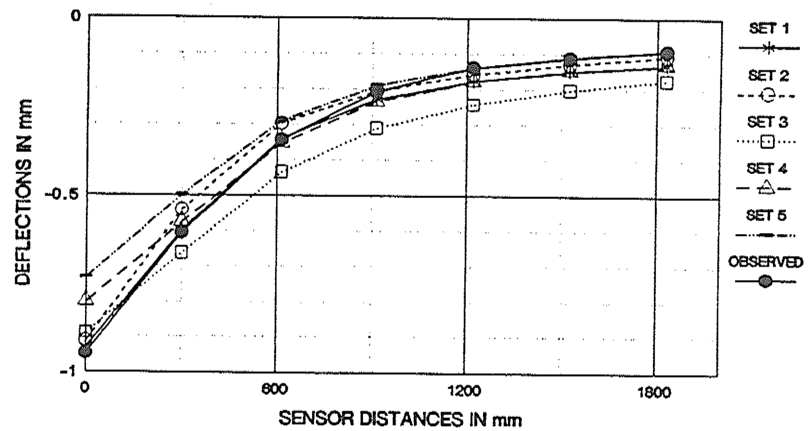

OPTIMIZING CRITERION: RMS VALUE OF DEFLECTIONS

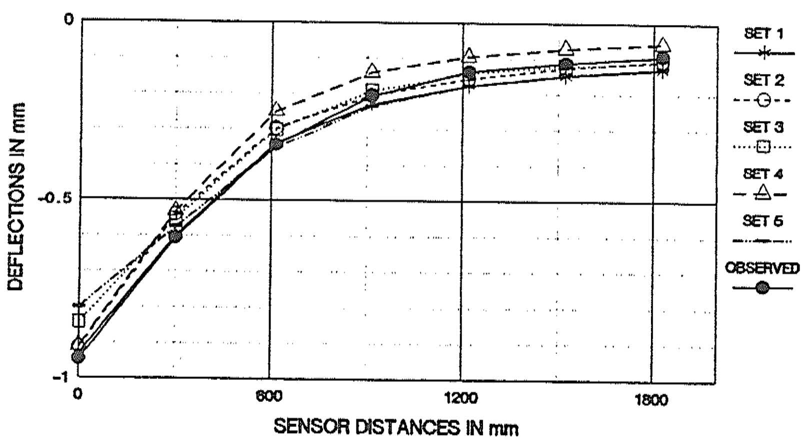

ANSYS FEM ANALYSIS : ISOTROPIC MODEL

BRANDON: RWY. 08-26: STA. 5 + 900: LOAD 1360 kPa

CALCULATED AND OBSERVED DEFLECTION BASINS

OPTIMIZING CRITERION: "AREA" OF DEFLECTION BASIN

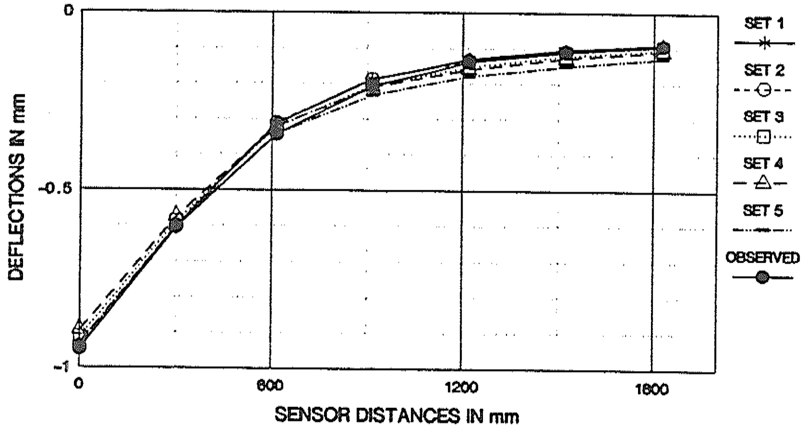

OPTIMIZING CRITERION: MAXIMUM DEFLECTION

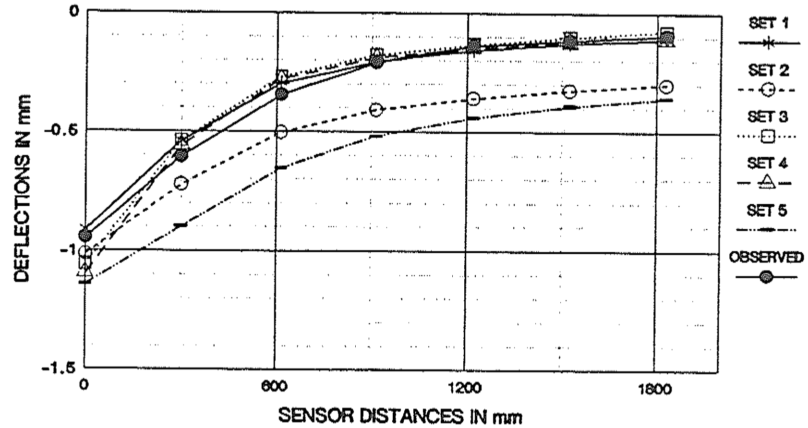

OPTIMIZING CRITERION: RMS VALUE OF DEFLECTIONS

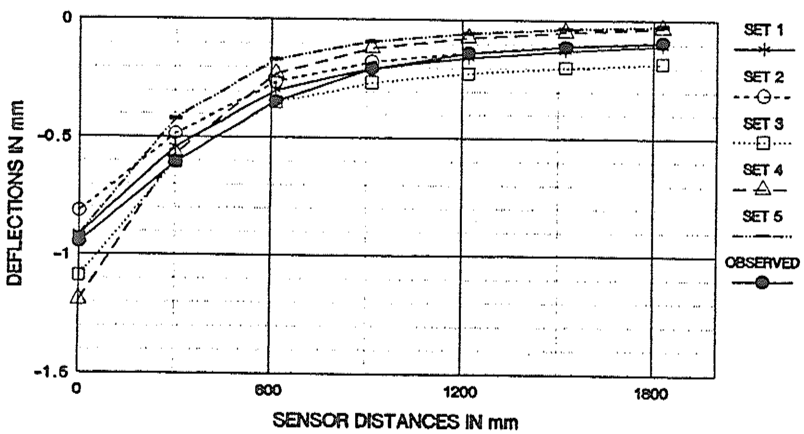

ANSYS FEM ANALYSIS : X-ANISOTROPIC MODEL

BRANDON: RWY. 08-26: STA. 5 + 900: LOAD 1360 kPa

CALCULATED AND OBSERVED DEFLECTION BASINS

OPTIMIZING CRITERION: "AREA" OF DEFLECTION BASIN

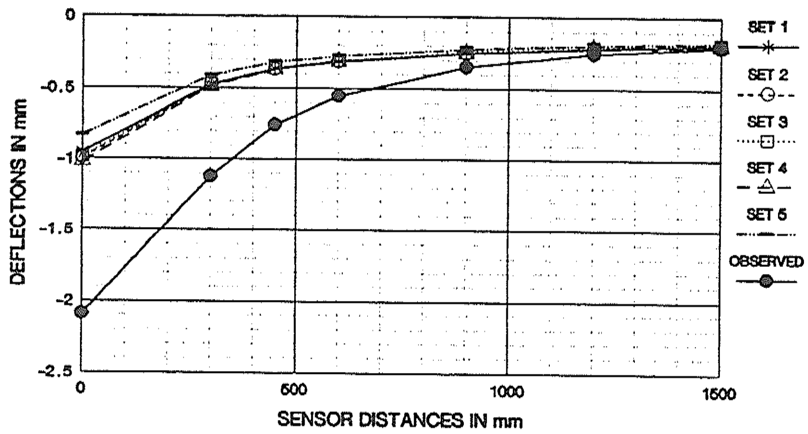

OPTIMIZING CRITERION: MAXIMUM DEFLECTION

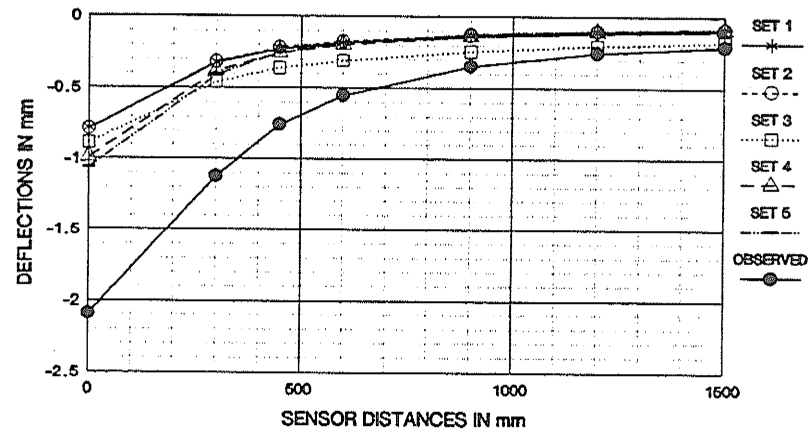

OPTIMIZING CRITERION: RMS VALUE OF DEFLECTIONS

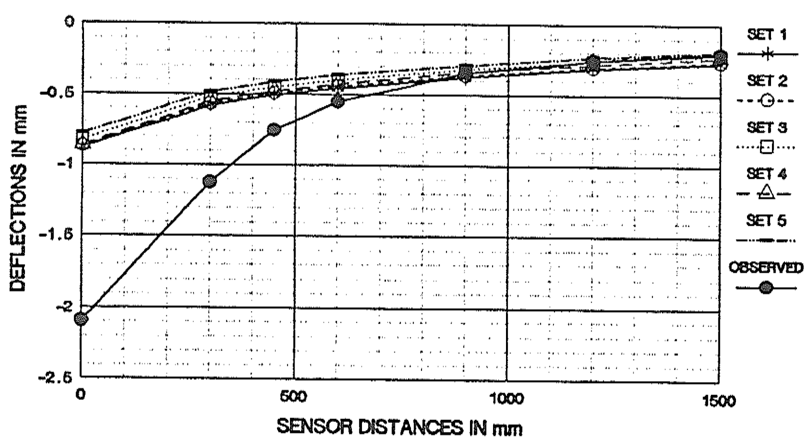

ANSYS FEM ANALYSIS : ISOTROPIC MODEL

ST. ANDREWS: RWY 13-31: STA. 5 + 660: LOAD 972 kPa

CALCULATED AND OBSERVED DEFLECTION BASINS

OPTIMIZING CRITERION: "AREA" OF DEFLECTION BASIN

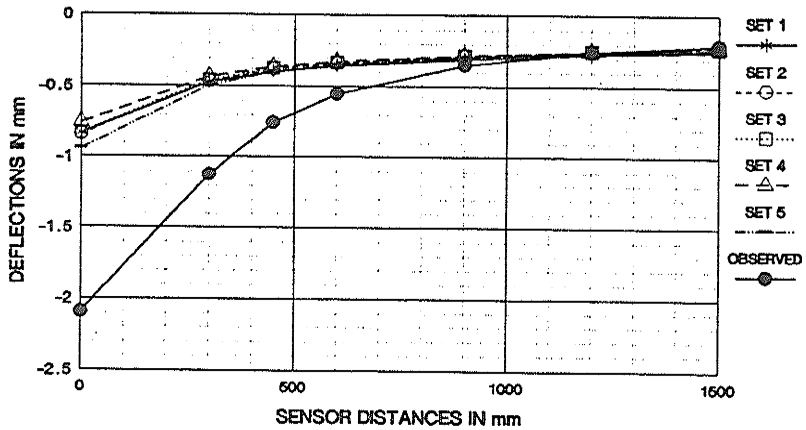

OPTIMIZING CRITERION: MAXIMUM DEFLECTION

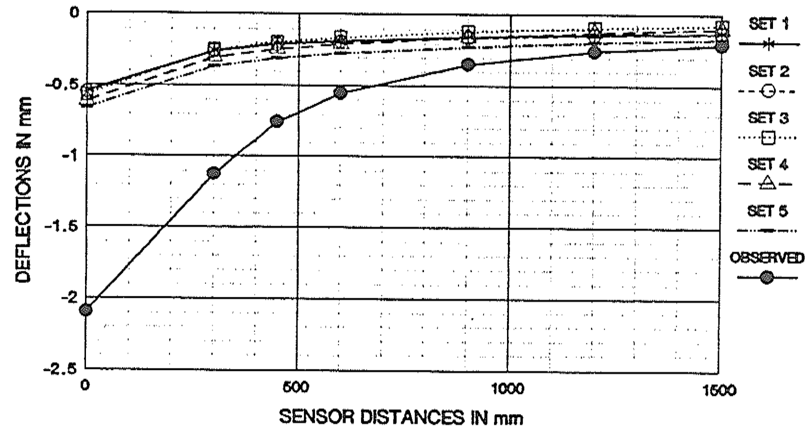

OPTIMIZING CRITERION: RMS VALUE OF DEFLECTIONS

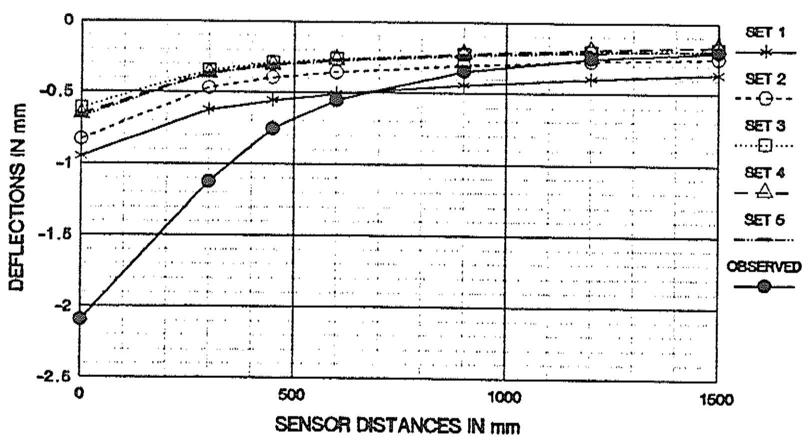

ANSYS FEM ANALYSIS : X-ANISOTROPIC MODEL

ST. ANDREWS: RWY 13-31: STA. 5+ 840: LOAD 972 kPa

CALCULATED AND OBSERVED DEFLECTION BASINS

OPTIMIZING CRITERION: "AREA" OF DEFLECTION BASIN

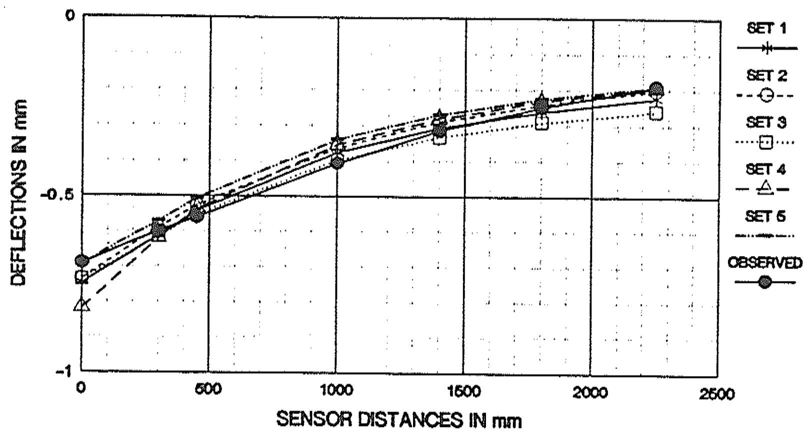

OPTIMIZING CRITERION: MAXIMUM DEFLECTION

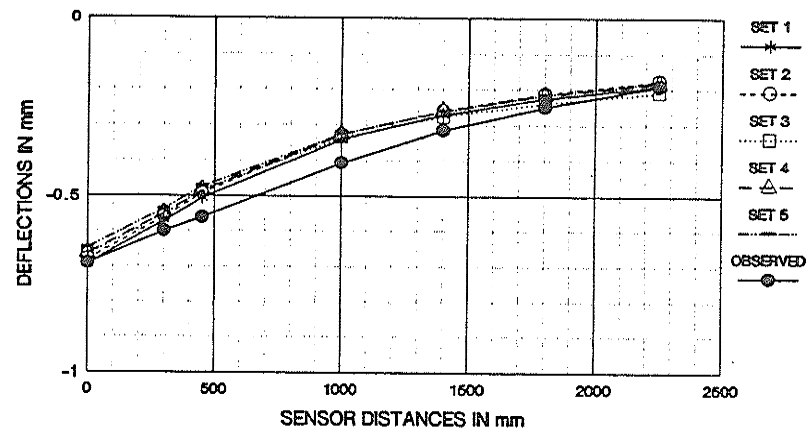

OPTIMIZING CRITERION: RMS VALUE OF DEFLECTIONS

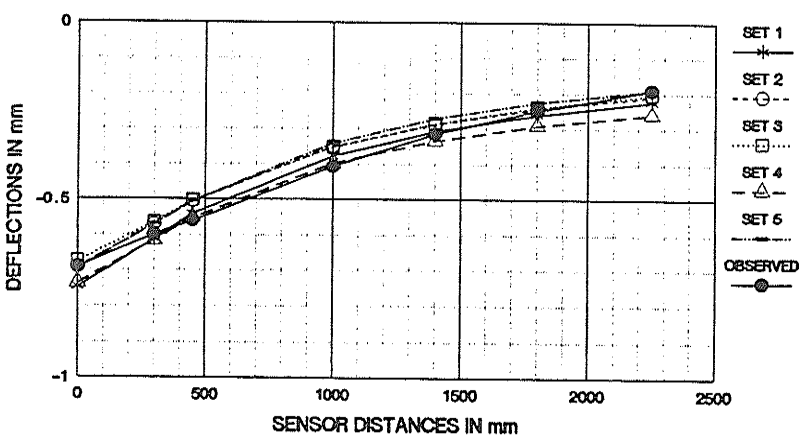

ANSYS FEM ANALYSIS : ISOTROPIC MODEL

REGINA: RWY. 12-30: STA. 5 + 990 L: LOAD 1485 kPa

CALCULATED AND OBSERVED DEFLECTION BASINS

OPTIMIZING CRITERION: "AREA" OF DEFLECTION BASIN

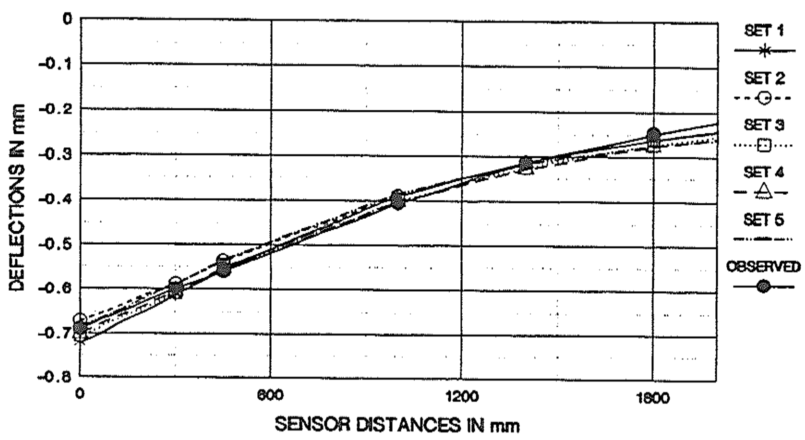

OPTIMIZING CRITERION: MAXIMUM DEFLECTION

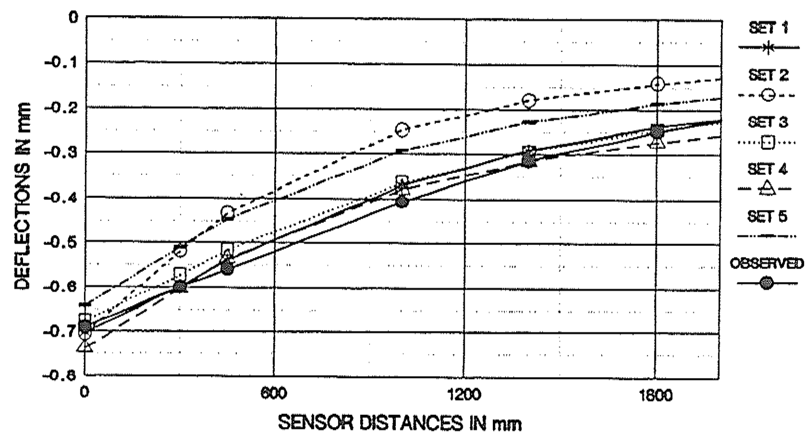

OPTIMIZING CRITERION: RMS VALUE OF DEFLECTIONS

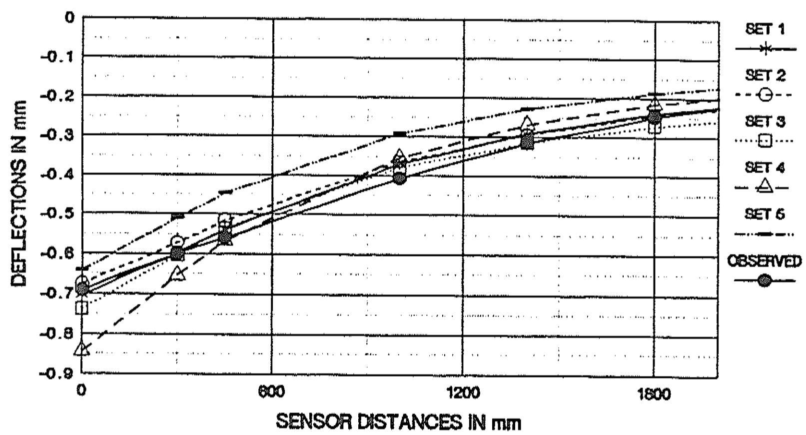

ANSYS FEM ANALYSIS : X-ANISOTROPIC MODEL

REGINA: RWY. 12-30: STA. 5 + 990: LOAD 1485 kPa

CALCULATED AND OBSERVED DEFLECTION BASINS

OPTIMIZING CRITERION: "AREA" OF DEFLECTION BASIN

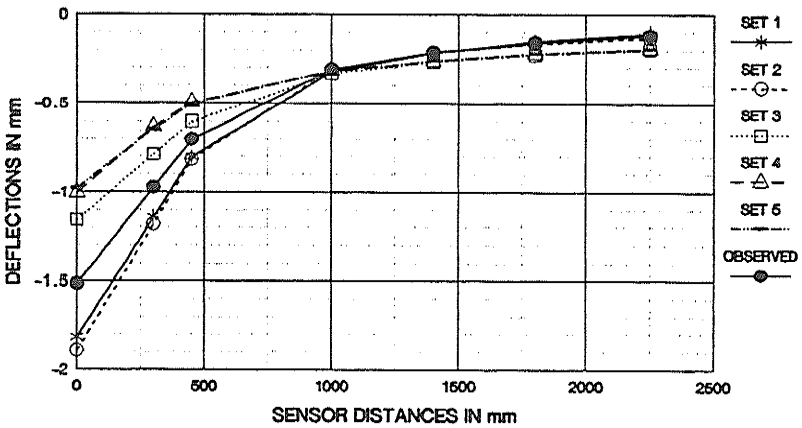

OPTIMIZING CRITERION: MAXIMUM DEFLECTION

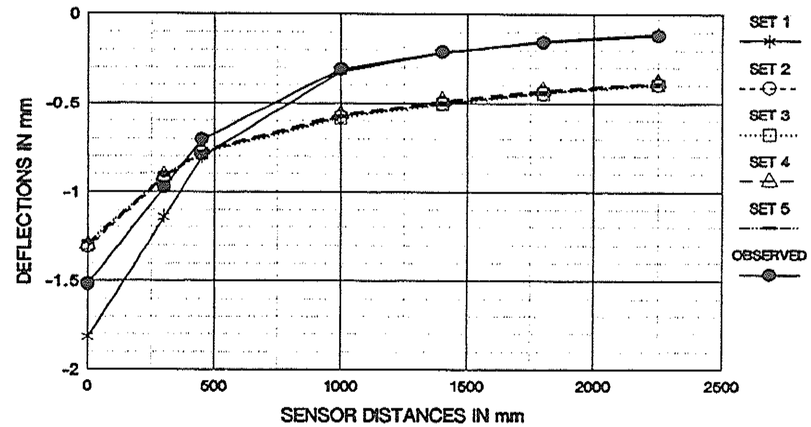

OPTIMIZING CRITERION: RMS VALUE OF DEFLECTIONS

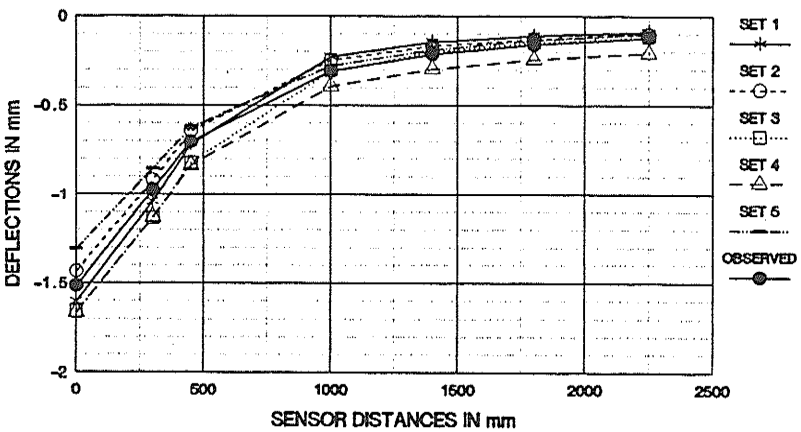

ANSYS FEM ANALYSIS : X-ANISOTROPIC MODEL

SASKATOON: RWY. 15-33:STA. 5 + 630 R:LOAD 1415 kPa

CALCULATED AND OBSERVED DEFLECTION BASINS

OPTIMIZING CRITERION: "AREA" OF DEFLECTION BASIN

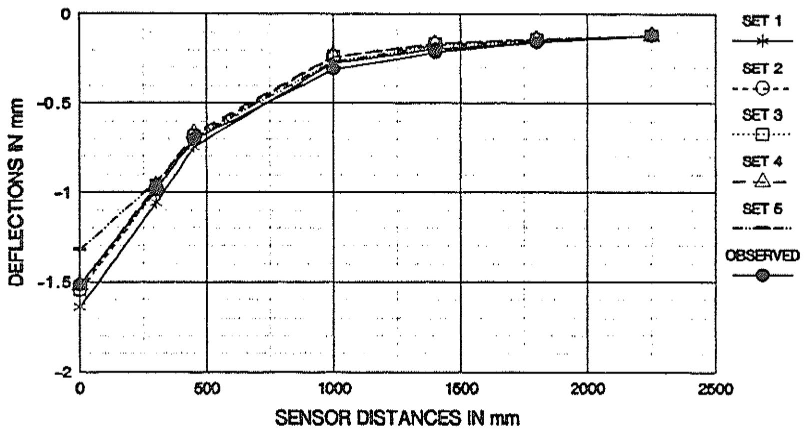

OPTIMIZING CRITERION: MAXIMUM DEFLECTION

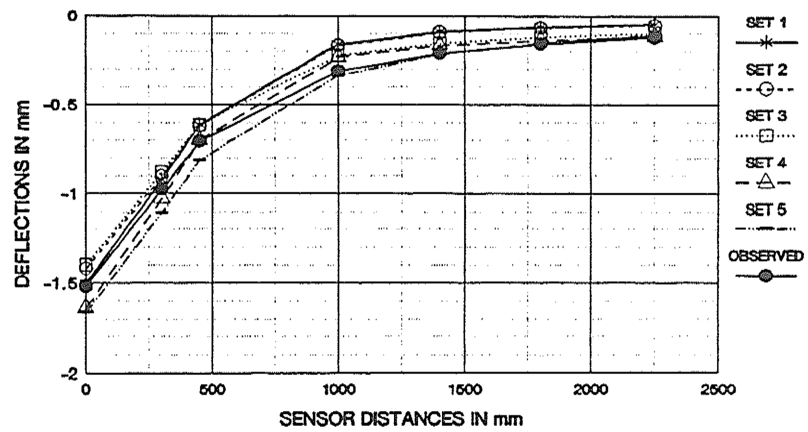

OPTIMIZING CRITERION: RMS VALUE OF DEFLECTIONS

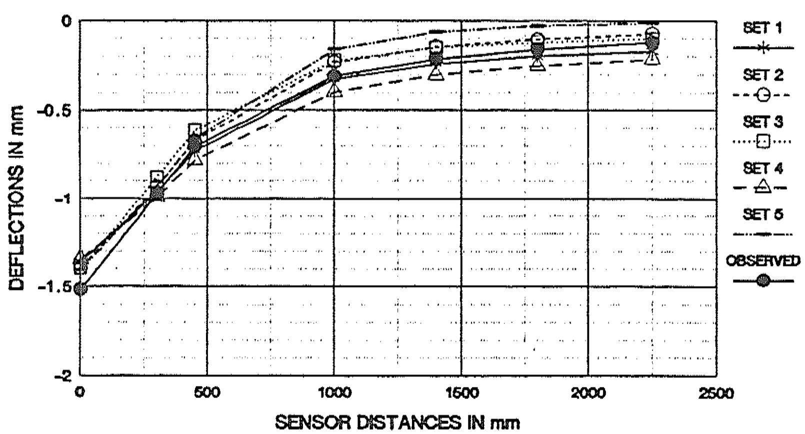

ANSYS FEM ANALYSIS : X-ANISOTROPIC MODEL

SASKATOON: RWY . 15-33:STA . 5 + 630 R:LOAD 1415 kPa

CALCULATED AND OBSERVED DEFLECTION BASINS

OPTIMIZING CRITERION: "AREA" OF DEFLECTION BASIN

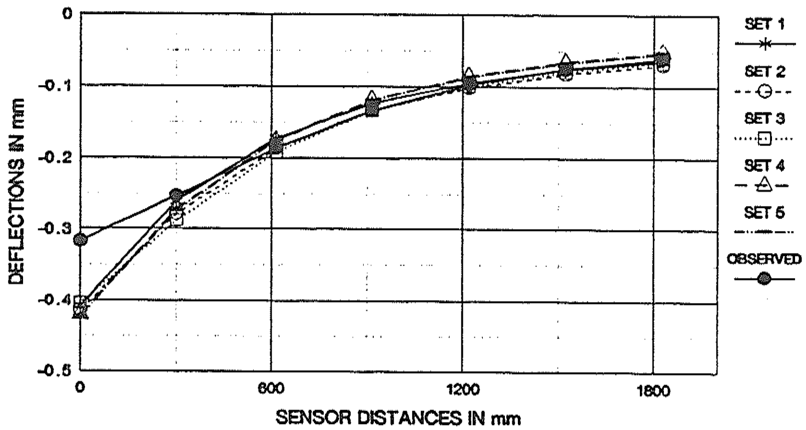

OPTIMIZING CRITERION: MAXIMUM DEFLECTION

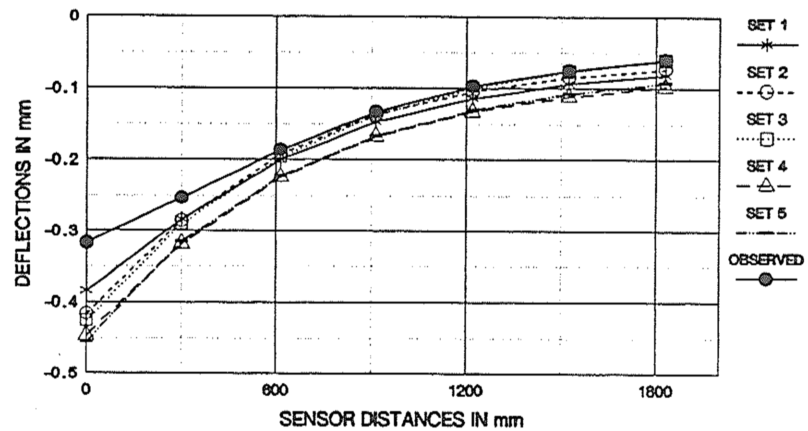

OPTIMIZING CRITERION: RMS VALUE OF DEFLECTIONS

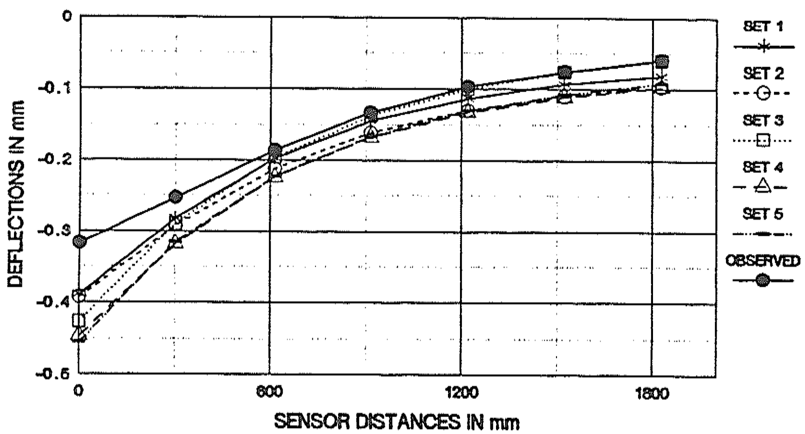

ANSYS FEM ANALYSIS : ISOTROPIC MODEL

THUNDER BAY: RWY 12–30: STA. 5 + 300 R LOAD: 1479 kPa.

CALCULATED AND OBSERVED DEFLECTION BASINS

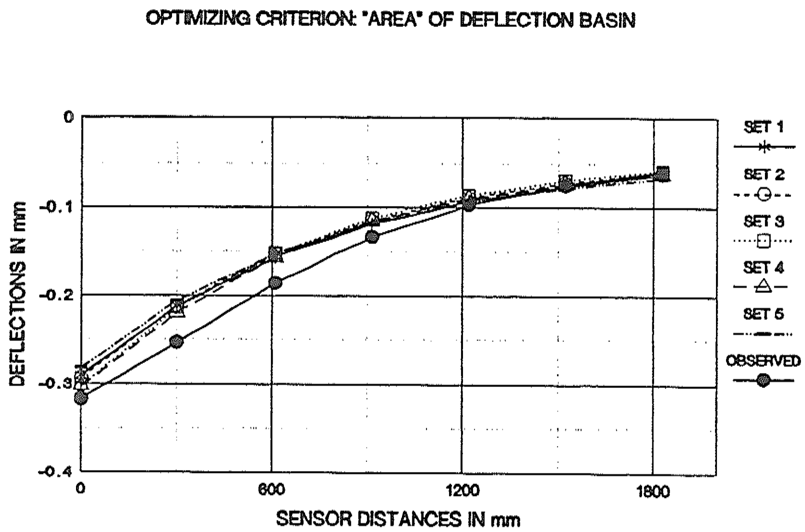

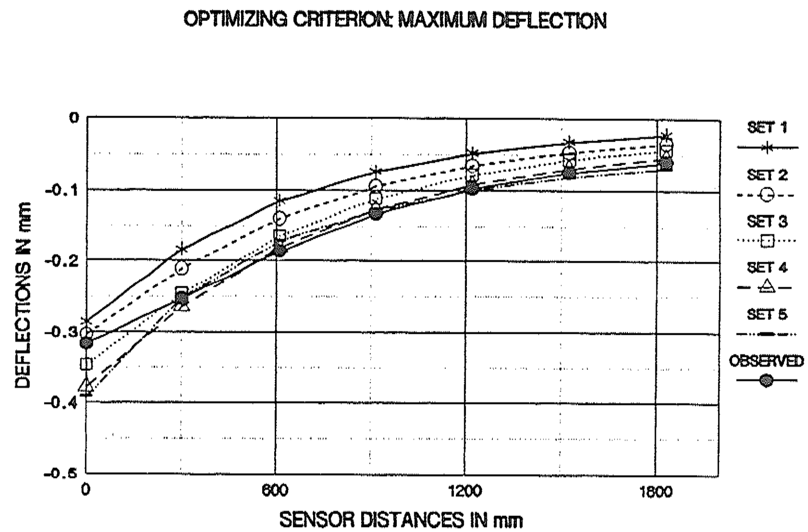

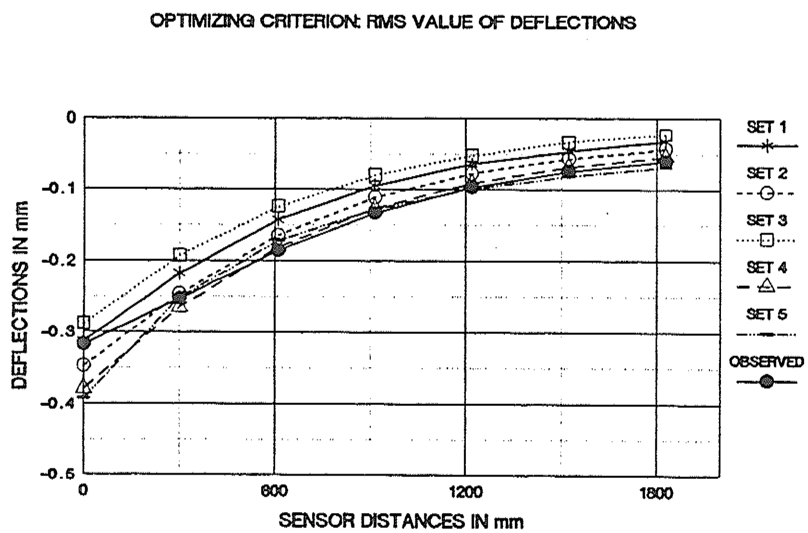

ANSYS FEM ANALYSIS : X-ANISOTROPIC MODEL

THUNDER BAY: RWY 12-30: STA. 5 + 300 R LOAD: 1479 kPa.

CALCULATED AND OBSERVED DEFLECTION BASINS

APPENDIX 6-III

SUMMARY OF MODULI FOR EACH SITE (TABLES)

ANSYS FEM ANALYSIS: ISOTROPIC MODEL.

ST.ANDREWS: RUNWAY 13-31: SUMMARY OF MODULI VALUES

OPTIMIZATION CRITERION: "AREA" OF DEFLECTION BASIN:

STATION	LOAD (kPa)	EY1	EY2	EY3
5 + 030	750	3893	151	80
5 + 120	750			
5 + 480	750	2075	165	84
5 + 660	750	4248	151	123
5 + 840	750	4691	155	68

OPTIMIZATION CRITERION: MAXIMUM DEFLECTION

STATION	LOAD (kPa)	EY1	EY2	EY3
5 + 030	750	1345	151	99
5 + 120	750			
5 + 480	750	3084	152	137
5 + 660	750	3815	157	122
5 + 840	750	2495	152	127

OPTIMIZATION CRITERION: RMS VALUE OF DEFLECTION

STATION	LOAD (kPa)	EY1	EY2	EY3
5 + 030	750	2842	151	73
5 + 120	750			
5 + 480	750	2339	164	75
5 + 660	750	3339	167	113
5 + 840	750	3082	158	67

ANSYS FEM ANALYSIS: ISOTROPIC MODEL.

ST.ANDREWS: RUNWAY 13-31: SUMMARY OF MODULI VALUES

OPTIMIZATION CRITERION: "AREA" OF DEFLECTION BASIN:

STATION	LOAD (kPa)	EY1	EY2	EY3
5 + 030	900	2980	157	62
5 + 120	900	3652	154	77
5 + 480	900	1794	153	91
5 + 660	900	3953	151	106
5 + 840	900	4242	151	72

OPTIMIZATION CRITERION: MAXIMUM DEFLECTION

STATION	LOAD (kPa)	EY1	EY2	EY3
5 + 030	900	3155	157	109
5 + 120	900	3433	152	143
5 + 480	900	1935	151	94
5 + 660	900	3859	157	121
5 + 840	900	1313	157	79

OPTIMIZATION CRITERION: RMS VALUE OF DEFLECTION

STATION	LOAD (kPa)	EY1	EY2	EY3
5 + 030	900	1340	152	50
5 + 120	900	1407	153	69
5 + 480	900	2908	153	82
5 + 660	900	3845	207	94
5 + 840	900	2611	153	69

ANSYS FEM ANALYSIS: ISOTROPIC MODEL.

ST.ANDREWS: RUNWAY 13-31: SUMMARY OF MODULI VALUES

OPTIMIZATION CRITERION: "AREA" OF DEFLECTION BASIN:

STATION	LOAD (kPa)	EY1	EY2	EY3
5 + 030	1100	4668	215	81
5 + 120	1100	2718	151	87
5 + 480	1100	4582	216	124
5 + 660	1100	3841	214	146
5 + 840	1100	4617	255	141

OPTIMIZATION CRITERION: MAXIMUM DEFLECTION

STATION	LOAD (kPa)	EY1	EY2	EY3
5 + 030	1100	4170	276	199
5 + 120	1100	3366	157	127
5 + 480	1100	4403	228	161
5 + 660	1100	4234	256	135
5 + 840	1100	4503	241	170

OPTIMIZATION CRITERION: RMS VALUE OF DEFLECTION

STATION	LOAD (kPa)	EY1	EY2	EY3
5 + 030	1100	4934	492	56
5 + 120	1100	1407	153	69
5 + 480	1100	3124	424	100
5 + 660	1100	4246	311	136
5 + 840	1100	4685	496	54

ANSYS FEM ANALYSIS: X-ANISOTROPIC MODEL

ST. ANDREWS: RUNWAY 13-31: SUMMARY OF MODULI VALUES

OPTIMIZATION CRITERION: "AREA" OF DEFLECTION BASIN

STATION	LOAD (kPa)	EY1	EY2	EX2	EY3	EX3	R2	R3
5 + 030	750.00	4027	160	175	68	88	1.10	1.31
5 + 120								
5 + 480		4632	158	141	68	94	0.89	1.39
5 + 660		1073	151	221	70	135	1.47	1.83
5 + 840		2641	151	125	51	120	0.83	2.34

OPTIMIZATION CRITERION: MAXIMUM DEFLECTION

STATION	LOAD (kPa)	EY1	EY2	EX2	EY3	EX3	R2	R3
5 + 030	750.00	3260	161	175	71	114	1.07	1.63
5 + 120								
5 + 480		2077	156	131	57	96	0.85	1.69
5 + 660		1782	167	300	74	125	1.85	1.75
5 + 840		4024	156	180	68	121	1.16	1.90

OPTIMIZATION CRITERION: RMS VALUE OF DEFLECTIONS

STATION	LOAD (kPa)	EY1	EY2	EX2	EY3	EX3	R2	R3
5 + 030	750.00	1138	151	218	51	107	1.45	2.09
5 + 120								
5 + 480		1181	152	364	60	121	2.40	1.99
5 + 660		3880	158	253	68	152	1.60	2.20
5 + 840		1745	155	182	64	103	1.17	1.68

ANSYS FEM ANALYSIS: X-ANISOTROPIC MODEL

ST. ANDREWS: RUNWAY 13-31: SUMMARY OF MODULI VALUES

OPTIMIZATION CRITERION: "AREA" OF DEFLECTION BASIN

STATION	LOAD (kPa)	EY1	EY2	EX2	EY3	EX3	R2	R3
5 + 030	900.00	1230	151	113	56	71	0.75	1.25
5 + 120		1463	151	186	51	97	1.24	1.91
5 + 480		1454	151	142	64	141	0.94	2.21
5 + 660		1877	151	214	52	61	1.42	1.18
5 + 840		1316	151	139	58	129	0.92	2.26

OPTIMIZATION CRITERION: MAXIMUM DEFLECTION

STATION	LOAD (kPa)	EY1	EY2	EX2	EY3	EX3	R2	R3
5 + 030	900.00	4309	156	223	57	123	1.44	2.18
5 + 120		2750	158	132	78	96	0.83	1.19
5 + 480		1308	153	182	67	127	1.19	1.90
5 + 660		1876	158	262	70	137	1.67	1.96
5 + 840		2283	151	152	51	104	1.00	2.04

OPTIMIZATION CRITERION: RMS VALUE OF DEFLECTIONS

STATION	LOAD (kPa)	EY1	EY2	EX2	EY3	EX3	R2	R3
5 + 030	900.00	4939	153	126	61	81	0.82	1.32
5 + 120		1334	169	132	59	54	0.80	0.92
5 + 480		3088	151	171	61	97	1.13	1.59
5 + 660		1591	157	306	85	102	1.95	1.24
5 + 840		2938	160	251	72	83	1.57	1.19

ANSYS FEM ANALYSIS: X-ANISOTROPIC MODEL

ST. ANDREWS: RUNWAY 13-31: SUMMARY OF MODULI

OPTIMIZATION CRITERION: "AREA" OF DEFLECTION

STATION	LOAD (kPa)	EY1	EY2	EX2	EY3	EX3	R2	R3
5 + 030	1100.00	2176	215	631	64	142	2.93	2.22
5 + 120		1406	151	117	52	75	0.78	1.46
5 + 480		4535	267	501	77	182	1.90	2.35
5 + 660		3471	391	1130	109	249	2.89	2.30
5 + 840		4607	285	683	114	177	2.39	1.55

OPTIMIZATION CRITERION: MAXIMUM DEFLECTION

STATION	LOAD (kPa)	EY1	EY2	EX2	EY3	EX3	R2	R3
5 + 030	1100.00	2342	476	824	144	323	1.75	2.18
5 + 120		1303	153	129	51	91	0.84	1.78
5 + 480		2298	467	836	164	380	1.84	2.26
5 + 660		2274	476	966	144	323	2.03	2.18
5 + 840		2352	476	831	144	323	1.76	2.18

OPTIMIZATION CRITERION: RMS VALUE OF DEFLECT

STATION	LOAD (kPa)	EY1	EY2	EX2	EY3	EX3	R2	R3
5 + 030	1100.00	3018	285	721	63	122	2.53	1.92
5 + 120		3759	167	260	80	132	1.60	1.66
5 + 480								
5 + 660		3036	377	924	120	203	2.47	1.80
5 + 840		3689	405	841	112	194	2.11	1.68

ANSYS FEM ANALYSIS: ISOTROPIC MODEL

BRANDON: RUNWAY 08-26: SUMMARY OF MODULI VALUES

OPTIMIZATION CRITERION: "AREA" OF DEFLECTION BASIN

STATION	LOAD (kPa)	EY1	EY2	EY3
5 + 400	600.00	1347	160	107
5 + 600		2186	155	153
5 + 900		3980	153	183
6 + 300		2531	151	147
6 + 500		3737	151	164

OPTIMIZATION CRITERION: MAXIMUM DEFLECTION

STATION	LOAD (kPa)	EY1	EY2	EY3
5 + 400	600.00	5698	171	132
5 + 600		5213	164	120
5 + 900		6352	171	146
6 + 300		6328	171	116
6 + 500		5518	171	134

OPTIMIZATION CRITERION: RMS VALUE OF DEFLECTION

STATION	LOAD (kPa)	EY1	EY2	EY3
5 + 400	600.00	5493	164	136
5 + 600		6345	183	141
5 + 900		5238	171	145
6 + 300		6589	164	119
6 + 500		5216	171	145

ANSYS FEM ANALYSIS: ISOTROPIC MODEL

BRANDON: RUNWAY 08-26: SUMMARY OF MODULI VALUES

OPTIMIZATION CRITERION: "AREA" OF DEFLECTION BASIN

STATION	LOAD (kPa)	EY1	EY2	EY3
5+400	800.00	1622	151	103
5+600		1701	152	138
5+900		4277	155	149
6+300		4982	151	142
6+500		6456	151	124

OPTIMIZATION CRITERION: MAXIMUM DEFLECTION

STATION	LOAD (kPa)	EY1	EY2	EY3
5+400	800.00	5467	164	140
5+600		4857	165	100
5+900		6329	171	132
6+300		6328	171	116
6+500		5694	171	129

OPTIMIZATION CRITERION: RMS VALUE OF DEFLECTION

STATION	LOAD (kPa)	EY1	EY2	EY3
5+400	800.00	2948	154	97
5+600		6000	171	116
5+900		5892	164	117
6+300		6331	171	116
6+500		6576	171	132

ANSYS FEM ANALYSIS: ISOTROPIC MODEL

BRANDON: RUNWAY 08-26: SUMMARY OF MODULI VALUES

OPTIMIZATION CRITERION: "AREA" OF DEFLECTION BASIN

STATION	LOAD (kPa)	EY1	EY2	EY3
5+400	1200.00	1417	151	83
5+600		1502	151	128
5+900		4483	153	158
6+300		2470	151	183
6+500		3405	152	197

OPTIMIZATION CRITERION: MAXIMUM DEFLECTION

STATION	LOAD (kPa)	EY1	EY2	EY3
5+400	1200.00	4457	165	157
5+600		5213	164	120
5+900		6329	171	116
6+300		6328	171	116
6+500		5909	171	124

OPTIMIZATION CRITERION: RMS VALUE OF DEFLECTION

STATION	LOAD (kPa)	EY1	EY2	EY3
5+400	1200.00	2940	152	93
5+600		6579	164	118
5+900		6098	164	119
6+300		6027	165	121
6+500		4724	164	135

ANSYS FEM ANALYSIS: ISOTROPIC MODEL

BRANDON: RUNWAY 08-26: SUMMARY OF MODULI VALUES

OPTIMIZATION CRITERION: "AREA" OF DEFLECTION BASIN

STATION	LOAD (kPa	EY1	EY2	EY3
5 + 400	1400.00	9948	151	132
5 + 600		9618	177	180
5 + 900		3982	151	139
6 + 300		1255	151	147
6 + 500		5358	151	124

OPTIMIZATION CRITERION: MAXIMUM DEFLECTION

STATION	LOAD (kPa	EY1	EY2	EY3
5 + 400	1400.00	9411	394	230
5 + 600		9284	364	240
5 + 900		6329	171	116
6 + 300		3036	152	117
6 + 500		5820	173	121

OPTIMIZATION CRITERION: RMS VALUE OF DEFLECTION

STATION	LOAD (kPa	EY1	EY2	EY3
5 + 400	1400.00	8881	324	175
5 + 600		9262	273	210
5 + 900		5006	164	162
6 + 300		3593	156	173
6 + 500		5182	168	137

ANSYS FEM ANALYSIS: X-ANISOTROPIC MODEL

BRANDON: RUNWAY 08-26: SUMMARY OF MODULI VALUES

OPTIMIZATION CRITERION: "AREA" OF DEFLECTION BASIN:

STATION	LOAD (kPa	EY1	EY2	EY3	EX3	EY4	EX4	R3	R4
4 + 950 (ECONOCRETE)	500.00	3529.87	18437.60	333.25	791.29	239.15	401.23	2.35	1.68
		EY1	EY2	EX2	EY3	EX3	R2	R3	
5 + 400		2428	151	349	57	134	2.31	2.36	
5 + 600		7204	162	134	124	86	0.83	0.69	
5 + 900		2604	173	166	154	152	0.96	0.98	
6 + 300		1673	151	244	112	83	1.62	0.74	
6 + 500		3067	186	181	114	109	0.97	0.97	

OPTIMIZATION CRITERION: MAXIMUM DEFLECTION

STATION	LOAD (kPa	EY1	EY2	EY3	EX3	EY4	EX4	R3	R4
4 + 950	500.00	4003	12940	412	696	206	350.68	1.69	1.70
		EY1	EY2	EX2	EY3	EX3	R2	R3	
5 + 400		3267	165	269	91	95	1.64	1.04	
5 + 600		5134	184	300	97	154	1.61	1.59	
5 + 900		5284	179	199	89	118	1.09	1.32	
6 + 300		4118	179	252	78	80	1.43	1.02	
6 + 500		5263	179	199	127	175	1.09	1.38	

OPTIMIZATION CRITERION: RMS VALUE OF DEFLECTIONS

STATION	LOAD (kPa	EY1	EY2	EY3	EX3	EY4	EX4	R3	R4
4 + 950	500.00	3599	11236	409	533	208	402.23	1.30	1.93
		EY1	EY2	EX2	EY3	EX3	R2	R3	
5 + 400		5134	184	287	97	151	1.55	1.56	
5 + 600		5134	184	300	125	217	1.63	1.73	
5 + 900		5134	184	300	125	201	1.63	1.61	
6 + 300		5673	179	175	110	156	0.98	1.41	
6 + 500		5134	184	300	154	258	1.63	1.68	

ANSYS FEM ANALYSIS: X-ANISOTROPIC MODEL

BRANDON: RUNWAY 08-26: SUMMARY OF MODULI VALUES

OPTIMIZATION CRITERION: "AREA" OF DEFLECTION BASIN:

STATION	LOAD (kPa)	EY1	EY2	EY3	EX3	EY4	EX4	R3	R4
4 + 950 (ECONOCRETE)	750.00	4525.76	13807.78	408.75	367.24	233.05	499.42	0.98	2.14
		EY1	EY2	EX2	EY3	EX3	R2	R3	
5 + 400		4362	155	124	95	139	0.80	1.49	
5 + 600		3159	195	178	95	84	0.91	0.86	
5 + 900		2496	200	198	100	94	0.99	0.94	
6 + 300		1980	191	190	84	90	0.99	1.13	
6 + 500		3536	182	223	115	119	1.23	1.04	

OPTIMIZATION CRITERION: MAXIMUM DEFLECTION

STATION	LOAD (kPa)	EY1	EY2	EY3	EX3	EY4	EX4	R3	R4
4 + 950 (ECONOCRETE)	750.00	4003	12940	412	690	206	357.73	1.71	1.72
		EY1	EY2	EX2	EY3	EX3	R2	R3	
5 + 400		3942	179	199	74	102	1.09	1.43	
5 + 600		3942	179	199	93	123	1.09	1.43	
5 + 900		6459	185	265	142	208	1.39	1.39	
6 + 300		4118	179	272	72	70	1.54	1.00	
6 + 500		5134	184	293	154	277	1.57	1.69	

OPTIMIZATION CRITERION: RMS VALUE OF DEFLECTIONS

STATION	LOAD (kPa)	EY1	EY2	EY3	EX3	EY4	EX4	R3	R4
4 + 950	750.00	4198	10245	439	717	201	319.40	1.68	1.60
		EY1	EY2	EX2	EY3	EX3	R2	R3	
5 + 400		2554	162	356	62	122	2.22	1.97	
5 + 600		3736	198	238	69	99	1.28	1.50	
5 + 900		2879	188	195	111	116	1.03	1.10	
6 + 300		3804	187	255	111	153	1.33	1.39	
6 + 500		4641	229	460	168	225	1.97	1.39	

ANSYS FEM ANALYSIS: X-ANISOTROPIC MODEL

BRANDON: RUNWAY 08-26: SUMMARY OF MODULI VALUES

OPTIMIZATION CRITERION: "AREA" OF DEFLECTION BASIN:

STATION	LOAD (kPa)	EY1	EY2	EY3	EX3	EY4	EX4	R3	R4
4 + 950	1100.00	4941	7498	451	676	238	497	1.50	2.09
		EY1	EY2	EX2	EY3	EX3	R2	R3	
5 + 400		1375	161	314	86	181	1.95	2.09	
5 + 600		2946	184	195	80	78	1.06	0.97	
5 + 900		3411	167	183	113	153	1.09	1.35	
6 + 300		3172	159	200	57	93	1.26	1.65	
6 + 500		3300	182	159	106	89	0.87	0.84	

OPTIMIZATION CRITERION: MAXIMUM DEFLECTION

STATION	LOAD (kPa)	EY1	EY2	EY3	EX3	EY4	EX4	R3	R4
4 + 950	1100.00	4579	12941	390	668	192	271	1.71	1.41
		EY1	EY2	EX2	EY3	EX3	R2	R3	
5 + 400		3185	171	137	92	96	0.80	1.05	
5 + 600		5287	200	203	78	73	1.03	0.94	
5 + 900		3942	180	200	102	133	1.09	1.30	
6 + 300		3942	179	184	86	102	1.01	1.19	
6 + 500		3942	179	199	102	132	1.09	1.29	

OPTIMIZATION CRITERION: RMS VALUE OF DEFLECTIONS

STATION	LOAD (kPa)	EY1	EY2	EY3	EX3	EY4	EX4	R3	R4
4 + 950	1100.00	4003	12940	412	644	206	358	1.56	1.73
		EY1	EY2	EX2	EY3	EX3	R2	R3	
5 + 400		2277	154	217	63	136	1	2.14	
5 + 600		2423	197	247	100	119	1	1.19	
5 + 900		3238	193	305	131	177	2	1.35	
6 + 300		3802	186	255	111	154	1	1.38	
6 + 500		3804	185	254	132	195	1	1.48	

ANSYS FEM ANALYSIS: X-ANISOTROPIC MODEL

BRANDON: RUNWAY 08-26: SUMMARY OF MODULI VALUES

OPTIMIZATION CRITERION: "AREA" OF DEFLECTION BASIN:

STATION	LOAD (kPa)	EY1	EY2	EY3	EX3	EY4	EX4	R3	R4
4 + 950	1400.00	5020	10227	500	313	231	451	0.63	1.95
		EY1	EY2	EX2	EY3	EX3	R2	R3	
5 + 400		9965	158	446	90	153	2.82	1.70	
5 + 600		9538	209	431	150	130	2.09	0.87	
5 + 900		4621	159	137	141	140	0.85	0.98	
6 + 300		4324	192	195	81	79	1.01	1.01	
6 + 500		3281	184	179	108	96	0.97	0.89	

OPTIMIZATION CRITERION: MAXIMUM DEFLECTION

STATION	LOAD (kPa)	EY1	EY2	EY3	EX3	EY4	EX4	R3	R4
4 + 950	1400.00	4003	12940	412	644	206	357.73	1.53	1.72
		EY1	EY2	EX2	EY3	EX3	R2	R3	
5 + 400		6410	657	1300	195	368	2.00	1.91	
5 + 600		8372	611	1549	249	586	2.53	2.36	
5 + 900		3733	174	236	99	109	1.36	1.24	
6 + 300		3529	177	154	74	88	0.86	1.26	
6 + 500		5104	199	201	130	166	1.04	1.43	

OPTIMIZATION CRITERION: RMS VALUE OF DEFLECTIONS

STATION	LOAD (kPa)	EY1	EY2	EY3	EX3	EY4	EX4	R3	R4
4 + 950	1400.00	4003	12940	420	644	206	357.73	1.53	1.72
		EY1	EY2	EX2	EY3	EX3	R2	R3	
5 + 400		9217	283	689	180	323	2.46	1.76	
5 + 600		9341	462	965	152	206	2.10	1.34	
5 + 900		2203	176	284	139	217	1.64	1.46	
6 + 300		1721	188	278	103	105	1.59	1.13	
6 + 500		2844	179	186	119	110	1.03	0.95	

ANSYS FEM ANALYSIS: ISOTROPIC MODEL.

REGINA: RUNWAY 12-30: SUMMARY OF MODULI VALUES

OPTIMIZATION CRITERION: "AREA" OF DEFLECTION BASIN:

STATION	LOAD (kPa)	EY1	EY2	EY3	EY4	EY5	EY6
5+510	700	6500	5347	2251	435	203	182
5+990		7850	3722	2215	312	237	184
6+290		5182	4331	2065	367	148	139
6+890		6460	6780	1159	339	191	108
7+310		2530	3617	32852	277	216	98

OPTIMIZATION CRITERION: MAXIMUM DEFLECTION

STATION	LOAD (kPa)	EY1	EY2	EY3	EY4	EY5	EY6
5+510	700	8784	3010	2393	460	191	169
5+990		7429	3072	2009	458	184	166
6+290		7022	2544	1705	476	216	146
6+890		5548	3921	1791	443	172	131
7+310		7944	4448	35467	395	207	94

OPTIMIZATION CRITERION: RMS VALUE OF DEFLECTIONS

STATION	LOAD (kPa)	EY1	EY2	EY3	EY4	EY5	EY6
5+510	700	8203	3142	2216	460	198	161
5+990		6699	3381	1989	462	192	130
6+290		6245	3345	1969	463	196	141
6+890		7316	3869	1856	471	157	101
7+310		6968	4778	32513	350	203	93

ANSYS FEM ANALYSIS: ISOTROPIC MODEL.

REGINA: RUNWAY 12-30: SUMMARY OF MODULI VALUES

OPTIMIZATION CRITERION: "AREA" OF DEFLECTION BASIN

STATION	LOAD (kPa)	EY1	EY2	EY3	EY4	EY5	EY6
5+510	1100	8228	4975	1947	425	196	177
5+990		5960	4061	1773	402	194	154
6+290		5828	5762	2205	268	154	113
6+890		2965	6109	1724	301	231	110
7+310		2750	2306	27592	264	178	94

OPTIMIZATION CRITERION: MAXIMUM DEFLECTION

STATION	LOAD (kPa)	EY1	EY2	EY3	EY4	EY5	EY6
5+510	1100	8525	3036	2295	445	190	174
5+990		7022	3251	2085	440	200	159
6+290		7295	2544	1638	475	212	145
6+890		6013	3814	1649	457	178	127
7+310		6517	3545	37887	338	218	87

OPTIMIZATION CRITERION: RMS VALUE OF DEFLECTIONS

STATION	LOAD (kPa)	EY1	EY2	EY3	EY4	EY5	EY6
5+510	1100	8843	2551	2184	476	187	156
5+990		7402	2539	1938	476	210	126
6+290		7127	3230	1793	474	191	118
6+890		5918	3932	1723	454	170	112
7+310		5927	4608	34572	308	220	89

ANSYS FEM ANALYSIS: ISOTROPIC MODEL.

REGINA: RUNWAY 12-30: SUMMARY OF MODULI VALUES

OPTIMIZATION CRITERION: "AREA" OF DEFLECTION BASIN:

STATION	LOAD (kPa)	EY1	EY2	EY3	EY4	EY5	EY6
5 + 510	1500	7677	3929	2336	450	176	172
5 + 990		4991	3929	2298	445	188	165
6 + 290		5209	3397	1948	467	161	143
6 + 890		5839	3102	1488	460	187	121
7 + 310		4161	5859	28964	299	137	133

OPTIMIZATION CRITERION: MAXIMUM DEFLECTION

STATION	LOAD (kPa)	EY1	EY2	EY3	EY4	EY5	EY6
5 + 510	1500	8017	3079	2036	460	190	177
5 + 990		8645	2859	1922	461	183	184
6 + 290		6438	3858	2327	459	197	158
6 + 890		5226	3864	1792	445	162	125
7 + 310		5557	4519	37703	326	220	85

OPTIMIZATION CRITERION: RMS VALUE OF DEFLECTIONS

STATION	LOAD (kPa)	EY1	EY2	EY3	EY4	EY5	EY6
5 + 510	1500	9130	2784	2145	466	194	171
5 + 990		7344	3120	2214	458	198	154
6 + 290		6831	3381	1994	462	192	131
6 + 890		4636	3014	1513	471	199	108
7 + 310		5272	4478	32873	349	205	103

ANSYS FEM ANALYSIS: X-ANISOTROPIC MODEL.

REGINA: RUNWAY 12-30: SUMMARY OF MODULI VALUES

OPTIMIZATION CRITERION: "AREA" OF DEFLECTION BASIN

STATIO	LOAD (kPa)	EY1	EY2	EY3	EY4	EX4	EY5	EX5	EY6	EX6	R4	R5	R6
5 + 510	700	8907	3513	2798	263	641	215	357	189	302	2.48	1.60	0.73
5 + 990	700	7408	6328	2743	282	319	195	216	169	178	1.13	1.09	1.31
6 + 290	700	6455	6486	2520	256	504	214	257	136	164	1.97	1.23	0.81
6 + 890	700	3398	3852	2892	287	656	232	234	92	92	2.29	1.01	2.24
7 + 310	700	4865	4008	28737	305	228	135	74	97	53	1.68	0.55	0.55

OPTIMIZATION CRITERION: MAXIMUM DEFLECTION

STATIO	LOAD (kpa)	EY1	EY2	EY3	EY4	EX4	EY5	EX5	EY6	EX6	R4	R5	R6
5 + 510	700	7716	3206	2289	416	797	171	276	177	274	1.90	1.52	1.83
5 + 990	700	7122	3370	2357	338	668	199	208	138	121	1.99	0.97	2.06
6 + 290	700	7084	3328	2239	373	814	206	212	139	122	2.15	0.97	2.06
6 + 890	700	6530	4058	2124	379	680	213	256	143	154	1.77	1.16	1.79
7 + 310	700	6570	5274	36104	346	395	181	267	110	161	1.13	1.54	1.54

OPTIMIZATION CRITERION: RMS VALUE OF DEFLECTION

STATIO	LOAD (kPa)	EY1	EY2	EY3	EY4	EX4	EY5	EX5	EY6	EX6	R4	R5	R6
5 + 510	700	8399	3195	2666	457	856	163	253	174	267	1.87	1.51	1.46
5 + 990	700	7581	2386	2385	324	656	184	165	141	128	2.05	0.90	2.14
6 + 290	700	6818	2373	2303	358	553	166	141	139	122	1.62	0.87	1.94
6 + 890	700	5531	4532	2218	373	667	200	242	125	137	1.80	1.14	1.88
7 + 310	700	7114	4845	34122	339	377	167	290	108	176	1.09	1.75	1.75

ANSYS FEM ANALYSIS: X-ANISOTROPIC MODEL.

REGINA: RUNWAY 12-30: SUMMARY OF MODULI VALUES

OPTIMIZATION CRITERION: "AREA" OF DEFLECTION BASIN

STATION	LOAD (kPa)	EY1	EY2	EY3	EY4	EX4	EY5	EX5	EY6	EX6	R4	R5	R6
5 + 510	1100												
5 + 990	1100	7142	5447	2602	292	356	204	317	151	236	1.22	1.56	1.20
6 + 290	1100	5722	7093	1343	253	262	171	344	134	253	1.03	1.97	2.30
6 + 890	1100	4421	6072	1504	254	224	213	413	86	173	0.88	1.97	1.23
7 + 310	1100	5992	4684	25925	296	467	234	169	108	75	1.62	0.72	0.72

OPTIMIZATION CRITERION: MAXIMUM DEFLECTION

STATION	LOAD (kPa)	EY1	EY2	EY3	EY4	EX4	EY5	EX5	EY6	EX6	R4	R5	R6
5 + 510	1100	8083	2663	1955	410	1002	170	289	192	330	2.46	1.70	1.25
5 + 990	1100	7015	2519	2343	353	592	208	187	166	142	1.76	0.87	1.49
6 + 290	1100	7352	2570	2459	375	696	204	190	151	137	1.87	0.90	1.96
6 + 890	1100	5513	4016	2251	377	627	184	256	143	188	1.63	1.33	1.75
7 + 310	1100	7430	4775	30179	256	249	168	310	94	163	0.97	1.92	1.92

OPTIMIZATION CRITERION: RMS VALUE OF DEFLECTION

STATION	LOAD (kPa)	EY1	EY2	EY3	EY4	EX4	EY5	EX5	EY6	EX6	R4	R5	R6
5 + 510	1100	7848	3195	2665	454	802	157	245	174	267	1.76	1.51	1.46
5 + 990	1100	8256	2962	2572	374	605	186	199	142	152	1.69	1.01	1.63
6 + 290	1100	7472	2527	2489	383	545	184	199	147	157	1.53	1.02	1.97
6 + 890	1100	6369	3283	2162	435	948	169	296	101	186	2.18	1.79	1.68
7 + 310	1100	6334	4478	33323	336	300	151	219	112	161	0.80	1.48	1.48

ANSYS FEM ANALYSIS: X-ANISOTROPIC MODEL.

REGINA: RUNWAY 12-30: SUMMARY OF MODULI VALUES

OPTIMIZATION CRITERION: "AREA" OF DEFLECTION BASIN

STATION	LOAD (kPa)	EY1	EY2	EY3	EY4	EX4	EY5	EX5	EY6	EX6	R4	R5	R6
5+510	1500	8888	3356	2466	425	886	181	226	175	220	2.16	1.24	1.84
5+990	1500	8324	2931	2741	375	558	191	190	142	139	1.51	0.94	1.69
6+290	1500	7385	2931	2626	412	556	191	180	142	130	1.40	0.90	1.75
6+890	1500	6336	4331	2340	405	673	186	250	132	160	1.66	1.27	1.76
7+310	1500	3188	3597	27829	255	238	186	96	105	54	0.94	0.52	0.52

OPTIMIZATION CRITERION: MAXIMUM DEFLECTION

STATION	LOAD (kPa)	EY1	EY2	EY3	EY4	EX4	EY5	EX5	EY6	EX6	R4	R5	R6
5+510	1500	9206	3087	1926	407	1049	149	230	178	299	2.60	1.63	1.68
5+990	1500	7180	2436	2203	352	522	219	273	184	210	1.54	1.21	1.14
6+290	1500	7430	2545	2324	359	623	212	265	167	196	1.72	1.19	1.18
6+890	1500	5806	4189	2466	365	789	184	270	126	170	2.14	1.43	1.35
7+310	1500	7007	4776	30701	256	239	181	282	94	140	0.93	1.63	1.49

OPTIMIZATION CRITERION: RMS VALUE OF DEFLECTION

STATION	LOAD (kPa)	EY1	EY2	EY3	EY4	EX4	EY5	EX5	EY6	EX6	R4	R5	R6
5+510	1500	8815	3023	2585	462	1082	155	250	183	301	2.35	1.59	1.52
5+990	1500	7341	2860	2568	377	596	185	201	164	165	1.66	1.01	1.89
6+290	1500	7908	2565	2392	334	526	195	227	140	168	1.66	1.12	1.92
6+890	1500	5830	4183	2305	423	757	201	258	129	153	1.75	1.25	1.75
7+310	1500	6177	3607	33147	335	324	154	223	115	164	0.90	1.49	1.49

ANSYS FEM ANALYSIS: ISOTROPIC MODEL.

SASKATOON: RUNWAY 15-33: SUMMARY OF MODULI VALUES

OPTIMIZATION CRITERION: "AREA" OF DEFLECTION BASIN

STATION	LOAD (kPa)	EY1	EY2	EY3	EY4	EY5
5 + 360	750	4505	1966	390	185	181
5 + 630	750	4505	1966	390	185	181
5 + 840	750	3796	2089	392	172	151
6 + 140	750	4527	1968	372	189	208
6 + 470	750	4250	1944	470	183	152

OPTIMIZATION CRITERION: MAXIMUM DEFLECTION

STATION	LOAD (kPa)	EY1	EY2	EY3	EY4	EY5
5 + 360	750	4549	1942	247	220	144
5 + 630	750	4549	1942	247	220	144
5 + 840	750	5409	2682	250	190	138
6 + 140	750	6268	3151	284	218	136
6 + 470	750	6207	3932	369	259	210

OPTIMIZATION CRITERION: RMS VALUE OF DEFLECTION

STATION	LOAD (kPa)	EY1	EY2	EY3	EY4	EY5
5 + 360	750	3341	1653	405	181	135
5 + 630	750	3341	1653	405	181	135
5 + 840	750	3542	1718	420	180	137
6 + 140	750	5175	2553	343	205	199
6 + 470	750	4268	1851	588	281	134

ANSYS FEM ANALYSIS: ISOTROPIC MODEL.

SASKATOON: RUNWAY 15-33: SUMMARY OF MODULI VALUES

OPTIMIZATION CRITERION: "AREA" OF DEFLECTION BASIN

STATION	LOAD (kPa)	EY1	EY2	EY3	EY4	EY5
5 + 360	1100	6127	2554	298	226	216
5 + 630	1100	6127	2554	298	226	216
5 + 840	1100	5538	1983	382	191	168
6 + 140	1100	5953	2503	526	239	223
6 + 470	1100	5066	1923	626	255	156

OPTIMIZATION CRITERION: MAXIMUM DEFLECTION

STATION	LOAD (kPa)	EY1	EY2	EY3	EY4	EY5
5 + 360	1100	3326	1653	409	231	135
5 + 630	1100	3326	1653	409	231	135
5 + 840	1100	2870	1516	667	256	104
6 + 140	1100	5938	2754	516	271	162
6 + 470	1100	5365	2112	600	243	141

OPTIMIZATION CRITERION: RMS VALUE OF DEFLECTION

STATION	LOAD (kPa)	EY1	EY2	EY3	EY4	EY5
5 + 360	1100	5607	2476	210	228	187
5 + 630	1100	5607	2476	210	228	187
5 + 840	1100	6202	2831	322	229	185
6 + 140	1100	6460	2502	254	265	229
6 + 470	1100	8394	3918	382	261	194

ANSYS FEM ANALYSIS: ISOTROPIC MODEL.

SASKATOON: RUNWAY 15-33: SUMMARY OF MODULI VALUES

OPTIMIZATION CRITERION: "AREA" OF DEFLECTION BASIN:

STATION	LOAD (kPa)	EY1	EY2	EY3	EY4	EY5
5 + 360	1400	5148	2577	340	232	208
5 + 630	1400	5723	2070	388	235	200
5 + 840	1400	4924	1983	412	194	161
6 + 140	1400	5863	2503	526	239	223
6 + 470	1400	4138	1943	614	199	183

OPTIMIZATION CRITERION: MAXIMUM DEFLECTION

STATION	LOAD (kPa)	EY1	EY2	EY3	EY4	EY5
5 + 360	1400	2771	1613	560	264	115
5 + 630	1400	2771	1613	560	264	115
5 + 840	1400	2721	1646	685	191	112
6 + 140	1400	4344	2000	663	281	106
6 + 470	1400	6926	3256	469	251	211

OPTIMIZATION CRITERION: RMS VALUE OF DEFLECTION

STATION	LOAD (kPa)	EY1	EY2	EY3	EY4	EY5
5 + 360	1400	4106	3675	220	155	217
5 + 630	1400	4106	3675	220	155	217
5 + 840	1400	3762	2913	236	257	120
6 + 140	1400	5564	3319	186	291	272
6 + 470	1400	7264	3879	367	270	195

ANSYS FEM ANALYSIS: X-ANISOTROPIC MODEL

SASKATOON: RUNWAY 15-33: SUMMARY OF MODULI VALUES

OPTIMIZATION CRITERION: "AREA" OF DEFLECTION BASIN.

STATION	LOAD (kPa)	EY1	EY2	EY3	EX3	EY4	EX4	EY5	EX5	R3	R4	R5
5 + 360	750.00	6718.97	1823.53	154.06	122.73	169.99	269.02	264.70	406.66	0.80	1.57	1.53
5 + 630	750.00	8677.58	4739.39	154.96	106.22	182.11	450.31	132.92	129.23	0.69	2.47	1.02
5 + 840	750.00	4757.82	4879.63	151.14	121.30	205.45	330.06	156.85	389.91	0.80	1.54	2.49
6 + 140	750.00	6243.00	4432.20	151.06	415.06	204.77	148.97	261.88	525.33	2.75	0.71	2.03
6 + 470	750.00	8708.99	4626.38	195.06	432.20	268.37	560.98	117.06	279.48	2.30	2.09	2.39

OPTIMIZATION CRITERION: MAXIMUM DEFLECTION

STATION	LOAD (kPa)	EY1	EY2	EY3	EX3	EY4	EX4	EY5	EX5	R3	R4	R5
5 + 360	750	5856	1520	155	181	264	283	124	241	1.17	1.03	1.87
5 + 630	750	5770	2682	179	255	219	392	180	322	1.43	1.71	1.69
5 + 840	750	5745	2505	205	232	221	455	162	272	1.20	1.99	1.64
6 + 140	750	6084	2685	206	247	221	457	161	271	1.29	1.99	1.64
6 + 470	750	7756	2956	200	332	221	436	179	352	1.85	2.04	1.90

OPTIMIZATION CRITERION: RMS VALUE OF DEFLECTIONS

STATION	LOAD (kPa)	EY1	EY2	EY3	EX3	EY4	EX4	EY5	EX5	R3	R4	R5
5 + 360	750	5078	1529	154	278	252	314	138	309	1.81	1.22	2.22
5 + 630	750	5640	2807	179	254	221	345	180	324	1.43	1.57	1.70
5 + 840	750	5107	4207	170	147	214	460	126	170	0.86	2.07	1.37
6 + 140	750	6102	2503	206	243	221	457	161	271	1.26	1.99	1.64
6 + 470	750	6920	3673	198	250	243	485	178	303	1.35	2.02	1.72

ANSYS FEM ANALYSIS: X-ANISOTROPIC MODEL

SASKATOON: RUNWAY 15-33: SUMMARY OF MODULI VALUES

OPTIMIZATION CRITERION: "AREA" OF DEFLECTION BASIN.

STATION	LOAD (kPa)	EY1	EY2	EY3	EX3	EY4	EX4	EY5	EX5	R3	R4	R5
5 + 360	1100	7012	2343	172	199	228	412	238	322	1.16	1.81	1.35
5 + 630	1100	5446	3732	157	213	183	422	106	257	1.35	2.31	2.44
5 + 840	1100	4768	4212	186	166	172	398	119	210	0.89	2.32	1.77
6 + 140	1100	9292	3975	178	268	273	305	274	220	1.54	1.13	0.80
6 + 470	1100											

OPTIMIZATION CRITERION: MAXIMUM DEFLECTION

STATION	LOAD (kPa)	EY1	EY2	EY3	EX3	EY4	EX4	EY5	EX5	R3	R4	R5
5 + 360	1100	6543	2503	206	239	206	403	161	271	1.24	1.90	1.64
5 + 630	1100	6752	2369	154	117	240	548	146	339	0.76	2.28	2.28
5 + 840	1100	6543	2503	206	233	221	457	161	271	1.20	1.99	1.64
6 + 140	1100	6079	2672	237	339	221	508	148	269	1.49	2.31	1.81
6 + 470	1100	8460	3330	213	442	250	210	228	433	2.16	0.82	1.87

OPTIMIZATION CRITERION: RMS VALUE OF DEFLECTIONS

STATION	LOAD (kPa)	EY1	EY2	EY3	EX3	EY4	EX4	EY5	EX5	R3	R4	R5
5 + 360	1100	5794	1640	174	236	224	296	182	384	1.35	1.35	2.09
5 + 630	1100	5727	3050	206	240	221	372	161	271	1.25	1.69	1.64
5 + 840	1100	5863	3537	206	257	214	388	131	185	1.35	1.82	1.50
6 + 140	1100	7347	2724	210	314	212	397	206	416	1.59	1.83	1.90
6 + 470	1100	6037	2995	292	351	226	417	161	291	1.40	1.89	1.80

ANSYS FEM ANALYSIS: X-ANISOTROPIC MODEL

SASKATOON: RUNWAY 15-33: SUMMARY OF MODULI VALUES

OPTIMIZATION CRITERION: "AREA" OF DEFLECTION BASIN:

STATION	LOAD (kPa)	EY1	EY2	EY3	EX3	EY4	EX4	EY5	EX5	R3	R4	R5
5 + 360	1400	8631	1703	187	381	194	366	193	183	2.04	1.90	0.95
5 + 630	1400	8486	2092	153	142	289	632	287	263	0.93	2.19	0.91
5 + 840	1400	6163	4441	163	269	194	482	132	204	1.65	2.49	1.54
6 + 140	1400	9193	4847	159	175	282	647	218	457	1.10	2.30	2.07
6 + 470	1400	7439	4027	299	666	192	473	119	183	2.22	2.46	1.56

OPTIMIZATION CRITERION: MAXIMUM DEFLECTION

STATION	LOAD (kPa)	EY1	EY2	EY3	EX3	EY4	EX4	EY5	EX5	R3	R4	R5
5 + 360	1400	7301	2885	198	288	243	454	189	323	1.60	1.92	1.66
5 + 630	1400	6962	1780	170	160	225	478	236	419	0.93	2.03	1.72
5 + 840	1400	7756	2935	200	279	220	433	179	352	1.52	2.04	1.90
6 + 140	1400	7756	2984	200	297	204	468	179	316	1.63	2.31	1.76
6 + 470	1400	7924	2833	366	668	250	447	175	176	1.94	1.85	1.02

OPTIMIZATION CRITERION: RMS VALUE OF DEFLECTIONS

STATION	LOAD (kPa)	EY1	EY2	EY3	EX3	EY4	EX4	EY5	EX5	R3	R4	R5
5 + 360	1400	6135	2503	206	243	221	457	192	347	1.27	1.99	1.64
5 + 630	1400	6103	3184	174	240	224	390	183	422	1.35	1.70	2.28
5 + 840	1400	7729	3802	196	338	204	491	132	214	1.92	2.41	1.67
6 + 140	1400	7346	2262	191	247	232	526	221	392	1.30	2.27	1.66
6 + 470	1400	6638	3752	315	482	214	432	130	251	1.55	2.11	2.00

ANSYS FEM ANALYSIS: ISOTROPIC MODEL.

THUNDER BAY : RUNWAY 12-30: SUMMARY OF MODULI VALUES

OPTIMIZATION CRITERION: "AREA" OF DEFLECTION BASIN

STATION	LOAD (kPa)	EY1	EY2	EY3	EY4	EY5	EY6
5 + 100	750	6219	3921	3492	287	278	233
5 + 300	750	6770	4798	2385	362	290	219
5 + 500	750	4166	5215	1784	24113	197	233
5 + 650	750	5305	4936	1989	22340	220	226
6 + 100	750	3941	5257	1609	22067	213	216
TBTXA740	750	5772	239	212	158		

OPTIMIZATION CRITERION: MAXIMUM DEFLECTION

STATION	LOAD (kPa)	EY1	EY2	EY3	EY4	EY5	EY6
5 + 100	750	6291	3958	2771	385	235	212
5 + 300	750	6291	3958	2771	385	235	212
5 + 500	750	5500	4246	2754	25741	272	222
5 + 650	750	7900	5667	1534	21161	289	249
6 + 100	750	6474	4844	2254	23634	263	228
TBTXA740	750	5762	406	199	153		

OPTIMIZATION CRITERION: RMS VALUE OF DEFLECTION

STATION	LOAD (kPa)	EY1	EY2	EY3	EY4	EY5	EY6
5 + 100	750	6334	3761	2897	340	265	192
5 + 300	750	6031	4732	3110	305	281	185
5 + 500	750	5931	4793	1504	22353	286	241
5 + 650	750	6701	4550	2422	24798	283	232
6 + 100	750	6384	5168	2099	22922	257	241
TBTXA740	750	5827	286	206	184		

ANSYS FEM ANALYSIS: ISOTROPIC MODEL.

THUNDER BAY : RUNWAY 12-30: SUMMARY OF MODULI VALUES

OPTIMIZATION CRITERION: "AREA" OF DEFLECTION BASIN

STATION	LOAD (kPa)	EY1	EY2	EY3	EY4	EY5	EY6
5 + 100	1000	7614	5091	3203	496	288	229
5 + 300	1000	7460	5120	3633	439	284	208
5 + 500	1000	5136	4420	1470	21021	262	112
5 + 650	1000	3658	5063	1785	27081	277	187
6 + 100	1000	3649	3569	2842	21860	290	114
TBTXA740	1000	7439	252	174	199		

OPTIMIZATION CRITERION: MAXIMUM DEFLECTION

STATION	LOAD (kPa)	EY1	EY2	EY3	EY4	EY5	EY6
5 + 100	1000	6291	3958	2771	385	235	212
5 + 300	1000	5813	4096	3115	315	280	183
5 + 500	1000	5690	3650	2550	29340	239	187
5 + 650	1000	6804	4699	2026	23360	279	230
6 + 100	1000	6021	3891	2025	28624	233	183
TBTXA740	1000	6269	368	198	167		

OPTIMIZATION CRITERION: RMS VALUE OF DEFLECTION

STATION	LOAD (kPa)	EY1	EY2	EY3	EY4	EY5	EY6
5 + 100	1000	5954	3573	2627	382	243	210
5 + 300	1000	4830	4340	3101	306	279	186
5 + 500	1000	5126	4303	1651	25103	260	192
5 + 650	1000	6808	4462	2057	23269	285	233
6 + 100	1000	5327	4126	2415	28638	210	183
TBTXA740	1000	5196	375	180	179		

ANSYS FEM ANALYSIS: ISOTROPIC MODEL.

THUNDER BAY : RUNWAY 12-30: SUMMARY OF MODULI VALUES

OPTIMIZATION CRITERION: "AREA" OF DEFLECTION BASIN

STATION	LOAD (kPa)	EY1	EY2	EY3	EY4	EY5	EY6
5 + 100	1300	6597	4151	3261	268	290	241
5 + 300	1300	5678	4983	2962	308	291	239
5 + 500	1300	5356	3425	2000	31224	232	183
5 + 650	1300	5281	4516	2724	24904	256	221
6 + 100	1300	5723	4027	2022	28609	229	180
TBTXA740	1300	7660	226	191	146		

OPTIMIZATION CRITERION: MAXIMUM DEFLECTION

STATION	LOAD (kPa)	EY1	EY2	EY3	EY4	EY5	EY6
5 + 100	1300	6031	4742	3216	307	281	186
5 + 300	1300	5959	4691	3132	306	280	212
5 + 500	1300	5690	3650	2550	29340	239	187
5 + 650	1300	6678	4242	2076	25792	272	219
6 + 100	1300	5782	4031	1993	31038	218	158
TBTXA740	1300	6269	365	198	167		

OPTIMIZATION CRITERION: RMS VALUE OF DEFLECTION

STATION	LOAD (kPa)	EY1	EY2	EY3	EY4	EY5	EY6
5 + 100	1300	5922	4160	2782	351	230	232
5 + 300	1300	5803	4322	2475	383	240	221
5 + 500	1300	4767	3638	1896	28347	216	174
5 + 650	1300	4592	3531	2280	26484	238	194
6 + 100	1300	5104	4022	2040	28579	210	176
TBTXA740	1300	5429	305	197	175		

ANSYS FEM ANALYSIS: ISOTROPIC MODEL.

THUNDER BAY : RUNWAY 12-30: SUMMARY OF MODULI VALUES

OPTIMIZATION CRITERION: "AREA" OF DEFLECTION BASIN

STATION	LOAD (kPa)	EY1	EY2	EY3	EY4	EY5	EY6
5 + 100	1500	7456	3245	3225	363	263	218
5 + 300	1500	7143	2707	3159	305	299	242
5 + 500	1500	5635	4024	2414	30008	225	179
5 + 650	1500	4895	4365	2910	30199	219	219
6 + 100	1500	5695	3920	2433	30863	236	168
TBTXA740	1500						

OPTIMIZATION CRITERION: MAXIMUM DEFLECTION

STATION	LOAD (kPa)	EY1	EY2	EY3	EY4	EY5	EY6
5 + 100	1500	6482	3054	3386	350	240	231
5 + 300	1500	6824	3508	3253	350	253	231
5 + 500	1500	5509	3644	2588	32836	207	183
5 + 650	1500	5509	3644	2588	32836	207	183
6 + 100	1500	5437	3844	2413	32384	203	166
TBTXA740	1500						

OPTIMIZATION CRITERION: RMS VALUE OF DEFLECTION

STATION	LOAD (kPa)	EY1	EY2	EY3	EY4	EY5	EY6
5 + 100	1500	7050	3759	3209	333	262	236
5 + 300	1500	6513	4076	3394	363	253	231
5 + 500	1500	5509	3644	2588	32836	207	183
5 + 650	1500	5912	3447	2386	32125	215	205
6 + 100	1500	6248	4170	2266	32284	207	162
TBTXA740	1500						

ANSYS FEM ANALYSIS: X-ANISOTROPIC MODEL.

THUNDER BAY : RUNWAY 12-30: SUMMARY OF MODULI VALUES

OPTIMIZATION CRITERION: "AREA" OF DEFLECTION BASIN

STATION	LOAD (kPa)	EY1	EY2	EY3	EY4	EX4	EY5	EX5	EY6	EX6	R4	R5	R6
5+100	750	7730	4703	3224	386	1056	288	389	206	475	2.74	1.35	2.31
5+300	750	6860	5761	2935	437	1265	251	563	167	414	2.88	2.25	2.49
5+500	750	7274	2242	3444	30722	30722	181	102	223	114	1.00	0.57	0.51
5+650	750	6248	2748	2581	36135	36135	268	564	130	68	1.00	2.12	0.52
6+100	750	3508	3572	3469	36410	36410	219	525	110	168	1.00	2.38	1.51
TBTXA740	750	4034			231	491	162	261	180	264	2.14	1.70	1.45

OPTIMIZATION CRITERION: MAXIMUM DEFLECTION

STATION	LOAD (kPa)	EY1	EY2	EY3	EY4	EX4	EY5	EX5	EY6	EX6	R4	R5	R6
5+100	750	6589	4070	2077	351	755	239	324	228	412	2.11	1.31	1.79
5+300	750	6685	4355	2089	346	612	241	366	234	465	1.77	1.50	2.00
5+500	750	6841	3953	2706	36503	36503	222	364	201	239	1.00	1.67	1.18
5+650	750	6815	4076	2601	32314	32314	250	374	193	230	1.00	1.50	1.28
6+100	750	6210	4263	3037	37571	37571	206	287	211	279	1.00	1.38	1.33
TBTXA740	750												

OPTIMIZATION CRITERION: RMS VALUE OF DEFLECTION

STATION	LOAD (kPa)	EY1	EY2	EY3	EY4	EX4	EY5	EX5	EY6	EX6	R4	R5	R6
5+100	750	6589	4070	2077	351	695	239	343	228	412	1.88	1.38	1.79
5+300	750	6685	4413	2089	360	620	241	386	234	464	1.77	1.58	2.00
5+500	750	6500	4895	2767	36015	36015	213	320	191	208	1.00	1.46	1.15
5+650	750	6724	3419	2833	30213	30213	251	309	190	256	1.00	1.27	1.42
6+100	750	6465	4497	2682	37395	37395	196	335	211	235	1.00	1.64	1.09
TBTXA740	750												

ANSYS FEM ANALYSIS: X-ANISOTROPIC MODEL.

THUNDER BAY : RUNWAY 12-30: SUMMARY OF MODULI VALUES

OPTIMIZATION CRITERION: "AREA" OF DEFLECTION BASIN

STATION	LOAD (kPa)	EY1	EY2	EY3	EY4	EX4	EY5	EX5	EY6	EX6	R4	R5	R6
5+100	1000	7796	5273	1457	426	752	286	647	219	422	1.78	2.26	1.92
5+300	1000	7890	5485	2485	425	1004	278	557	209	255	2.37	2.00	1.29
5+500	1000	3949	2464	3578	23631	23631	275	177	202	111	1.00	0.65	0.55
5+650	1000	4850	2385	1724	37568	37568	176	411	218	111	1.00	2.32	0.51
6+100	1000	6014	3705	1187	21658	21658	277	238	110	85	1.00	0.90	0.78
TBTXA740	1000	6021			240	415	153	318	188	188	1.74	2.07	1.33

OPTIMIZATION CRITERION: MAXIMUM DEFLECTION

STATION	LOAD (kPa)	EY1	EY2	EY3	EY4	EX4	EY5	EX5	EY6	EX6	R4	R5	R6
5+100	1000	6589	4070	2077	351	695	239	343	228	412	1.88	1.38	1.79
5+300	1000	6685	4370	2089	362	633	241	376	233	464	1.77	1.54	2.00
5+500	1000	5358	4235	2631	31432	31432	188	250	193	276	1.00	1.38	1.38
5+650	1000	6288	4369	2937	37648	37648	214	343	212	291	1.00	1.63	1.37
6+100	1000	6125	3612	3112	29773	29773	189	298	175	192	1.00	1.63	1.07
TBTXA740	1000	5857			409	833	162	215	151	282	2.11	1.23	1.93

OPTIMIZATION CRITERION: RMS VALUE OF DEFLECTION

STATION	LOAD (kPa)	EY1	EY2	EY3	EY4	EX4	EY5	EX5	EY6	EX6	R4	R5	R6
5+100	1000	6589	4070	2077	358	701	239	343	228	412	1.88	1.38	1.79
5+300	1000	6685	4473	2089	360	620	241	386	234	465	1.77	1.58	2.00
5+500	1000	6167	4228	2536	33184	33184	209	303	191	230	1.00	1.45	1.19
5+650	1000	6815	4076	2601	32314	32314	250	374	193	230	1.00	1.50	1.28
6+100	1000	6167	4228	2536	33184	33184	209	303	191	230	1.00	1.45	1.19
TBTXA740	1000	5352			327	699	170	284	146	319	2.10	1.63	2.22

ANSYS FEM ANALYSIS: X-ANISOTROPIC MODEL.

THUNDER BAY : RUNWAY 12-30: SUMMARY OF MODULI VALUES

OPTIMIZATION CRITERION: "AREA" OF DEFLECTION BASIN

STATION	LOAD (kPa)	EY1	EY2	EY3	EY4	EX4	EY5	EX5	EY6	EX6	R4	R5	R6
5+100	1000	7796	5273	1457	426	752	286	647	219	422	1.78	2.26	1.92
5+300	1000	7890	5485	2485	425	1004	278	557	209	255	2.37	2.00	1.29
5+500	1000	3949	2464	3578	23631	23631	275	177	202	111	1.00	0.65	0.55
5+650	1000	4850	2385	1724	37568	37568	176	411	218	111	1.00	2.32	0.51
6+100	1000	6014	3705	1187	21658	21658	277	238	110	85	1.00	0.90	0.78
TBTXA740	1000	6021			240	415	153	318	188	188	1.74	2.07	1.33

OPTIMIZATION CRITERION: MAXIMUM DEFLECTION

STATION	LOAD (kPa)	EY1	EY2	EY3	EY4	EX4	EY5	EX5	EY6	EX6	R4	R5	R6
5+100	1000	6589	4070	2077	351	695	239	343	228	412	1.88	1.38	1.79
5+300	1000	6685	4370	2089	362	633	241	376	233	464	1.77	1.54	2.00
5+500	1000	5358	4235	2631	31432	31432	188	250	193	276	1.00	1.38	1.38
5+650	1000	6288	4369	2937	37648	37648	214	343	212	291	1.00	1.63	1.37
6+100	1000	6125	3612	3112	29773	29773	189	298	175	192	1.00	1.63	1.07
TBTXA740	1000	5857			409	833	162	215	151	282	2.11	1.23	1.93

OPTIMIZATION CRITERION: RMS VALUE OF DEFLECTION

STATION	LOAD (kPa)	EY1	EY2	EY3	EY4	EX4	EY5	EX5	EY6	EX6	R4	R5	R6
5+100	1000	6589	4070	2077	358	701	239	343	228	412	1.88	1.38	1.79
5+300	1000	6685	4473	2089	360	620	241	386	234	465	1.77	1.58	2.00
5+500	1000	6167	4228	2536	33184	33184	209	303	191	230	1.00	1.45	1.19
5+650	1000	6815	4076	2601	32314	32314	250	374	193	230	1.00	1.50	1.28
6+100	1000	6167	4228	2536	33184	33184	209	303	191	230	1.00	1.45	1.19
TBTXA740	1000	5352			327	699	170	284	146	319	2.10	1.63	2.22

ANSYS FEM ANALYSIS: X-ANISOTROPIC MODEL.

THUNDER BAY : RUNWAY 12-30: SUMMARY OF MODULI VALUES

OPTIMIZATION CRITERION: "AREA" OF DEFLECTION BASIN

STATION	LOAD (kPa)	EY1	EY2	EY3	EY4	EX4	EY5	EX5	EY6	EX6	R4	R5	R6
5+100	1300	7730	4703	3224	386	1056	288	389	206	475	2.74	1.35	2.31
5+300	1300	7775	4613	2065	362	991	296	556	233	150	2.69	1.87	0.64
5+500	1300	4329	2910	2986	20896	20896	263	260	122	78	1.00	0.96	0.65
5+650	1300	7099	2434	1552	22786	22786	273	519	207	182	1.00	1.92	0.91
6+100	1300	4142	2607	1841	28205	28205	191	182	149	126	1.00	0.95	0.85
TBTXA740	1300	4904			283	363	151	257	180	329	1.29	1.74	1.81

OPTIMIZATION CRITERION: MAXIMUM DEFLECTION

STATION	LOAD (kPa)	EY1	EY2	EY3	EY4	EX4	EY5	EX5	EY6	EX6	R4	R5	R6
5+100	1300	6589	4070	2077	351	695	239	343	228	412	1.88	1.38	1.79
5+300	1300	6685	4388	2089	367	638	241	383	233	464	1.77	1.57	2.00
5+500	1300	6006	4401	2704	32202	32202	194	284	202	266	1.00	1.46	1.28
5+650	1300	6210	4263	3037	37571	37571	206	287	211	287	1.00	1.38	1.36
6+100	1300	6314	3552	2760	27883	27883	215	235	139	146	1.00	1.11	1.02
TBTXA740	1300	5964			376	594	173	255	152	267	1.62	1.42	1.76

OPTIMIZATION CRITERION: RMS VALUE OF DEFLECTION

STATION	LOAD (kPa)	EY1	EY2	EY3	EY4	EX4	EY5	EX5	EY6	EX6	R4	R5	R6
5+100	1300	6589	4070	2077	364	705	239	337	228	412	1.88	1.36	1.79
5+300	1300	6685	4556	2089	360	620	241	375	234	465	1.77	1.54	2.00
5+500	1300	6167	4228	2536	33184	33184	209	303	191	230	1.00	1.45	1.19
5+650	1300	6837	4339	2842	35323	35323	235	339	182	220	1.00	1.45	1.27
6+100	1300	6244	3388	3118	29169	29169	206	274	158	173	1.00	1.37	1.03
TBTXA740	1300	5368			280	447	197	352	167	266	1.70	1.77	1.62

ANSYS FEM ANALYSIS: X-ANISOTROPIC MODEL.

THUNDER BAY : RUNWAY 12-30: SUMMARY OF MODULI VALUES

OPTIMIZATION CRITERION: "AREA" OF DEFLECTION BASIN

STATION	LOAD (kPa)	EY1	EY2	EY3	EY4	EX4	EY5	EX5	EY6	EX6	R4	R5	R6
5+100	1500	7730	4703	3224	386	1056	288	389	206	475	2.74	1.35	2.31
5+300	1500	7500	5897	3966	411	1028	296	402	222	518	2.57	1.36	2.34
5+500	1500	3039	3645	1388	36389	36389	234	540	102	70	1.00	2.32	0.69
5+650	1500	5092	4229	1025	34097	34097	174	372	132	105	1.00	2.09	0.82
6+100	1500	3434	3276	1466	35196	35196	150	208	101	120	1.00	1.39	1.20
TBTXA740	1500												

OPTIMIZATION CRITERION: MAXIMUM DEFLECTION

STATION	LOAD (kPa)	EY1	EY2	EY3	EY4	EX4	EY5	EX5	EY6	EX6	R4	R5	R6
5+100	1500	6589	4070	2077	351	695	239	343	228	412	1.88	1.38	1.79
5+300	1500	6685	4397	2089	367	637	241	387	233	464	1.77	1.58	2.00
5+500	1500	4881	3697	2624	24779	24779	217	292	153	148	1.00	1.31	0.93
5+650	1500	6095	4153	3525	30724	30724	184	244	192	221	1.00	1.36	1.12
6+100	1500	6162	3662	2527	30273	30273	225	306	126	145	1.00	1.31	1.18
TBTXA740	1500												

OPTIMIZATION CRITERION: RMS VALUE OF DEFLECTION

STATION	LOAD (kPa)	EY1	EY2	EY3	EY4	EX4	EY5	EX5	EY6	EX6	R4	R5	R6
5+100	1500	6722	3919	2323	334	626	250	442	229	454	1.89	1.71	2.00
5+300	1500	6685	4617	2089	360	620	241	338	234	465	1.77	1.40	2.00
5+500	1500	5717	3104	2141	29498	29498	223	326	159	159	1.00	1.53	1.00
5+650	1500	5872	4528	2965	25227	25227	202	365	170	170	1.00	1.85	1.00
6+100	1500	6076	2817	2454	32226	32226	243	431	155	155	1.00	1.72	1.00
TBTXA740	1500												

APPENDIX 6-IV

SUMMARY OF MODULI FOR EACH SITE (CHARTS)

ANSYS FEM ANALYSIS

BRANDON: RWY. 08-26: PROFILE OF MODULI OF BOUND LAYERS

OPTIMIZING CRITERION: "AREA" OF DEFLECTION BASIN

(BOTH ISOTROPIC AND X-ANISOTROPIC CASES)

LOAD STEP 1: (600 kPa)

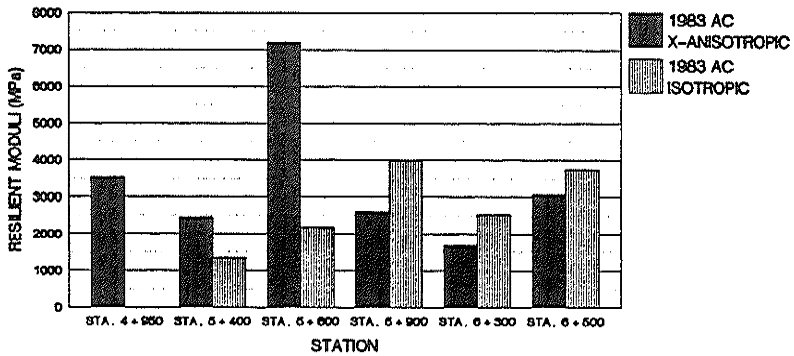

LOAD STEP 2: (800 kPa)

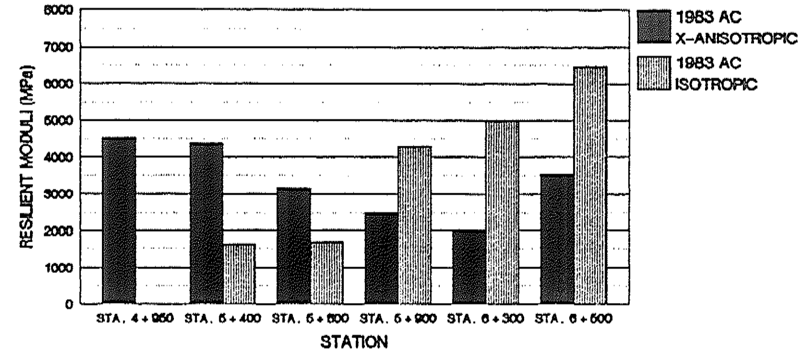

LOAD STEP 3: (1200 kPa)

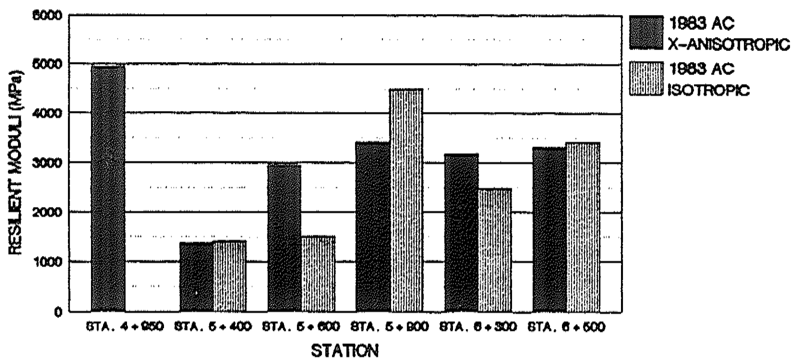

LOAD STEP 4: (1400 kPa)

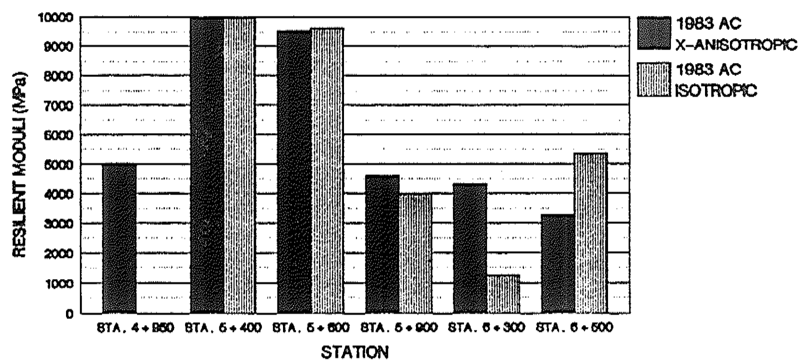

ANSYS FEM ANALYSIS

BRANDON: RWY . 08-26: PROFILE OF MODULI OF BOUND LAYERS

OPTIMIZING CRITERION: MAXIMUM DEFLECTION

(BOTH ISOTROPIC AND X-ANISOTROPIC CASES)

LOAD STEP 1: (600 kPa)

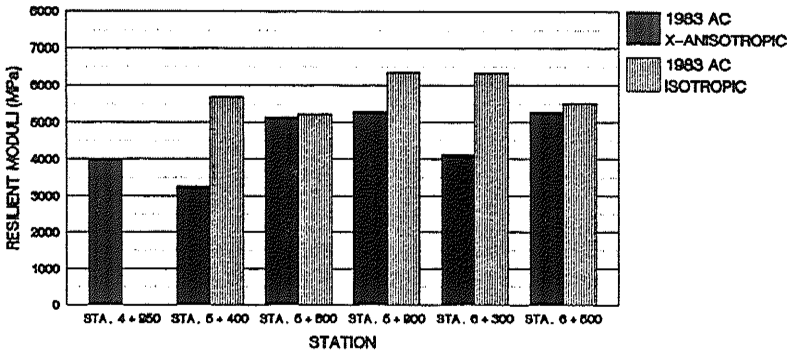

LOAD STEP 2: (800 kPa)

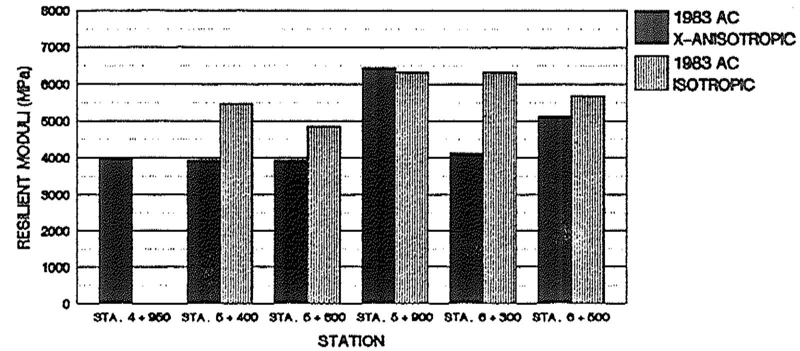

LOAD STEP 3: (1200 kPa)

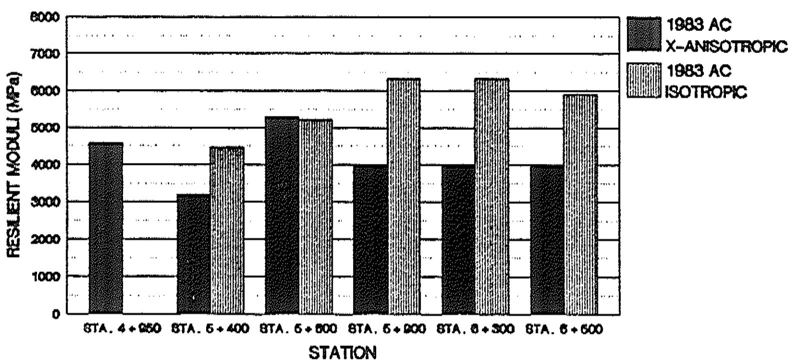

LOAD STEP 4: (1400 kPa)

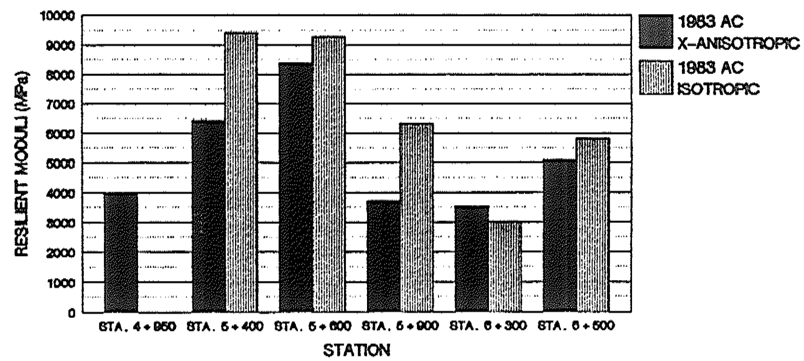

ANSYS FEM ANALYSIS

BRANDON: RWY. 08-26: PROFILE OF MODULI OF BOUND LAYERS

OPTIMIZING CRITERION: RMS VALUE OF DEFLECTIONS

(BOTH ISOTROPIC AND X-ANISOTROPIC CASES)

LOAD STEP 1: (600 kPa)

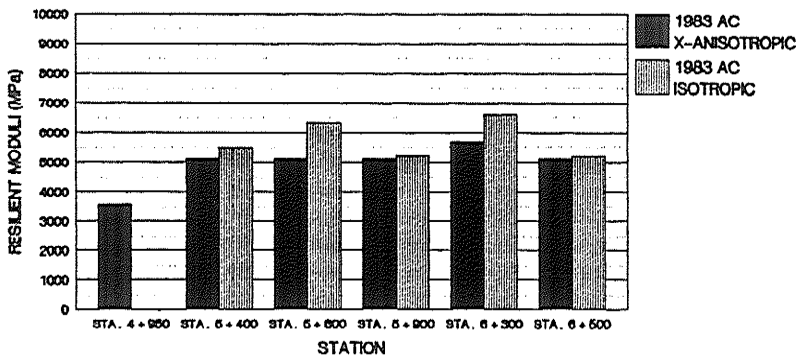

LOAD STEP 2: (800 kPa)

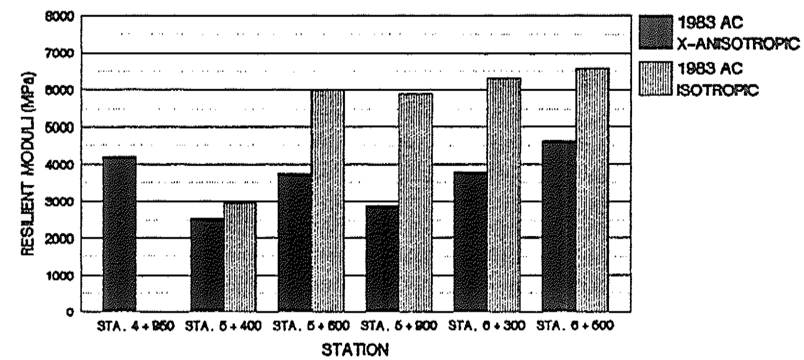

LOAD STEP 3: (1200 kPa)

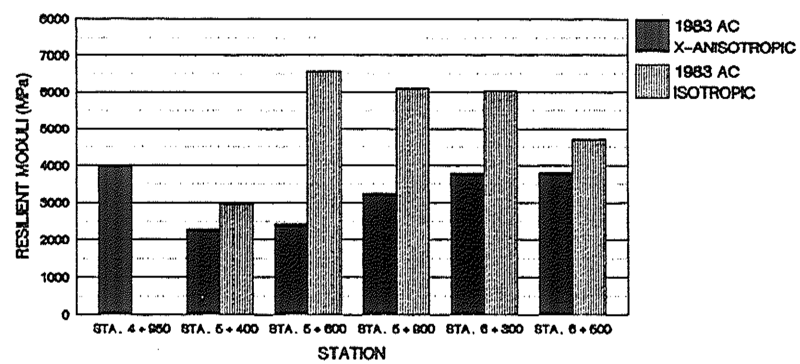

LOAD STEP 4: (1400 kPa)

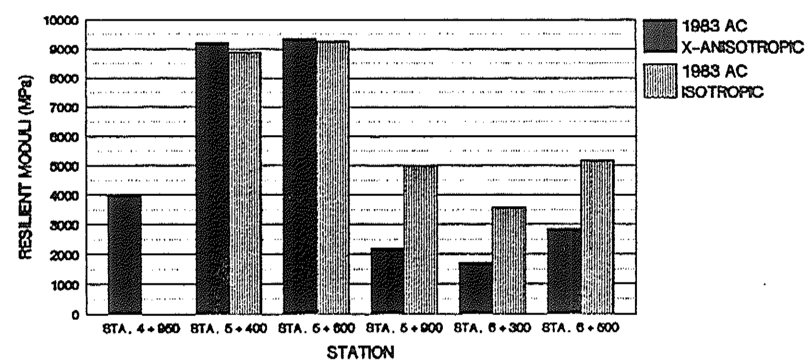

ANSYS FEM ANALYSIS

BRANDON: RWY. 08-26: PROFILE OF MODULI OF UNBOUND LAYERS

OPTIMIZING CRITERION: "AREA" OF DEFLECTION BASIN

(BOTH ISOTROPIC AND X-ANISOTROPIC CASES)

LOAD STEP 1: (600 kPa)

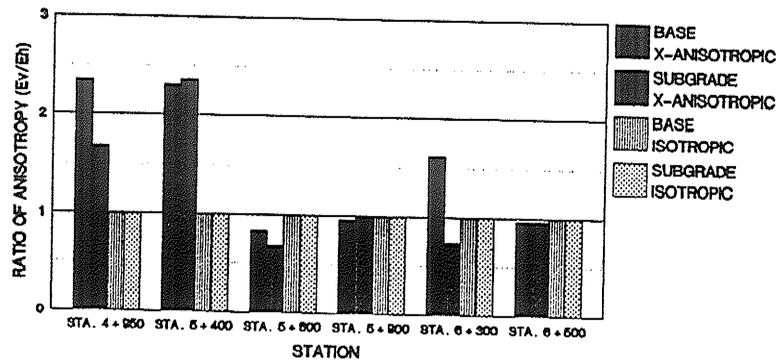

LOAD STEP 2: (800 kPa)

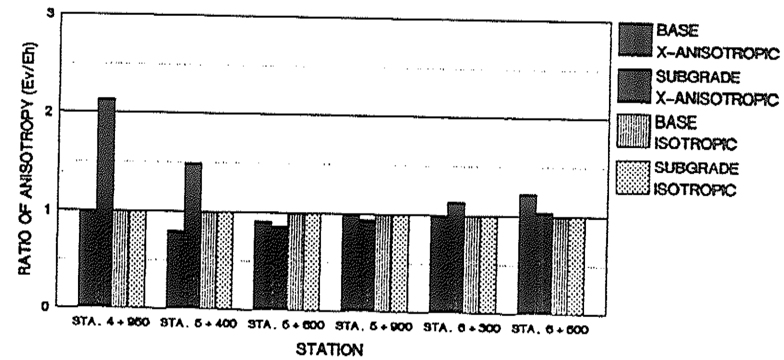

LOAD STEP 3: (1200 kPa)

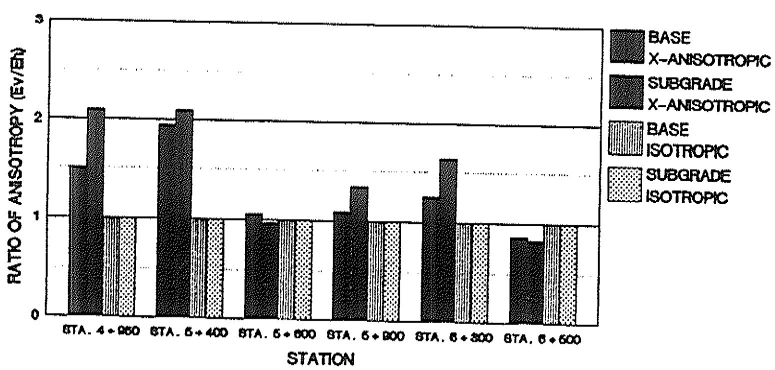

LOAD STEP 4: (1400 kPa)

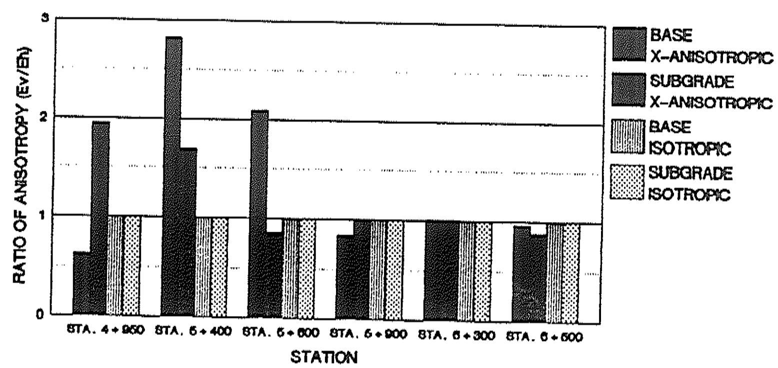

ANSYS FEM ANALYSIS

BRANDON: RWY . 08-26: PROFILE OF MODULI OF UNBOUND LAYERS

OPTIMIZING CRITERION: MAXIMUM DEFLECTION

(BOTH ISOTROPIC AND X-ANISOTROPIC CASES)

LOAD STEP 1: (600 kPa)

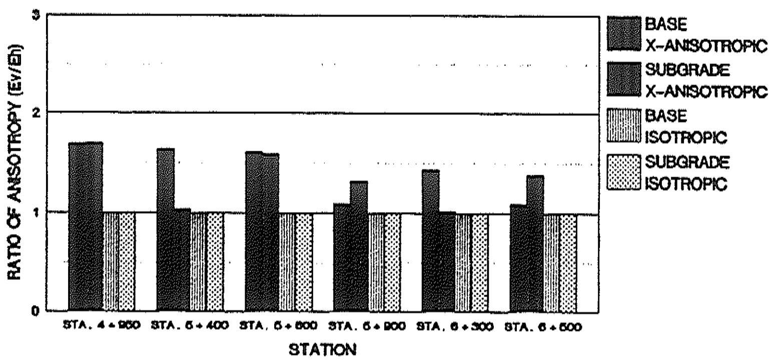

LOAD STEP 2: (800 kPa)

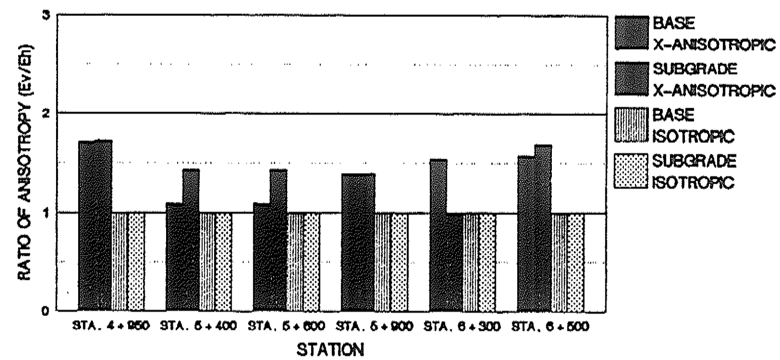

LOAD STEP 3: (1200 kPa)

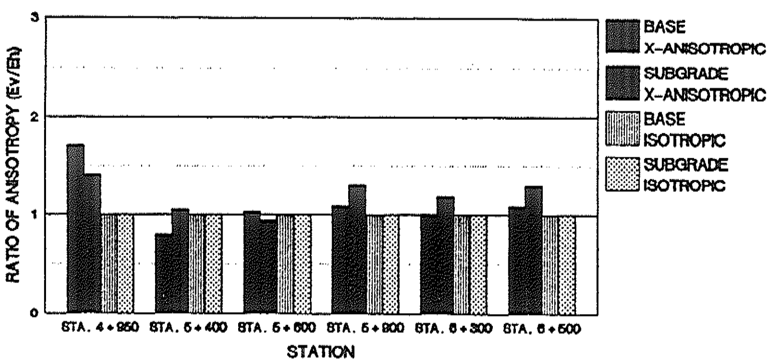

LOAD STEP 4: (1400 kPa)

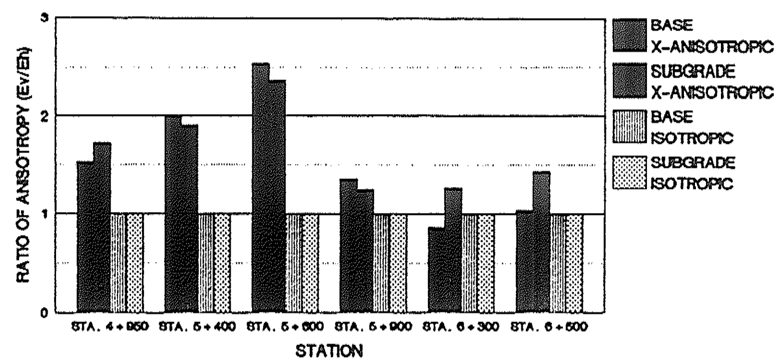

ANSYS FEM ANALYSIS

BRANDON: RWY. 08–26: PROFILE OF MODULI OF UNBOUND LAYERS

OPTIMIZING CRITERION: RMS VALUE OF DEFLECTIONS

(BOTH ISOTROPIC AND X-ANISOTROPIC CASES)

LOAD STEP 1: (600 kPa)

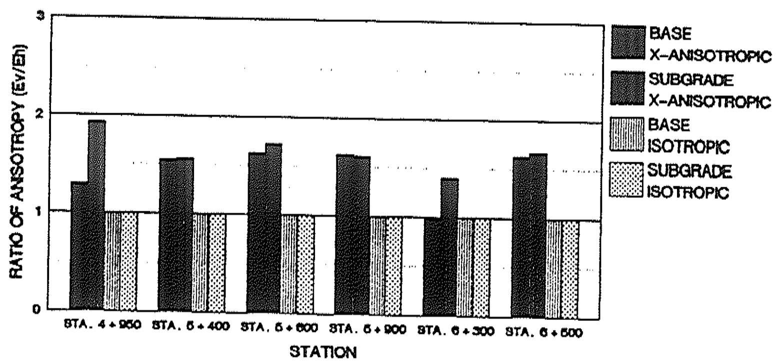

LOAD STEP 2: (800 kPa)

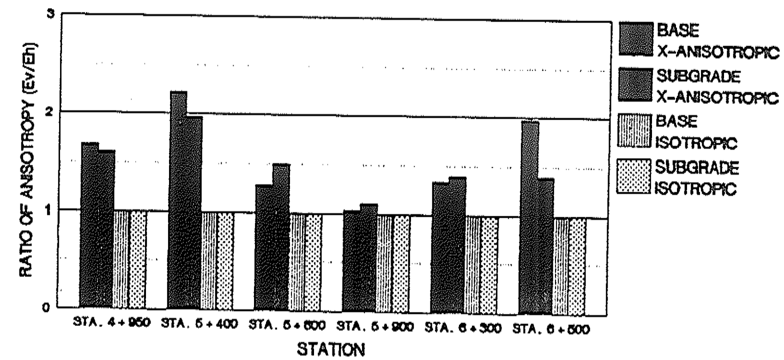

LOAD STEP 3: (1200 kPa)

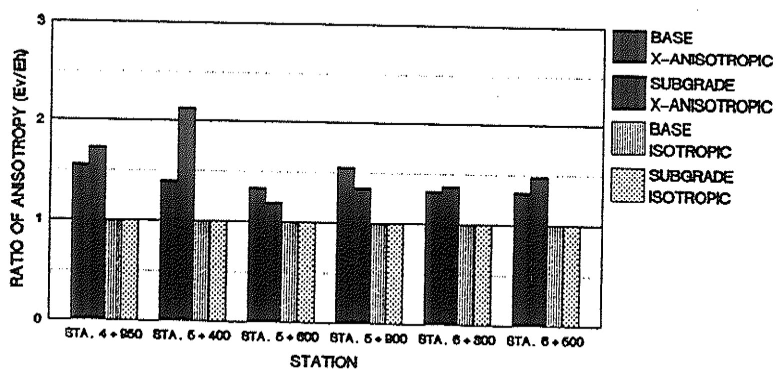

LOAD STEP 4: (1400 kPa)

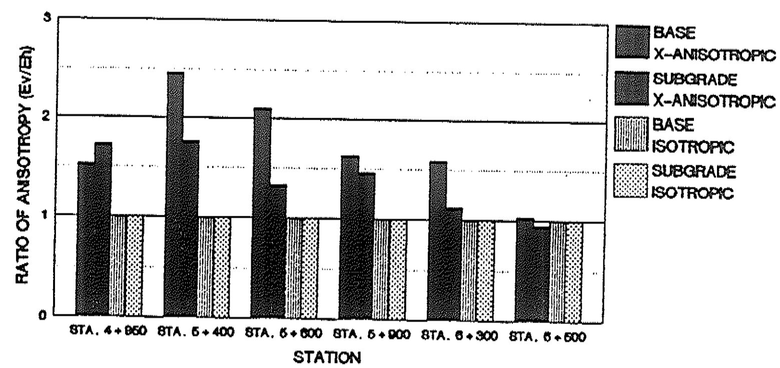

LOAD STEP 1: (500 kPa)

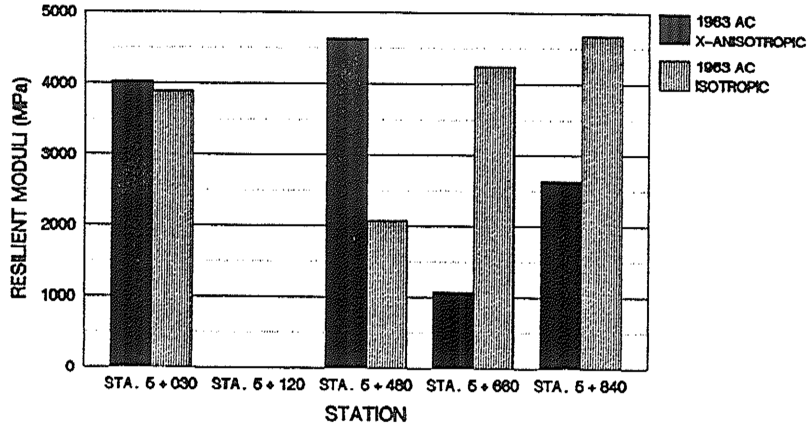

LOAD STEP 2: (750 kPa)

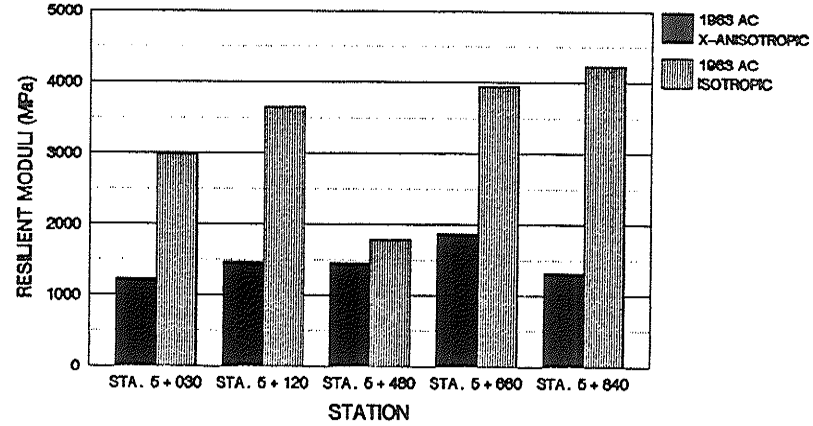

LOAD STEP 3: (1000 kPa)

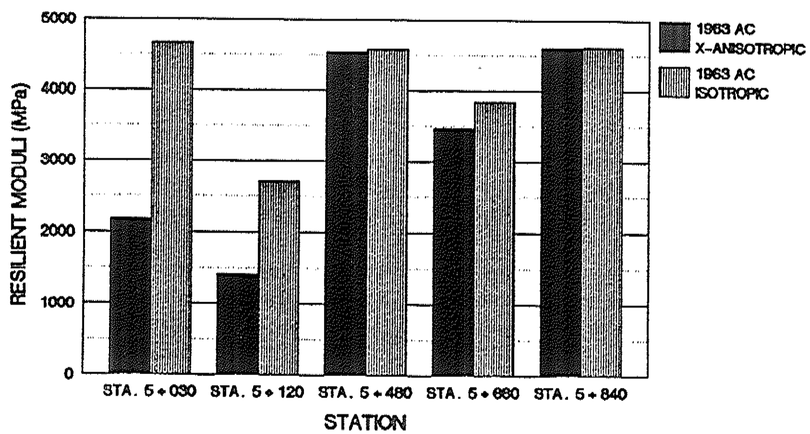

ANSYS FEM ANALYSIS

ST. ANDREWS RWY. 13-31: PROFILE OF MODULI OF BOUND MATERIALS

OPTIMIZING CRITERION: "AREA" OF BASIN

(BOTH ISOTROPIC AND X-ANISOTROPIC CASES)

LOAD STEP 1: (500 kPa)

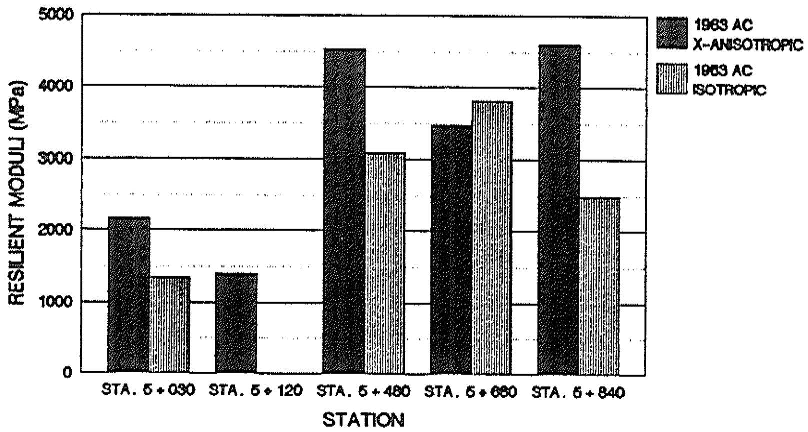

LOAD STEP 2: (750 kPa)

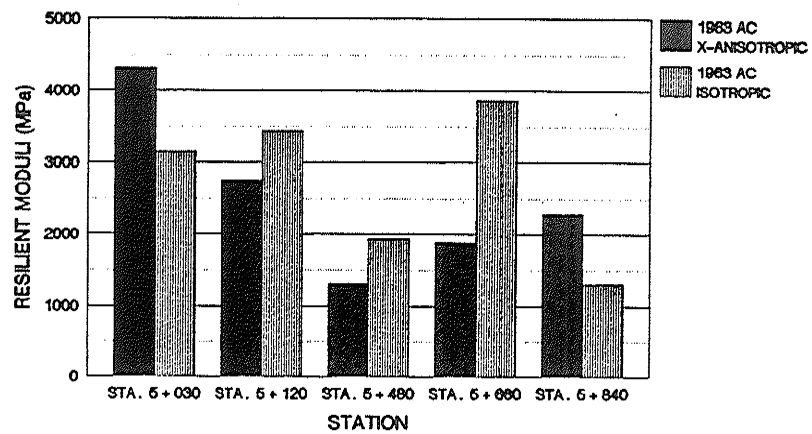

LOAD STEP 3: (1000 kPa)

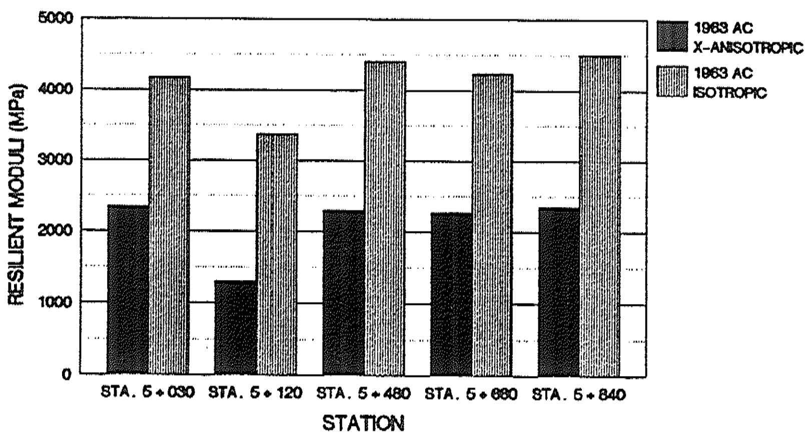

ANSYS FEM ANALYSIS

ST. ANDREWS RWY. 13-31: PROFILE OF MODULI OF BOUND MATERIALS

OPTIMIZING CRITERION: MAXIMUM DEFLECTION

(BOTH ISOTROPIC AND X-ANISOTROPIC MODELS)

LOAD STEP 1: (500 kPa)

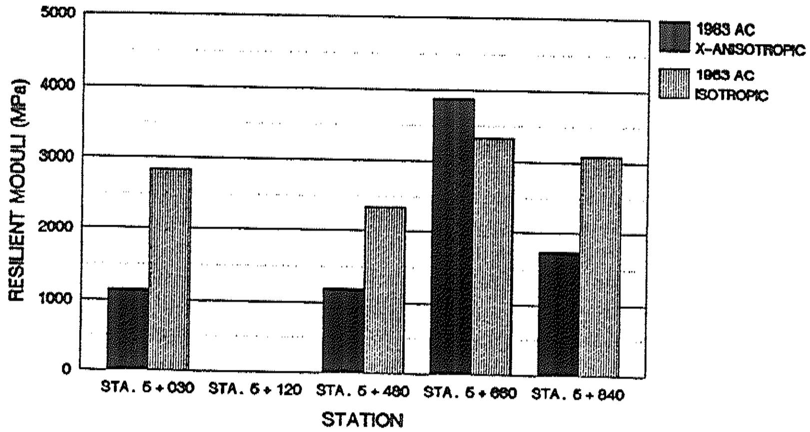

LOAD STEP 2: (750 kPa)

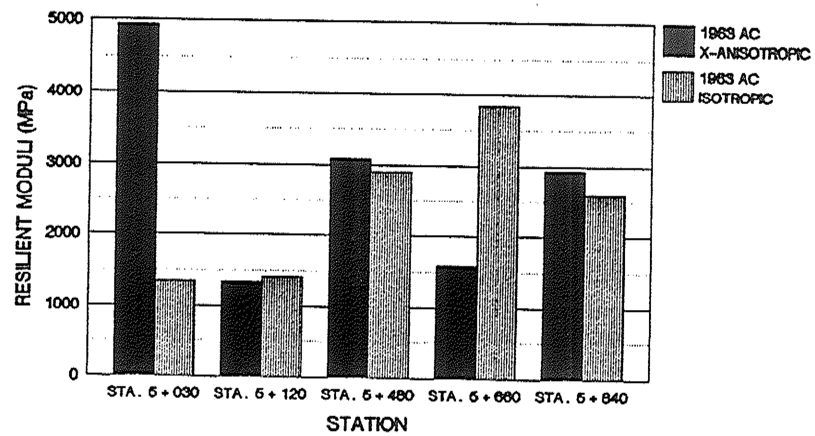

LOAD STEP 3: (1000 kPa)

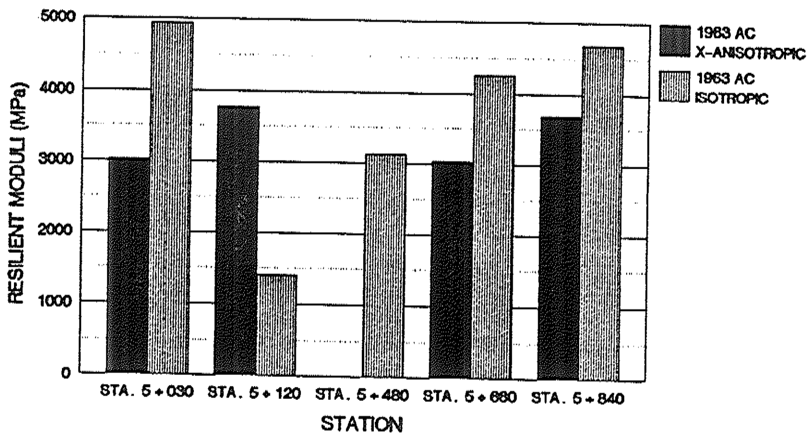

ANSYS FEM ANALYSIS

STANDREWS RWY. 13-31: PROFILE OF MODULI OF BOUND MATERIALS

OPTIMIZING CRITERION: RMS VALUE OF DEFLECTIONS

(BOTH ISOTROPIC AND X-ANISOTROPIC MODELS)

LOAD STEP 1: (500 kPa)

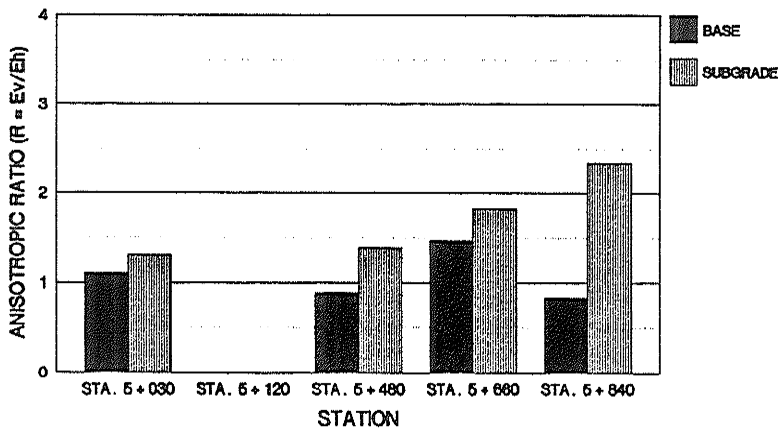

LOAD STEP 2: (750 kPa)

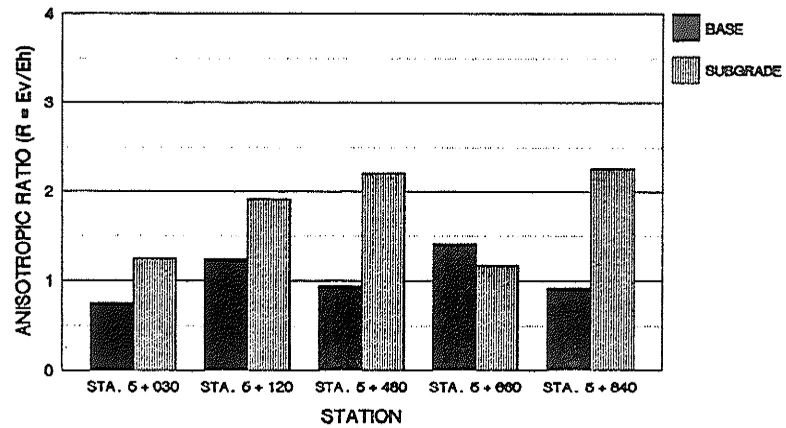

LOAD STEP 3: (1000 kPa)

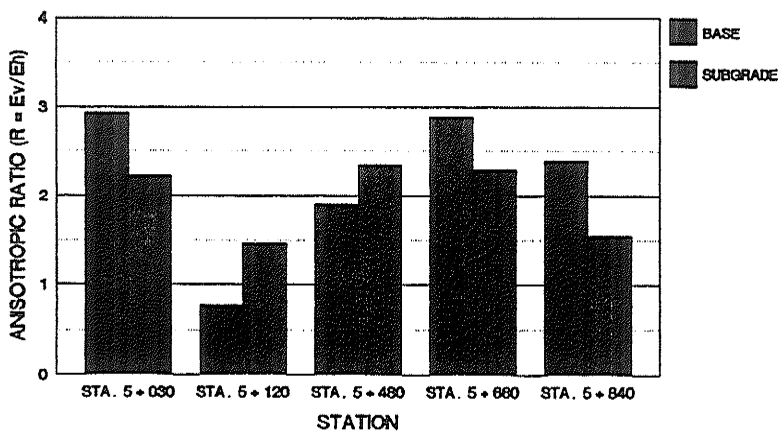

ANSYS FEM ANALYSIS

ST. ANDREWS RWY. 13–31: PROFILE OF MODULI OF UNBOUND MATERIALS

OPTIMIZING CRITERION: "AREA" OF BASIN

(BOTH ISOTROPIC AND X-ANISOTROPIC CASES)

LOAD STEP 1: (500 kPa)

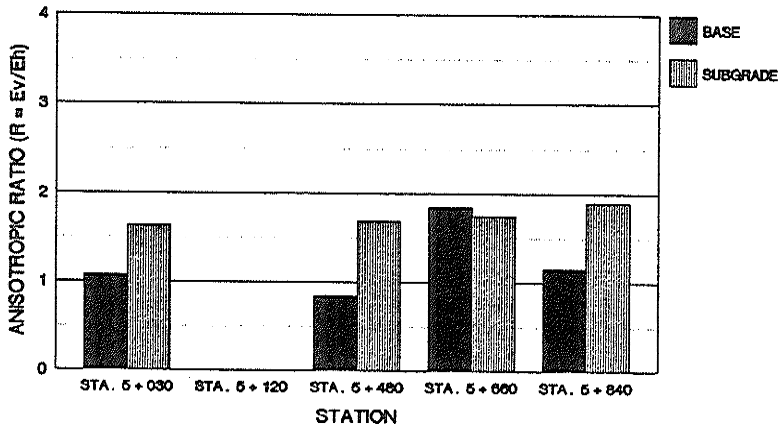

LOAD STEP 2: (750 kPa)

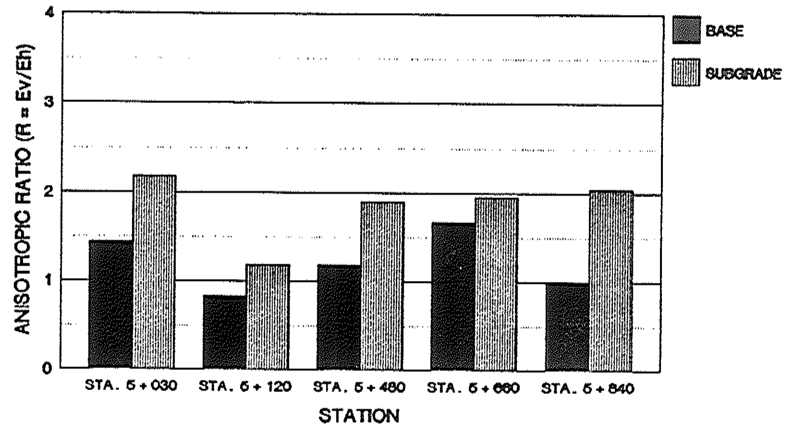

LOAD STEP 3: (1000 kPa)

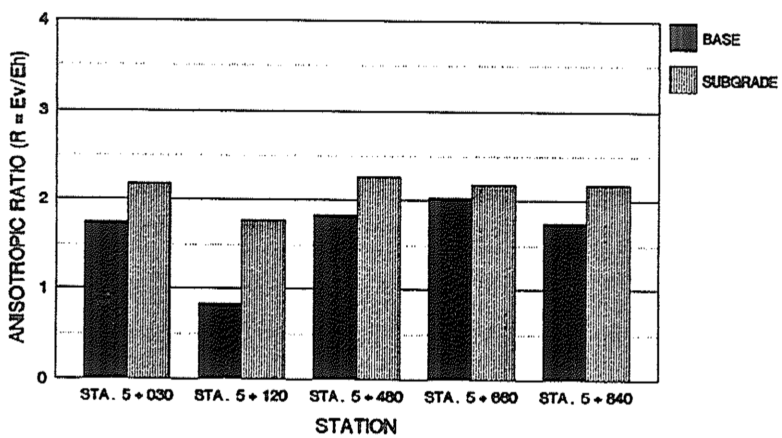

ANSYS FEM ANALYSIS

ST. ANDREWS RWY. 13-31: PROFILE OF MODULI OF UNBOUND MATERIALS

OPTIMIZING CRITERION: MAXIMUM DEFLECTION

(BOTH ISOTROPIC AND X-ANISOTROPIC MODELS)

LOAD STEP 1: (500 kPa)

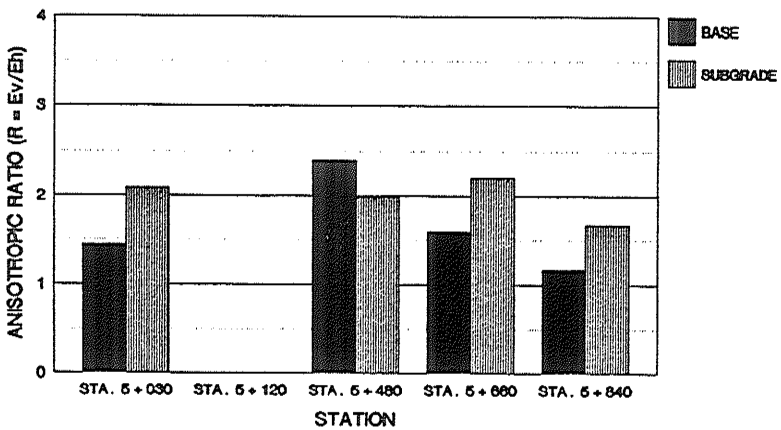

LOAD STEP 2: (750 kPa)

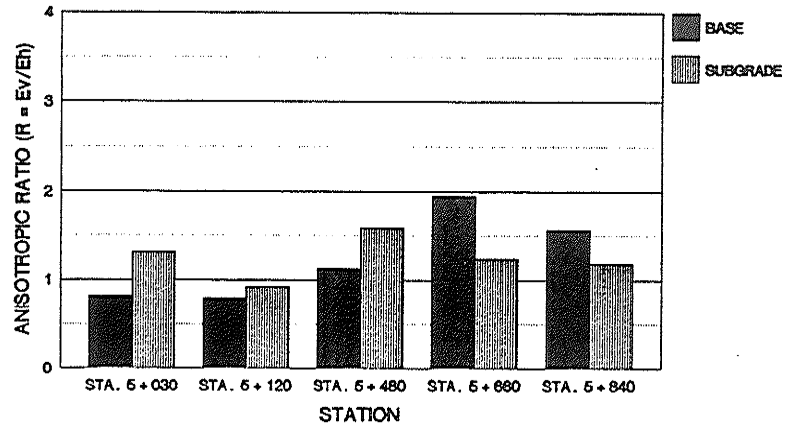

LOAD STEP 3: (1000 kPa)

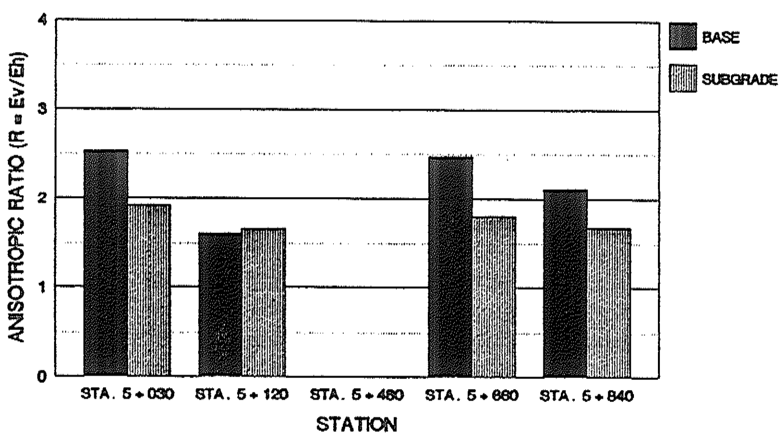

ANSYS FEM ANALYSIS

STANDREWS RWY. 13-31: PROFILE OF MODULI OF UNBOUND MATERIALS

OPTIMIZING CRITERION: RMS VALUE OF DEFLECTIONS

(BOTH ISOTROPIC AND X-ANISOTROPIC MODELS)

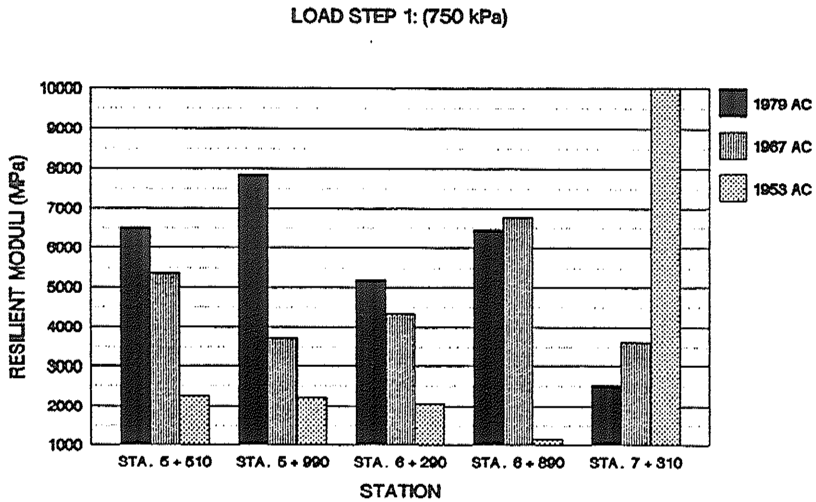

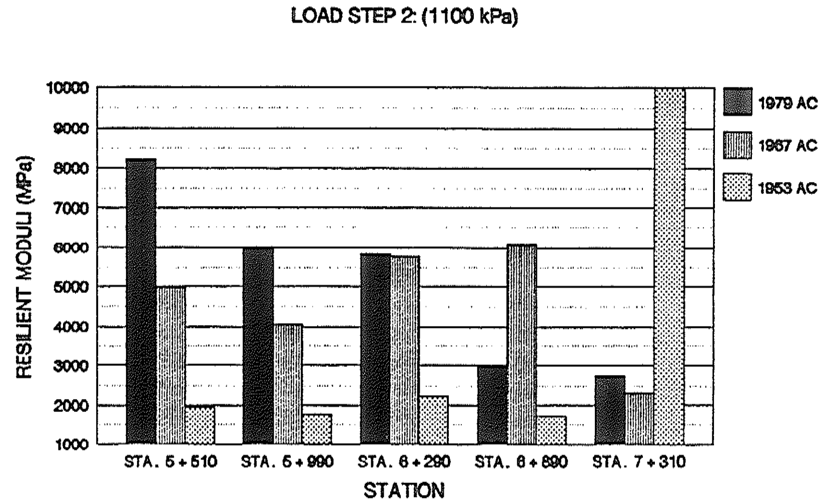

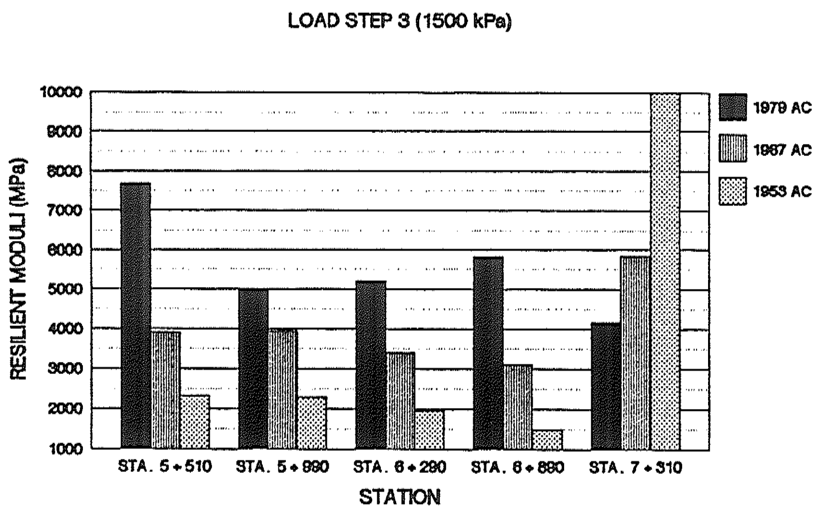

ANSYS FEM ANALYSIS: ISOTROPIC MODEL

REGINA RWY. 12-30: PROFILE OF AC MODULI

OPTIMIZING CRITERION: "AREA" OF BASIN

LOAD STEP 1: (750 kPa)

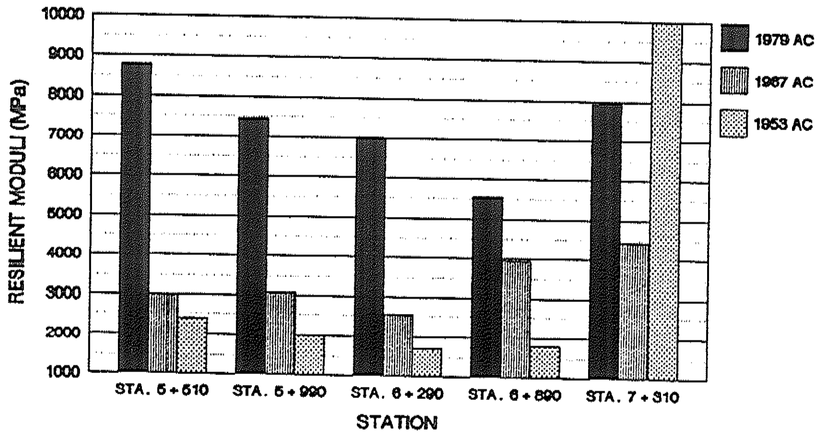

LOAD STEP 2: (1100 kPa)

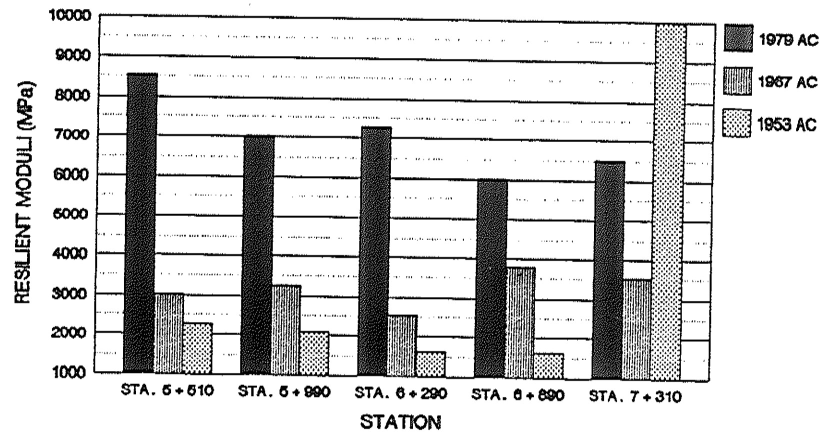

LOAD STEP 3: (1500 kPa)

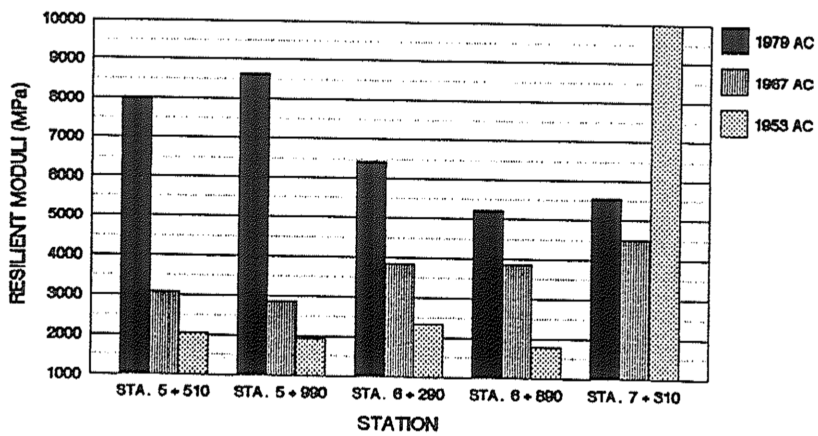

ANSYS FEM ANALYSIS: ISOTROPIC MODEL

REGINA RWY. 12–30: PROFILE OF AC MODULI

OPTIMIZING CRITERION: MAXIMUM DEFLECTION

LOAD STEP 1: (750 kPa)

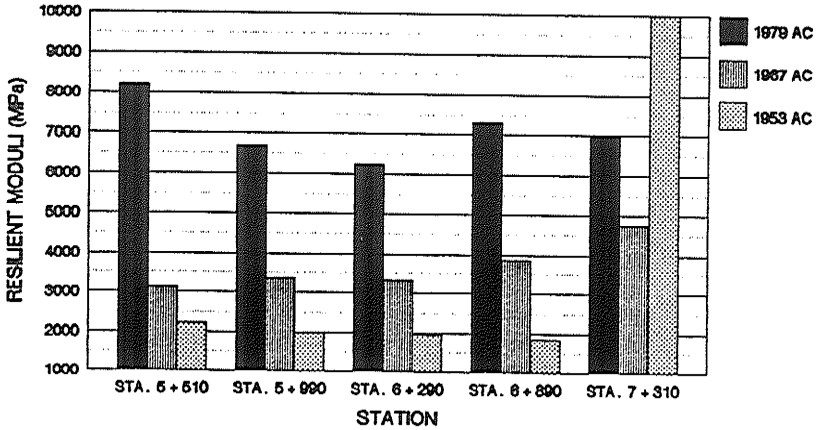

LOAD STEP 2: (1100 kPa)

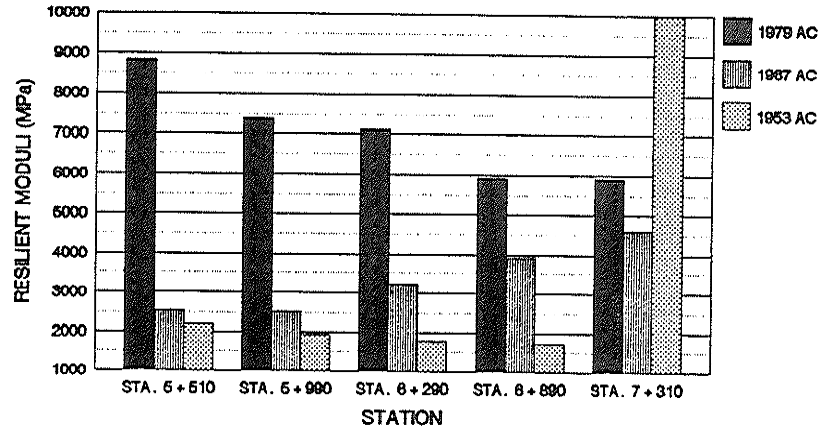

LOAD STEP 3: (1500 kPa)

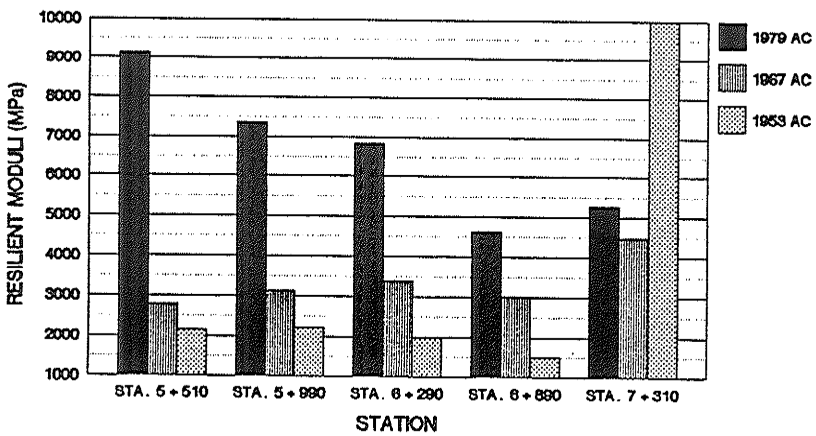

ANSYS FEM ANALYSIS: ISOTROPIC MODEL

REGINA RWY. 12-30: PROFILE OF AC MODULI

OPTIMIZING CRITERION: RMS VALUE OF DEFLECTIONS

LOAD STEP 1 (750 kPa)

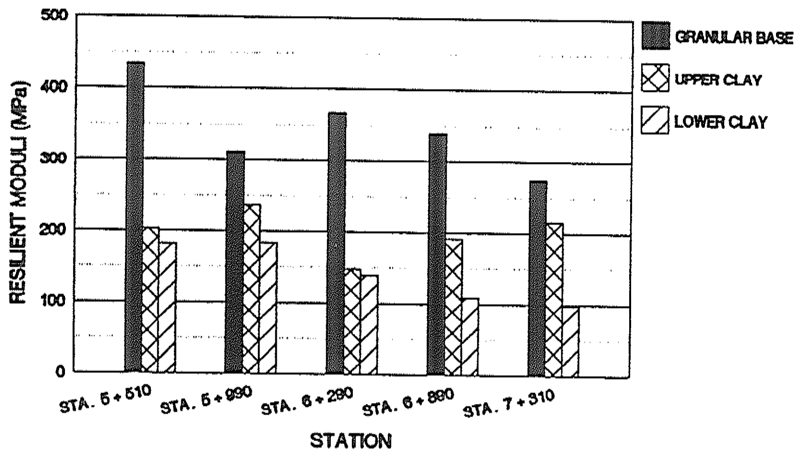

LOAD STEP 2 (1100 kPa)

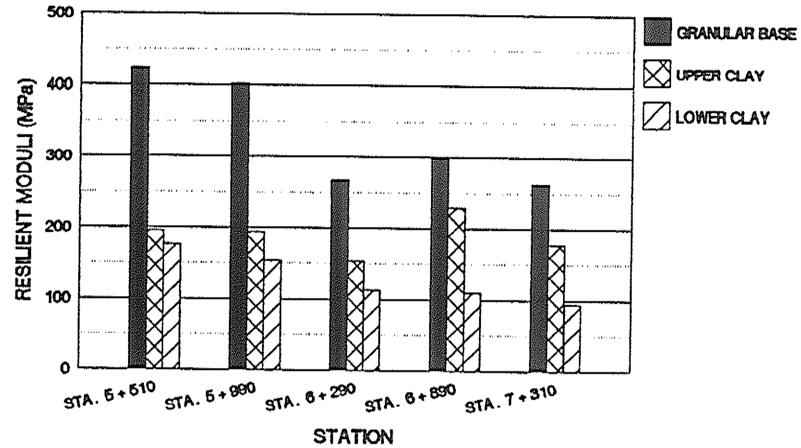

LOAD STEP 3 (1500 kPa)

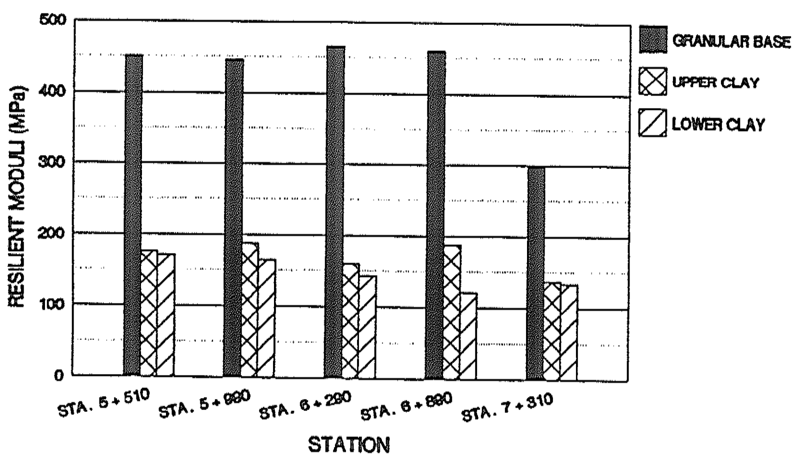

ANSYS FEM ANALYSIS: ISOTROPIC MODEL

REGINA RWY. 12–30: PROFILE OF MODULI OF UNBOUND LAYERS

OPTIMIZING CRITERION: "AREA" OF BASIN

LOAD STEP 1 (750 kPa)

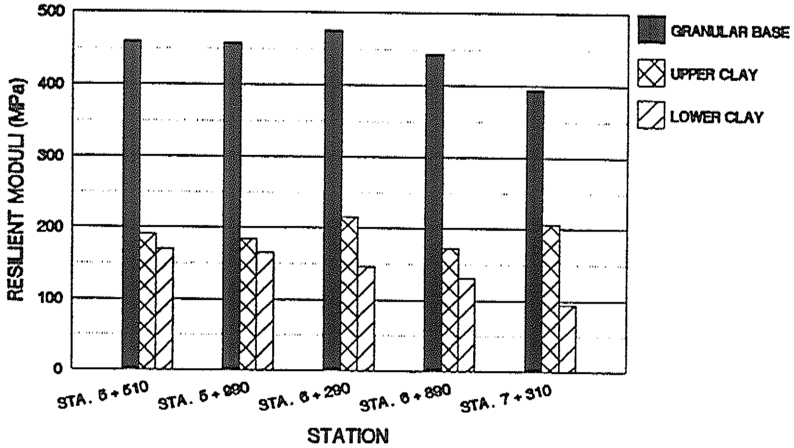

LOAD STEP 2 (1100 kPa)

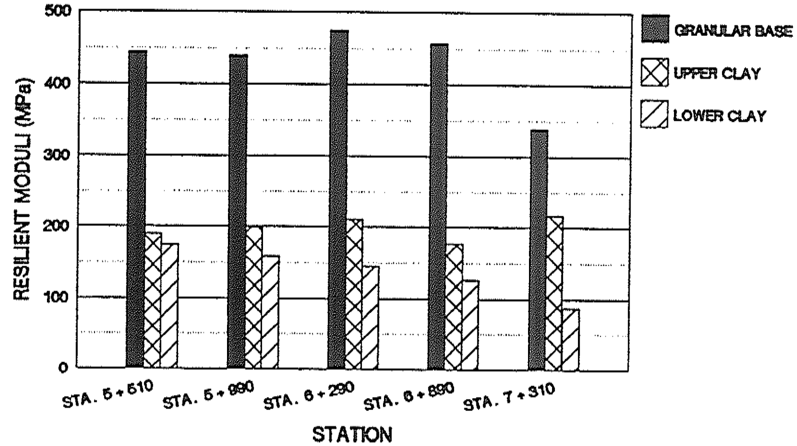

LOAD STEP 3 (1500 kPa)

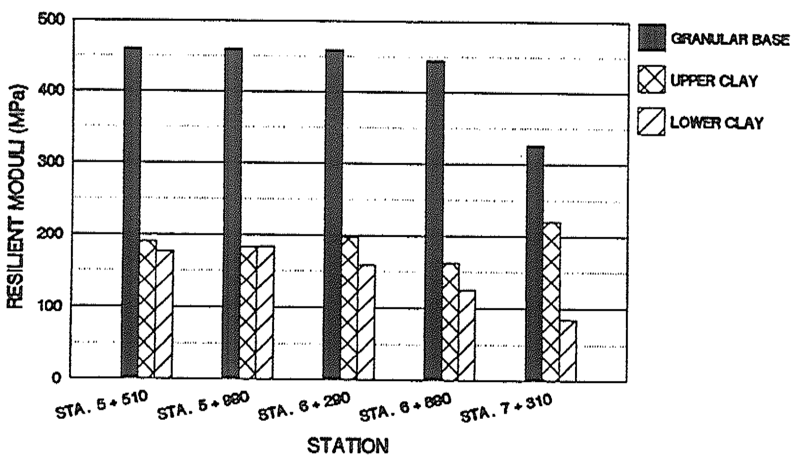

ANSYS FEM ANALYSIS: ISOTROPIC MODEL

REGINA RWY. 12–30: PROFILE OF MODULI OF UNBOUND LAYERS

OPTIMIZING CRITERION: MAXIMUM DEFLECTION

LOAD STEP 1 (750 kPa)

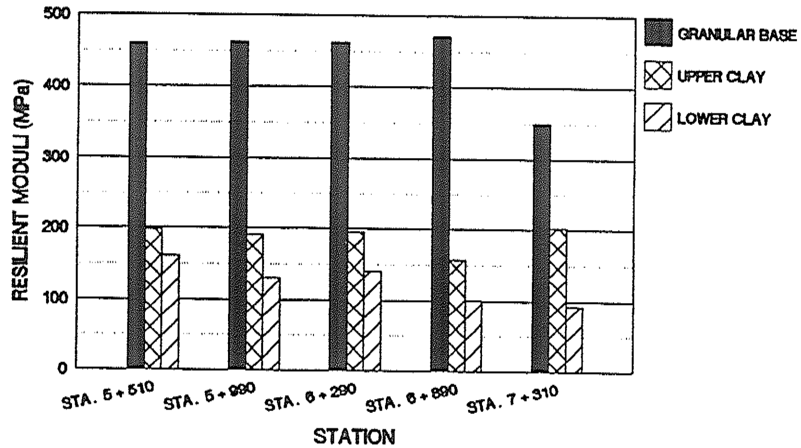

LOAD STEP 2 (1100 kPa)

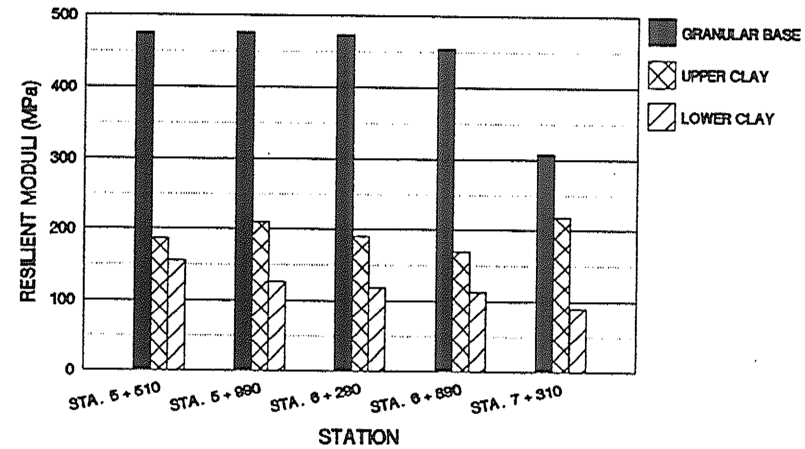

LOAD STEP 3 (1500 kPa)

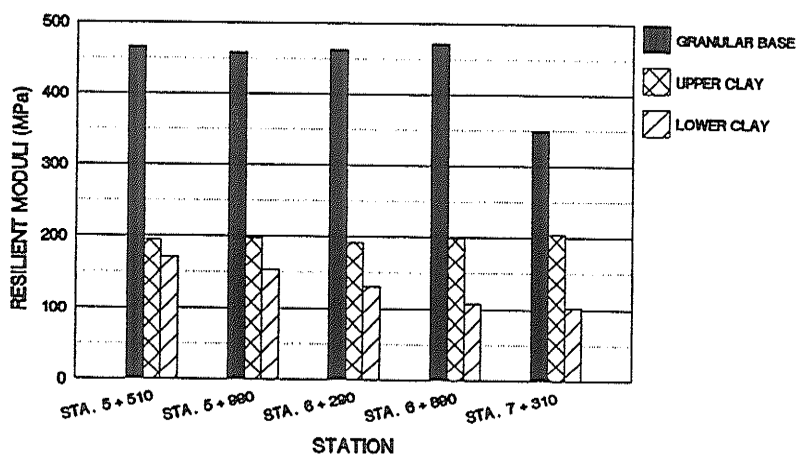

ANSYS FEM ANALYSIS: ISOTROPIC MODEL

REGINA RWY. 12-30: PROFILE OF MODULI OF UNBOUND LAYERS

OPTIMIZING CRITERION: RMS VALUE OF DEFLECTIONS

LOAD STEP 1: (750 kPa)

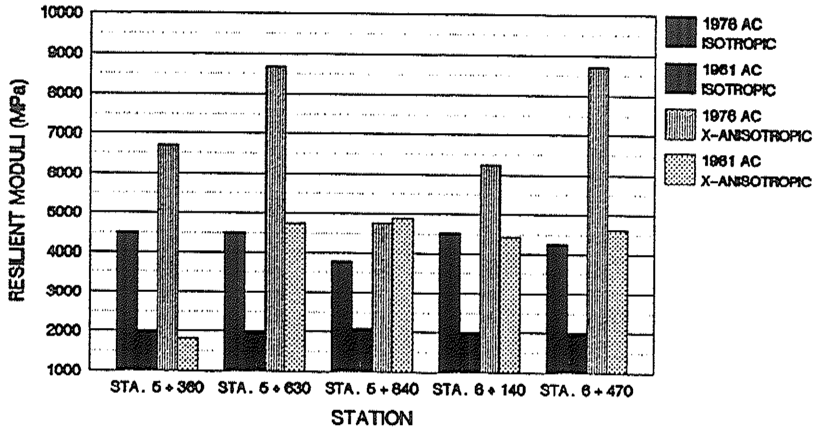

LOAD STEP 2: (1100 kPa)

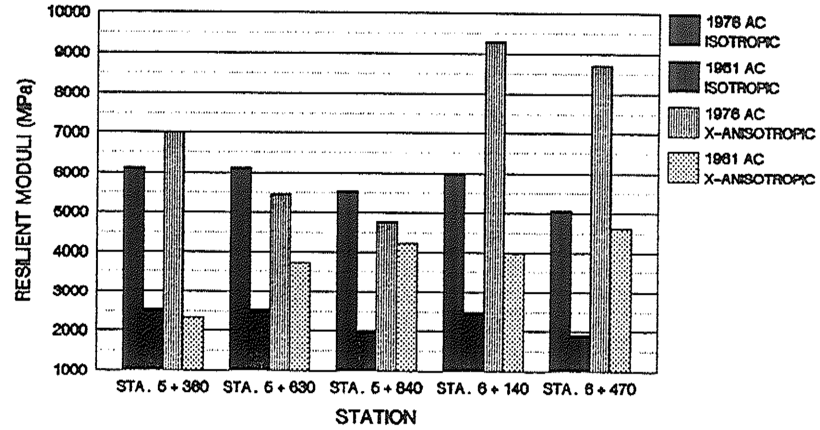

LOAD STEP 3: (1400 kPa)

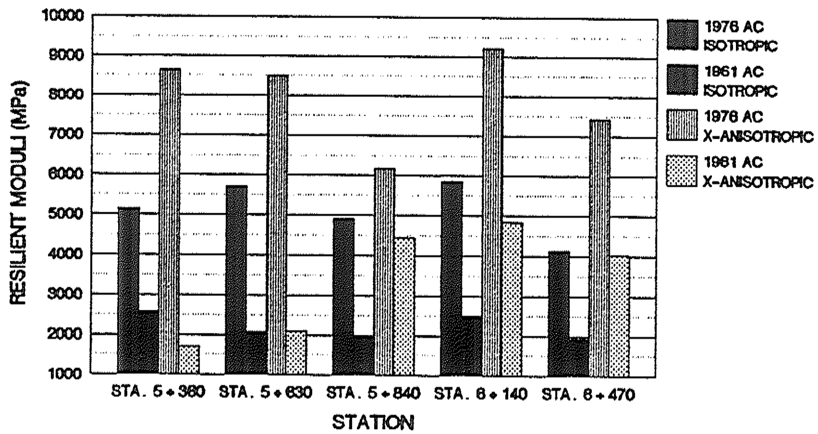

ANSYS FEM ANALYSIS

SASKATOON: RWY. 15-33: PROFILE OF MODULI OF BOUND LAYERS

OPTIMIZING CRITERION: "AREA" OF BASIN

(BOTH ISOTROPIC AND X-ANISOTROPIC CASES)

LOAD STEP 1: (750 kPa)

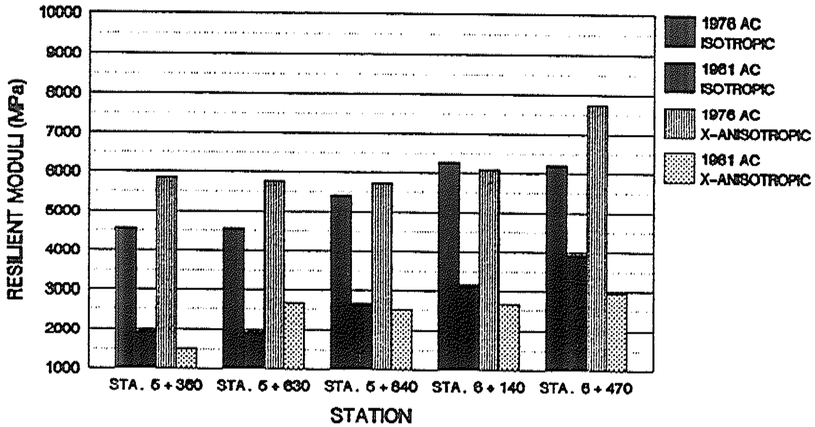

LOAD STEP 2: (1100 kPa)

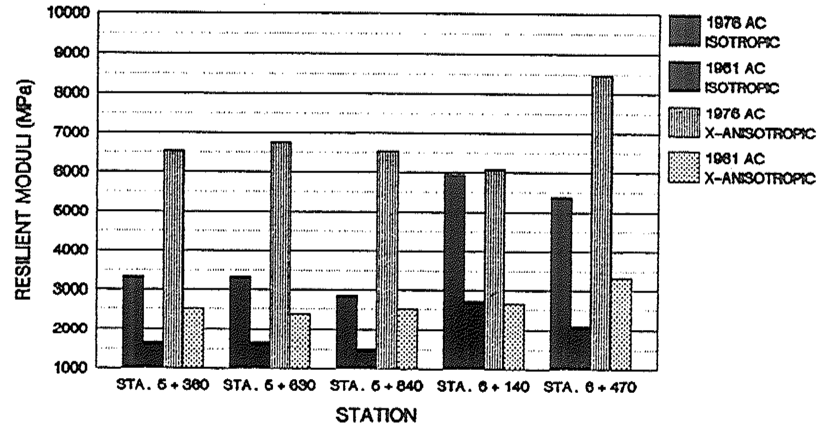

LOAD STEP 3: (1400 kPa)

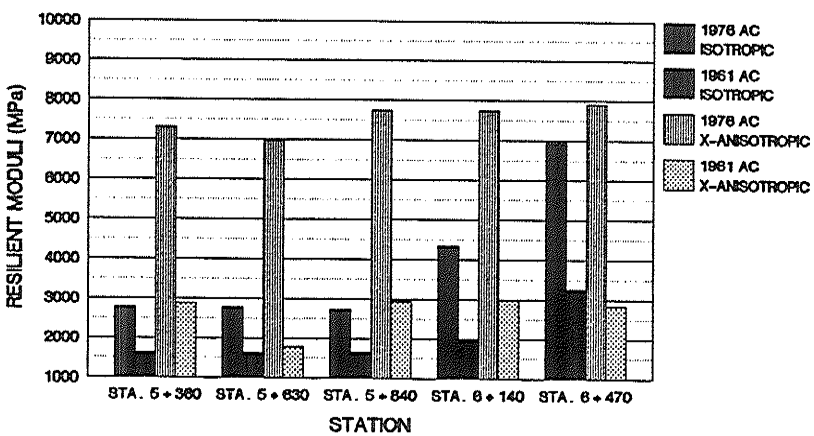

ANSYS FEM ANALYSIS

SASKATOON: RWY. 15-33: PROFILE OF MODULI OF BOUND LAYERS

OPTIMIZING CRITERION: MAXIMUM DEFLECTION

(BOTH ISOTROPIC AND X-ANISOTROPIC CASES)

LOAD STEP 1: (750 kPa)

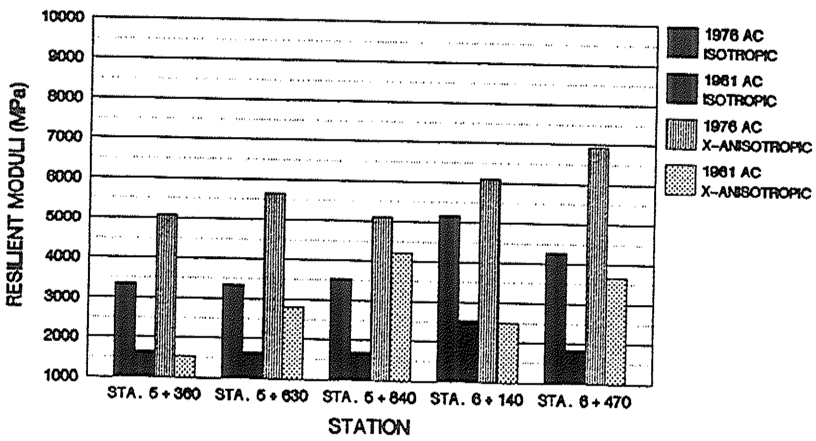

LOAD STEP 2: (1100 kPa)

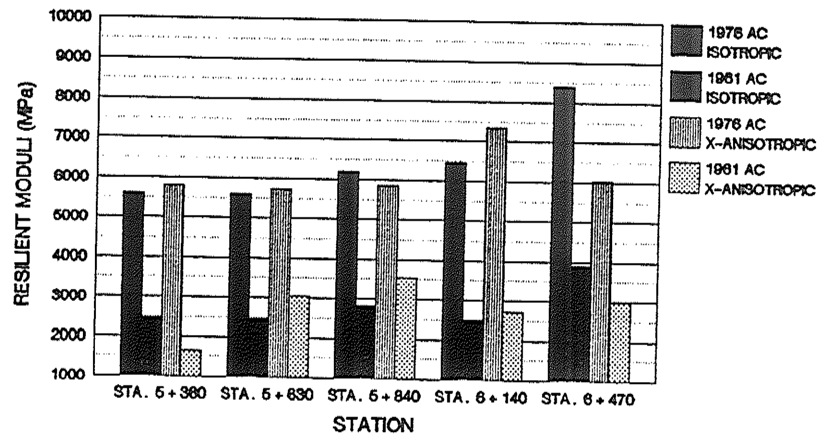

LOAD STEP 3: (1400 kPa)

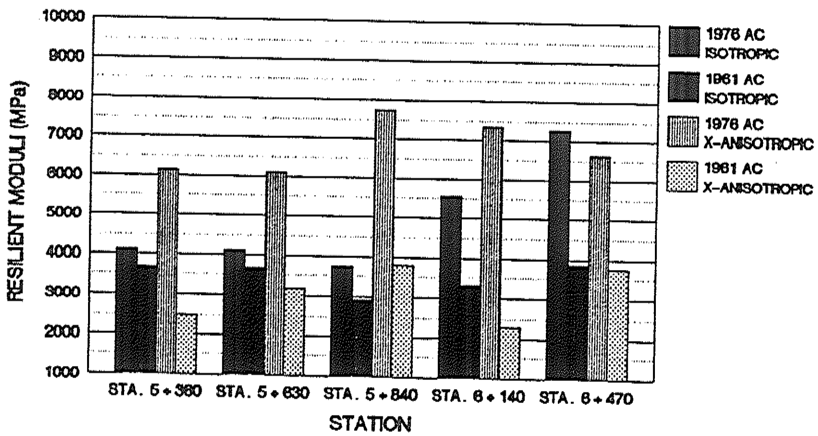

ANSYS FEM ANALYSIS

SASKATOON: RWY. 15-33: PROFILE OF MODULI OF BOUND LAYERS

OPTIMIZING CRITERION: RMS VALUE OF DEFLECTIONS

(BOTH ISOTROPIC AND X-ANISOTROPIC CASES)

LOAD STEP 1 (750 kPa)

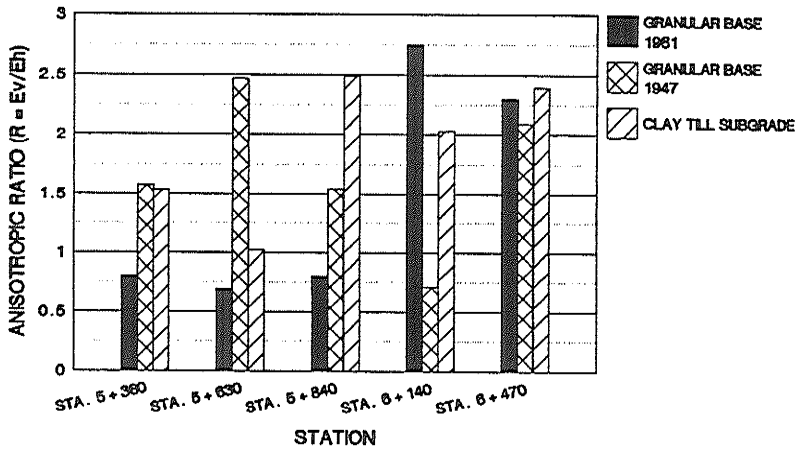

LOAD STEP 2 (1100 kPa)

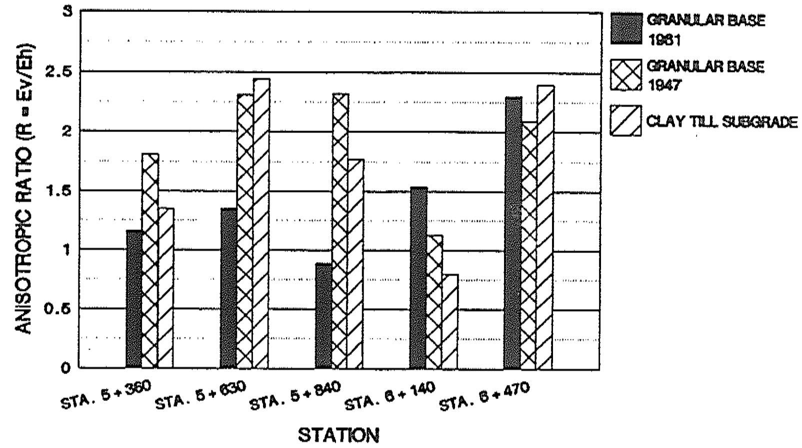

LOAD STEP 3 (1500 kPa)

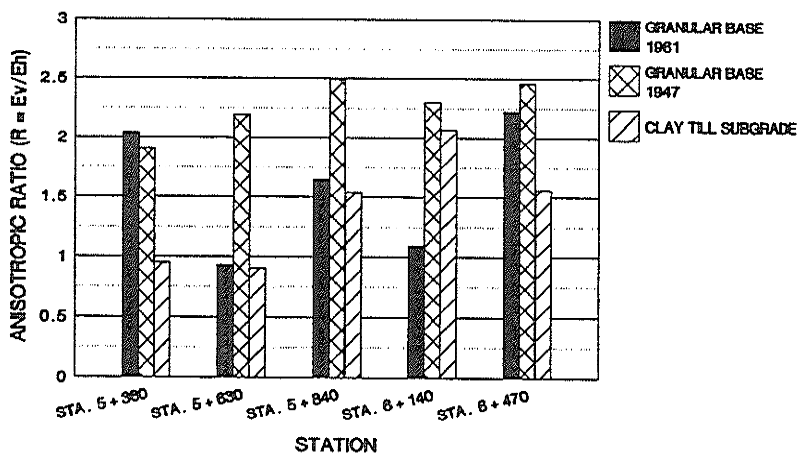

ANSYS FEM ANALYSIS

SASKATOON: RWY. 15-33: PROFILE OF MODULI OF UNBOUND LAYERS

OPTIMIZING CRITERION: "AREA" OF DEFLECTION BASIN

(BOTH ISOTROPIC AND X-ANISOTROPIC CASES)

LOAD STEP 1 (750 kPa)

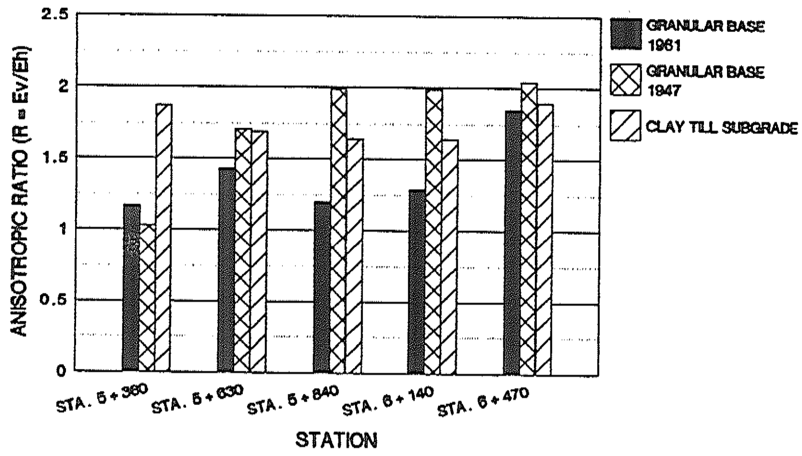

LOAD STEP 2 (1100 kPa)

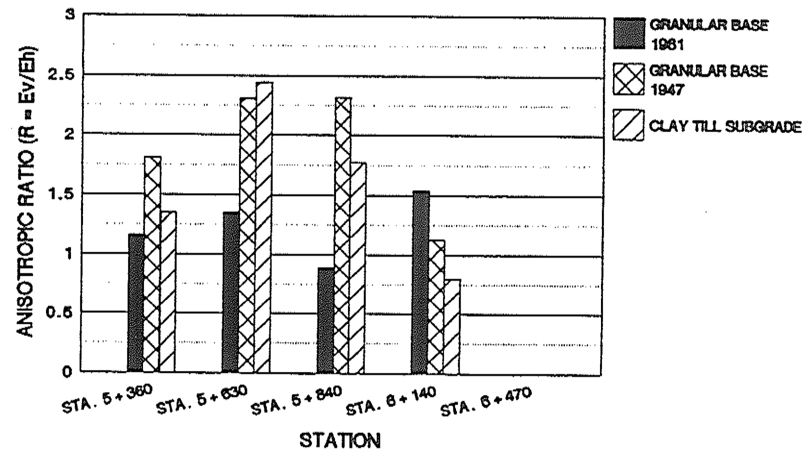

LOAD STEP 3 (1500 kPa)

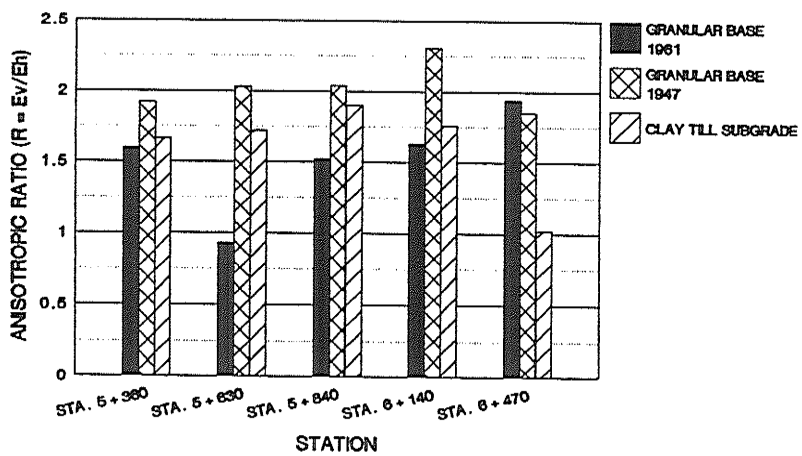

ANSYS FEM ANALYSIS

SASKATOON: RWY. 15-33: PROFILE OF MODULI OF UNBOUND LAYERS

OPTIMIZING CRITERION: MAXIMUM DEFLECTION

(BOTH ISOTROPIC AND X-ANISOTROPIC CASES)

LOAD STEP 1 (750 kPa)

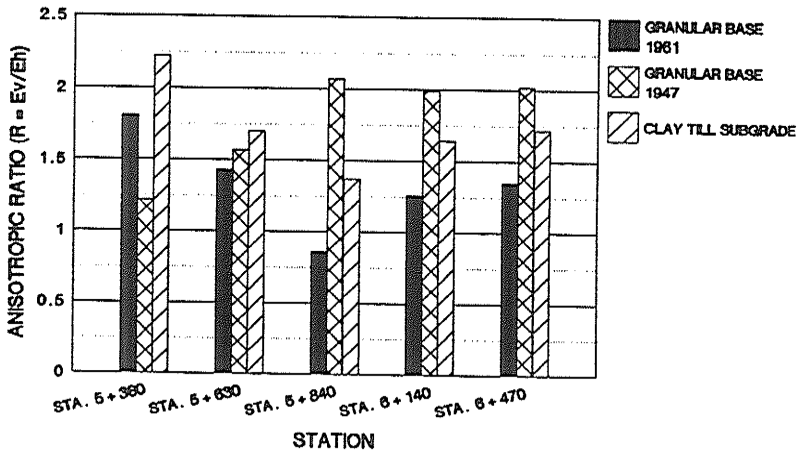

LOAD STEP 2 (1100 kPa)

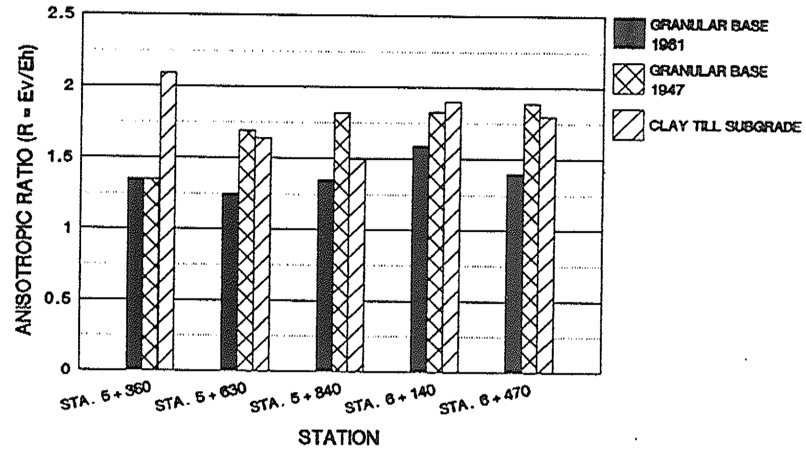

LOAD STEP 2 (1100 kPa)

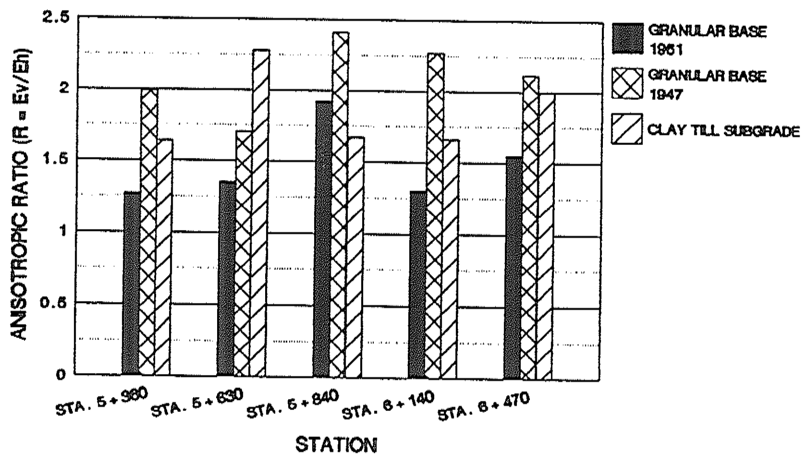

ANSYS FEM ANALYSIS

SASKATOON: RWY. 15-33: PROFILE OF MODULI OF UNBOUND LAYERS

OPTIMIZING CRITERION: RMS VALUE OF DEFLECTIONS

(BOTH ISOTROPIC AND X-ANISOTROPIC CASES)

ANSYS FEM ANALYSIS

THUNDER BAY: RWY. 12–30: PROFILE OF MODULI OF BOUND LAYERS

OPTIMIZING CRITERION: "AREA" OF DEFLECTION BASIN

(BOTH ISOTROPIC AND X-ANISOTROPIC CASES)

LOAD STEP 1: (750 kPa)

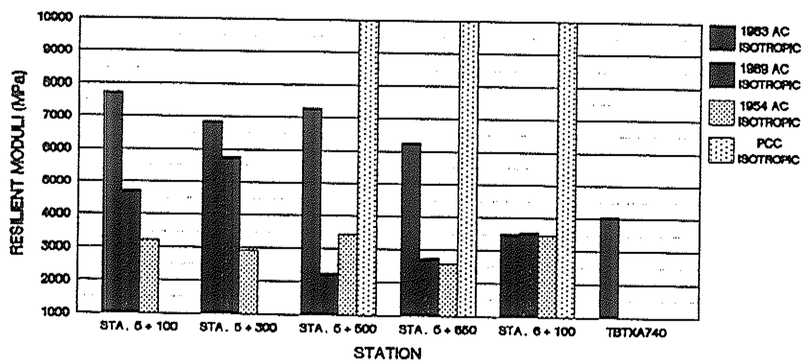

LOAD STEP 2: (1100 kPa)

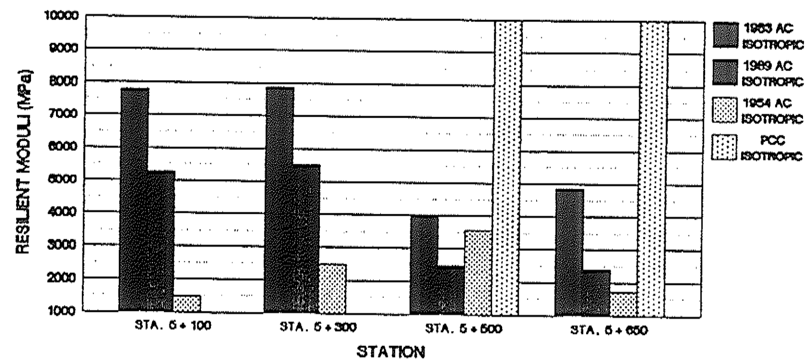

LOAD STEP 3: (1300 kPa)

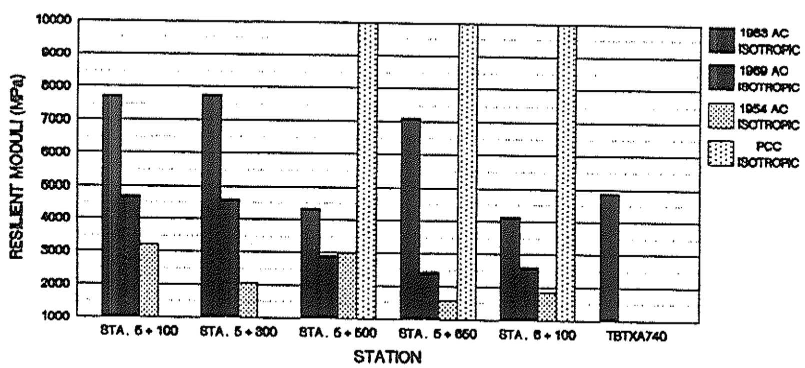

LOAD STEP 4: (1500 kPa)

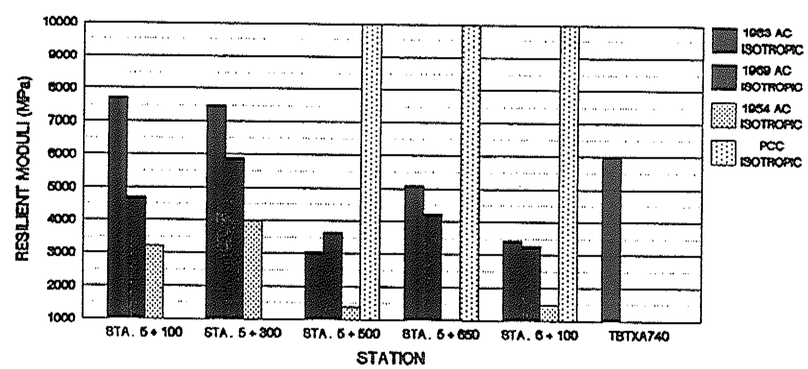

ANSYS FEM ANALYSIS

THUNDER BAY: RWY. 12-30: PROFILE OF MODULI OF BOUND LAYERS

OPTIMIZING CRITERION: MAXIMUM DEFLECTION

(BOTH ISOTROPIC AND X-ANISOTROPIC CASES)

LOAD STEP 1: (750 kPa)

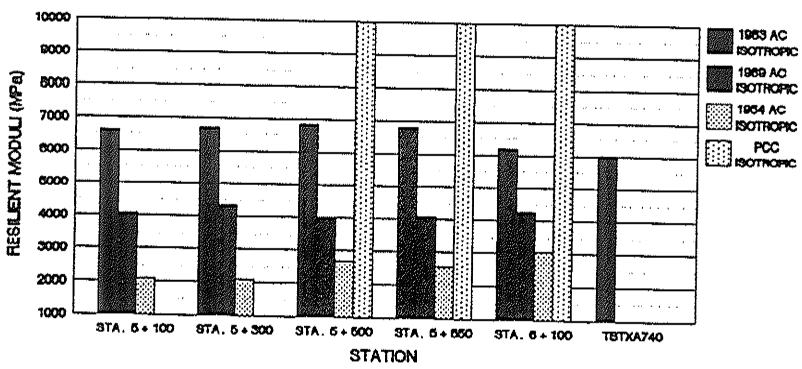

LOAD STEP 2: (1100 kPa)

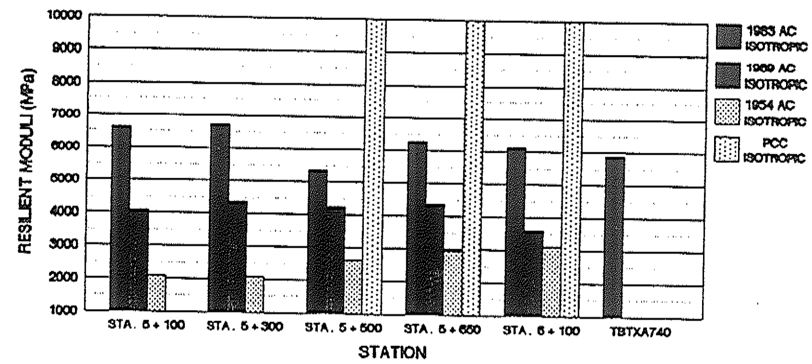

LOAD STEP 3: (1300 kPa)

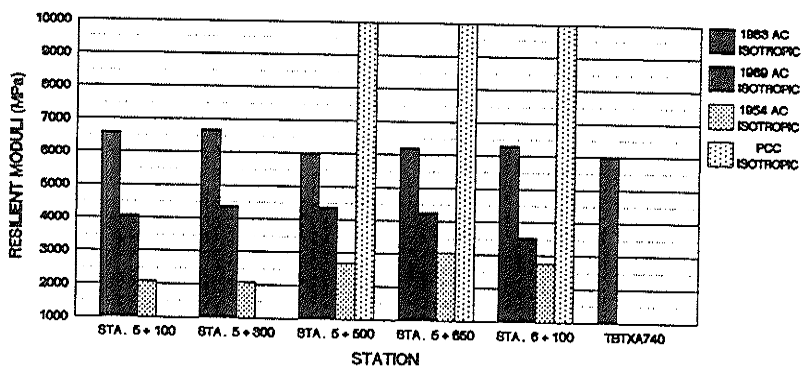

LOAD STEP 4: (1500 kPa)

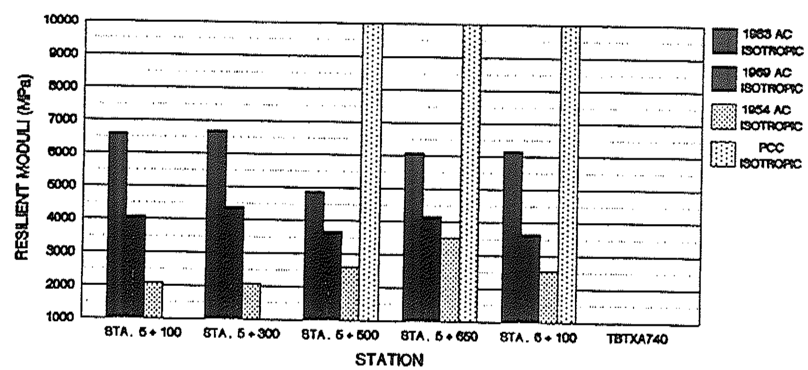

ANSYS FEM ANALYSIS

THUNDER BAY: RWY. 12-30: PROFILE OF MODULI OF BOUND LAYERS

OPTIMIZING CRITERION: RMS VALUE OF DEFLECTIONS

(BOTH ISOTROPIC AND X-ANISOTROPIC CASES)

LOAD STEP 1: (750 kPa)

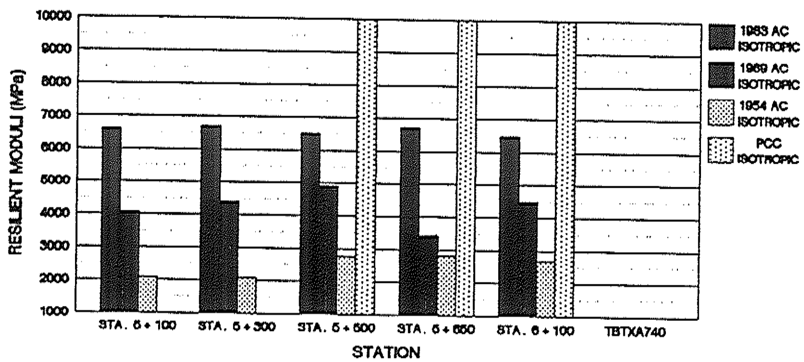

LOAD STEP 2: (1100 kPa)

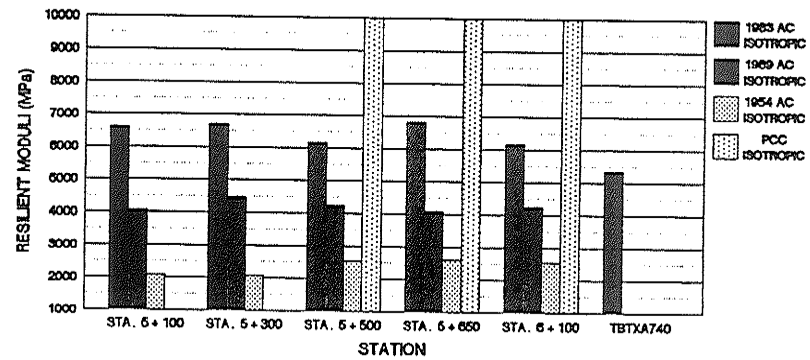

LOAD STEP 3: (1300 kPa)

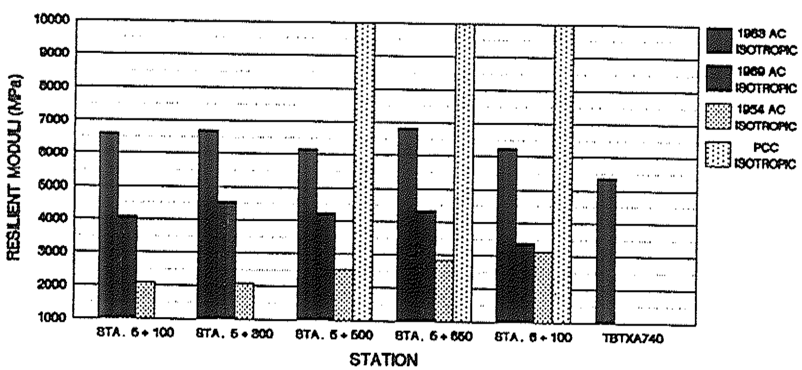

LOAD STEP 4: (1500 kPa)

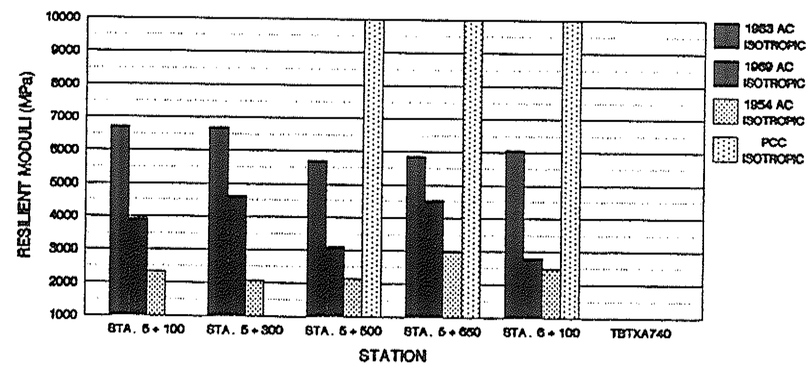

ANSYS FEM ANALYSIS

THUNDER BAY: RWY. 12-30: PROFILE OF MODULI OF UNBOUND LAYERS

OPTIMIZING CRITERION: "AREA" OF DEFLECTION BASIN

(BOTH ISOTROPIC AND X-ANISOTROPIC CASES)

LOAD STEP 1: (750 kPa)

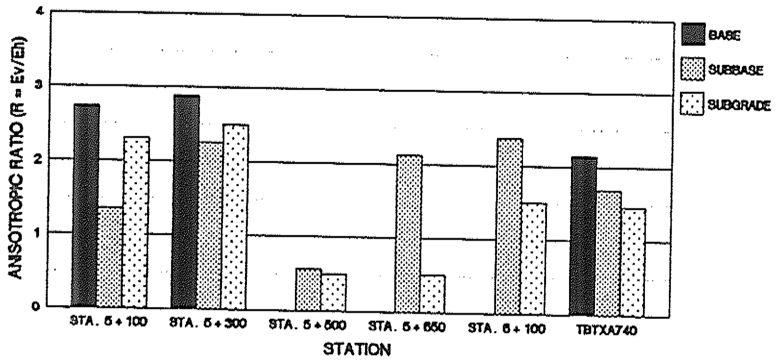

LOAD STEP 2: (1100 kPa)

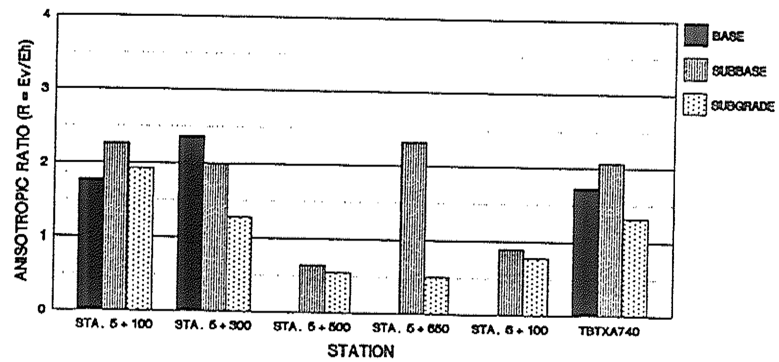

LOAD STEP 3: (1300 kPa)

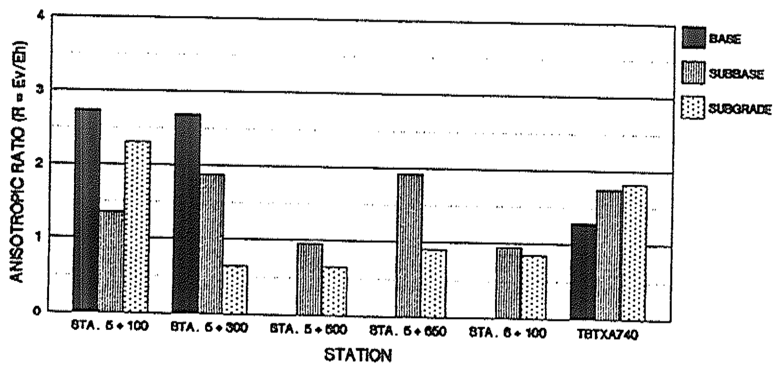

LOAD STEP 4: (1500 kPa)

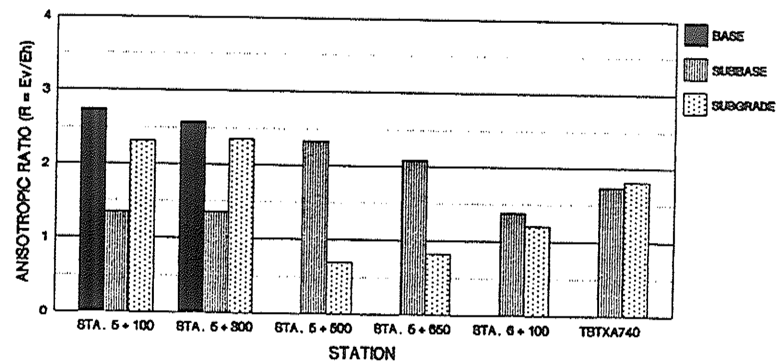

ANSYS FEM ANALYSIS

THUNDER BAY: RWY. 12-30: PROFILE OF MODULI OF UNBOUND LAYERS

OPTIMIZING CRITERION: MAXIMUM DEFLECTION

(BOTH ISOTROPIC AND X-ANISOTROPIC CASES)

LOAD STEP 1: (750 kPa)

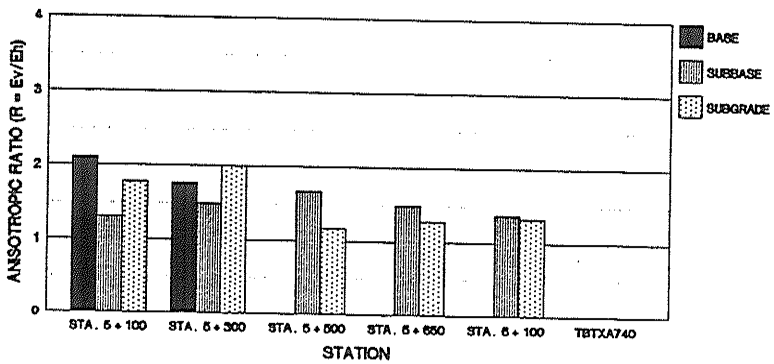

LOAD STEP 2: (1100 kPa)

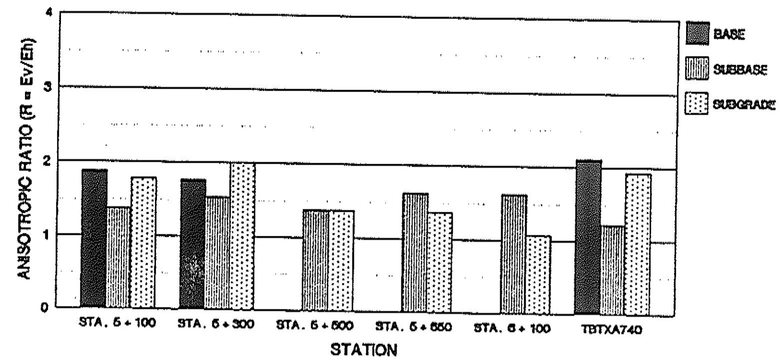

LOAD STEP 3: (1300 kPa)

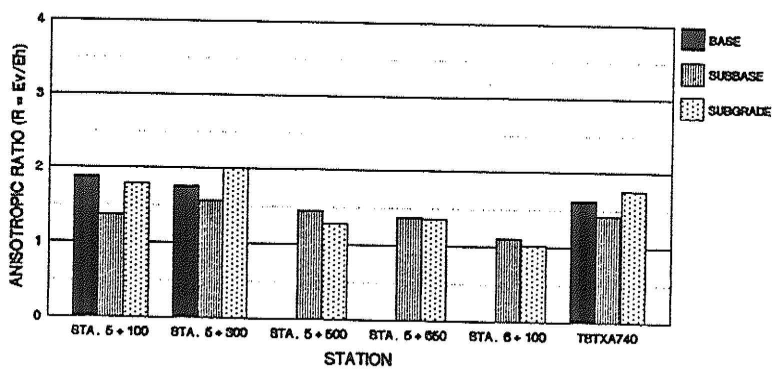

LOAD STEP 4: (1500 kPa)

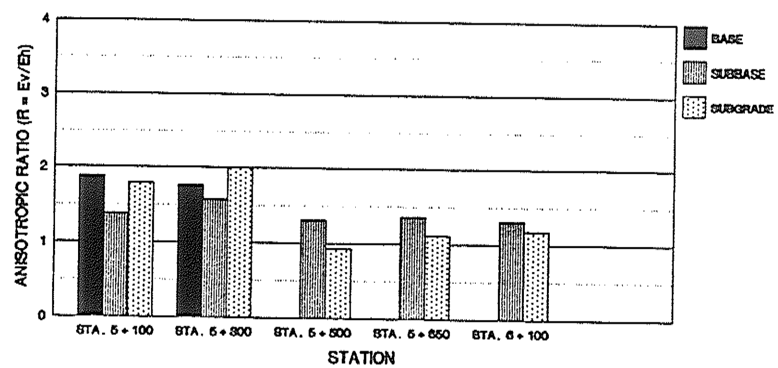

ANSYS FEM ANALYSIS

THUNDER BAY: RWY. 12-30: PROFILE OF MODULI OF UNBOUND LAYERS

OPTIMIZING CRITERION: RMS VALUE OF DEFLECTIONS

(BOTH ISOTROPIC AND X-ANISOTROPIC CASES)

LOAD STEP 1: (750 kPa)

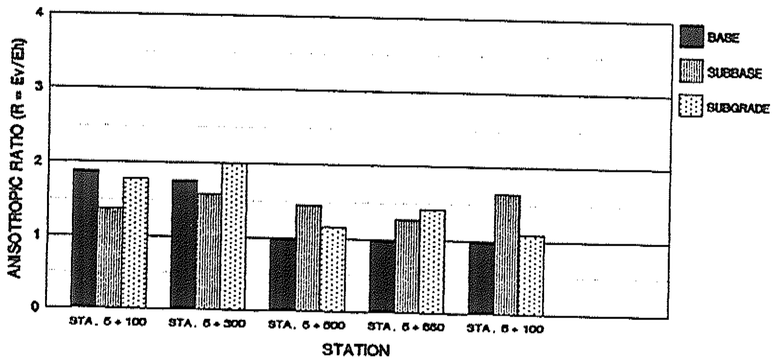

LOAD STEP 2: (1100 kPa)

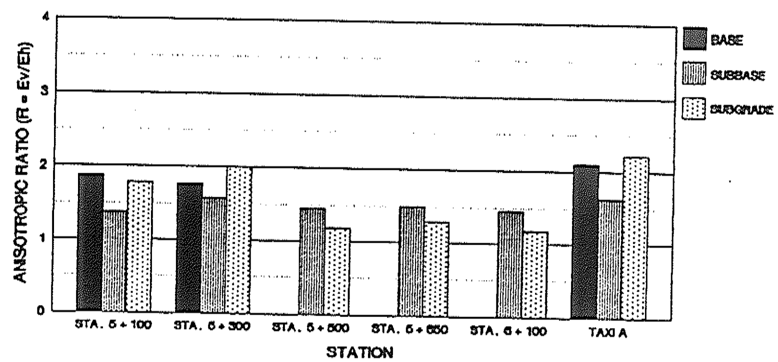

LOAD STEP 3: (1300 kPa)

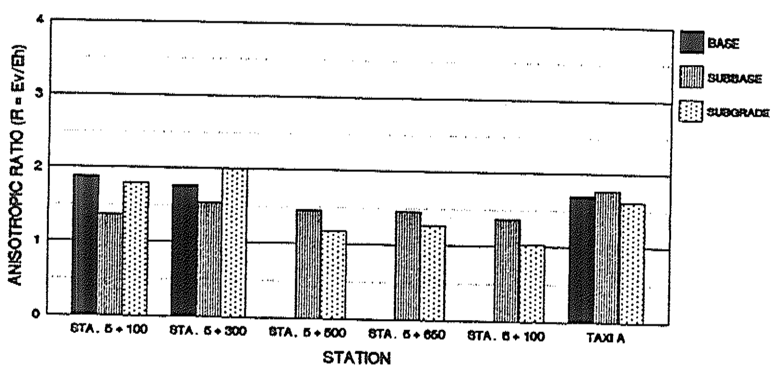

LOAD STEP 4: (1500 kPa)

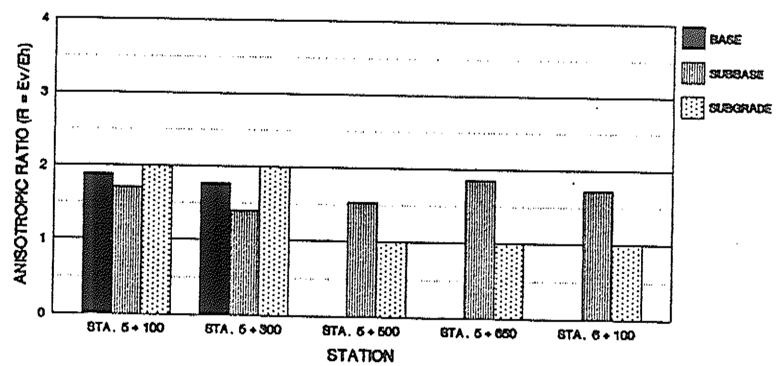

APPENDIX 6-V

STRESS DISTRIBUTION ALONG THE CENTRELINE OF LOAD

OPTIMIZING CRITERION: 'AREA' OF DEFLECTION BASIN

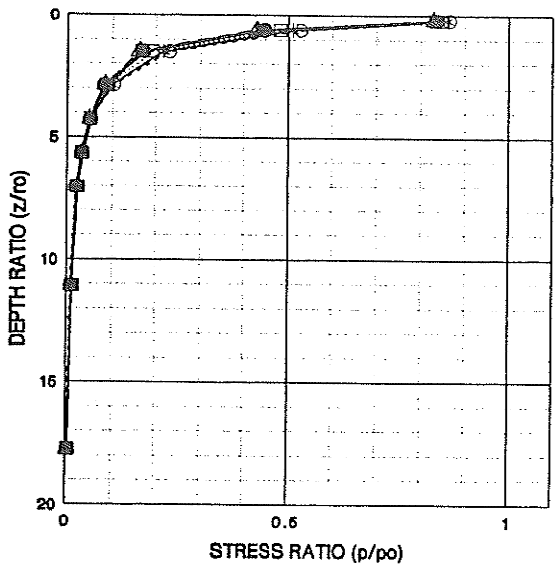

OPTIMIZING CRITERION: MAXIMUM DEFLECTION

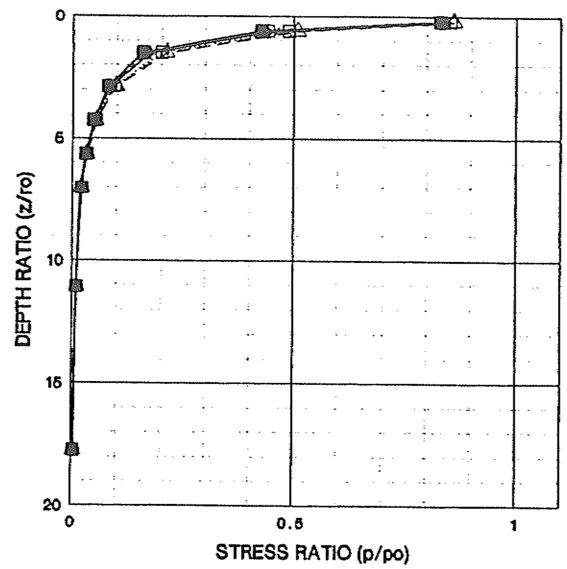

OPTIMIZING CRITERION: RMS VALUE OF DEFLECTIONS

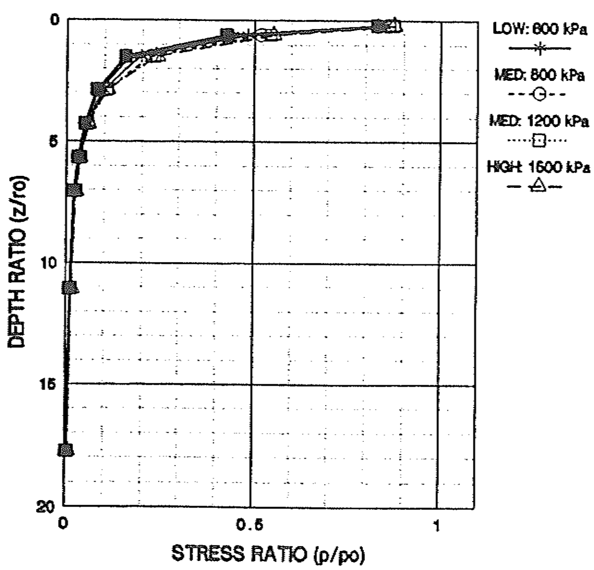

ANSYS FEM ANALYSIS

BRANDON: RWY. 08-26: STA. 5 + 900

DISTRIBUTION OF VERTICAL STRESSES ON C.L. OF LOADS

(ISOTROPIC ABD X-ANISOTROPIC MODELS)

OPTIMIZING CRITERION: "AREA" OF DEFLECTION BASIN

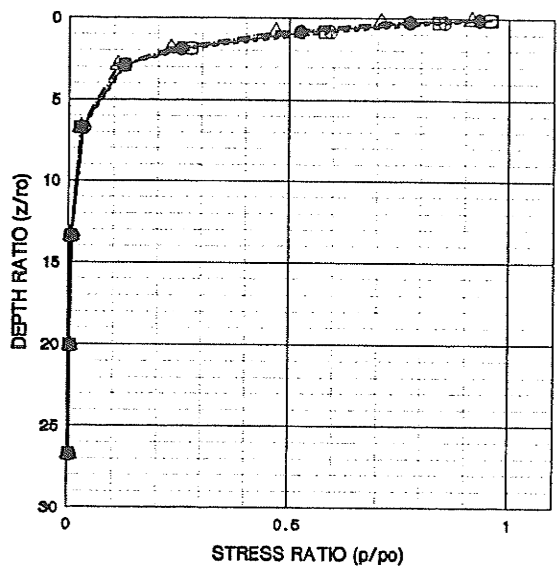

OPTIMIZING CRITERION: MAXIMUM DEFLECTION

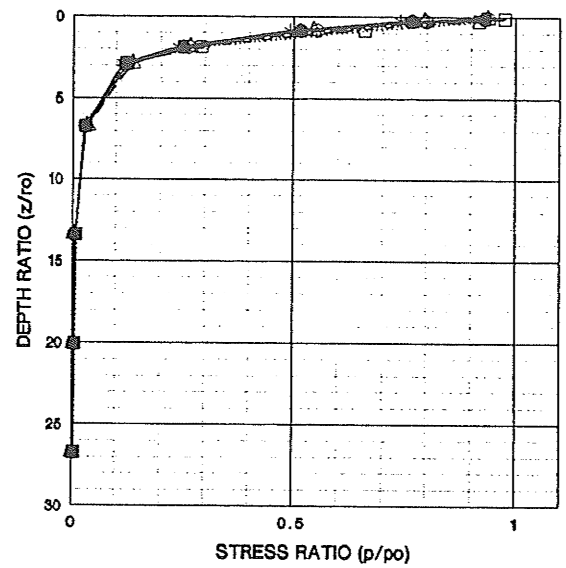

OPTIMIZING CRITERION: RMS VALUE OF DEFLECTIONS

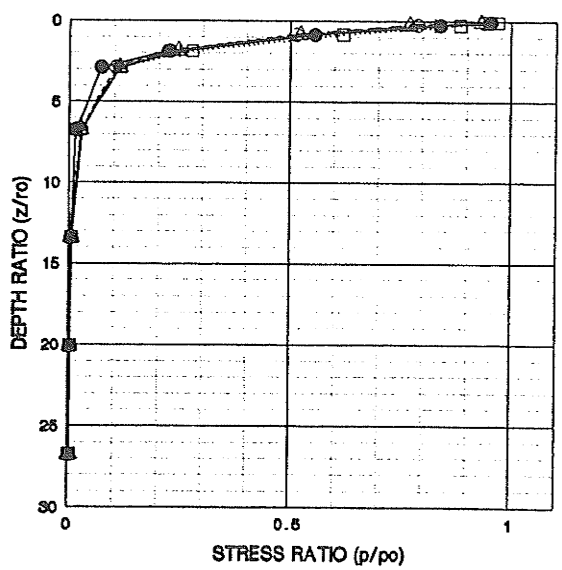

LOW: 500 kPa

MED: 700 kPa

HIGH: 1000 kPa

ANSYS FEM ANALYSIS

ST. ANDREWS: RWY. 13-31: STA. 5 + 840

DISTRIBUTION OF VERTICAL STRESSES ON C.L. OF LOADS

(BOTH ISOTROPIC AND ANISOTROPIC MODELS)

OPTIMIZING CRITERION: "AREA" OF DEFLECTION BASIN

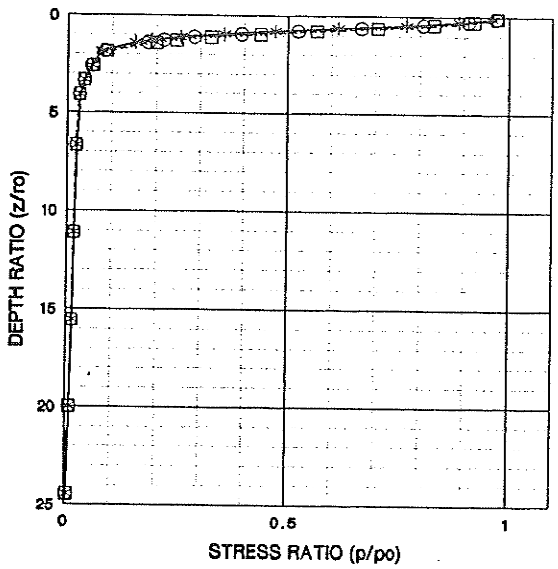

OPTIMIZING CRITERION: MAXIMUM DEFLECTION

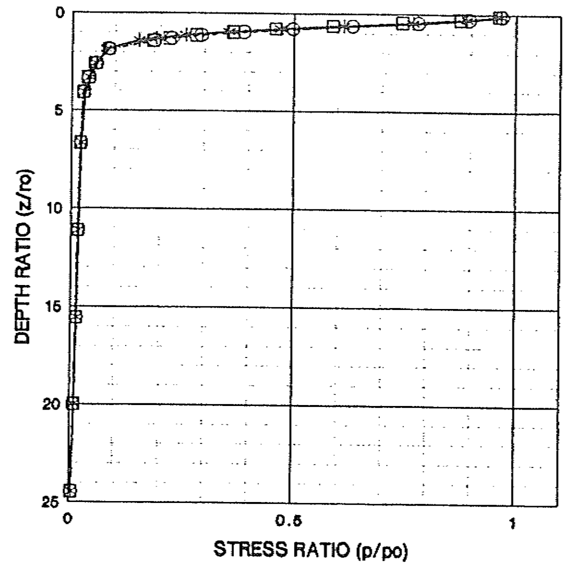

OPTIMIZING CRITERION: RMS VALUE OF DEFLECTIONS

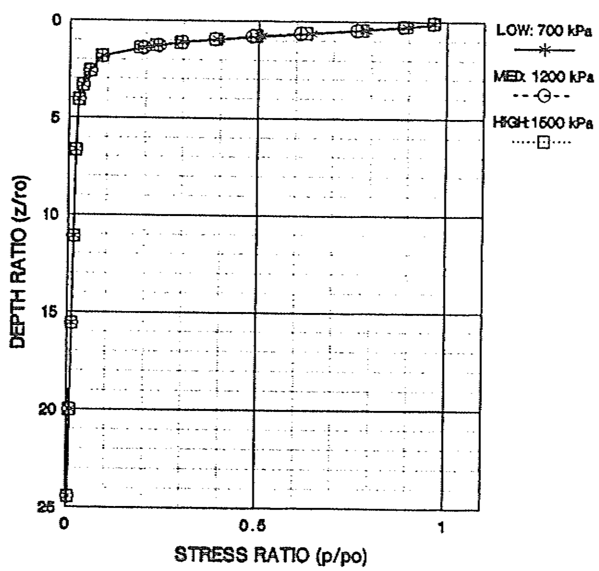

ANSYS FEM ANALYSIS : ISOTROPIC MODEL

REGINA: RWY. 12-30: STA. 5 + 990 L

DISTRIBUTION OF VERTICAL STRESSES ON C.L. OF LOADS

OPTIMIZING CRITERION: "AREA" OF DEFLECTION BASIN

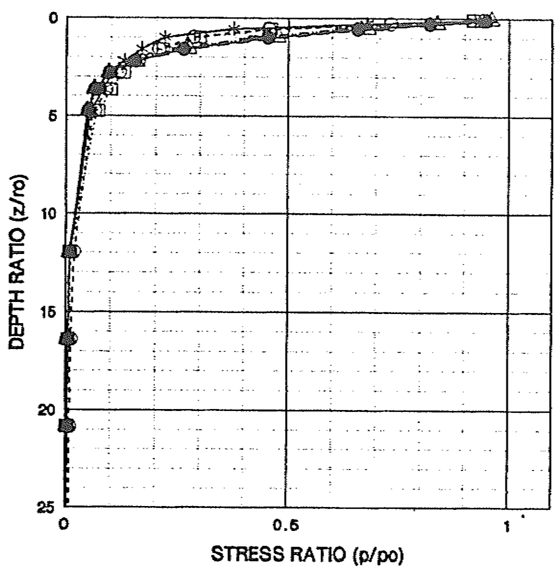

OPTIMIZING CRITERION: MAXIMUM DEFLECTION

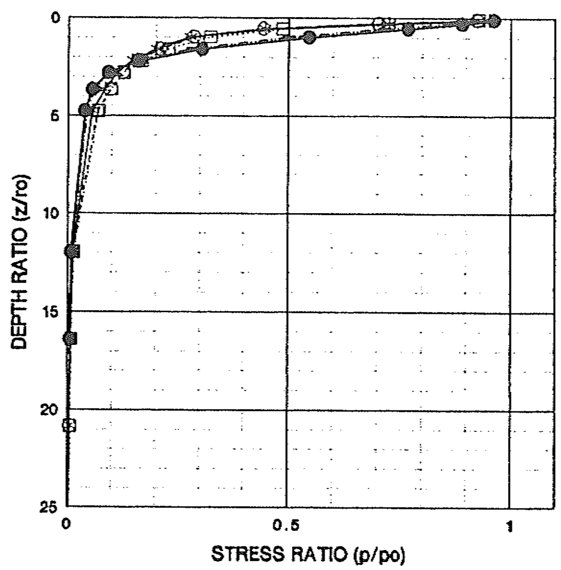

OPTIMIZING CRITERION: RMS VALUE OF DEFLECTIONS

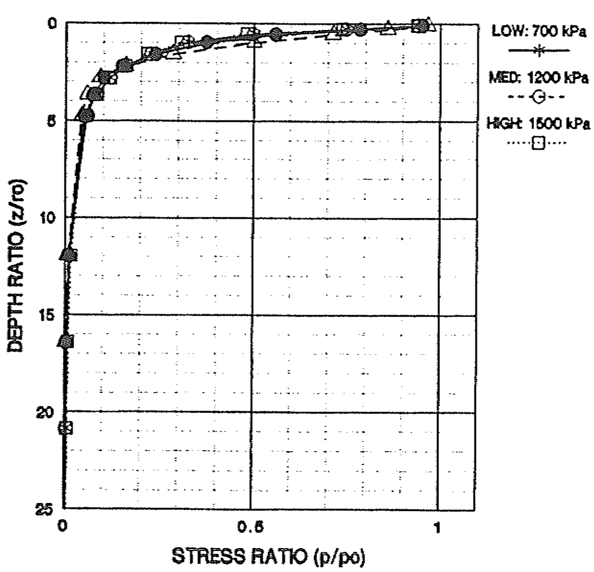

ANSYS FEM ANALYSIS

SASKATOON: RWY. 15-33:STA. 5 + 630 R

DISTRIBUTION OF VERTICAL STRESSES ON C.L. OF LOADS

(BOTH ISOTROPIC AND X-ANISOTROPIC MODELS)

OPTIMIZING CRITERION: "AREA" OF DEFLECTION BASIN

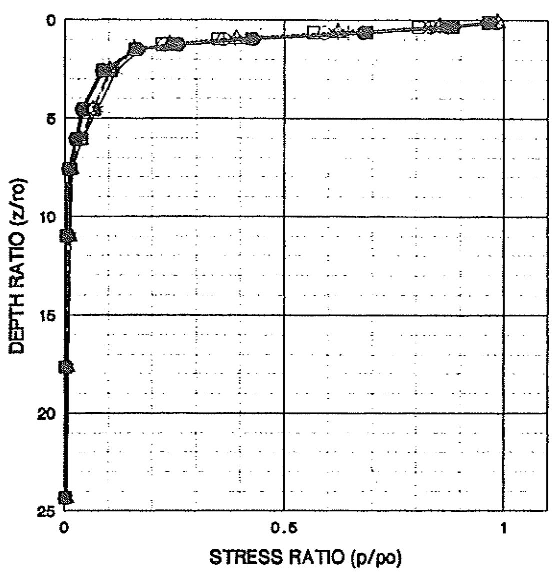

OPTIMIZING CRITERION: MAXIMUM DEFLECTION

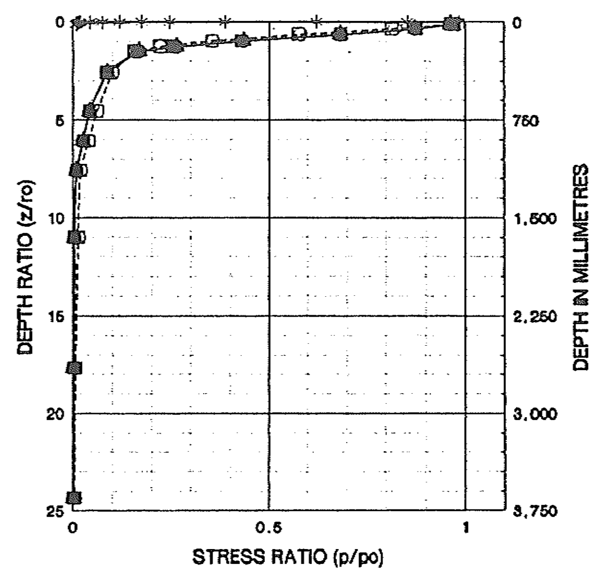

OPTIMIZING CRITERION: RMS VALUE OF DEFLECTIONS

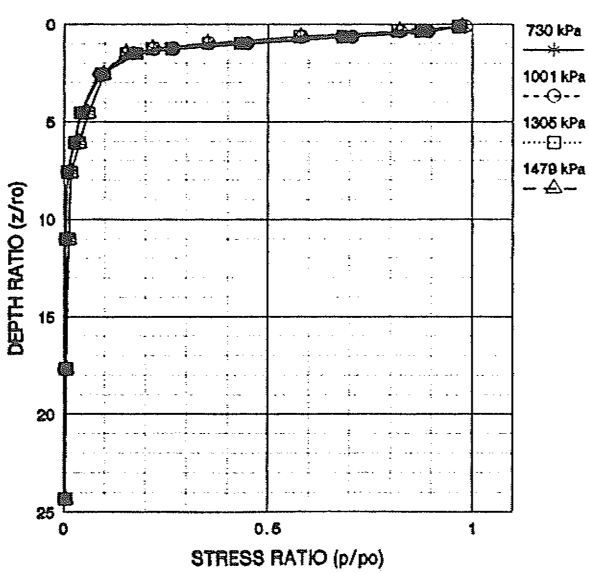

ANSYS FEM ANALYSIS

THUNDER BAY: RWY. 12-30: STA. 5 + 300 R.

DISTRIBUTION OF VERTICAL STRESSES ON C.L. OF LOADS

(ISOTROPIC AND ANISOTROPIC MODELS)